HAL
open science

Tailoring common hydrogels into 3D cell culture templates.

Aurélien Pasturel

To cite this version:

Aurélien Pasturel. Tailoring common hydrogels into 3D cell culture templates.. Cellular Biology. Université de Bordeaux, 2019. English. NNT : 2019BORD0302 . tel-03035011

HAL Id: tel-03035011

https://theses.hal.science/tel-03035011v1

Submitted on 2 Dec 2020

HAL is a multi-disciplinary open access archive for the deposit and dissemination of scientific research documents, whether they are published or not. The documents may come from teaching and research institutions in France or abroad, or from public or private research centers.

L'archive ouverte pluridisciplinaire **HAL**, est destinée au dépôt et à la diffusion de documents scientifiques de niveau recherche, publiés ou non, émanant des établissements d'enseignement et de recherche français ou étrangers, des laboratoires publics ou privés.

université de BORDEAUX

ALVEOLE – CNRS UMR 5297

Tailoring common hydrogels into 3D cell culture templates

Thèse pour l'obtention du grade de docteur de l'université de Bordeaux effectuée sous la direction de Vincent Studer.

Aurélien Pasturel
30/09/2019

Thèse présentée pour obtenir le grade de

Docteur de l'université de Bordeaux

Ecole doctorale sciences de la vie et de la santé

Spécialité : bio-imagerie.

Par Aurélien Pasturel

Tailoring common hydrogels into 3D cell culture templates

Sous la direction de Vincent Studer

Soutenue le 4 Décembre 2019

Membres du Jury

Vincent Studer	Directeur de recherche CNRS Bordeaux	Directeur de thèse
Joelle Amédée-Vilamitjana	Directeur de Recherche INSERM Bordeaux	Présidente du Jury
Xavier Gidrol	Directeur de Recherche, CEA Grenoble	Rapporteur
Nicolas Rivron	Project Leadear IMBA Wien	Rapporteur
Gaëlle Recher	Chargé de recherche CNRS Bordeaux	Examinateur
Aurélien Duboin	Ingénieur Alvéole Paris	Examinateur
Olivier Théodoly	Directeur de Recherche CNRS Marseille	Examinateur

Abstract/Résumé

Tailoring hydrogels into biomimetic templates represents a crucial step to build better *in-vitro* models but it is to date still challenging. Indeed, these synthetic or natural polymeric networks are often so frail they can't be processed through standard micro-fabrication. Here, we combine a ultra-violet pattern projector with gas permeable microreactors to control gas, reagents and photon distribution and *in fine*, the reaction kinetics in space and time. Doing so, enabled a generic chemistry that can structure, liquefy or decorate (locally functionalize) common hydrogels. Altogether these three hydrogel engineering operations form a flexible toolbox that supports the most commonly used hydrogels: i.e. Matrigel, Agar-agar, poly(ethylene-glycol) and poly(acryl-amide). We successfully applied this solution to grow cells into standardized micro-niches demonstrating that it can readily address cell culture challenges such has controlled adhesion on topographical structures, standardization of spheroids or culture on shaped Matrigel.

Keywords: Hydrogel, 3D cell culture, Photo-chemistry, Radical-chemistry

L'ingénierie d'hydrogels ; leur structuration et fonctionnalisation à l'échelle cellulaire, est une étape clé pour aboutir à de modèles in-vitro plus physiologiques. À ce jour, elle reste difficile car ces matériaux polymères, mous et riches en eau, sont souvent trop fragiles pour la micro-fabrication traditionnelle. Pour pallier à ce fait, nous avons combinée illumination ultraviolette structurée et chambres de réaction perméables au gaz nous offrant la maitrise sur la distribution de photons, les réactifs et les gaz présents à chaque instant et en tout point d'un champ d'illumination. Nous pouvons ainsi contrôler une photochimie adaptée aux hydrogels les plus répandus et structurer, décorer ou liquéfier ces matériaux. Ensemble ces trois opérations forment une boite à outil complète adaptée aux substrats les plus communs que sont Matrigel, Agar, Poly(acrylamide) et Poly(éthylène-glycol). Nous avons par la suite fabriqué des micro-niches en hydrogel permettant la culture standardisée de lignées cellulaire et de neurones primaires soit par adhésion sur des topographies ou par auto-organisation en sphéroïdes. Ceci démontre que la plateforme est à même de répondre à des enjeux importants de culture cellulaire tridimensionnelle.

Mots Clés : Hydrogel, 3D cell culture, Photo-chimie , Chimie radicalaire

Remerciements

Je tiens premièrement, à remercier mes supérieurs Romuald Vally et Vincent Studer qui m'ont fait confiance et m'ont donné la latitude nécessaire pour mener à bien ce projet alors que j'ai dû partager mon temps entre Bordeaux, Paris et Avignon. Grace à vous tous s'est littéralement déroulé comme sur des rails.

Je souhaite ensuite remercier les membres d'Alvéole et de Quattrocento, en particulier Aurélien Duboin et Luc Talini, qui m'ont tous accueilli avant même le début de ce doctorat, qui ont cru en moi et m'ont donné une chance alors que j'avais ma motivation pour seul atout.

Bien sûr, je remercie les personnes qui ont partagé mon quotidien à bordeaux notamment Pierre Oliver, Sarah et Nathalie mais aussi les membres des équipes Sibarita, Nagerl et l'IINS en général. Que ce soit par vos conseils avisés, vos encouragements ou vos enseignements, votre patience et votre égard envers moi ont été d'une aide inestimable.

Je remercie aussi ma compagne, ma famille et mes amis qui ont toujours su trouver les mots et me redonner courage dans les moments difficiles. C'est en m'inspirant de vos qualités à tous que je suis parvenu jusqu'ici.

Enfin, j'aimerais adresser une pensée aux proches regrettés, partis au cours de ces trois années. Merci pour tout ce que vous m'avez appris, je ne serais pas là sans vous non plus.

Outline

General Introduction 1
Preamble 1
Hydrogels in Biology 5
Engineered versus extracted matrixes 7
Perspectives in 3D cell culture: tailored templates 13
Altering mater with light 15
Photochemistry: a straight path to hydrogel tailoring 17
Oxygen and benzophenones 23
Closing thoughts 27
Chapter 1 : Mastering Z 28
Introduction 28
Molding 29
Flow Focusing 32
Meniscus Pinning 35
Discussion : 37
Experiments 39
Front polymerization: NOA Slides 39
Conclusions on “NOA-Slides” 43
Oxygen-controlled polymerization 44
From silicone microwells to microreactors 46
Gas-Controlled Polymerization 50
Conclusions on gas-controlled polymerization 55
Flux-Controlled Polymerization 56
Conclusions on flux-controlled polymerization 61
Cell culture: Revert the antifouling or make use of it 62
Chapter’s conclusion: kinetics to control Z 66
Chapter 2 Decoration 67
Introduction 67
Microcontact Printing 68
Light-based micropatterning 70
Flow-generated chemical gradients 72
Discussion 74
Experiments 76

Gel transfer: lift off patterning. 76
Photo-linkers: bridging poly(ethylene-glycol) and biomolecules 82
Synergy: queuing structure with decoration 89
Cell culture: topographical and chemical cues combined 92
Chapter's conclusion: Are linkers superior? 95
Chapter 3 Going Wide 97
Introduction 97
Benzophenones: a deeper dive in the world of photo-initiators. 98
Experiments 100
Decoration of native gels 100
Conclusions on native-crosslinking 108
Photo-scission: Debuts 109
Photo-scission: improvements 113
Cell culture : controlling cell growth on visco-elastic gels 121
Chapter's conclusion: uncharted territories 123
Conclusion 125
Preamble: 125
Impossible structures: 126
Preserving the gel and the cells: The orthogonality conundrum 129
Square meters of micron sized niches? The question of scale 132
Closing words: 134
Appendix I : Common methods 136
Appendix II : BioRxiv Preprint 137
Bibliography 145
Index of Figures 150
Index Of tables 151

General Introduction

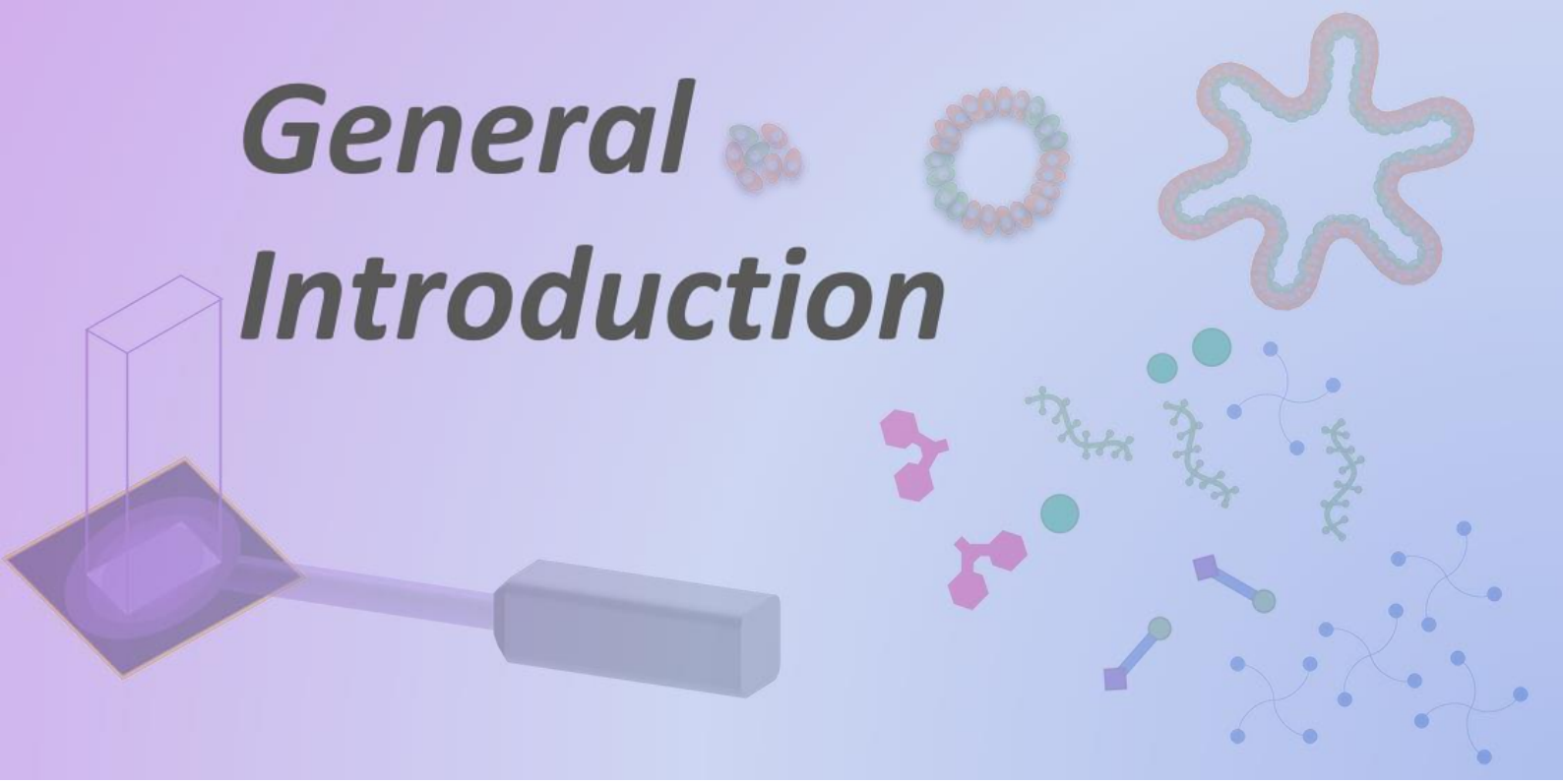

Preamble

When the material is more liquid than solid how can one shape or functionalize it?

From the seminal works in tumor micro-environment[1] to the most recent developments in organoïds[2], hydrogels have paved the way towards physiologically relevant cell-based models. Indeed, these soft polymeric networks, made of synthetic or natural molecules, offer several improvements over glass slides and Petri dishes: i) They are water permeable allowing nutrients to diffuse through ii) Their softness is comparable to that of organs iii) Cells can be cultivated in tridimensional configurations within these meshes. However, organs also display specific shapes and patterns of biomolecules which govern cell behavior and are poorly replicated by homogeneous matrixes. Standardizing cell culture will require templates and micro-niches engineered from these soft hydrogel materials[2–4].

To fine tune the structural and chemical properties of these extracellular matrix mimics, scientists have extensively relied on hardware and chemistry[5]. Laser ablation[6] and extrusion-based 3D printing[7] are used to structure hydrogels which lack photosensitive properties . Alternatively, hydrogels were chemically modified to achieve photopolymerization[8], photo-degradation or functionnalization[9–11] using light structuration methods such as photomasks, 2-photon raster scanning or digital micromirror devices[12].

However, I argue that this over-reliance on hardware and chemical modification had its toll on the overall cohesion of this scientific topic. Each solution was made unique: domineering its own field but poorly transferrable to other research teams. As a result, a gap grows between hardware[12], chemistry[10] and biology-oriented[13] hydrogel research. The first field designs more[14] and more[15] complex set-ups to reach the desired engineering capabilities, using cells as a proof of viability. This “tool-making” field is

usually the furthest astray from biology. The second, develops finely tailorable hydrogels[9,16] that go in pair with hardware set-ups. Additionally, they also fashion custom hydrogels to create organoids[17] and/or differentiate[18,19] stem cells, often competing with the gold-standard that is Matrigel. The latter community uses Matrigel as it is successful and well documented[1,20]. They make for the lack of control over the matrix parameters by adding soluble factors to monitor cell self-organization and reach highly heterogenous cellular structures such as minibrains[2,21]. As tool makers, we tried to bridge the gap with biology by introducing a simple and generic solution. Thus, instead of introducing new features to our previously built platform[22], we tried to keep the same configuration while pushing further it's capabilities.

Z-stages and 2 photon illumination were avoided for the additional complexity they bring despite being common solutions to control the reactions in the Z axis. Commercially available reagents were favored over home-made chemicals in an effort to make the technology as accessible as possible. Instead we catered on universal radical reactions namely : benzophenone photo-chemistry[23] , oxygen-radical interactions[22,24] and photo grafting linkers[25].

To fully take advantage of these chemical mechanisms, our platform combines a structured illumination module docked to a microscope and polydimethylsiloxane (silicone) microreactors to control the gas, reagent and photon distribution during the engineering process (**Figure 1**). During the course of this manuscript I will present the successive developments that led to the emergence of this platform.

The introductory section will offer a broad picture of hydrogel research as well as light-based hydrogel engineering strategies. Each experimental chapter will also offer a state of the art in hydrogel engineering strategies although from a user perspective in an attempt to understand the needs and challenges.

The first challenge that we try to solve is related to the control of hydrogel shape (**Figure 1 Blue Panel**). Eventually the well-known inhibition of polymerization[24] by oxygen is exploited. Applications relevant to tridimensional cell culture such as vascular structures and spheroid standardization are also presented.

In a second part, we cover the subject of decoration that is the methods to locally functionalize a gel with biomolecules. After trials and errors, we adopt the well-tested photo-linkers[25] in combination with cell adhesive poly-electrolytes[26] (poly-L-lysin) to decorate bio-inert gels such as poly-ethylene glycol (**Figure 1 Green Panel**). We demonstrate that the workflow allows for quantitative decoration and functionalization of topographies as cell lines and neurons are gown on these biomolecule patterns.

In the latest chapter, we shed light on the unique uses of benzophenone photo-initiators. We first demonstrate that gelation and decoration can be applied on many hydrogels thanks to benzophenone chemistry. We then expand our reaction portfolio by introducing photo scission i.e. our original contribution to hydrogel structuration (**Figure 1 Yellow Panel**). This subtractive manufacturing method relies on oxygen/benzophenone interaction to liquefy native hydrogels such as Matrigel or Agar-agar while preserving the remaining areas. We exploit this to cultivate neurons on Matrigel structures that were previously impossible to obtain.

In the conclusion we'll discuss the pros and cons of our strategy by raising the three following questions:

What are the tasks that our platform struggles at?
Should one opt for crude chemistry when working with frail materials and cells?
How can we reach the inevitable requirement for large scale production?

In doing so, we'll try to point at the necessary enhancements that will ultimately improve and/or simplify our emerging toolbox.

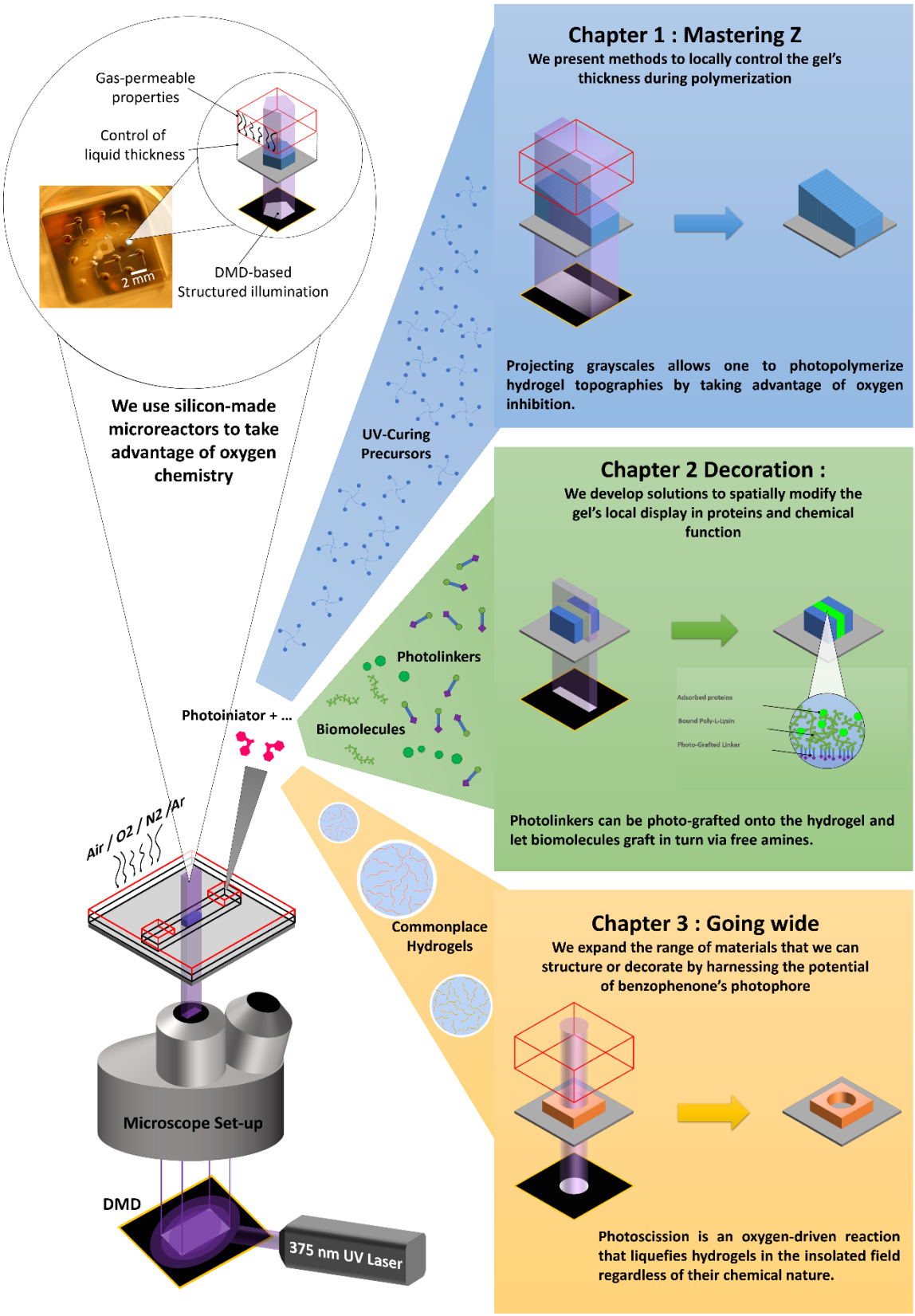

Figure 1 **| *Introducing the platform and the chapters.***

Right, *the platform is presented with gas permeable silicone microreactors used in this paper showing the upper (red) and lower (black) silicone stencil designs stacked onto a glass slide (gray). Below lies the schematics of the microscope objectives (gray) , the digital micromirror device (black with gold trim), and the 375nm expanded and collimated laser beam (purple).* ***Middle,*** *schematics of the reagents with : hydrogel precursors (blue 4-branched stars) , photo-initiator (pink) , photo-linkers (purple and green) , biomolecules (green), agar (yellow) and Matrigel (pink)* ***Left,*** *The chapters are presented with schematics of the realizations made in this manuscript showing cured hydrogel (blue) , decorated hydrogel (blue for the gel green for the decoration) photo-scissionned Matrigel (Pink)*

Hydrogels in Biology

Hydrogels are polymeric networks with the characteristic properties of solids (resistance to flow) at the macroscale and of liquids (diffusion of solutes) at the nanoscale. These matrixes are formed through a process called gelation by which highly elongated and often branched molecules, the precursors, bind to each other. Going in pair with the high diversity of gel precursors, an equally high variety exists in gelation modes and binding nature[27] **(Table 1 second column)**. To offer a few examples: Matrigel and collagen form non-covalent bonds following an increase in temperature. Alginate gelifies via ionic-bridges in the presence of calcium. Agar-agar precursors must be heated then form covalent ester bonds upon cooling. Poly-acrylamide covalently reticulates through radical initiation.

Due to their high hydrophilicity, the molecules composing the network support a lot of water within the mesh creating a biocompatible matrix. Indeed, proteins and other biomolecules are stable and diffuse within these materials. As such, hydrogels like agar and poly-acryl-amide are the historical staple for nucleic acid and protein electrophoresis respectively. Cell culture can also be performed on top or within these substrates **(Table 1 third column)**. Bio-active gels like Matrigel and type I collagen promote the colonization of cells since they contain adhesion molecules and the necessary growth factors. On the other hand, bio-inert gels like agar or poly(ethylene-glycol) do not contain any adhesion molecules. These inert materials support the growth of cells and/or spheroids that require low attachment or are alternatively complemented with the adequate growth and adhesion proteins.

In the recent years, hydrogels have attracted more interest as the need for improved in-vitro models rises. Cell culture, traditionally performed on glassware and petri-dishes, shows its limits in replicating and more importantly predicting in-vivo outcomes[28,29]. Indeed, such substrates exhibit flat features and stiffnesses that are almost never encountered in vivo. Additionally, such materials do not support the flow and/or diffusion of solutes within their mesh. As a consequence, many cells types display altered or degraded phenotype and functionality when cultivated on glass or plastic. Among the tremendous emerging solutions to improve the physiological relevance of in-vitro models (organ on chips, bioprinting, spheroids etc…), hydrogels offer a unique blend of simplicity and efficiency while also supporting the other technologies. Whether one wants to fill microfluidic compartments with cells or exploit the stem-cell's self-organization to obtain organoids, hydrogels are likely to be the material of choice.

Naturally derived matrixes		
Material	Mode of gelation	Notable features
Basement Membrane Extract	Going from 4 to 37C°	Sourced from rat, Cell adhesive, rich in laminin and growth factors, Well documented
Collagen	Going from 4 to 37C°, pH neutralization	Sourced from rat or bovine tendon, Cell adhesive,
Alginate	Ionic crosslinking with calcium	Sourced from algae, Cell repellant
Agar	Cooling after ebulition	Sourced from algae, Cell repellant, Well documented
Hyaluronic Acid	Depends on chemical modification	Sourced from bacteria bioproduction, Interract with cell receptors but not adhesive

Engineered and synthetic precursors		
Material	Mode of gelation	Notable features
Polyacrylamide	Radical crosslinking	High range of tunable stiffness, Well documented
Poly-(ethylene-glycol)	Depends on chemical modification	« Blank slate », bioinert and FDA approved, Highly engineered; Well documented
PolyPeptides	Self assembly into fibers	Usefull in very soft (neural) substrates

Color coding: PolyPeptides, Poly-Osides, Poly-Ethylenes, Poly-Amides

***Table 1* | A wide array of hydrogels support different types of cell culture studies.**

Adapted from : A practical guide to hydrogels for 3D cell culture Stephen Caliari Jason Burdick Nature Methods 2018[27] . Authors sort the hydrogel in three categories: Naturally derived, Synthetic and Hybrid materials while in this review we consider engineered materials which encompasses synthetic and hybrid hydrogels as opposed to extracted (naturally derive) matrixes.

A high number of hydrogels were developed to meet the growing demand, each precursor fitting one or more applications. As the next part will illustrate, in the race for the optimal matrix (or library), two strategies are competing.

Engineered versus extracted matrixes

Some hydrogels are decellularized extracts coming from specific organs and organisms while others intend to contain the minimal number of factors to recapitulate the cellular micro-environment.

The former strategy represents a utilitarian posture. It is unlikely that we'll know and understand all the relevant factors that govern the cell behavior anytime soon. Until then, decellularized matrixes extracted from organs should provide the truest to life hydrogel substrates. Starting in 1987, the pioneering work of Mina Bissel demonstrated that cell lines could recover most of their original functionalities when embedded within laminin rich hydrogels compared to their Petri dish equivalents[30] **(Figure 2 first reference)**. Later on, they used extracellular matrixes from healthy and malignant donors to study their effect on cell morphology. The exact composition of the gel was unknown but despite this drawback, the origin of the gel served as a reference and made for a convenient shortcut from material science towards biology. Many other laboratories adapted this methodology to their needs, the series of work saw an increase in the model complexity culminating with the whole brain organoïds developed by Lancaster and colleagues[21] **(Figure 2 last reference)**.

This last work exemplifies the utilitarian philosophy supporting extracted hydrogels : Matrigel , the hydrogel used in this work, contains more than a thousand different molecules most of which are not yet identified[20]. Despite this drawback, the brain organoïds can readily serve as a tool to study development and pathology and the workflow is being adapted in other laboratories[2].

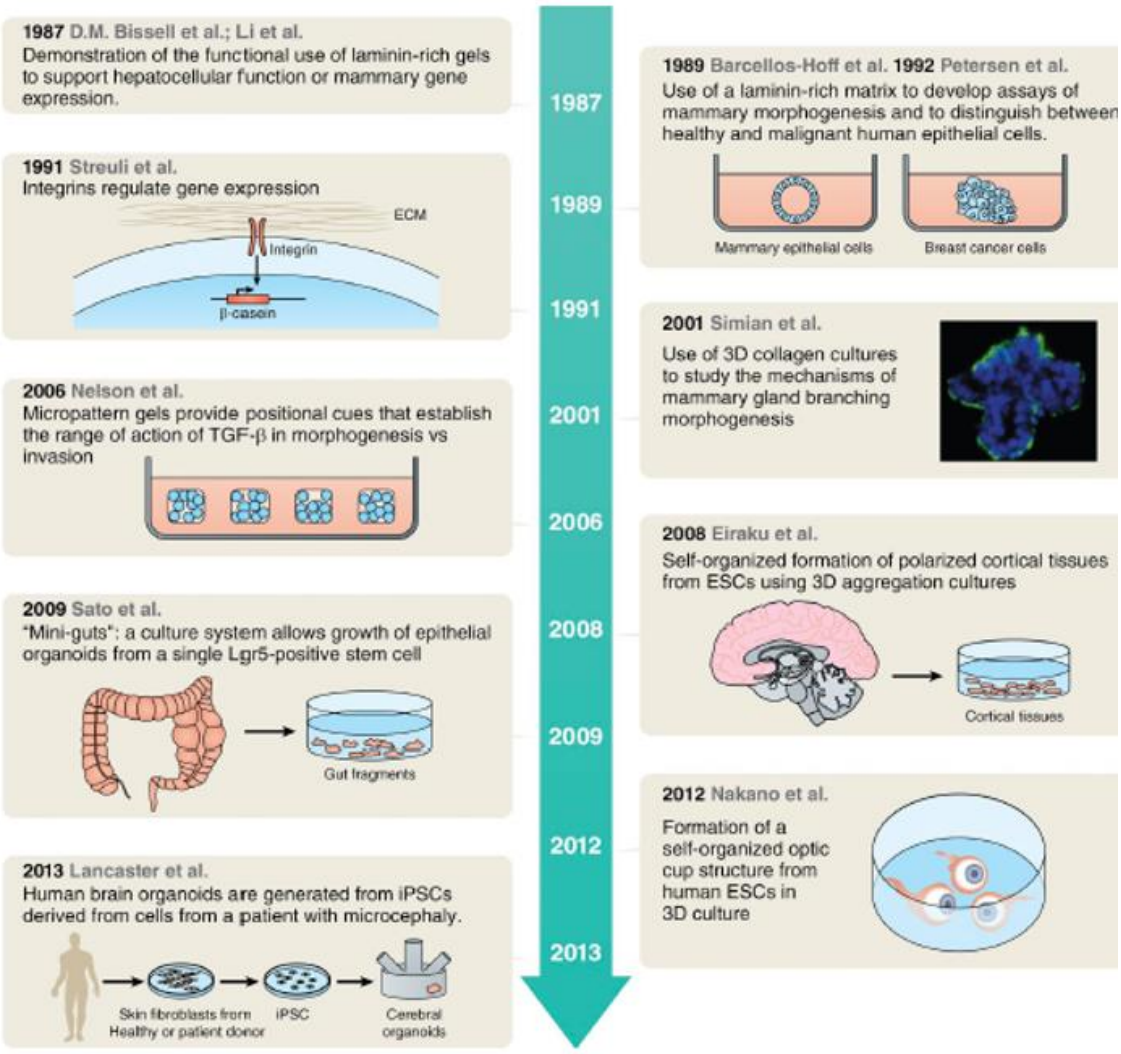

Figure 2 **| *Naturally derived matrixes have paved the history of three-dimensional cell culture.***

Extracted from : Organoids : a historical perspective in thinking in three dimensions Mina Bissel Journal of cell biology 2017[1]. Important breakthroughs are presented in chronological order, note the recurrence of collagen and laminin rich hydrogels. The pioneering works of the authors were performed in laminin rich extracts about thirty years ago and the same type of hydrogels are still used today in the most advanced organoid experiments.

The opposite strategy is a synthetic biology posture. Many of the factors contained within the naturally derived hydrogels may not be useful or even be detrimental to the organotypic culture that one may try to reach. The matrix-related effects on cell behavior can't be controlled unless we understand them. And in return we can't understand them unless we build an extracellular matrix with our own means. In their work on designer matrixes for intestinal organoid development[17], Gjorevsky and colleagues demonstrated that gut-organoïd development required the substrate to soften during the cell culture **(Figure 3 A)**. This matrix-softening was a key property of Matrigel and could be successfully replicated using enzymatically cleavable moieties within the poly(ethylene-glycol) hydrogel that had

been designed. This led to a production a stable and fully functional gut organoids within well-defined and minimal matrixes **(Figure 3 B)**.

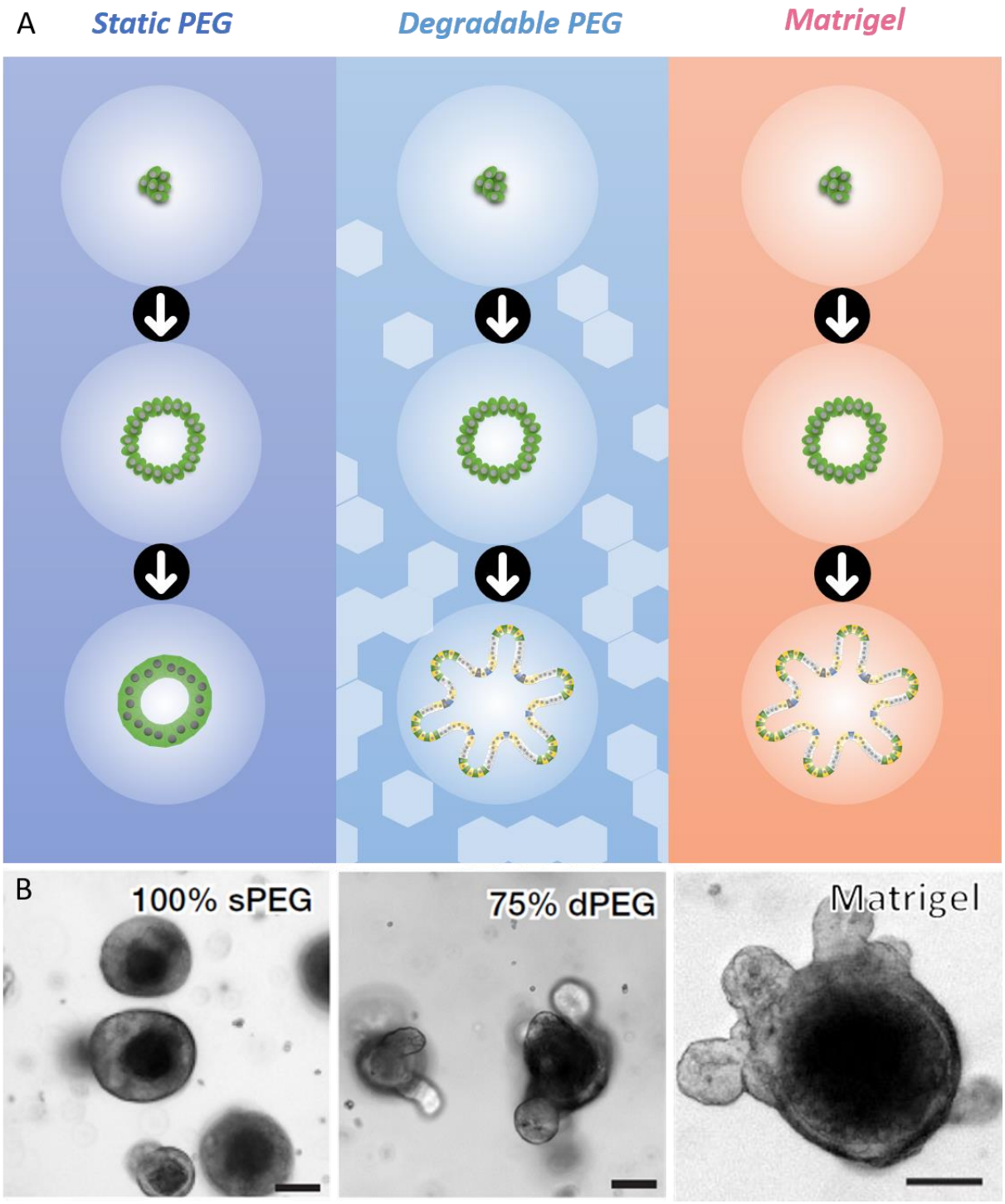

Figure 3 **| Engineered matrixes can improve organoid generation.**

Adapted from : Designer matrices for intestinal stem cell and organoid culture MP Lutolf Nature letters 2016[17]. **A,** Schematics representing the growth of gut organoïds in the three different matrixes. **B,** Bright microscopy images of the gut organoids obtained in their respective hydrogel: note the generation of vilis in the case of degradable poly-ethylene-glycol and Matrigel whereas the static , covalent hydrogel blocks the formation of such structures.

In another telling example Chaudhuri et al. conceived hydrogels with tunable stress relaxation to study its effect on stem cell differentiation[18]. Viscosity and elasticity usually intertwine using organ-derived materials but alginates precursors of variable length and poly-ethylene spacers solved this challenge **(Figure 4 A)**. The researchers succeeded in modifying the stress relaxation (viscosity) of the hydrogels while maintaining the same stiffness (elasticity) and observed that cells were very responsive towards viscosity **(Figure 4 B)**.

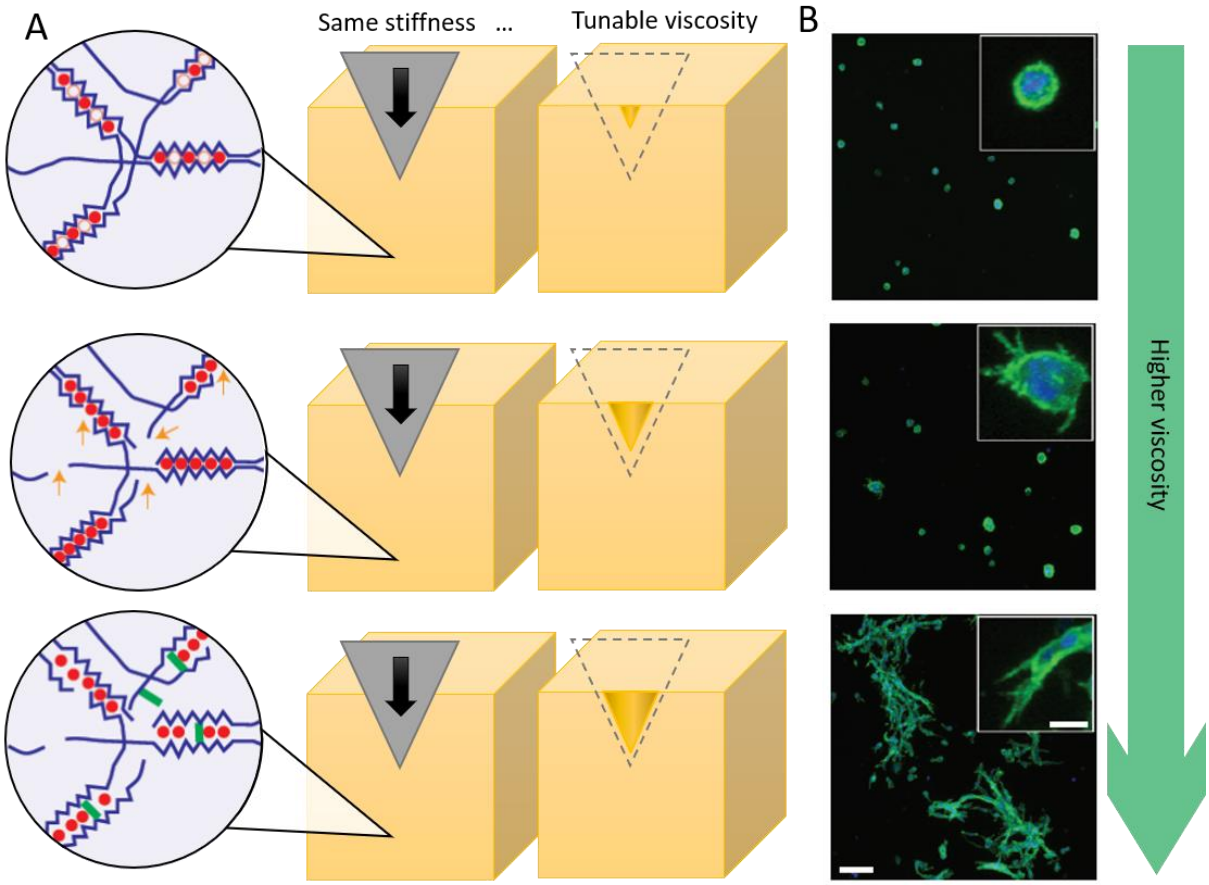

***Figure 4* | Engineered matrixes allow better control of mechanical parameters.**

Adapted from : Hydrogels with tunable stress relaxation regulate stem cell fate and activity DJ Mooney Nature materials 2015[18]. **A,** Design principles for hydrogels with tunable viscosities: alginate strands are represented in blue with calcium crosslinks in red, poly(ethyleneglycol) spacers are in green. All the gels display the same initial resistance to deformation (elasticity) but they do not recover their initial shape (viscosity) the same way. **B,** Fluorescence microscopy images of cell spreading in gels with growing stress relaxation showing Actin (green), Nucleus (DAPI, Blue). With the same amount of adhesion factors the cells are more likely to spread when the viscosity is high.

The mechanical properties are not the only tunable parameter with synthetic hydrogels; customized gels can also harbor functional adhesion motifs to promote adhesion, angiogenesis or neurite outgrowth. This is especially relevant in the optimization of implantable biomaterials for regenerative medicine. In 2019, Dos Santos et al.[19] used a combination of vinyl-modified elastin-like peptides, cysteine terminated IKVAV peptides and starshaped thiol terminated poly(ethylene-glycol) to create

hydrogels promoting angiogenesis and innervation **(Figure 5)**. Under radical crosslinking alkene and thiol functionalities bind to each other leading to the formation of a gel containing adjustable quantities of IKVAV sequences and poly(ethylene-glycol). They were thus able to find an optimum ratio for the different factors leading to successful neurite outgrowth and angiogenesis **(Figure 5 B C)**.

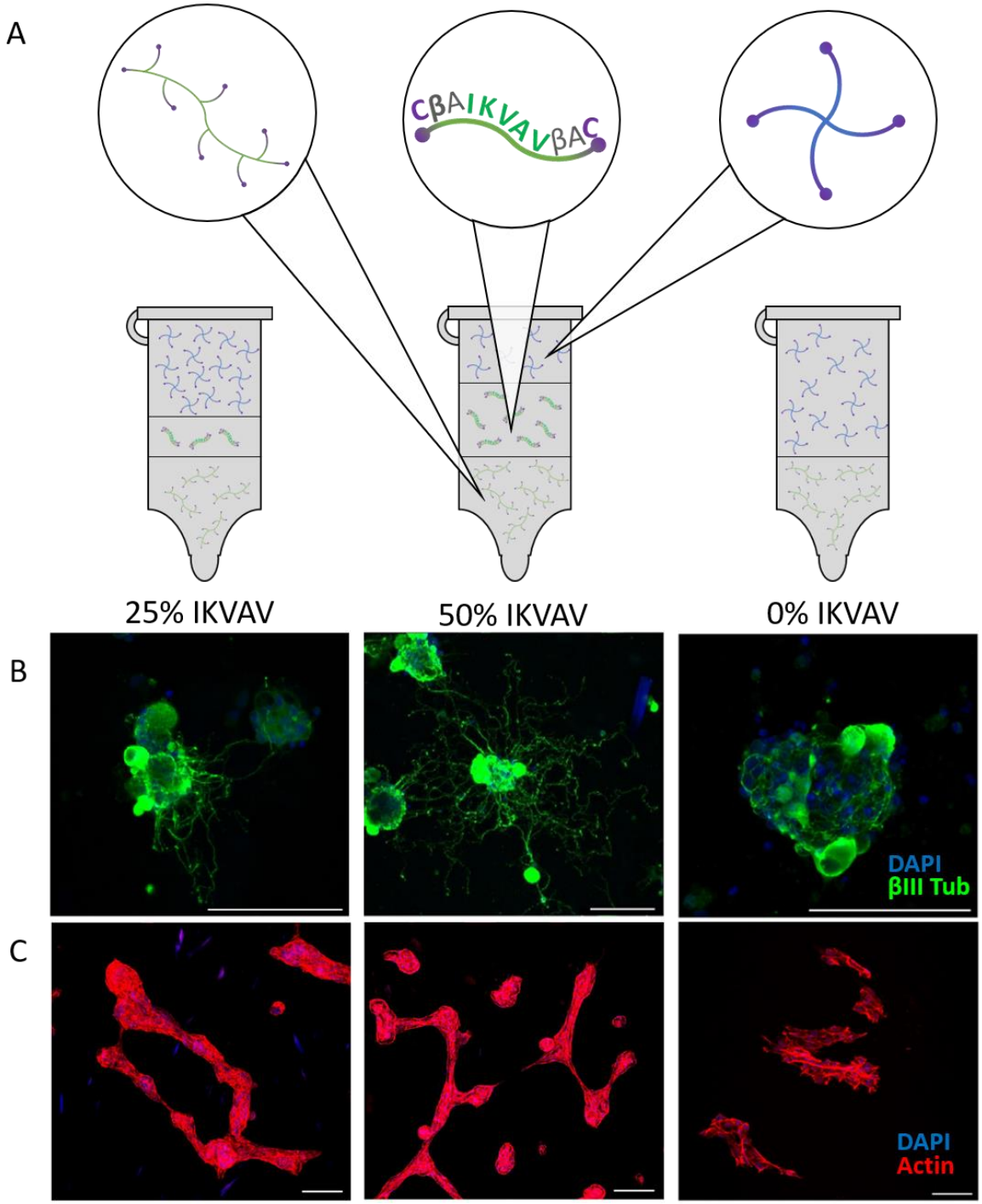

Figure 5 **| *Engineered matrixes allow better control of biological factors.***

Adapted from : Development of a cell-free and growth factor-free hydrogel capable of inducing angiogenesis and innervation after subcutaneous implantation J Amédée Acta Biomaterialia 2019. **A,** Design principles for hydrogels with tunable bifunctionalities showing the schematic structure of elastin like peptide (left panel), IKVAV peptide (middle panel) and star-shaped poly(ethylene-glycol) (right panel) **B,** Fluorescence microscopy images of neurons spreading on each gel showing BIII tubulin (green), Nucleus (DAPI, Blue). **C,** Fluorescence microscopy images of bone marrow endothelial cells spreading on each gel showing BIII tubulin (green), Nucleus (DAPI, Blue). 50% IKVAV proved to be an optimum to favor neurite outgrowth and angiogenesis.

Overall each strategy is valid: extracted matrixes provide a ready to use, general purpose solution for early developments while designer matrixes provide longer-term solutions for niche applications. Nonetheless, the quest for the perfect matrix led to a tremendous (at times puzzling) diversity of hydrogels currently in use across the globe. We thus made numerous efforts to be as generic as possible while implementing our hydrogel structuration and decoration protocols.

No matter the material, hydrogels can't promote standardized and relevant cell culture if the conditions are not controlled at the cellular scale[2–4]. Indeed, when trying to replicate the heterogeneous features of organs, homogeneous matrixes are not sufficient. In the next section, we discuss the currents trends in today's tridimensional cell culture highlighting the necessity to turn hydrogels into cell culture templates.

Perspectives in 3D cell culture: tailored templates

Stem cells can self-organize up to a certain degree. After their inclusion at random within a hydrogel only a few of the initial aggregates give birth to functional organoids. This led scientist to hypothesize that controlling the initial cell culture conditions was instrumental in the standardization of organoid generation. Three recent reviews from some of the top research teams in 3D cell culture point towards this direction[2–4] **(Figure 6)**.

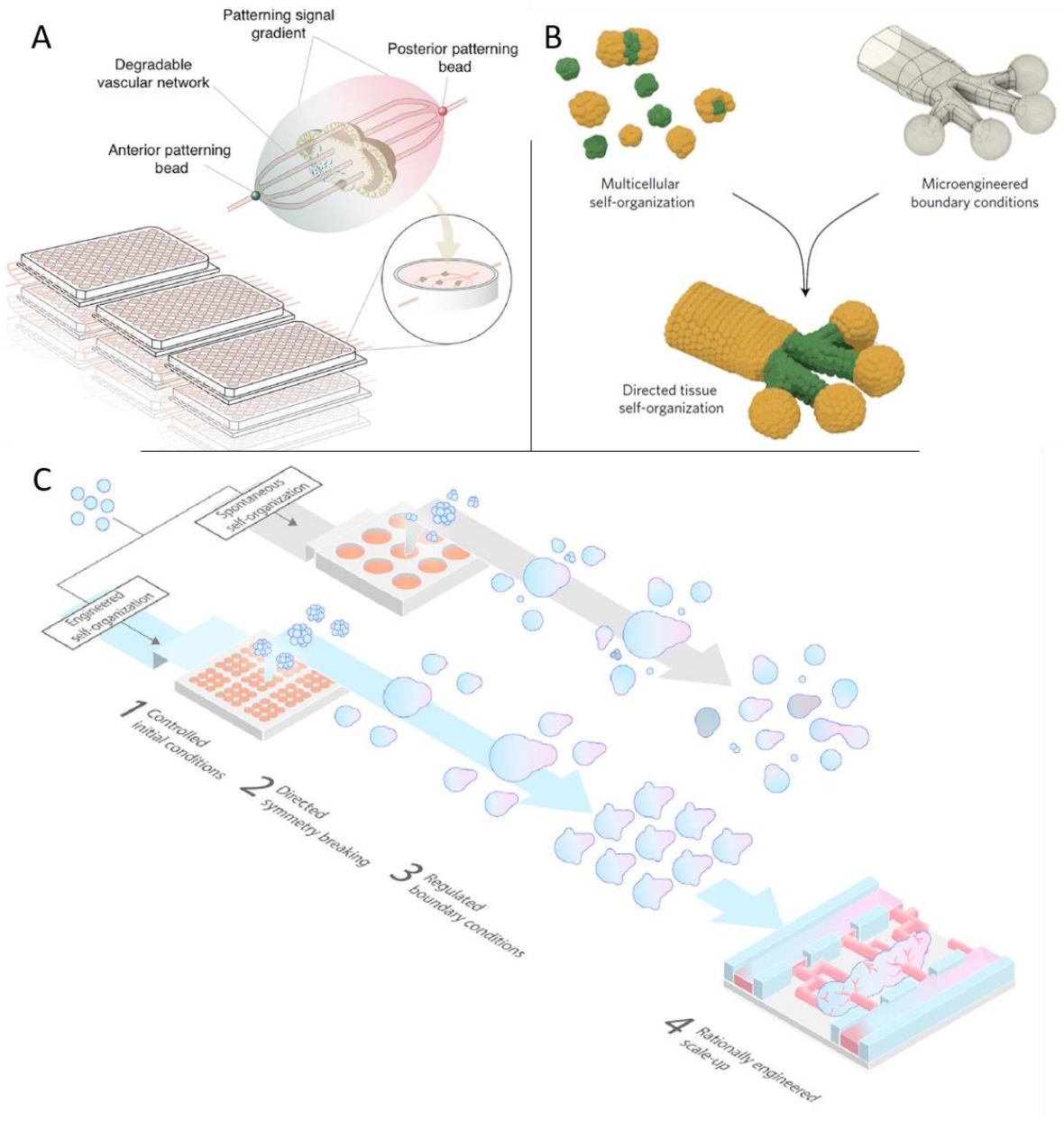

***Figure 6* | When hydrogel and micro-engineering meet: rationalizing organoid generation.**

Extracted from : **A,** Stem Cell Models of the human brain Development Madeline Lancaster 2018[2]. **B,** Convergence of microengineering and cellular self-organization towards functional tissue manufacturing Manuel Thery 2018[3]. **C,** Engineering Stem Cell Organization to build better organoïds M.P. Lutolf 2019[4]. Each figure shows the author's philosophy in improving and standardizing organoid culture. Note the multiple emergence of the concepts of boundaries, and patterning for symmetry breaking.

All three reviews agree that biomolecules and boundary conditions have to work in concert to guide the cell's self-organization. Interestingly, each author offers a different perspective in how to achieve greater complexity. Lancaster et al. suggests to implement flow and diffusing biomolecules to create an antero-posterior gradient. Thery and colleagues would use the cell's self-patterning potential and boundary condition to achieve symmetry breaking. Finally, Lutolf et al. suggest an integrated four step process with controlled initial conditions, human induced symmetry breaking, regulated growth then scale up with the help of perfusion.

To implement all the concepts introduced above, hydrogels must be shaped and tethered with biomolecules in a spatially controlled manner. In short, hydrogels must depart from homogeneous matrixes to become heterogenous biomimetic or bio-tutoring templates.

The most basic methods to achieve such feats rely on the fabrication of stamps with micron sized-features to mold hydrogels or ink them with proteins[13]. These techniques are seeing use within laboratories however they have one important drawback: hydrogels are often too brittle to sustain physical contact.

Light, on the other hand, can initiate a wide array of chemical reactions to alter the structural or chemical properties of materials without exerting a mechanical strain. The next half of this introduction illustrate the principles and applications of light-matter interactions in the field of hydrogel engineering.

Altering mater with light

Upon absorption of a photon with the adequate wavelength (or two photons with the double of the wavelength), molecules composing the material can become unstable and react with other agents in the vicinity (**Figure 7**). The range of reactions is very large including but not restricted to polymerization, grafting and degradation. In the case of hydrogels, the absorbing molecules can be the mesh itself or photo-initiators diluted in or covalently bound to the structure.

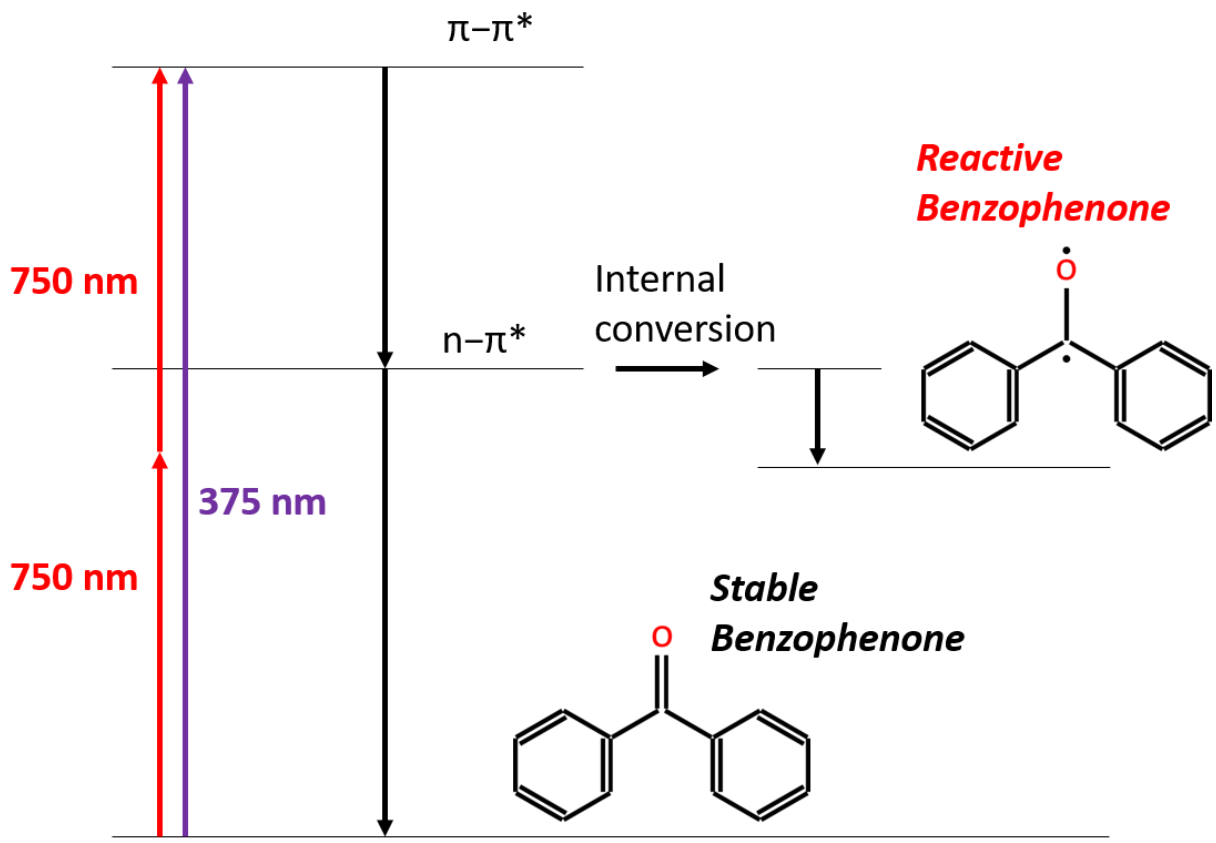

***Figure 7* | Principles of light-matter interaction with the oversimplified example of benzophenone.**

A Jablonski's diagram showing how the photo-initiator benzophenone can go from stable to reactive by absorbing one ultraviolet (purple) or two infrared (red) photons. Note that the molecules goes through successive relaxations and internal conversions (blacks arrows) before reaching the reactive state.

Light-induced chemical reactions are a powerful tool by themselves, yet it is the structuration of such illumination that makes hydrogel tailoring possible. In the recent years, spatially controlled illumination appeared as a very promising candidate to locally alter a hydrogel's shape and chemical display.

Thanks to three major technologies, subparts of a material can be irradiated while the remaining area stays intact **(Figure 8)**.

In raster-scanning techniques, two-photon laser beams focalize the illumination at a single focal point that is scanned along a tri-dimensional shape **(Figure 8 left)**. This process relies on the simultaneous absorption of two photons by the molecules of the sample which requires nano-to femtosecond laser pulses. Each photon brings half of the activation energy so that the material is only altered in a small voxel at the focal point. The tridimensional shape is then produced by illuminating voxel by voxel giving exquisite flexibility and resolution at the expanse of being increasingly time consuming as the scale expands.

On the other hand, photomasks offer the most scalable yet least flexible solution **(Figure 8 right)**. They consist in a layer of absorbing material with transparent patterns letting light through in specific areas. In combination with an illumination source, photomasks shape light only in two dimensions.

Digital micromirrors devices are arrays of micron-scaled mirrors that can be independently controlled to reflect light onto the sample ('ON' position) or outwards ('OFF' position) **(Figure 8 middle)**. They offer a digital alternative to photomasks since arbitrary bidimensional shapes can be projected but they also have unique capabilities. First, patterns can change dynamically during the insolation, second, the local intensity can be modulated on a 8-bit basis since each mirror can flip 'ON' and 'OFF' at high (10KHz) rates. However, when the scale increases beyond the boundaries of the device, this methodology encounters the same type of limitations as raster scanning methods.

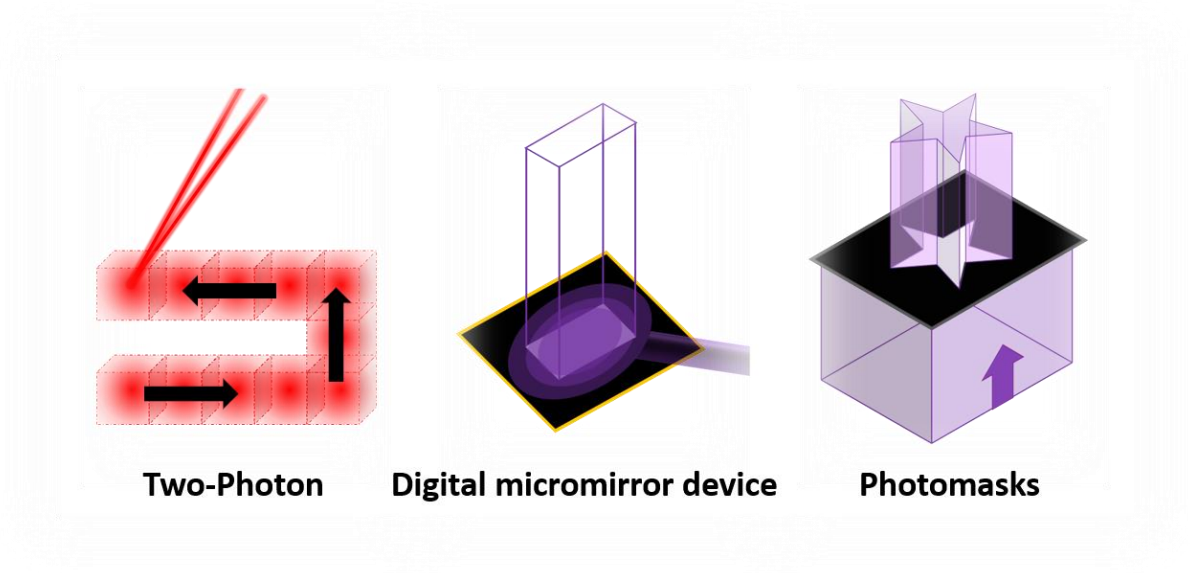

Figure 8 **| *The three major light structuration methodologies.***

Two photon lasers (in red) scan the sample in all three axes, illuminating voxels in rapid succession to form a shape. Digital micromirror devices (black with gold trim) can reflect light on a pixel basis to create extruded bidimensional shapes. Photomasks (black with silver trim) are crafted to let light pass through in distinct area forming extruded shapes.

Dedicated photo-chemistries go in pair with light structuration. Together they synergize into light-based hydrogel-tailoring solutions:

Photochemistry: a straight path to hydrogel tailoring

First and foremost, hydrogel gelation can be light-triggered with photo-initiators when vinyl groups are present at the extremities of the precursor[8]. Upon irradiation, the photo-initiators absorb the light and form radicals: highly reactive species that can start crosslinking. Radicals are especially reactive towards dense electronic concentrations making vinyl moieties (acrylate, methacrylate …) ideal crosslinking targets. The activated vinyl extremities of the precursors then react with other molecules leading to gelation. Most synthetic and naturally derived precursors can be found with vinyl modifications which makes this method very popular[31–34]. Additionally, one can stop the insolation at any time to tune the crosslinking rate and thus the hydrogel's stiffness, several scientific article can attest for this[35–37]. The works of Yin and colleagues in 2018 represent one of the most advanced attempts at utilizing this later concept for cell culture[35] **(Figure 9)**. They combined stereolithography, digital micromirror devices, and photopolymerizable chemistry together to obtain an automated hydrogel structuration platform. A moving stage in the polymerization chamber controlled the polymerization in the Z axis while the micromirror array ensured control over the two remaining dimensions **(Figure 9 A)**. The dynamic insolation capacities of the platform allowed parts of the resulting structure to receive ultra-violet light for prolonged periods and thus led to a higher local crosslinking rate. With this tool, they created hydrogel tubes with soft and stiff sides. When cells were seeded upon such structures, they naturally migrated towards the stiffer parts **(Figure 9 B)**.

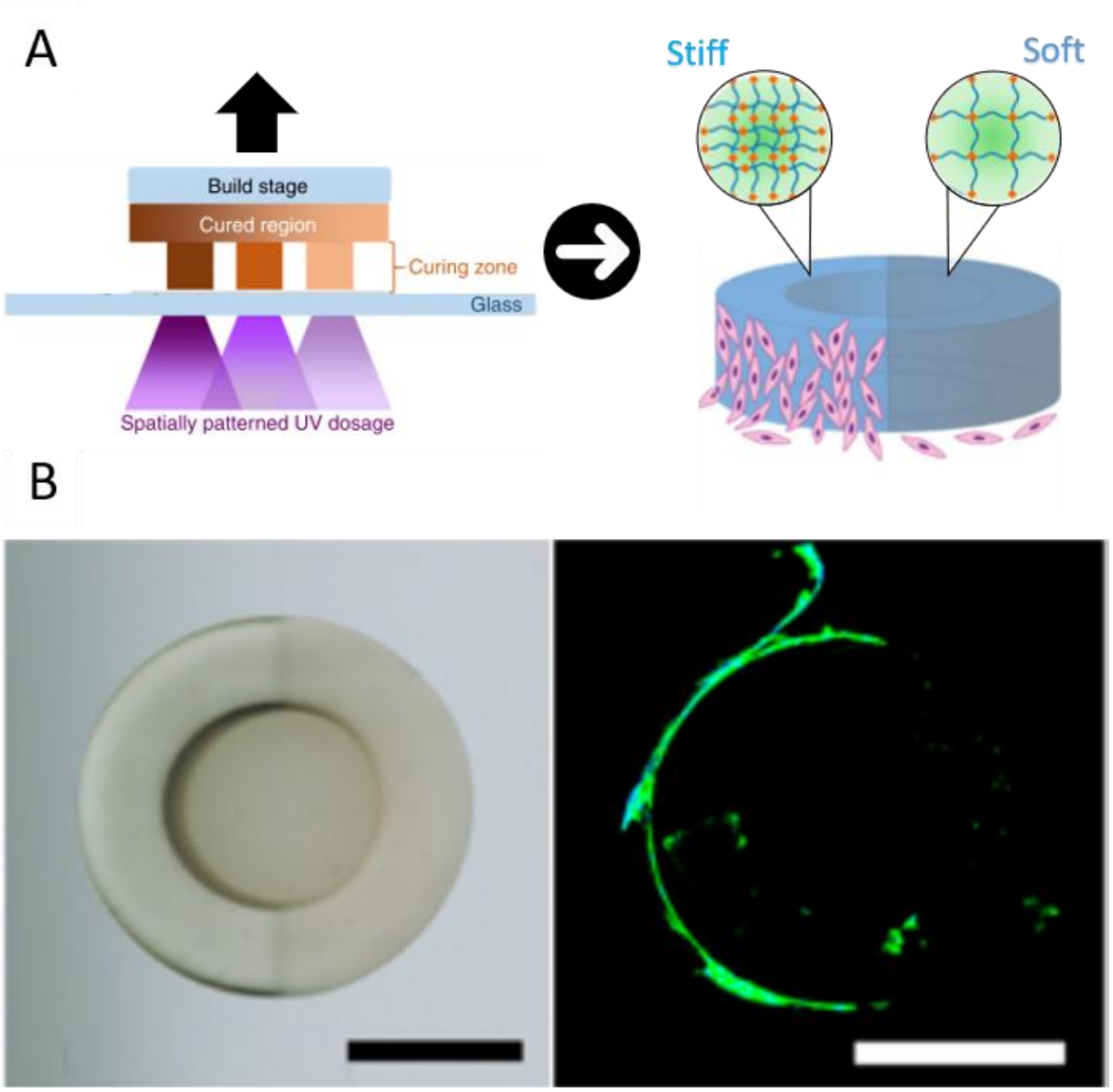

Figure 9 **| *Using light structuration to photo-cure hydrogel precursors.***

Adapted from : Orthogonal programming of Orthogonal programming of heterogeneous micro-mechano-environments and geometries in three-dimensional bio-stereolithography Hang Yin Nature Communications 2018[35]. **A,** Here a digital micro mirror is combined with stereolithography to photopolymerize hydrogel structures. The Ultra-violet dose can be tuned during the building process allowing the production of objects with stiff and soft parts. **B,** From left to right : bright field microscopy images of the resulting hydrogels with a stiff (right) and soft (left) part. Confocal Fluorescence microscopy images of cells colonizing the hydrogels with actin (green) and nucleus (blue).

While light-based additive manufacturing is solely achieved through photo-initiators and chemical modification, there are also subtractive methods which offer more flexibility. Hydrogel degradation is achieved through high-intensity biphotonic laser pulses[6,38–40] while chemical modification[6,9,16,41,42] can unlock this reaction under gentler conditions. In the first case the very high energies delivered to the sample at the focal point of the laser beam, ionize and liquefy the mesh in short timescales[6]. Due to the use of two-photon illumination, this technique is well suited for the generation of channels within

hydrogel layers. The pioneering work of Sarig Nadir and colleagues in 2009 attests for that[40]: with nano and femtosecond laser pulses, they carved micron-sized channels within poly-ethylene glycol hydrogels and were able to guide neurite outgrowth. Despite their chemical diversity, many hydrogels can undergo laser-based micro ablation[6]. As a consequence, other research laboratories adapted the technology to their material of choice in order to create channels or microniches[6,38–40,43] **(Figure 10)**.

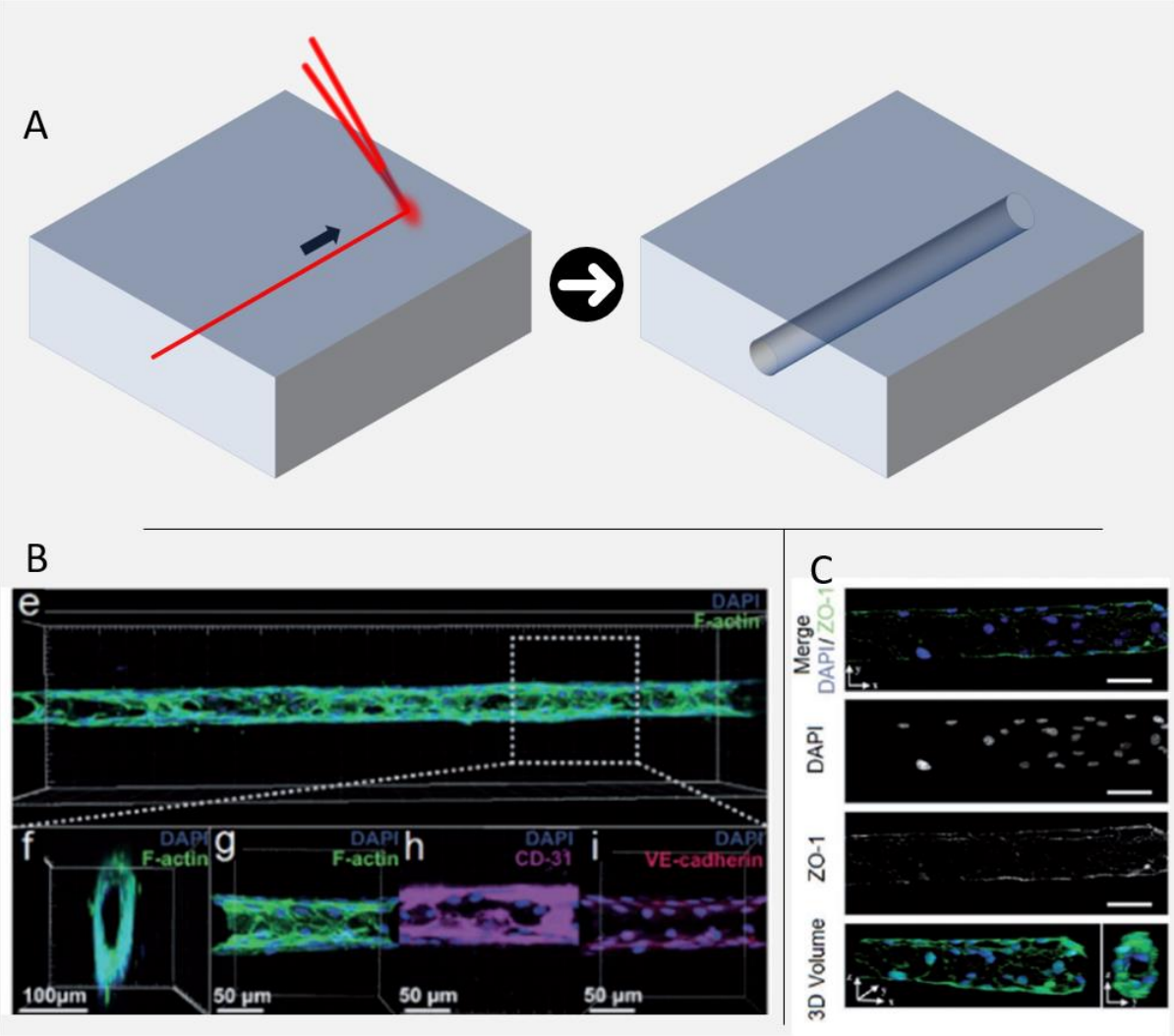

Figure 10 **| *Using light structuration to photo-degrade hydrogels.***

Adapted from: Fundamentals of Laser-Based Hydrogel Degradation and Applications in Cell and Tissue Engineering Shantanu Pradhan Advanced HealthCare Materials 2017[6]. **A,** In laser assisted hydrogel degradation a infrared two-photon beam (red) is scanned inside the mesh of a cured hydrogel (blue) the gel is quickly degraded at the focal point leading to the generation of channels. This very straightforward process has been adopted by various laboratories. **B,** Vascular networks realized by Lutolf et al. **C,** Vascular networks realized by West et al.

In the presence of cells, photo-degradation speed can be a limiting factor especially when one need to raster-scan the sample[39]. In such cases, chemical modification can facilitate hydrogel degradation[9,16,41,42]. Orto-nitrophenyl moieties break upon visible light irradiation and, when included within the precursor chain, allow for quicker and gentler degradation conditions. In 2014, Tsang and

colleagues synthesized photodegradable hydrogels through the combination of gelatin precursors and linkers that incorporated photodegradable nitrophenyl functionalities at each extremity[42] **(Figure 11)**. The resulting hydrogels did not require two photon illumination and could be quickly degraded using simple photomasks. They carved grooves within these light-sensitive compounds **(Figure 11 B)** in order to align cardiomyocytes thus improving their functionality.

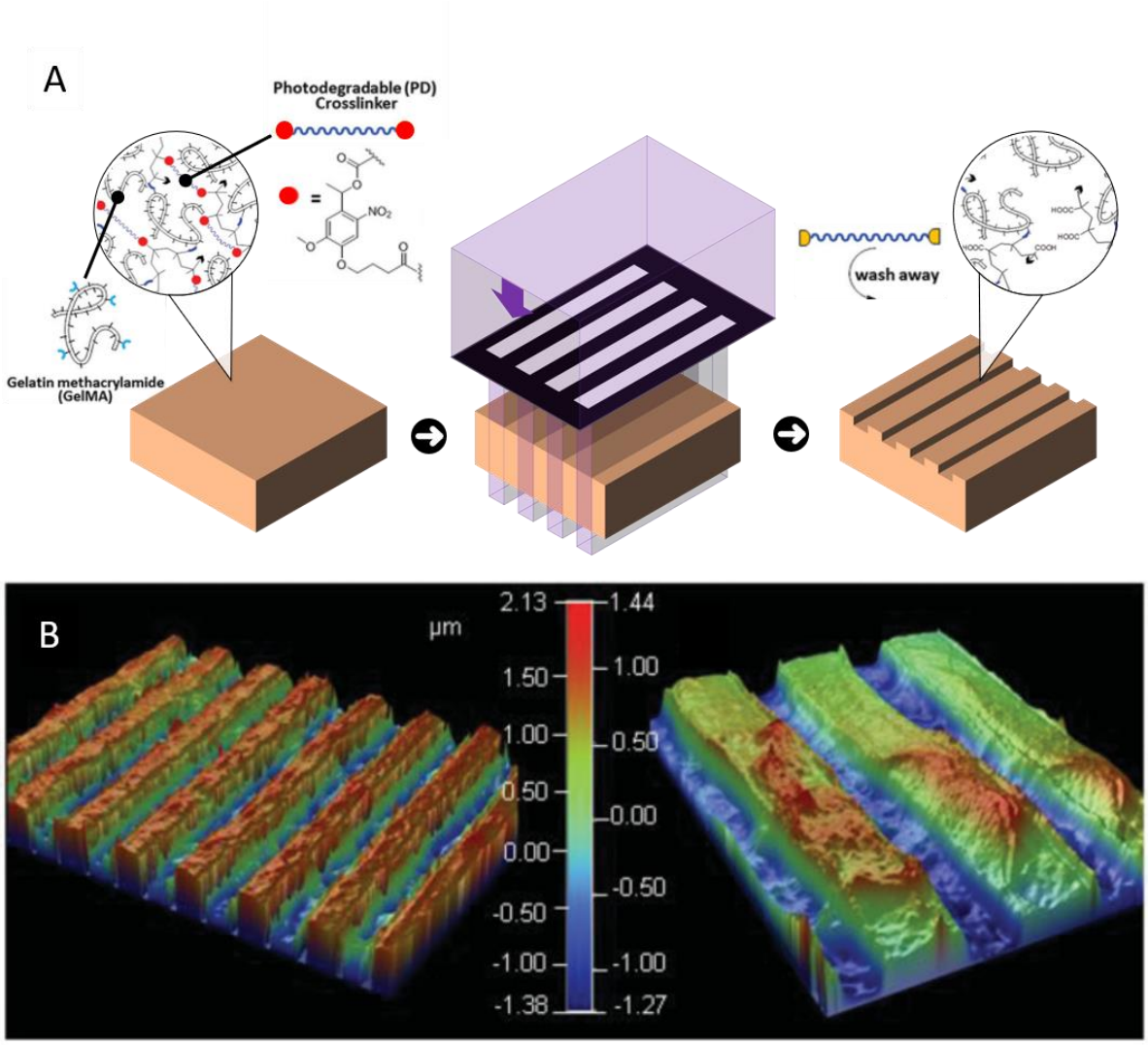

Figure 11 **| *Chemically engineered hydrogels for photodegradation.***

Adapted from: Facile One-Step micropatterning using photodegradable gelatin hydrogels for improved cardiomyocyte organization and alignment Kelly MC Tsang Advanced Functional Materials 2014[42]. **A,** Design principle for photodegradable hydrogels : gelatin methacrylate (pink) is crosslinked with a photodegradable spacer (blue) containing ortho-nitrophenyl moieties (red points). The resulting hydrogel can be photodegraded through ultraviolet irradiation (purple) using a photomask (black with silver trim). **B,** micro-structured hydrogels: profilometry reconstruction of the resulting topographies.

Additive and subtractive manufacturing cover the structuration needs for hydrogels however spatial tethering of biomolecules is also required. Light-based hydrogel functionalization exclusively relies on chemicals that can be specifically designed biomolecules[16,44,45] or more all-purpose photo-linkers[25,46,47].

In the former case, biomolecules of interest are chemically modified with functionalities allowing them to graft and/or detach from the hydrogel upon light irradiation. This represents a precise and orthogonal approach to hydrogel functionalization that often requires the hydrogel precursors to include the chemical moieties that go in pair with the designed biomolecules. This is perfectly exemplified in the recent works of Shadish et al in 2019[44] **(Figure 12)**. In this paper they created mutant conjugates of biomolecules with Sortase reactive extremities. The Sortase enzyme then substituted the reactive ends with click-based functionalities incorporating photograftable or photolabile groups **(Figure 12 A)**. The hydrogels precursors were also chemically modified with complementary chemical functions to support the tethering of biomolecules. In fine, they were able to photo-graft and/or photo-release the grafted biomolecules from the gels using either photomasks or two-photon illumination set-ups **(Figure 12 B)**. Overall, the sortase enzymatic substitution is elegant in that it provides a site-controlled and modular platform to functionalize biomolecules with any of the linkers developed by the group.

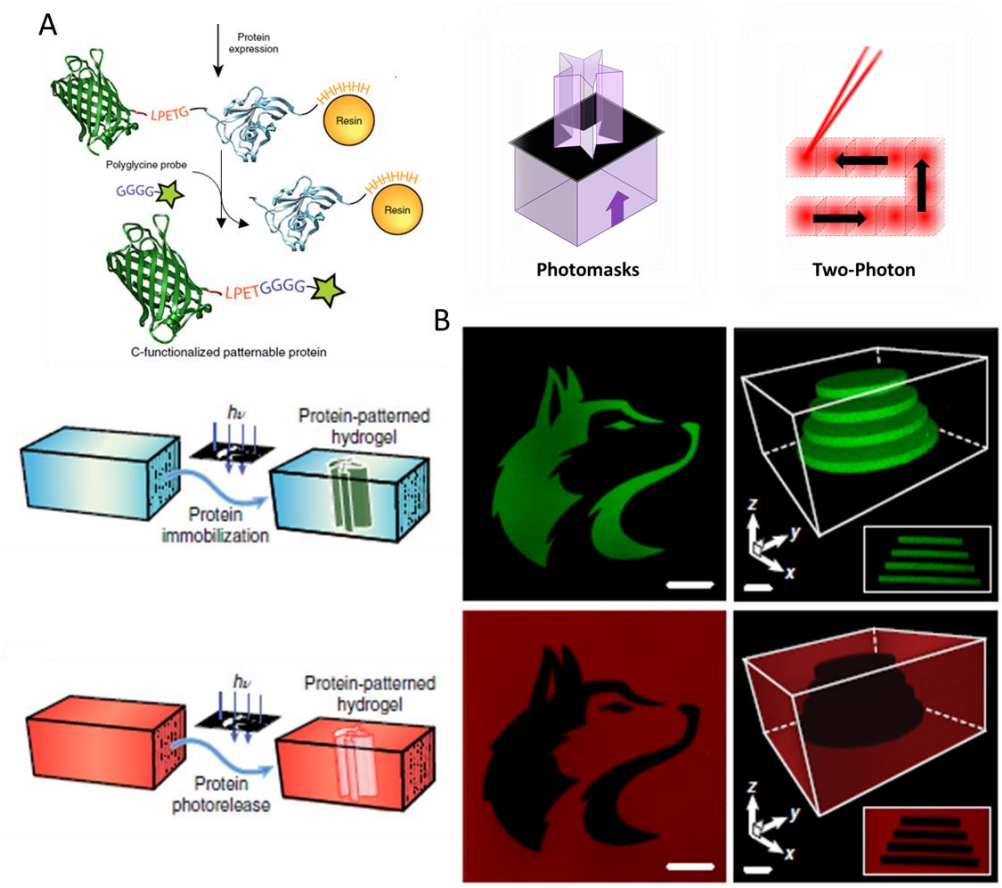

Figure 12 **| *Chemically engineered hydrogels for dynamic and spatial presentation of biomolecules.***

Adapted from: Bioactive site-specifically modified proteins for 4D patterning of gel biomaterials, Cole Deforest Nature Materials 2019[44]. **A,** Protein functionalization workflow: the target protein (green) is expressed with a linker sequence, the Sortase enzyme (blue) and a poly-histidine tag for immobilization. The photolinker-containing probe displays a poly-glycine tag which is a cleavage sequence for the Sortase. The protein is then C-grafted with a pho-tolinker for light based decoration.**B,** Epifluorescence microscopy images and 3D reconstructions of hydrogels decorated with the functionalized proteins through photoimmoblization (green) of photorelease (red) using either mask or two photon set-ups.

There are also more generic photo-linkers which do not require extended know-how in organic chemistry. Sulfo-SANPAH, Sulfo-LC-SDA and acryl-poly(ethylene-glycol)succinimidyl-valerate are among those. These hetero-bifunctional linkers incorporate radical or photo-reactive moieties which can graft onto hydrogels upon photo-initiatior activation. On the other end lies an activated ester which reacts with free amines contained within the protein's lysins and N-terminus. In short, one extremity binds to the gel under irradiation while the other binds the protein. Photo-linkers will be described in more detail later in this manuscprit as they were extensively used during the course of this work.

In retrospect, photo-initiators support most of the light-based hydrogel tailoring state of the art. Some are incorporated directly in the precursors or photo-linkers to respectively break and graft upon irradiation. Others are free to enable vinyl-linker grafting and gelation. The use of photo-initiators is often debated in the tridimensional cell culture community as the generated free-radicals are cytotoxic. Thus, many of the ongoing efforts are gearing towards cytocompatible photoreactions. Another way around is to let go on the cytocompatibility and tailor the hydrogels before cell seeding. Embracing that workflow, one can take advantage of the very unique properties of radical reactions such as oxygen inhibition and benzophenone photo-chemistry.

Oxygen and benzophenones

Oxygen inhibition of polymerization is a mechanism through which radicals react with oxygen instead of precursors stopping or hindering their assembly into networks. In practical terms, unless one removes oxygen from the reaction chamber, polymerization is impossible close to a gas-permeable material (such as silicone). Well known from the microfabrication and additive manufacturing specialists, this reaction in usually seen as detrimental. Nonetheless, it is possible to control oxygen inhibition and take advantage of it : many examples can be found in the litterature[24,48–50]. In a recent article, Tumbleston and colleagues[24] introduced the continuous liquid interface process **(Figure 13)**. This additive manufacturing method, uses oxygen flow through a gas permeable window below the polymerization tank in order to produce tridimensional shapes from top to bottom in a continuous fashion rather than layer by layer. A dynamic imaging unit projects slices of the object synchronized with the stage elevation while oxygen inhibition ensures that a continuous liquid interface separates the polymerized bulk from the window. This work also provided a comprehensive study of the oxygen inhibition as a function of gas content and photon flux both of which were crucial in the success of this work **(Figure 13 A)**.

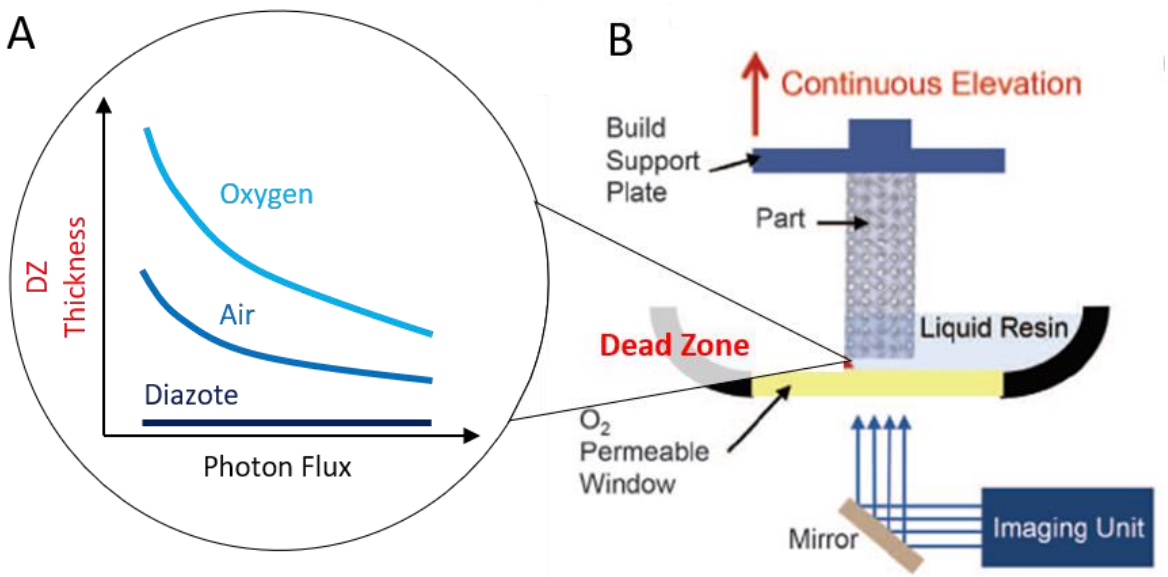

Figure 13 **| *Oxygen inhibited stereolithography*.**

Adapted from: Continuous liquid interface production of 3D objects J. M. Desimone Science 2015[24].**A,** Characteristics of the oxygen inhibition deadzone as a function of photon flux and gas content **B,** Schematics of the stereolithography set-up used by the team.

In addition to inhibition, oxygen also plays another, less well known, role. In conjunction with benzophenones oxygen can induce the photodegradation (which we call photo-scission) of polymers[22,51]. Benzophenones are unique photo-initiators in that they can abstract hydrogens from a

carbon backbone upon irradiation[23] thus forming a carbo-radical **(Figure 14 first line)**. Di-Oxygen can then add onto the carboradical forming an hydroperoxyl group which initiates a chain breaking reaction **Figure 14 second line)**. The exact mechanisms by which poly(ethyleneglycol) is degraded is not known however hypothesis can be drawn from the work of pinto et al[51] who worked on the photoscission of polystyrene. The hydroperoxyl group may either break upon irradiation forming an oxy-radical. This oxyradical will then react with another of its kind breaking one chain while the other turns into an alcohol **(Figure 14 third and fourth line)**. Alternatively, the hydroperoxyl can decompose, breaking the chain and releasing water in the case of poly(styrene) **(Figure 14 fifth line)**.

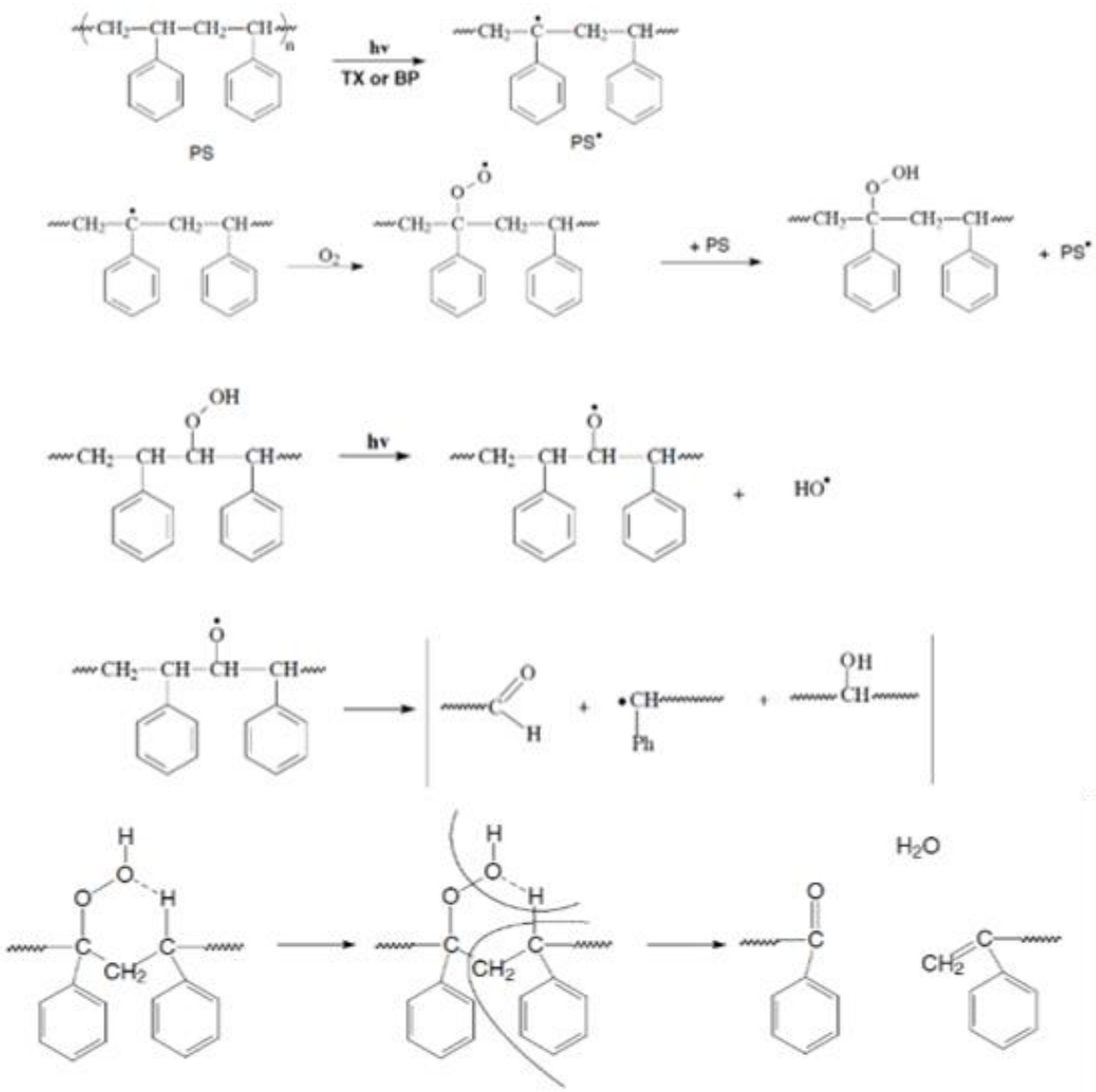

Figure 14 **| *Oxygen induced photo-scission.***

Left Panel, Mechanism for the photodegradation of poly-styrene extracted from Photodegradation of Polystyrene Films Containing ultra-violet-Visible Sensitizers Leticia Pinto Journal of Research Updates in Polymer Science 2013[51].

The photo-scission of poly(ethylene-glycol) saw application in the field of cell culture with the light induced molecular adsorption of proteins[22] **(Figure 15)** The technology emerged within our team and consist in photo-scissionning anti-adhesive poly-ethylene glycol layers with a benzophenone-based photo-initiator and a digitally modulated illumination field **(Figure 15 A)**. Following this step, proteins can adsorb on the degraded areas of the anti-adhesive layer and subsequently let cells attach on the patterns generated **(Figure 15 B)**.

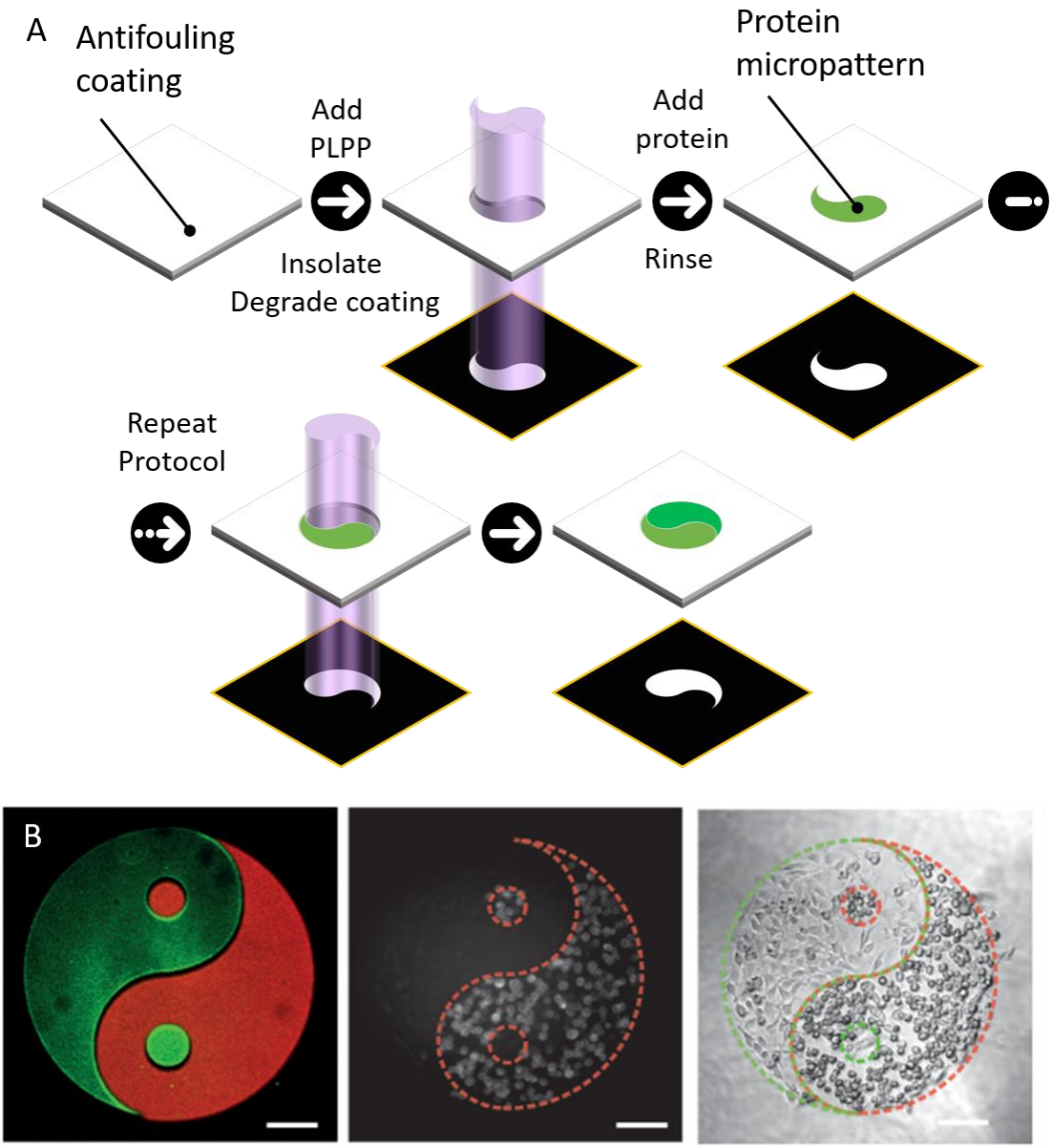

***Figure 15* | Using photo-scission to tutor cell adhesion.**

Adapted from: Multiprotein printing via light induced molecule adsorption. V. Studer Advanced Materials 2016[22]. **A,** Surface functionalization workflow: ultraviolet light is used in conjunction with a photo-initiator to locally erase a bio-inert poly-(ethylene-glycol) layer. Proteins can then adsorb onto the surface and the process can be repeated. **B,** Control of cell adhesion and coculture from left to right : epifluorescence microscopy image of a glass slide functionalized with two different proteins. Epifluorescence microscopy image of the first cell population. Brightfield microscopy images of the two co-cultivated cell types.

We initially thought that photo-scission was solely restricted to nanoscale poly-(ethylene-glycol) brushes but we wanted to explore whether this reaction could be successfully transferred to micron-scale hydrogel layers.

Closing thoughts

It is within this context that my work started: a hefty amount of solutions existed, most of them already operational among the pioneering laboratories. The general trend for those solutions was (and still is): i) to improve the biocompatibility of the chemical reactions through feats of chemical engineering. ii) to ensure complete design flexibility with two-photon illumination or stereolithography. I deliberately chose not to follow these trends: in my view, we had not enough know-how chemistry-wise and platform developments would have led us astray from applied science. I saw this restriction as an opportunity to breed creativity and rely on the unique traits of our methodology (benzophenone/oxygen chemistry, digital/widefield/quantitative illumination) to yield original results. I also took time to explore what the other teams where doing when they lacked the all-powerful platforms such as those introduced above. Thus, each of the following experimental chapters will start with a brief review of commonplace strategies to shape (chapter1) and decorate (chapter2) hydrogels. Doing so we highlighted the fact that most 3D cell culture assays can be performed with rather simple shapes and decoration patterns.

Structuration appears to be of higher demand than decoration as it is an easy way to assemble spheroids, create vasculatures and promote cell alignment. In the following part we try to tackle the challenge of shaping hydrogels in three dimensions with a bidimensional widefield projection system.

Chapter 1
Mastering Z

Introduction

Organs display complex shapes: from the stratified layers of skin, through villus found in the intestine up to the kidney tubules. Although cells can self-organize up to a high degrees of complexity[1] it is thought that no further hierarchy can emerge without boundary conditions[2–4]. To recapitulate the features of organs it is thus necessary to create tridimensional templates that can tutor the cell's self-organization.

As we previously mentioned, molding is the traditional method to shape hydrogels but it's not the only one. Flow focusing and meniscus pinning are also in use within pioneering laboratories. The simplicity of these protocols allowed them to succeed in transferring into biological research which makes them a great source of inspiration.

Accordingly, the goal of this introduction is to present these simple techniques and what they achieved before diving into the experimental section. This will help in identifying what kind of objects are highly sought after while also highlighting the importance of controlling the local thickness when shaping hydrogels.

Molding

In the absence of turn-key solutions, biologists have devised original ways to shape hydrogels. When the gel can withstand it, molding remains the most straightforward option[52–57] **(Figure 16 A)**. Dingle and colleagues[57] molded agar-agar into cups to standardize the culture of neuro-spheres. Interestingly, neurons and glial cells formed spheres that synthesized a laminin rich matrix while inhibitory and excitatory circuits were observed **(Figure 16 B)**.

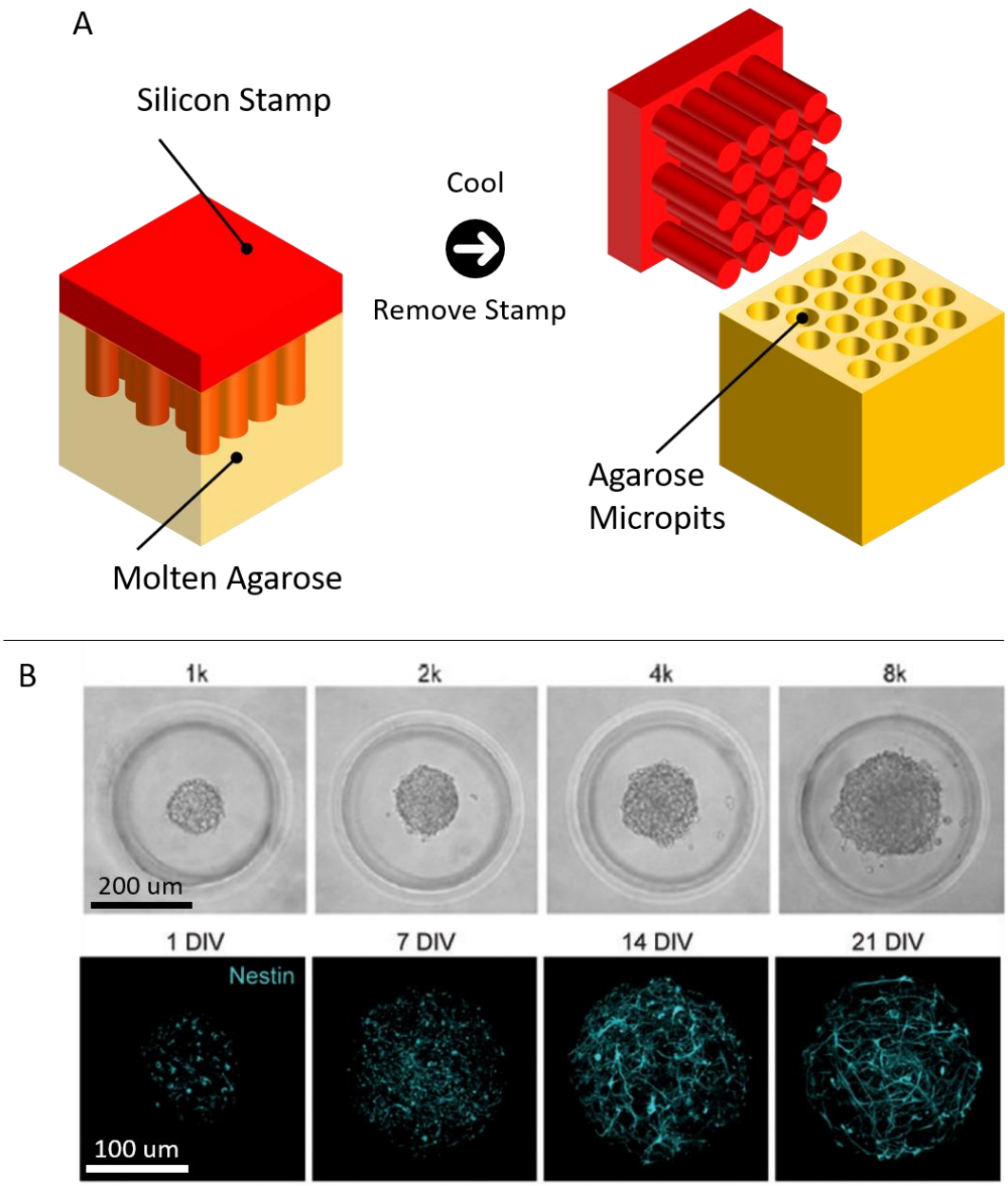

Figure 16 **| *Molding Agar to produce cortical neurospheres.***

Adapted from: Three dimensional neural spheroid culture an in vitro model for cortical studies J. Kauer, D. Hoffman Kim Tissue Engineering 2015[57]. **A,** Schematics illustrating the generation of agar (yellow) micropits from a silicone stamp (red) **B,** Brightfield microscopy images and epifluorescence images of the resulting neurospheres tagged for nestin. Note the size increases with cell seeding count and the spheres grow in size over time eventually forming axonal networks.

In another example Rivron and colleagues[56] generated blastoïds (blastocysts mimics) using the same micromolded agar templates **(Figure 17 A)**. To successfully produce standardized blastoids they cocultivated trophoblast and embryonic stem cells together. The adequate cocktail of differentiation factors led the cells to self-organize with the embryonic cells catering inside a hollow sphere formed by the trophoblasts (**Figure 17 A-B)**.

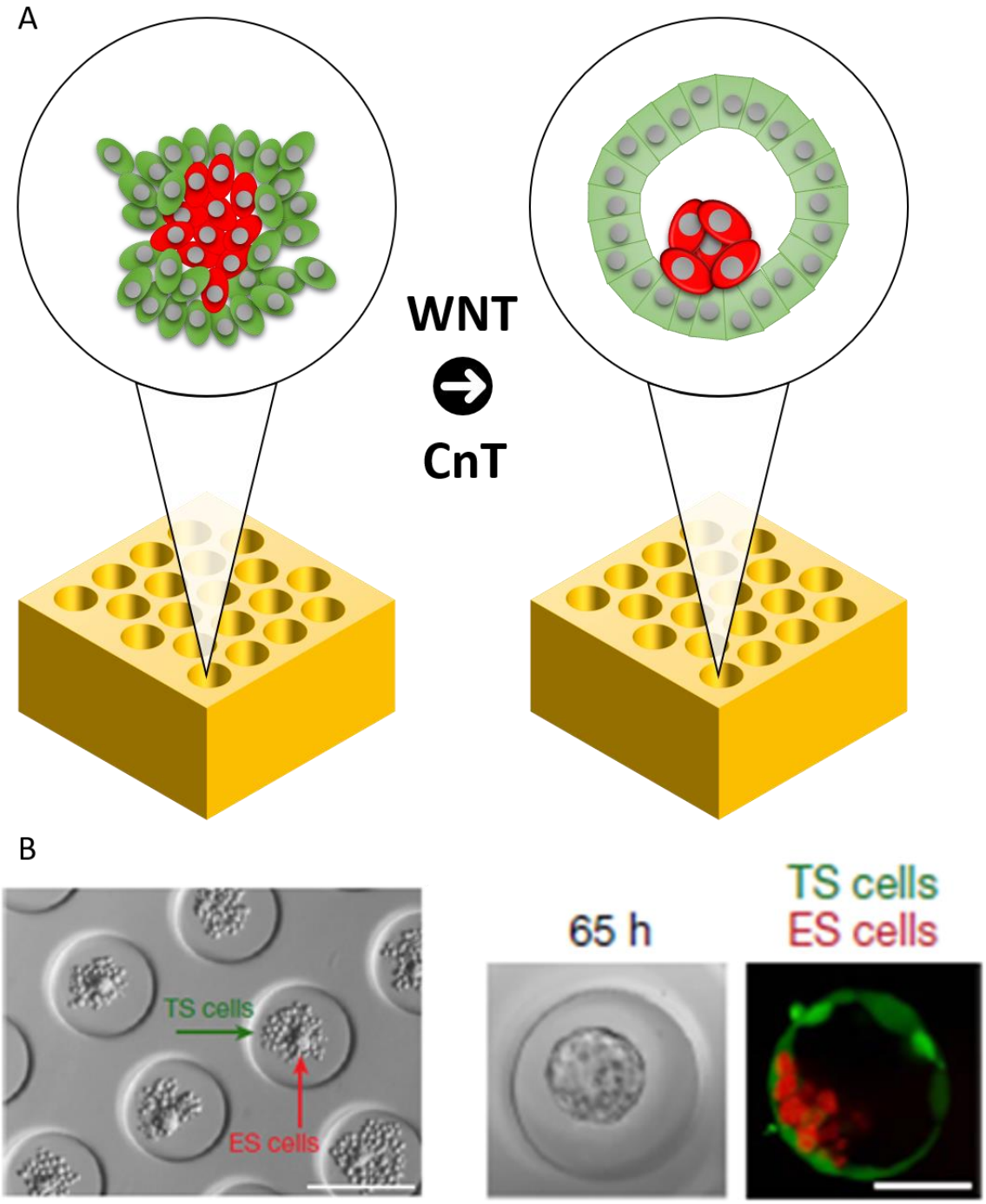

Figure 17 **| *Molding Agar to produce blastoïds.***

Adapted from: Blastocyst-like structures generated solely from stem cells N. Rivron Niels Geijsen Nature 2018[56]. **A,** Schematics illustrating the production of blastoïds with agar (yellow) trophoblastic stem cells (green) and embryonic stem cells (red) **B,** Brightfield microscopy images and epifluorescence images of the cells growing in the wells before and after blastoïd's self assembly.

With needles as a mold, Alimperti et al[52] created collagen tubules and studied the inflammation process using a coculture of fibroblast and endothelial cells **(Figure 18)**. They optimized the ratio of endothelial to mesenchymal stem cells observing that only a handful of configurations led to the formation of a leak-tight tubule. Following the injection lipo-polysaccharide as a pro-inflammatory factor, mural cells detached from the vessels confirming a suspected fibrosis mechanism that was not yet observed in culture.

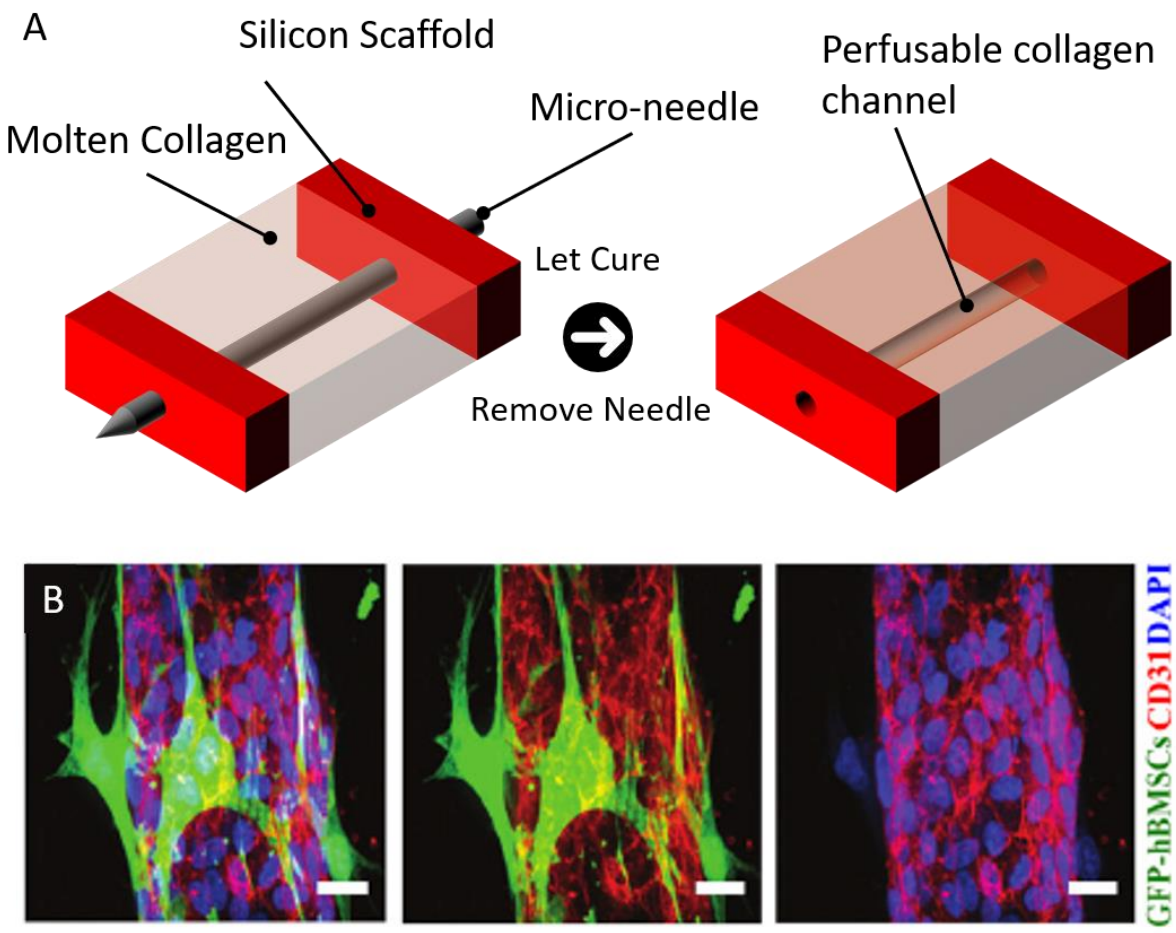

Figure 18 **| *Molding Collagen into tubules.***

Adapted from: Three-dimensional biomimetic vascular model reveals a RhoA, Rac1, and N-cadherin balance in mural cell–endothelial cell-regulated barrier function V Bajaj et Al. PNAS 2017.[52] **A,** Creating collagen (pink) tubules with a needle (gray) a silicone scaffold (red) **B,** epifluorescence microscopy image of the resulting vasculature showing mesenchymal stem cells (GFP, green) the cells nuclei (DAPI, blue) and CD31.

Aside from the examples presented above, readers may be interested in the works of Celeste Nelson's laboratory who use molding to study cell mechanics and auto organization[53,54]. Molding is truly the most straightforward and popular hydrogel structuration method; it is worth noting however that the fabrication of the stamp may not be as easy.

Flow Focusing

Hydrogel precursors come in liquid state until they cure, this gives the opportunity of shaping gels through control of the flow parameters[58–64]. Droplet generation is one way of using flow as a structuration modality, while less flexible than molding, it can achieve a very high throughput. Using flow-focusing microfluidics, it is possible to encapsulate single cells in microbeads at very high rates to study their development[58–62].

Traditionally cells are encapsulated in alginate droplets[60,61] that start gelling once in contact with a calcium-rich solution. By precisely controlling the temperature, other scientists adapted this protocol on Matrigel[59,62].

Recently, Laperrousaz et al used this technique to encapsulate single cancer cell lines in Matrigel microbeads to create clonal organoïds[59] **(Figure 18 A)**. Conveniently, the resulting acini like structures could be transfected and analyzed in high throughput using large-particle flow cytometry. This is in contrast with other structuration methods were the hydrogel is bound to a surface, here the cells and their micro-template can be handled with pipettes. As they show, cells aggregated into chaotic spheroids or acini-like organoids depending on the clone's genetic background **(Figure 19 B)**. Testing different cells lines also demonstrated that each lineage generated a specific ratio of each cancer phenotype.

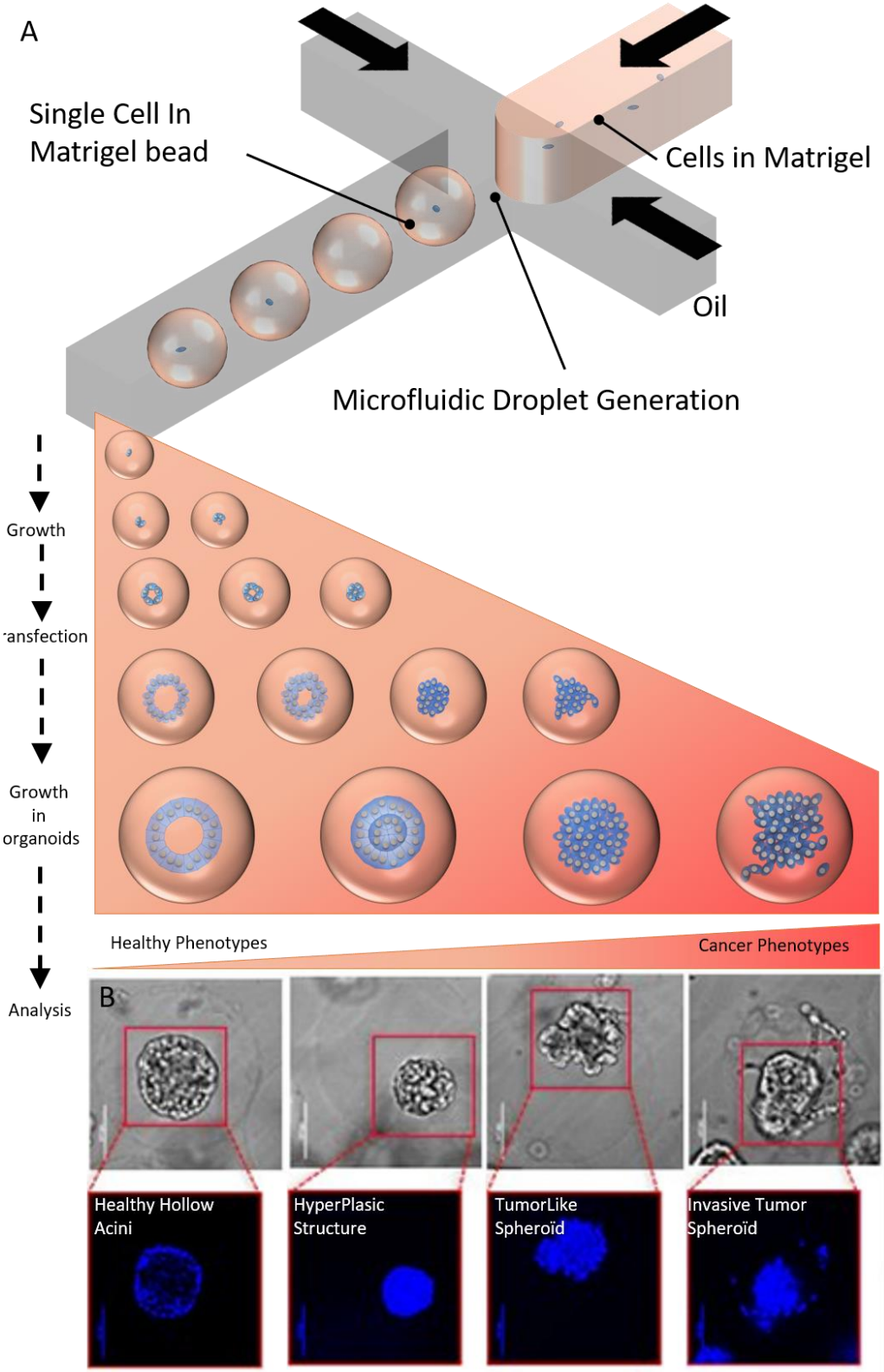

Figure 19 **| *Flow focusing to create clonal organoid capsules***

Adapted from Direct transfection of clonal organoids in Matrigel microbeads A promising approach toward organoid-based genetic screens X. Gidrol Nucleic Acids Research 2018[59] **A,** Experimental workflow displaying cell encapsulation by microfluidic flow-focusing, organoid culture in the microbeads , transfection and analysis **B,** organoid subpopulations as a function of cell lines.

By adjusting the flow rates, flow focusing can not only create droplets but also tubes[63,64]. In 2019, Andrique and colleagues used this principle to engineer functional mimics of blood vessel (vesseloïds) [64] **(Figure 20)**. They co-encapsulated endothelial cells and smooth muscle cells in alginate tubules using a double flow-focusing system **(Figure 20 A)**. The cells spontaneously grew into hollow tubules after one day in culture **(Figure 20 B)**. Conveniently the vessels could be subsequently perfused, they thus demonstrated that the vesseloïds were leak-proof, contractile and excitable.

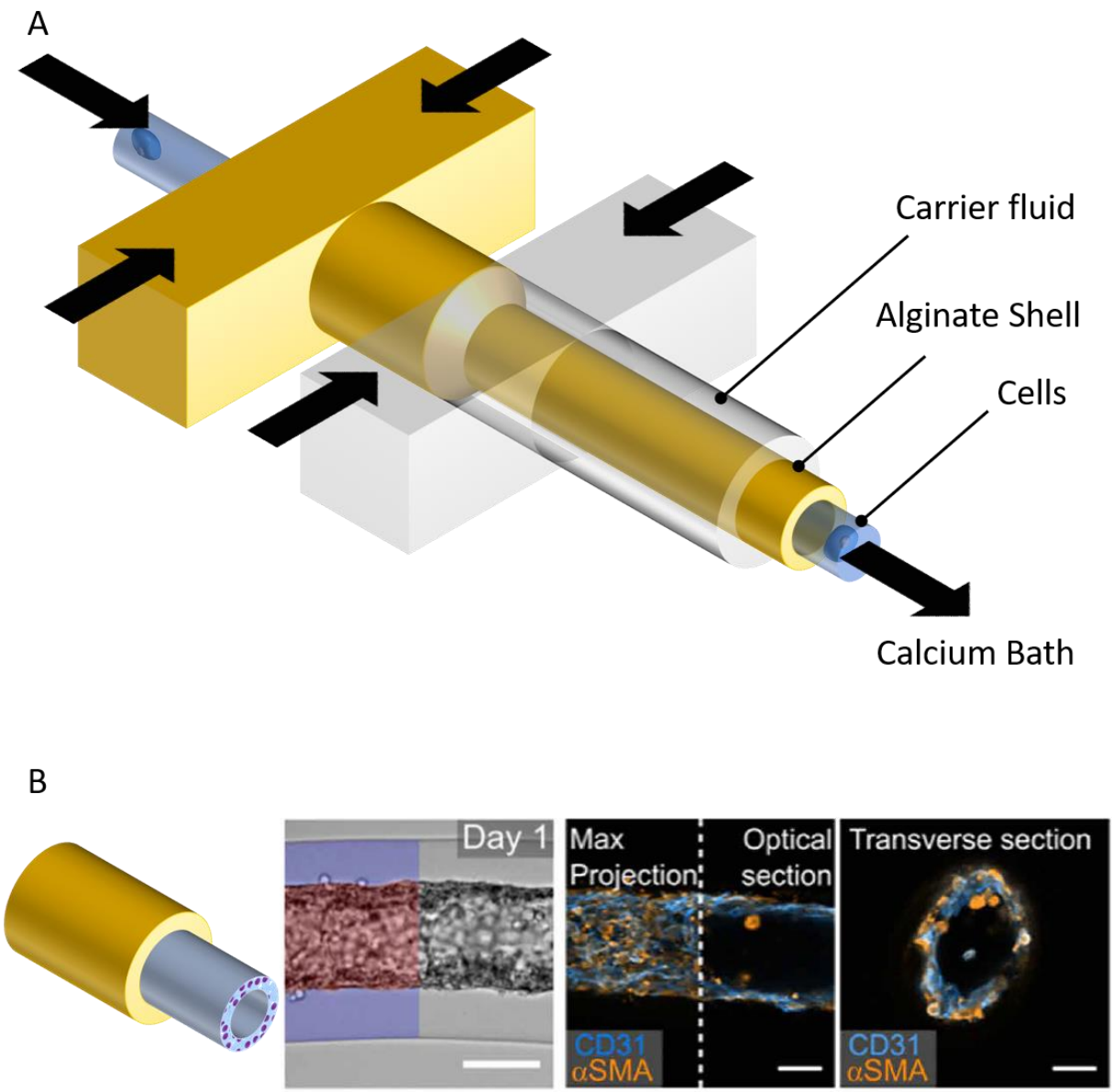

Figure 20 **| *Flow focusing to create tubules and vessels***

Adapted from : A model of guided cell self-organization for rapid and spontaneous formation of functional vessels P. Nassoy et al. Science Advances 2018[64] **A,** Experimental workflow displaying cell encapsulation in alginate (yellow) by flow-focusing, **B,** Schematic , brightfield and confocal microscopy images showing the resulting vesseloïds.

While minimalistic in terms of shaping, it's the throughput, ease of handling and analysis that set flow focusing apart from the other techniques.

Meniscus Pinning

Last but not least, it is also possible to use meniscus pinning to confine hydrogels to specific compartments of a device[65–69]. Upon injection in a chamber the flowing gel will be stopped by microfabricated hydrophobic obstacles and let to cure **(Figure 21 A left and right)**. This later creates a permeable interface where cells inside and outside the gel can come in contact and interact. Horizontal obstacles called phase-guides allowed Moreno and colleagues to create an in-vitro model of the blood-brain barrier in a 96 well plate format[69]. They differentiated dopaminergic neurons derived from induced pluripotent stem cells encapsulated in the hydrogel generating a vascularized and functional neural network **(Figure 21 left)**. Jeon et al used a similar device with vertical plastic posts to study tumor extravasation[65] . The device consisted of a central hydrogel channel separating two lateral compartments designed for flow. In the central hydrogel chamber, endothelial cells self-organized into vasculatures that connected each side **(Figure 21 right)**. In the device cancer started to behave as expected from their in-vivo counterparts they crossed the mural cells and went into the circulating flow.

Design simplicity and ease of use for non-experts make meniscus pinning devices particularly fit for industrialization and commercialization. Unsurprisingly, the two aforementioned devices are now sold by two companies respectively Mimetas (Netherlands) and AIM Biotech (United States of America). A growing number of scientific articles emerged from those devices[66–68].

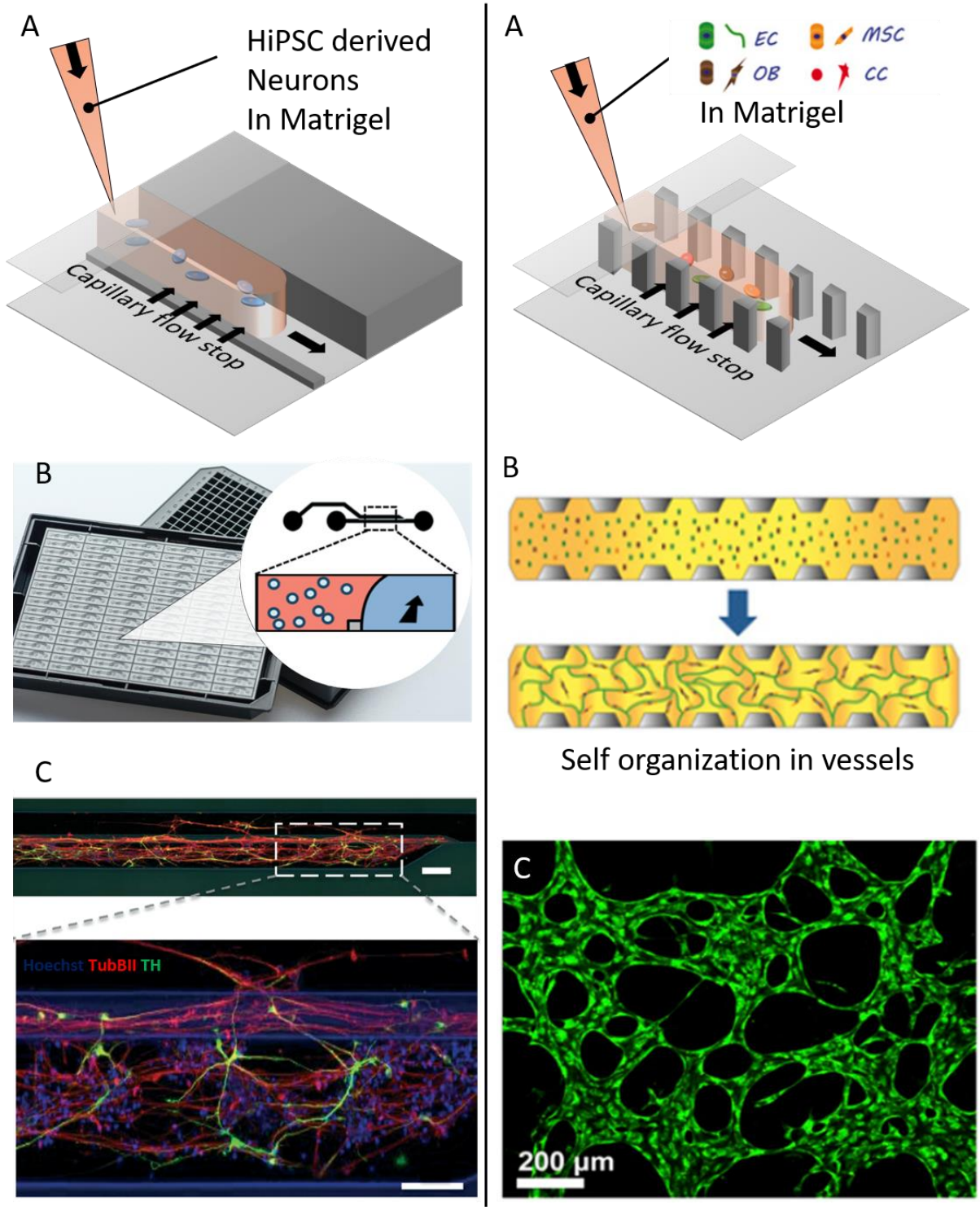

Figure 21 **| *Meniscus pinning as a tool to create hydrogel barriers and vasculatures.***

Left, cell culture compartments Adapted from P. Vulto Lab on Chip 2015[69]: Differentiation of neuroepithelial stem cells into functional dopaminergic neurons in 3D microfluidic cell culture. **A,** Technology principle: horizontal phases guides (grey) restrain hydrogels (pink) with embedded cells (light blue) in subparts of the channel allowing subsequent perfusion. **B,** design of the cell culture plate with 384 well format with 96 underlying microfluidic chambers. **C,** Confocal fluorescence microscopy images of the resulting in-vitro models with stem cell derived neurons labelling as follows: cells nuclei (Hoechst, blue), TubBIII (red) and TH (green). **Right Panel, vasculatures:** adapted from Human 3D vascularized organotypic microfluidic assays to study breast cancer cell extravasation R.D. Kamm PNAS 2015[65] **A**, Technology principle: vertical posts (grey) restrain hydrogels (pink) with embedded endothelial (green), mesenchymal (orange) , osteoblast (brown) and cancer cells (red). **B,** After seeding, the cells spontaneously assemble into vascular structures connecting each side of the chamber. **C**, epifluorescence microscopy images of the resulting vascular structures.

Discussion :

In the works presented above, hydrogel structuration mostly consists in simple shapes with little flexibility over experimental design. Wells and capsules, chambers and barriers, channels and vasculatures seem to be the three main building blocks employed in 3D cell culture. The former ensures a confined environment with controlled initial conditions (cell number, boundaries). The second defines functional subgroups within the sample to separate cell populations or perfusion from culture compartments. The latter supports the dynamic nature of the cell's micro-environment where molecules can quickly diffuse and gradients can be established.

One important lesson can be extracted from this review: when trying to build tridimensional cell cultures models, it is important to use the cell behavior to our advantage. In the works above the researchers obtained physiologically relevant data from those simple templates because the cell's self-organization did the rest of the structuration.

Light structuration is able to replicate those building blocks; however, it requires Z-control **(Table 2)**.

Using digital micromirrors alone can only produce extruded bidimensional shape out of photopolymerizable precursors. This can produce primitive structures but most of them are not sufficiently relevant building blocks **(Table 2 column 1)**. While complete Z-control appeared as a difficult initial goal **(Table 2 column 3)**, topographical polymerization seemed more feasible while also enabling a good degree of flexibility in the range of possible blocks **(Table 2 column 2)**.

In the coming experimental section, we test two hypotheses to control the local thickness of the gel:

First, frontal polymerization where the gel's polymerization starts from the surface a propagates along the Z axis. This reaction, while straightforward, will eventually show its limits both in terms of reproducibility and range of useable hydrogels.

In the second time, we will harness oxygen-inhibited polymerization where a controlled layer of oxygen will fix the gel's polymerization thickness depending on gas content and/or photon flux. This technology will prove much more robust making it a viable engineering process for cell culture.

	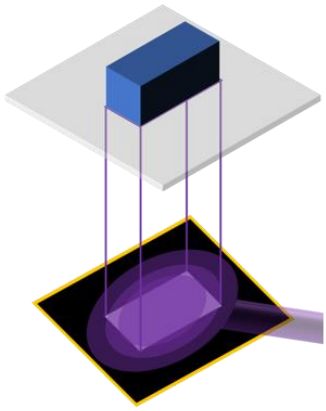 ***Extrusion level :*** *Thickness is that of the liquid.* *Allows for bidimensionnal shapes extruded along the Z-axis.*	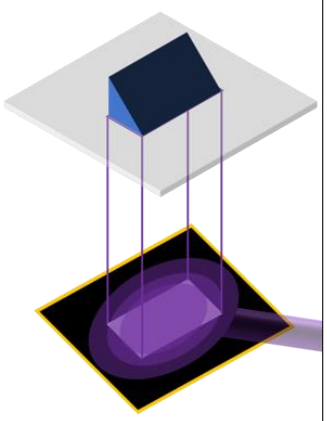 ***Topography level :*** *Thickness is under control.* *Allows for landscapes and open structures.*	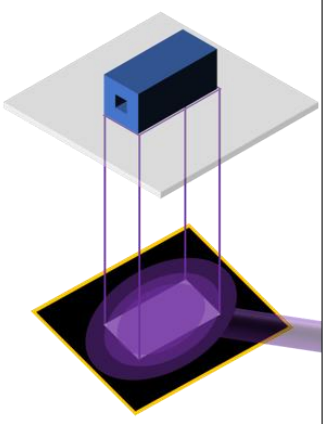 ***Tridimensionnal level :*** *Thickness and offsets are under control.* *Allows for any shapes and internal features*
Wells and Capsules 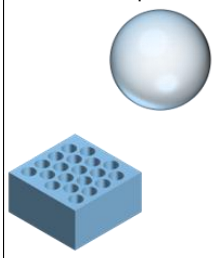	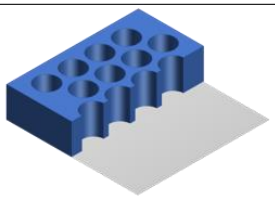 *Wells are through-holes cells are confronted to a stiff bottom*	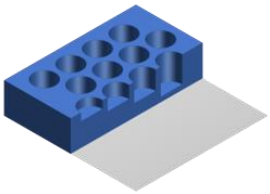 *Wells are now « complete » Their depth and slope can be tuned with ease.*	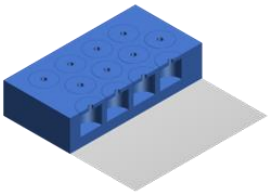 *Open Capsules can further confine the cells in controlled envirronments*
Compartments and Barriers 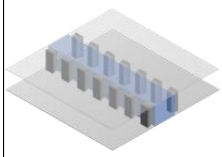	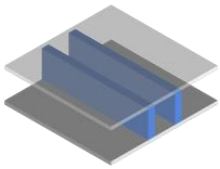 *Chambers are separated by vertical walls, cells only encounter hydrogel on the Z axis*	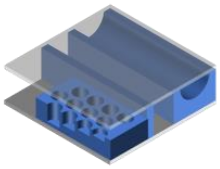 *Chambers are separated by vertical walls, wells and floors can be added to specific parts.*	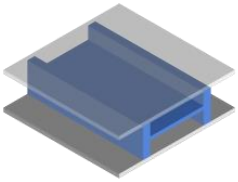 *Barriers can horizontally or vertically seperate chambers + All preceding features*
Channels and Perfusion 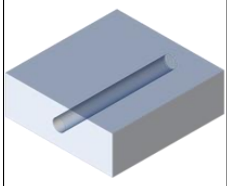	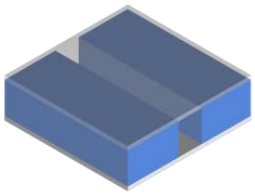 *Channels are vertical walls, cells only encounter hydrogel on the Z axis*	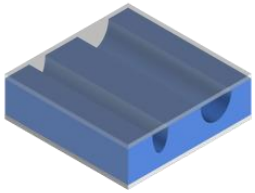 *Channels are walls, vertical or not, with a floor of tunable depth.*	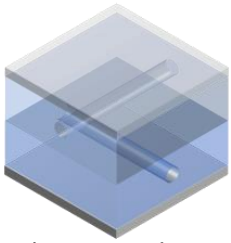 *Channels are « complete » and can intertwine*

Table 2 **| Three functional bricks support hydrogels templates, Z structuration is crucial in their production by light.**

The three levels of Z-control are presented in columns with their respective advantages when it comes to create wells/capsules, chamber/compartments and channels. Note that some structure can be done with relatively low Z-control while other can only be complete with total control over the polymerization in the Z axis.

Experiments

Front polymerization: NOA Slides

Front polymerization describes a type of chemical reaction were a propagating curing surface advances through the liquid material[70]. If the dimension of propagation happens to be the Z axis, the curing thickness becomes correlated with the polymerization time. Jao T. Cabral and colleagues made extensive use of this principle to control the curing thickness of photopolymerizable resins first for microfluidic applications[71] then later as a generic structuration solution[72] **(Figure 22 top)**. Following this process, Zhao et al. made origami out of poly(ethylene-glycol) monomers showing that frontal polymerization could also be applied on hydrogels[73] **(Figure 22 bottom left)**. Eventually, Stoecklin and colleagues demonstrated that the curing of hydrogels could be initiated from the interface of half-baked photopolymerized resins[74] **(Figure 22 bottom right)**. Together, these results led us to hypothesize that a propagating hydrogel-curing front could be triggered from the surface of resin-coated glass slides. Then, the curing thickness would be controlled by adjusting the insolation time on specific areas to stop the advancing reaction **(Figure 23)**.

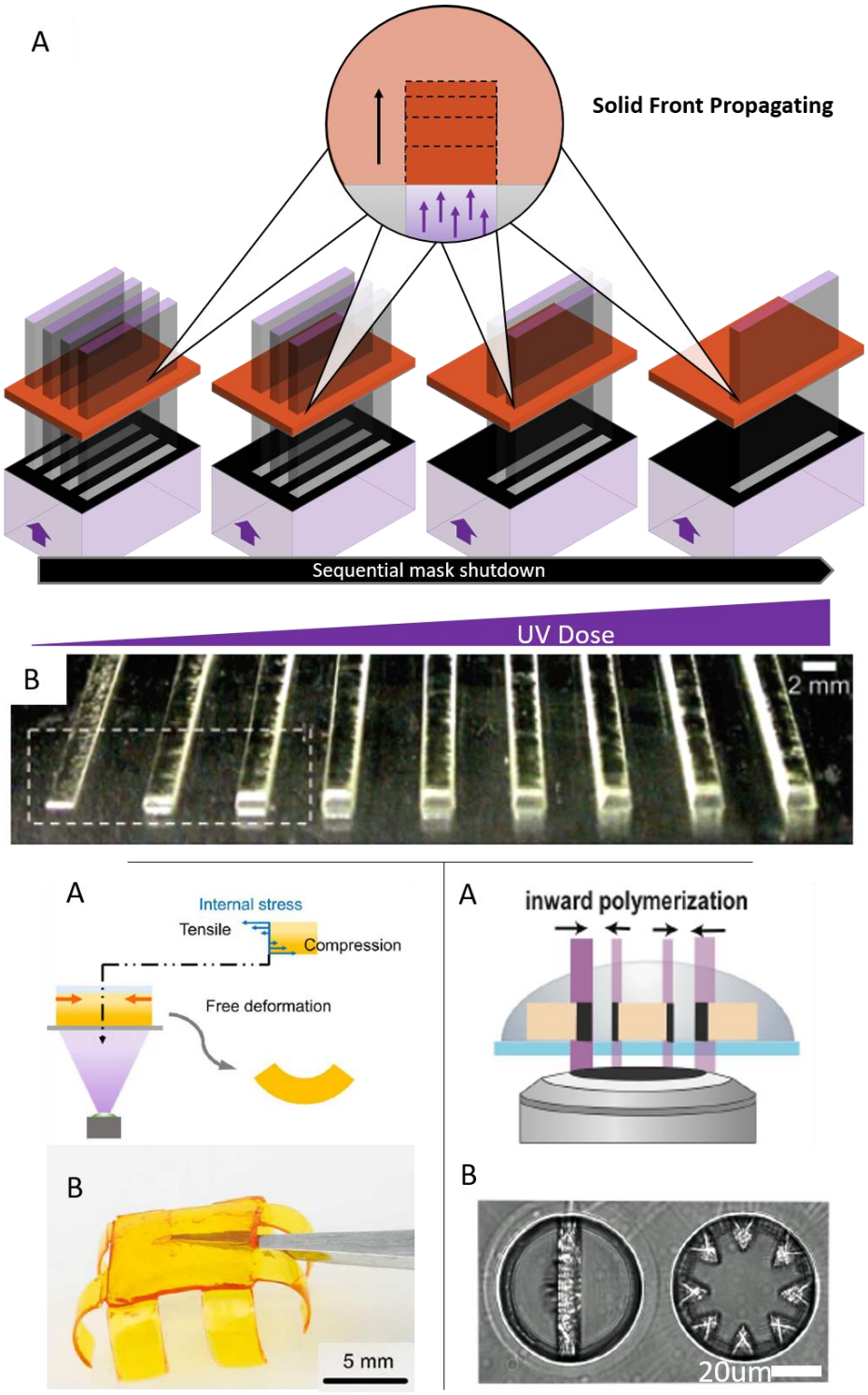

Figure 22 **|** ***Frontal photopolymerization.***

Top, Basic frontal photopolymerization principle Adapted from: Frontal Polymerization JA Pojman et al. Polymer Science a comprehensive reference 2012[70]. **A,** Upon irradiation the resin (brown) cures in depth over time (dots). **B.** As the photographs show the higher the irradiation dose the thicker the resulting resin. **Down Left, Frontal polymerization applied to hydrogels** Adapted from: Origami by frontal photopolymerization Zeang Zhao and colleagues Science Advances 2017[73]. **A,** Here frontal polymerization cures an hydrogel layers (in yellow). **B,** the resulting curing gradient allow the flat structures to bend after reticulation. **Lower Panel, Hydrogel Frontal polymerization starting from a half-baked resin** Adapted from: A New Approach to Design Artificial 3D Microniches with Combined Chemical, Topographical, and Rheological Cues. V Viasnoff Advanced Biosystems 2018[74]. **A,** pits made of resin are partially cured. The resin-embedded photo-initiator starts a frontal polymerization of the hydrogel precursors. **B,** brightfield microscopy images of the pits with hydrogel features.

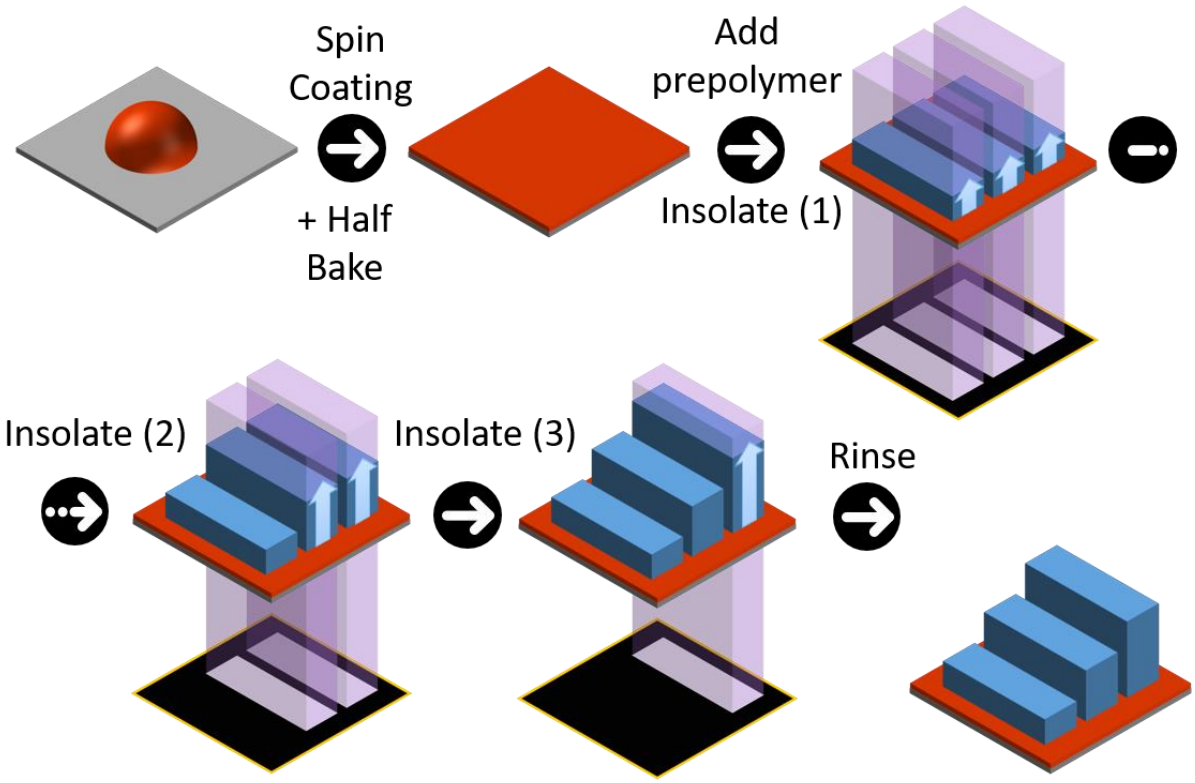

Figure 23 **| *Fabrication of NOA-slides for photopolymerization and use thereof.***

Schematics of the protocol: A drop of photocurable resin (brown) is deposited on a glass slide and subsequently spin-coated and half-baked to form a homogeneous and reactive layer. Following the incubation of a photopolymerizable hydrogel, ultra-violet insolation triggers a growing polymerization from the bottom to the top. Thickness is thus regulated by the ultra-violet-dose.

Methods:

Preparation of NOA-Slides: NOA 81 (Norland Optical adhesive, UK) was spin coated at the surface of 22x22 mm 170 um thick glass coverslip (Schott Nexterion, Schott Jena, Germany) at 4500 rpm for 60 seconds. The resulting thin layer of NOA was then "half-baked" using a ultra-violet-oven (UV-KUB, KLOE, France) at maximum power (40 mw/cm²) for 10 to 30 seconds. 250 um thick, xurographed silicone layers with microwells (silicone stencils, Alvéole, France) were then added to the surface. A second silicone layer was added on top to control the liquid thickness.

Front Polymerization of poly(ethylene glycol) di-acrylate: Solutions containing the prepolymer (molecular weight 700, Sigma) were added to each well of the microreactors grayscale patterns were then insolated using the PRIMO set-up in normal mode. In this scenario, each pixel has a continuous insolation time proportional to the gray level. To help in the structure's characterization 1mg/mL of 4-arm-poly(ethyleneglycol)-Biotin was added to the mix and the structure's surface was subsequently coated with cyanine-5-labelled streptavidin.

Characterization of the resulting hydrogel structure: Structures were resolved using confocal microscopy after flipping the sample upside down in order to avoid optical aberrations.

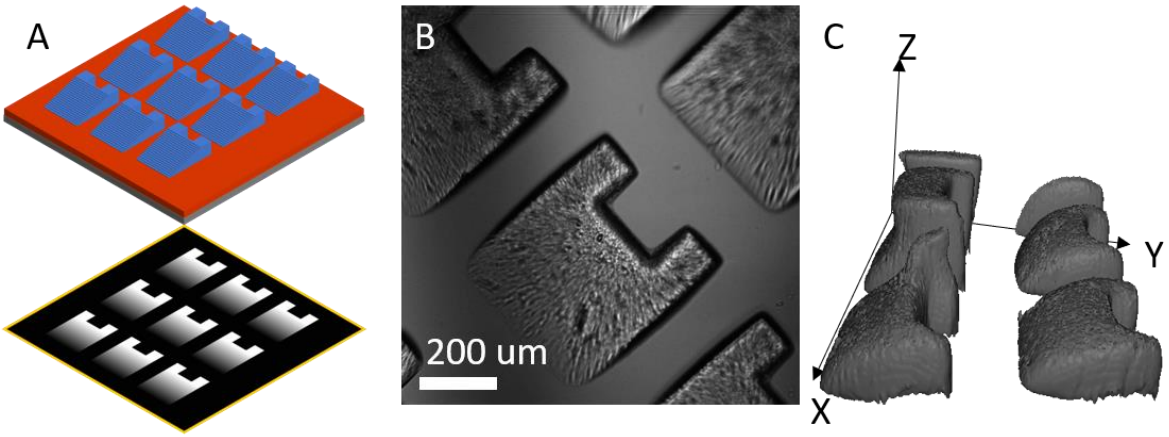

Figure 24 **| *Frontal polymerization is unreliable***

A, Schematics of hydrogel slopes made using NOA slide showing the projected pattern (grayscale gold border) and the NOA slide (gray-brown) with the expected hydrogel structure (blue) **B,** brightfield microscopy image showing the resulting hydrogel structures **C,** Confocal microscopy reconstruction of said structures.

Analysis:

We demonstrate the control of the polymerization thickness for short precursors like poly(ethylene-glycol) diacrylate with molecular weight 700 and below **(Figure 24 A-B)**. However, calibrating the reaction proved difficult as the reaction kinetic is fast and sensitive to the homogeneity of the resin layer. The consequences of a poorly controlled kinetic become visible as some structures display an aberrant thickness **(Figure 24 C)**. The resin displays batch to batch variability further complicating the optimization steps.

Conclusions on “NOA-Slides”

Front polymerization may appear simple and straightforward but its limitations make it ill-suited for hydrogel structuration. As the results tend to show, there is a high variability in the shapes one can obtain from this reaction. A possible explanation arose when we observed that the resin-contained photo-initiator can diffuse into the precursor’s solution. Indeed, we were able to polymerize the precursor solution once removed from the NOA-slide substrates.

To make matters worse, only short (molecular weight < 700) poly-ethylene-glycol prepolymers are able to cure using this process. Any attempts with longer chain length proved unsuccessful (molecular weight 10K).

This poses substantial issues:

First and foremost, the shorter the precursor is and the less water-soluble it becomes. Short length precursors are more resins than they are hydrogels. Unsurprisingly, the long chain precursor did not photopolymerize after being put in contact then removed from the NOA-slides.

Second, extensive literature suggested that long chain precursors were more likely to support efficient cell culture[17,19,75]. We wanted a reaction that would be useable with a wide range of materials especially those that were already successful.

Oxygen inhibition appeared as more generic mechanism so we opted to abandon the frontal polymerization path in favor of the gas-controlled polymerization.

Oxygen-controlled polymerization

Oxygen inhibition of polymerization is a chemical reaction well known to complicate the research of scientists working with many different kinds of photopolymerizable materials. As its name implies, oxygen species quench the monomer and/or photo-initiator radicals inducing side reactions that do not contribute to chain elongation and gelation. This reaction is especially noticeable at the vicinity of gas permeable objects such as silicone-made materials. Here oxygen creates an inhibition layer the so-called dead-zone were polymerization is simply impossible. I had the opportunity to observe oxygen inhibition in action as I was photopolymerizing short and long chain precursors close to the borders of silicone microwells **(Figure 25)**. I was thus confident that this mechanism could be generic enough to help in the structuration of many photopolymerizable materials.

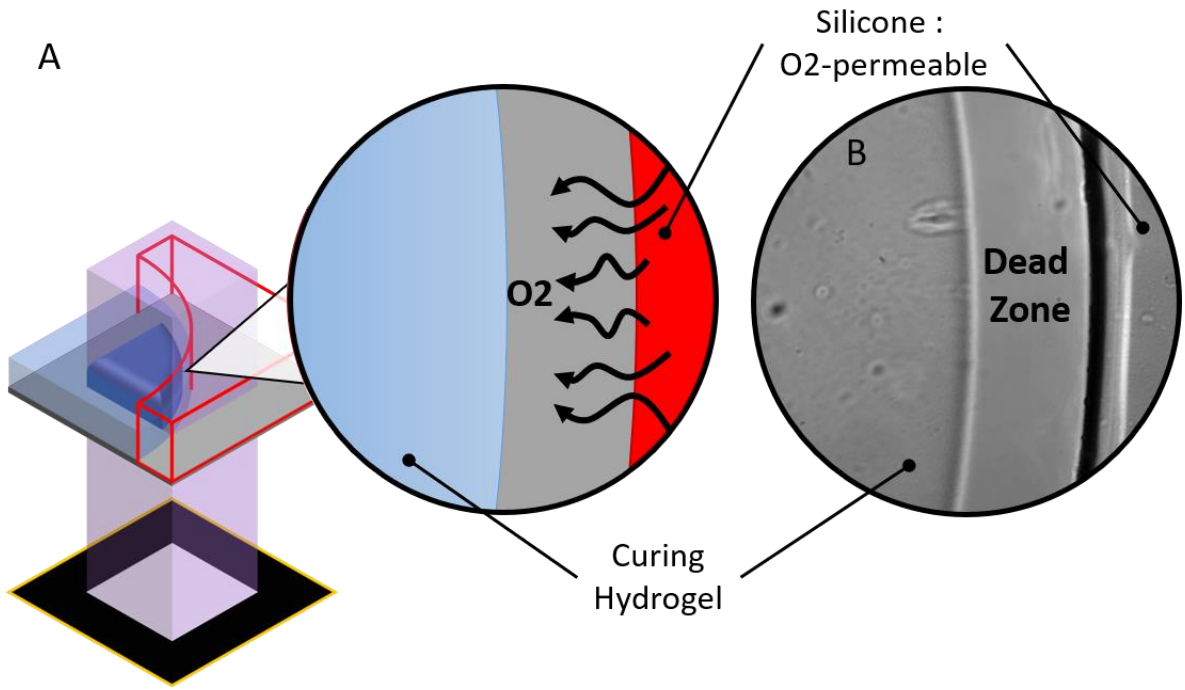

Figure 25 **| *Oxygen inhibition is easily observed near silicone.***

A, Schematics of an experiment were a square is projected with the digital micro-mirror device (black gold-trim). The insolated area (purple) overextends beyond the boundaries of the silicone (red) micro-well so that the photopolymerizable precursor (light blue) should form a gel(blue) that reaches the silicone. **B,** In fact, as the brightfield microscopy image in the insert demonstrates, a non-polymerized dead-zone can be observed at the vicinity of the silicone.

Although it was at first, an undesirable side reaction, oxygen inhibition recently became harnessed to generate hydrogel microparticles[48,50] or achieve feats of 3D printing[15,24,35]. On this last subject, the extensive work done by Tumbleston and colleagues[24] have gathered a lot of interest in the field of additive manufacturing and proved instrumental in my understanding and later exploitation of the mechanism **(Figure 24)**.

Other research labs quickly adopted this smart technology by copying[35] and/or adapting[15] the experimental set-up were a moving Z stage controls the polymerization thickness. In these papers, oxygen inhibition is a mean to maintain a continuous liquid interface at the bottom of the printing chamber. We hypothesized that we could alleviate the need for moving parts by directly exploiting the deadzone properties to control the polymerization thickness. Indeed, oxygen inhibition depends both on the oxygen content and the projected photon flux **(Figure 26)**.

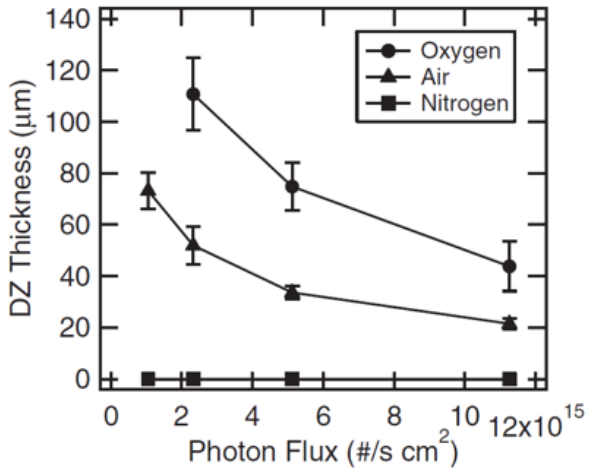

Extracted from: Continuous liquid interface production of 3D objects J. M. Desimone Science 2015[24].Histogram representing the oxygen inhibition's (dead zone) thickness as a function of oxygen content and photon flux.

***Figure 26* | Inhibition depends on oxygen concentration and photon flux.**

Those properties offer two technical gateways to kinetically control the polymerization thickness: either use a gas-controlled chamber to control oxygen's pressure or modulate the photon flux via the digital micromirror's capacities. We thus implemented an easy way to control and stabilize oxygen flow in our set-up: we fabricated gas-permeable microreactors.

From silicone microwells to microreactors

With the microreactors, we transferred the mechanism that we could observe in the horizontal plane from X, Y to top down by adding a silicone ceiling to our microwells **(Figure 27)**.

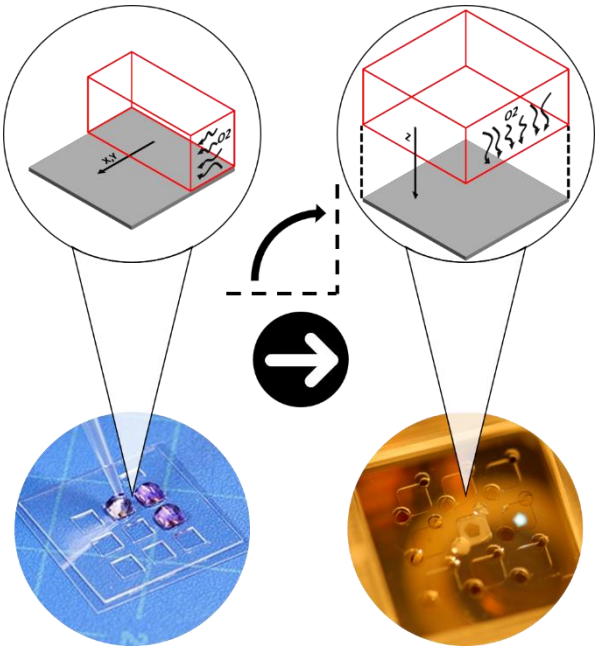

Top, Schematics representing the silicone (red) layer with perfusing oxygen and its major flow direction (black arrows). **Below,** Photographs of the corresponding silicone microwells and silicone microreactors.

Figure 27 | ***From wells to microreactors.***

As a base-material we opted to use silicone stencils as they can assemble into modular objects where the oxygen's flow and the liquid's thickness are both under control. The fabrication of those silicone stencils does not involve soft lithography, instead, a cutting plotter cuts them out of commercial silicone foils of standardized thickness (250 um) **(Figure 28)**. This process was inspired by the pioneering publication of Bartholomeuz and colleagues in 2012[76].

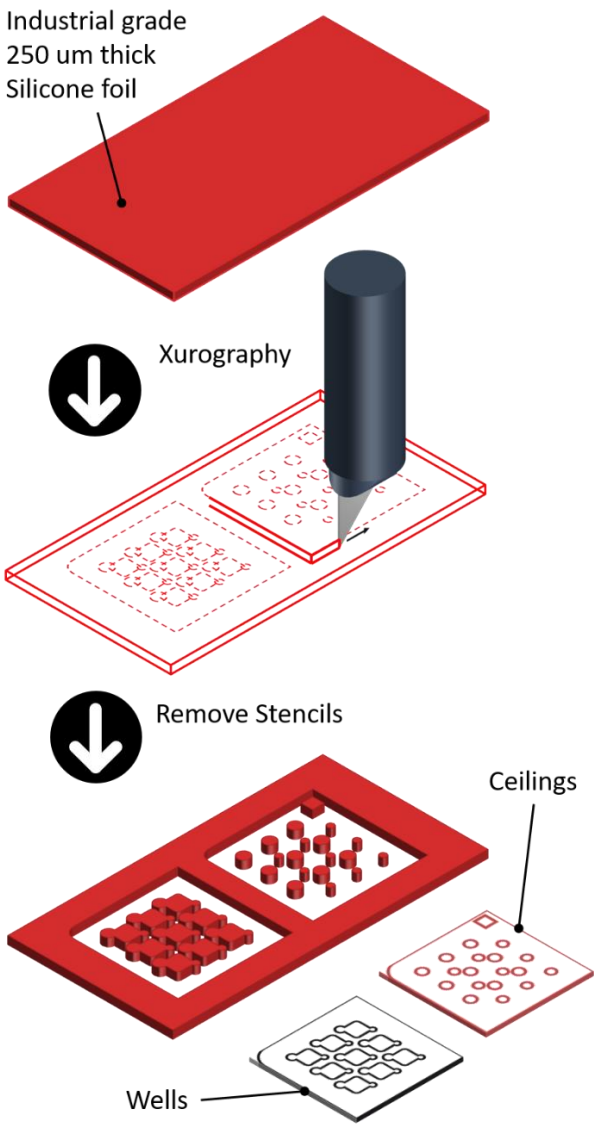

Schematics representing a 250 um thick silicone foil (red) being process by a cutting plotter (black). to extract two silicone stencils for the wells and the ceilings (black and red respectively).

Figure 28 | ***The xurography process***

Once cut, two complementary (wells and ceiling) stencils are stacked onto a glass slide **(Figure 29 top)** to form a single or an array of microreactors with two or more entries depending on the design. The complete device can then fit onto the set-up's microscope stage for structuration **(Figure 29 bottom)**.

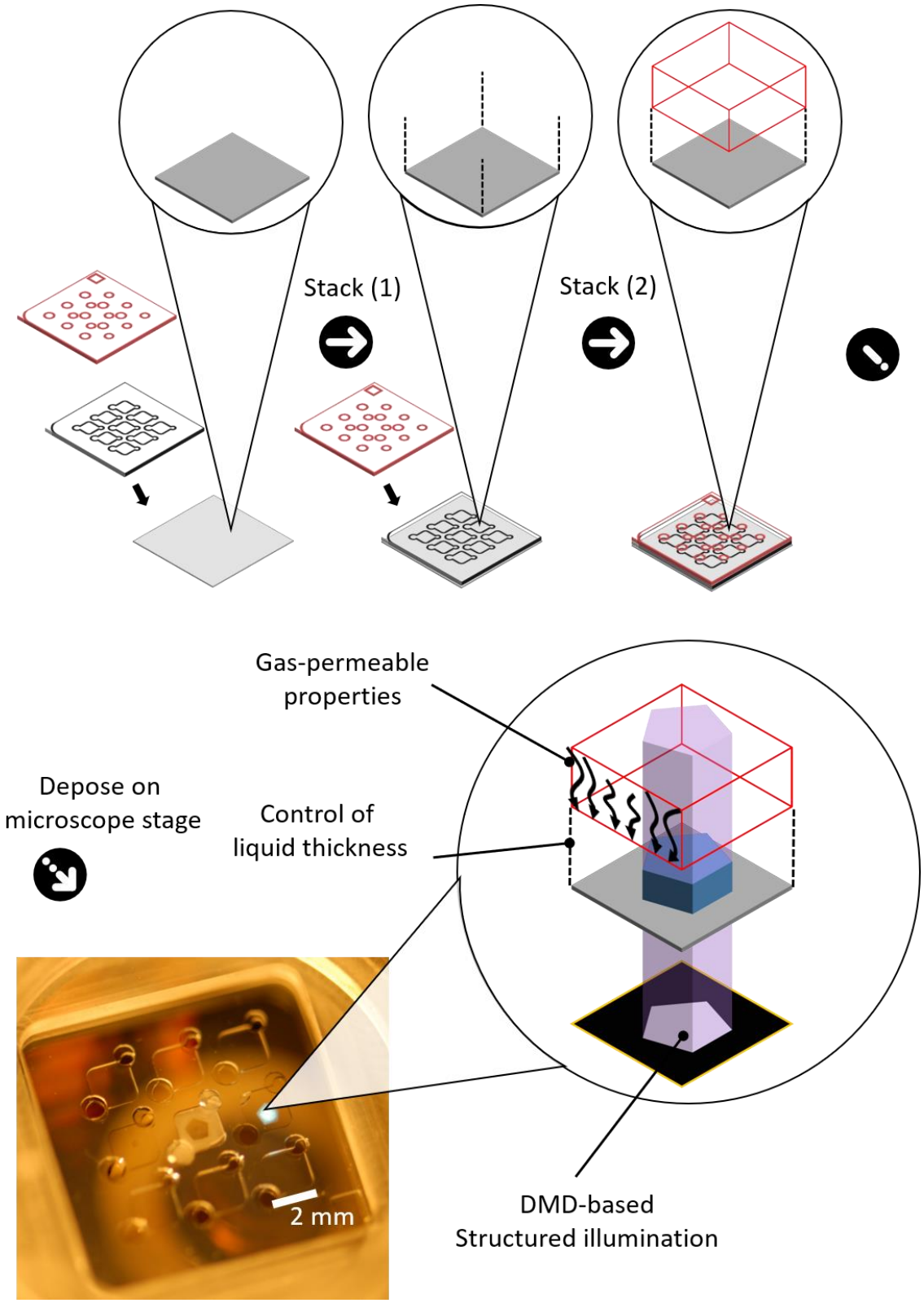

Figure 29 **| Assembly of gas permeable microreactors and use thereof.**

Two silicone foils with xurographed features (a.k.a. Stencils) are stacked onto a microscopy glass coverslip to form multiple reactions microchambers. This configuration is meant to control the precursor-solution's thickness as well as providing a gas source in the form of the ceiling.

Compared to what could be achieved with soft lithography, the stencils are much thinner meaning the end device is flat and can be imaged through the glass slide or the silicone window if needed. Secondly the ceiling is removable so that the enclosed device can be reopened again to facilitate cell seeding after structuration. Alternatively, the ceiling can serve as a closed chamber the later create compartments and channels.

This later aspect is the subject of the next part. Inspired by previous works done with the same illumination module[77], we thought we could use the micro-reactors as standardized chip that could be subsequently customized with photopolymerized hydrogels features.

The next section will describe the use of gas content to control and/or nullify oxygen inhibition in the realization of fluidic systems.

Gas-Controlled Polymerization

Here, the control of the gel thickness was achieved by changing the atmospheric content in order to shrink/expand the dead-zone **(Figure 30)**. Once incubated with precursors and photo-initiator, the complete device was placed within a sealed enclosure were argon, azote, air, or oxygen could be perfused. To characterize this methodology, we polymerized and measured the thickness of pillar-arrays in different atmospheric conditions **(Figure 30)**.

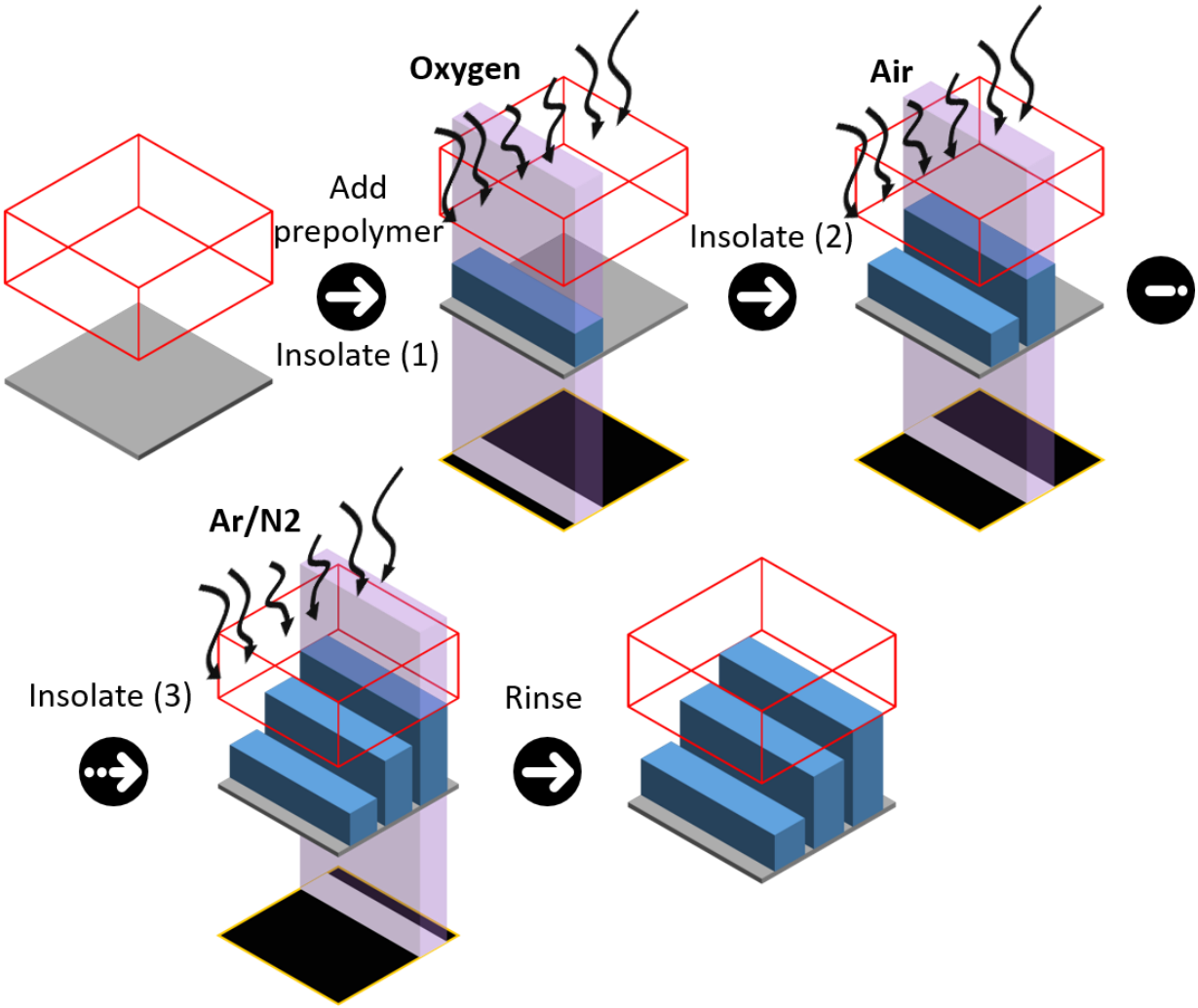

Figure 30 **| *Gas-controlled photopolymerization and use thereof.***

Hydrogels prepolymers are incubated inside microreactors then sealed in a gas-perfused chamber. Each thickness of the structure is then separately photo-polymerized under a specific oxygen content.

Methods:

Gas-controlled polymerization of 4-arm-poly(ethylene-glycol)-acrylate precursor solutions: Precursor gel solutions containing 50 mg/mL monomer and 1X PLPP as photo-initiator were incubated inside the silicone microreactors. The reactors were then placed in a confined chamber allowing the perfusion of

argon, diazoate, oxygen or air. Gels were cured by projecting patterns at 128 mw/cm² for 20, 30 and 100 sec respectively.

Characterization of the resulting hydrogel structure: The resulting gels were rinsed with PBS, incubated with 0.3 um carboxy-fluorescent beads and rinsed again with PBS. Their height was measured by focusing beads at the top and then at the bottom of the gels and deduced from the z stage displacement of the microscope.

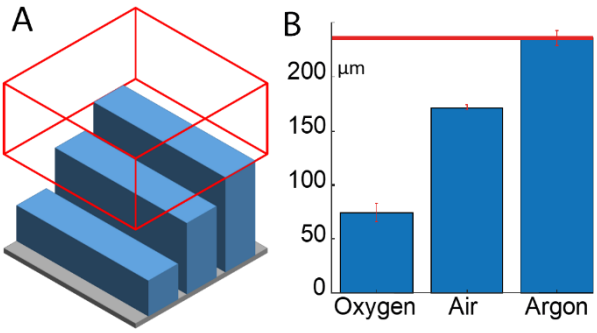

A, Schematics of hydrogel 3-stage structures obtained via gas-controlled polymerization using 100%, 20% and 0% oxygen as in Fig (4). **B,** Histogram displaying the resulting hydrogel thickness in microns for each gas condition and the ceiling (red line).

Figure 31 | ***Characterization of hydrogel thickness in gas-controlled polymerization***

Analysis:

In sharp contrast with the "NOA-Slide" results, controlling the gas-content above the micro-reactors ensures a precise and reproducible thickness control. The hydrogel thickness is clearly inversely correlated with the amount of oxygen perfusing from the ceiling above **(Figure 31 B oxygen and air)**. Furthermore, when oxygen is depleted from the whole reactor **(Figure 31 B argon)**, the cured gel reaches the ceiling effectively forming a wall.

Since, Decock and colleagues[77] demonstrated the use of the same set-up to photopolymerize channels inside microfluidic devices, we hypothesized that we could achieve similar feats yet with a twist of our own.

Indeed, to bypass the issue of oxygen inhibition they had to use other resins while here we can enable or disable oxygen inhibition to produce multi-height features with ease **(Figure 32, Figure 33)**.

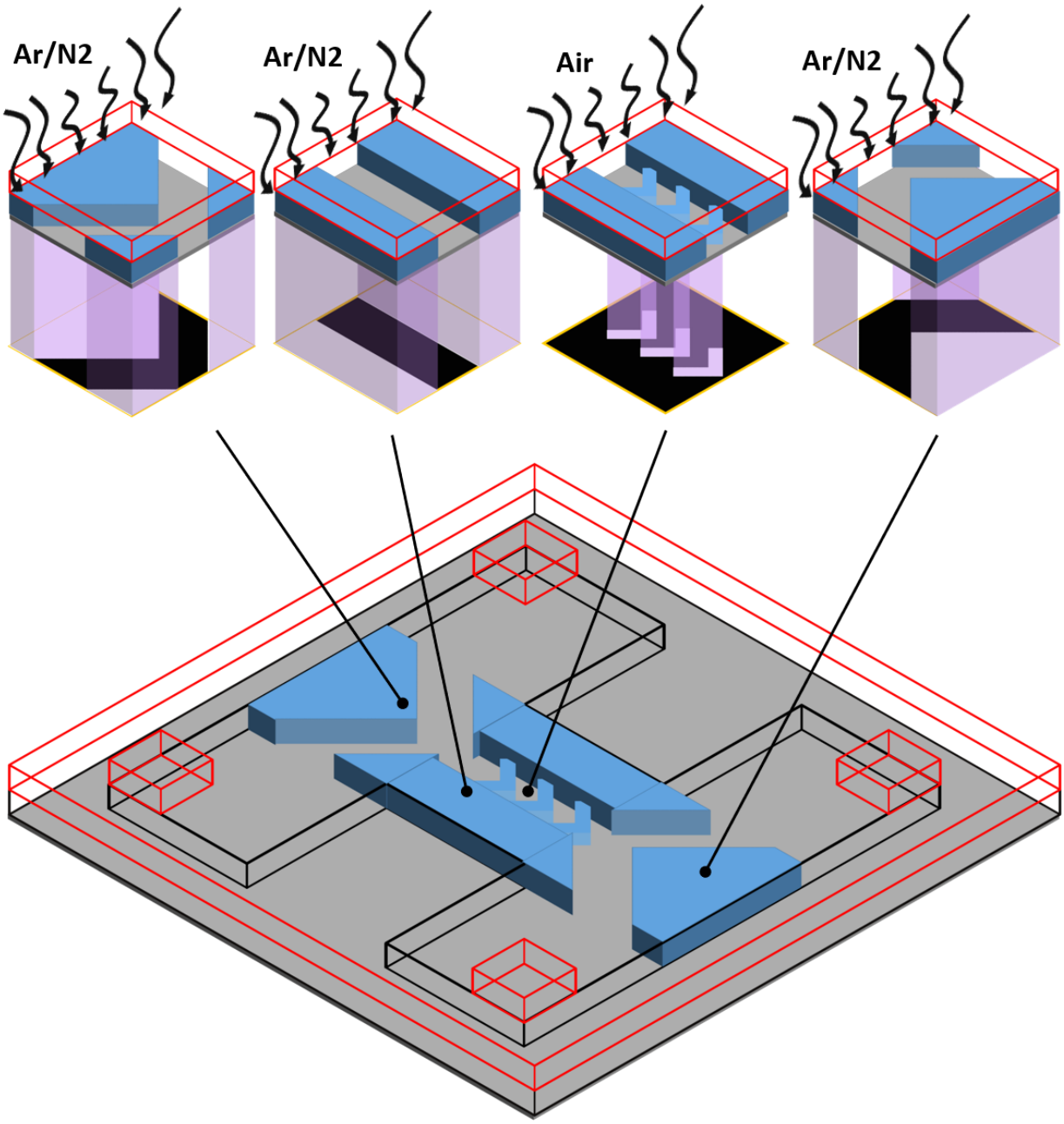

Figure 32 **| *In-situ polymerization of chambers and channels.***

In the schematic, successive insolation field of view are queued to polymerize and stitch hydrogel channels (blue) into a silicone micro-reactor (gray for glass, black for first layer, red for ceiling). Note that one can tune on and off oxygen inhibition by changing the gas content effectively allowing the generation of multiple stages as seen for the herringbone mixer in the central chamber.

Methods:

Perfusing Spiral: to create the spiral, a solution consisting of 5% 4-Arm-poly(ethylene-glycol)-Acrylate diluted in PLPP 1X was injected inside the channels of a 6 entry silicone reactor. All the ultra-violet illumination steps were performed using a 4X objective. During argon perfusion, a spiral is insolated

during 30 sec at max power: 128 mW/cm². The resulting gels were rinsed with PBS, incubated with 3 um carboxy-fluorescent beads and drop deposition on one extremity generated a flow.

Diffusion gradient: a solution consisting of 5% 4-Arm-poly(ethylene-glycol)-Acrylate diluted in PLPP 1X was injected inside the channels of a 6-entry silicone reactor. All the ultra-violet illumination steps were performed using a 4X objective. During argon perfusion, a diffusion chamber made of parallel bars is insolated during 20 sec at max power: 128 mW/cm². The resulting gels were rinsed with PBS. Once the channels created and rinsed, the upper chamber was filled with a solution of 1mg/mL GFP and let to diffuse through the gel for one hour.

Herringbone mixer: a solution consisting of 5% 4-arm-poly(ethylene-glycol)-Acrylate diluted in PLPP 1X was injected inside the channels of a 6-entry silicone reactor. During argon perfusion, two parallel flow channels are generated in two overlapping fields of projection during 30 sec at max power: 128 mW/cm². Argon Perfusion is stopped and a second pattern consisting of the mixer features is projected using the same parameters. The resulting gels were rinsed with PBS, incubated with 3 um carboxy-fluorescent beads in the middle chamber. Pipette aspiration at the exit of the circuit generated a sufficient flow to observe the mixing effects.

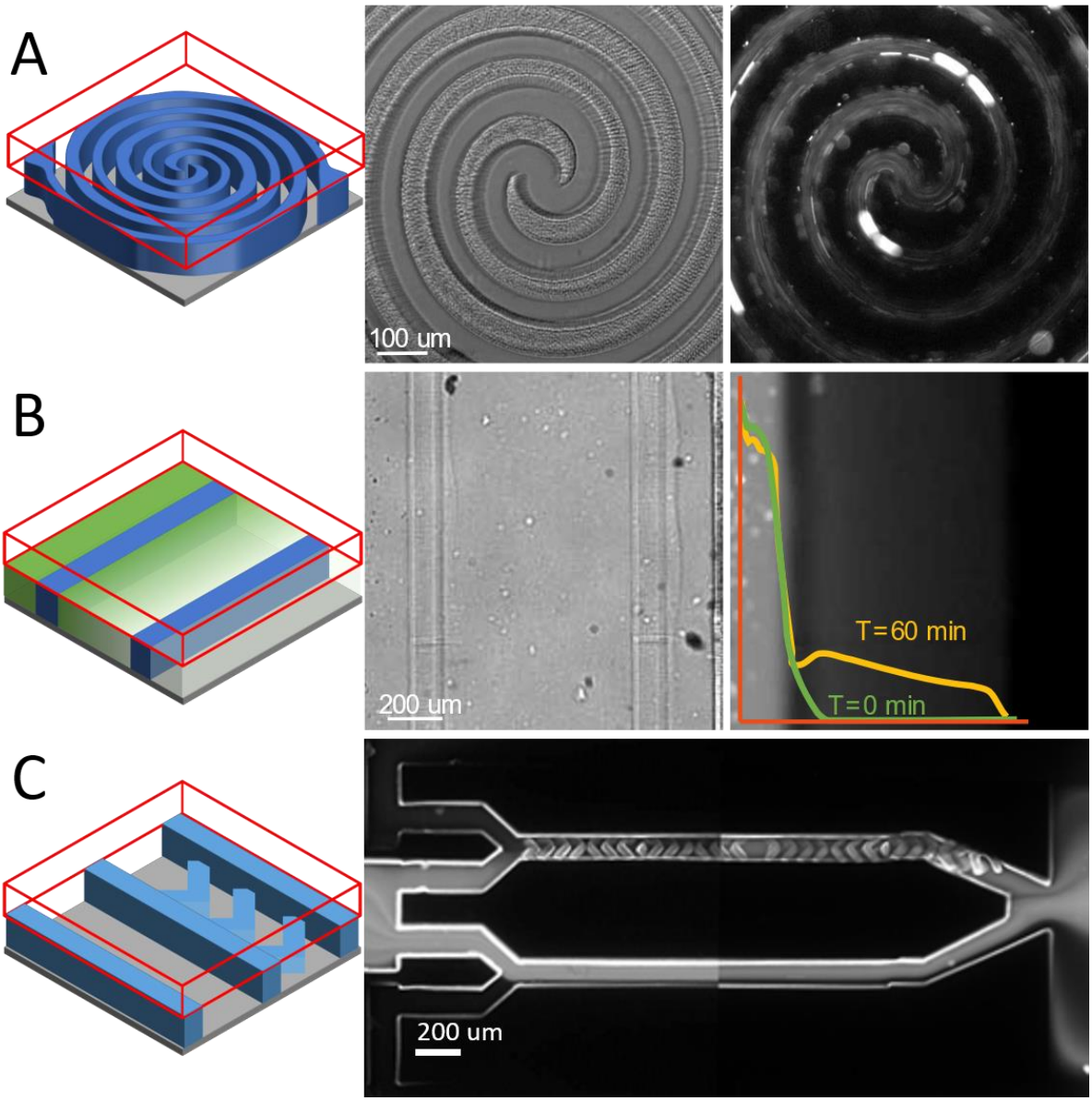

Figure 33 **| *Fabrication of fluidic devices using gas-controlled polymerization***

A, Schematics, brightfield and epifluorescence images of a perfused hydrogel spiral. The spiral is perfused with a solution containing beads to highlight flow and sealing of the channels. **B,** Schematics, brightfield and epifluorescence images of a gradient generation chamber using protein diffusion through the hydrogel. **C,** Schematics and epifluorescence images of a herringbone mixer resulting from two insolation steps.

Analysis:

This figure illustrates the unique traits of gas-controlled polymerization in the realization of fluidic devices. By nullifying oxygen inhibition one can directly polymerize channels with elaborate geometries **(Figure 33 A)**. Hydrogel barriers are semi-permeable allowing diffusion gradients to form within the chambers **(Figure 33 B)**. Also, multi-height structures can be created with ease compared to traditional soft-lithography techniques as we illustrated with the realization of a herringbone mixer **(Figure 33 C)**.

Conclusions on gas-controlled polymerization

More than the control of thickness, it is the possibility to switch oxygen inhibition "ON" and "OFF" that set's gas-controlled polymerization apart. In traditional soft lithography, multilayered fluidic devices are notoriously complicated to produce due to alignment procedures, here creating two stages is a matter of enabling oxygen or not.

Being able to create hydrogel barriers is also a great asset as such channels are semi-permeable. This permeability is conveniently tunable as Decock et al. demonstrated in their work[77]. Both the ultraviolet dose and the precursor's content can be adjusted to reach the desired pore size.

However, this methodology implies tubing and gases which are not always available in standard laboratories. Overall, I'd argue that this technique suits more a microfabrication than a cell biology context despite its evident advantages (chambers and gradients). We thus looked for a structuration method that could be performed in ambient air. This is where photon-flux modulation of the dead-zone proved the most interesting.

Flux-Controlled Polymerization

As previously stated, oxygen inhibition fluctuates according to the projected photon-flux[24]. The more photons are sent to the sample and the thinner the inhibition layer becomes. Here, we demonstrate the control of the polymerization thickness using the laser power or projected gray levels **(see Altering mater with light)** instead of perfusing gases **(Figure 34)**. This makes the system simpler while also enabling the direct polymerization of slopes and topographical features **(Figure 35 A-B)**. Additionally, we study our capacity to fix the gel thickness while tuning the ultra-violet dose that the material receives **(Figure 35 C-E)**. This has significant applications since the ultra-violet dose can directly influence the stiffness[35–37] and permeability[77] for acrylate-hydrogels.

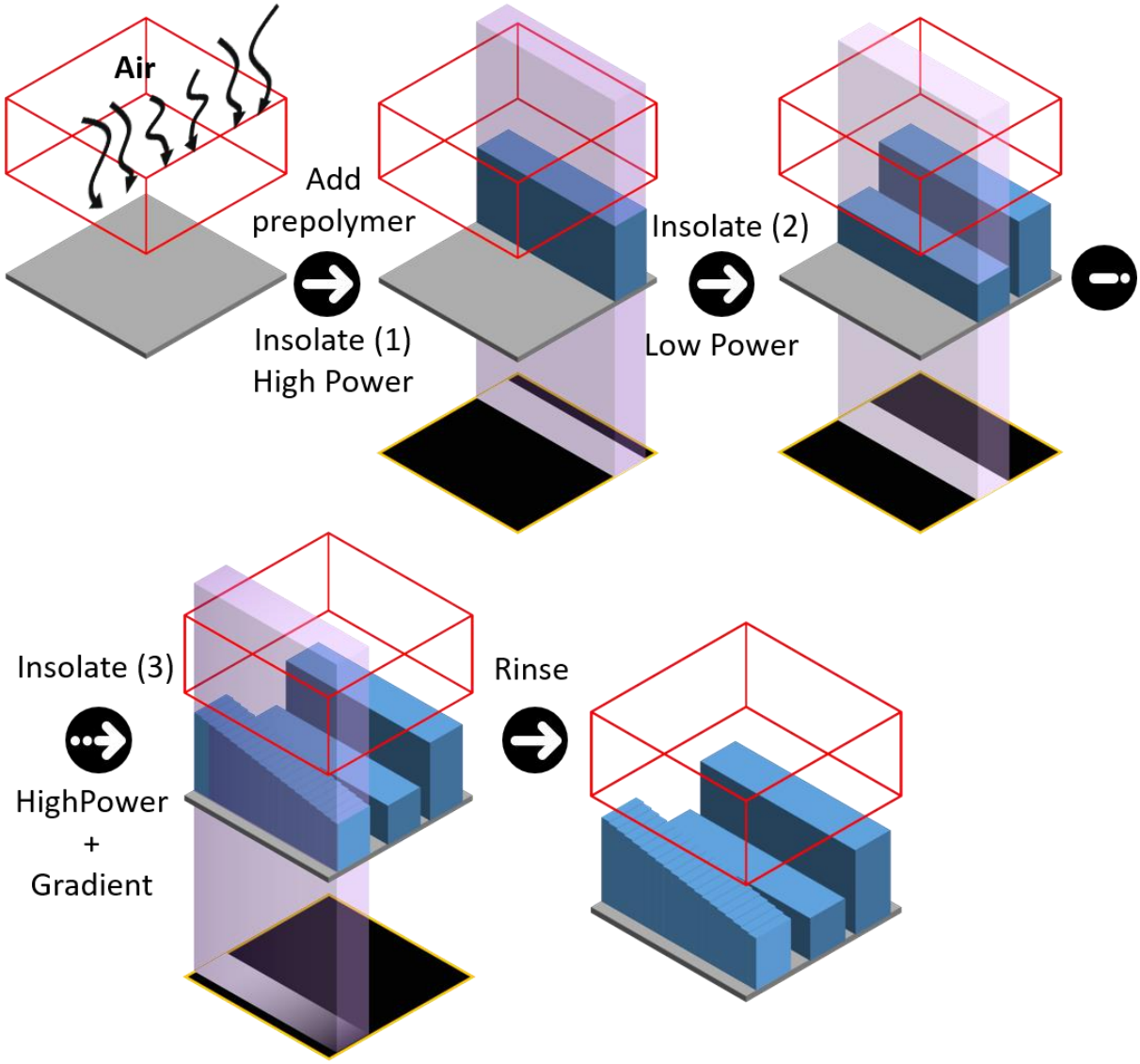

Figure 34 **| *Flux-controlled polymerization, principle and uses.***

Hydrogels prepolymers are incubated inside microreactors under air atmosphere. Different thicknesses result from tuning the laser power before each successive insolation. Alternatively, slopes are generated by projecting gray-levels.

Methods:

Z-controlled polymerization of 4-arm-poly(ethylene-glycol)-acrylate precursor solutions: A solution consisting of 5% 4-Arm-poly(ethylene-glycol)-Acrylate diluted in PLPP 1X was injected inside each well of a 9 wells microreactor. In each well a pattern consisting of 32 wide squares was projected under air at different powers and times: 128 mw/cm² 30 sec; 96 mw/cm² 36 sec; 78 mw/cm² 45 sec; 58 mw/cm² 60 sec; 38 mw/cm² 90 sec; 26.5 mw/cm² 135 sec. Alternatively, grayscale patterns with decreasing gray values of 255, 210, 189, 166, 145 and 128 were insolated for 30, 35, 40, 55, 105 and 180 sec respectively.

Characterization of the gel thickness: The resulting gels were rinsed with PBS, incubated with 0.3um carboxy-fluorescent beads and rinsed again with PBS. Their height was measured by focusing beads at the top and then at the bottom of the gels and deduced from the z stage displacement of the microscope.

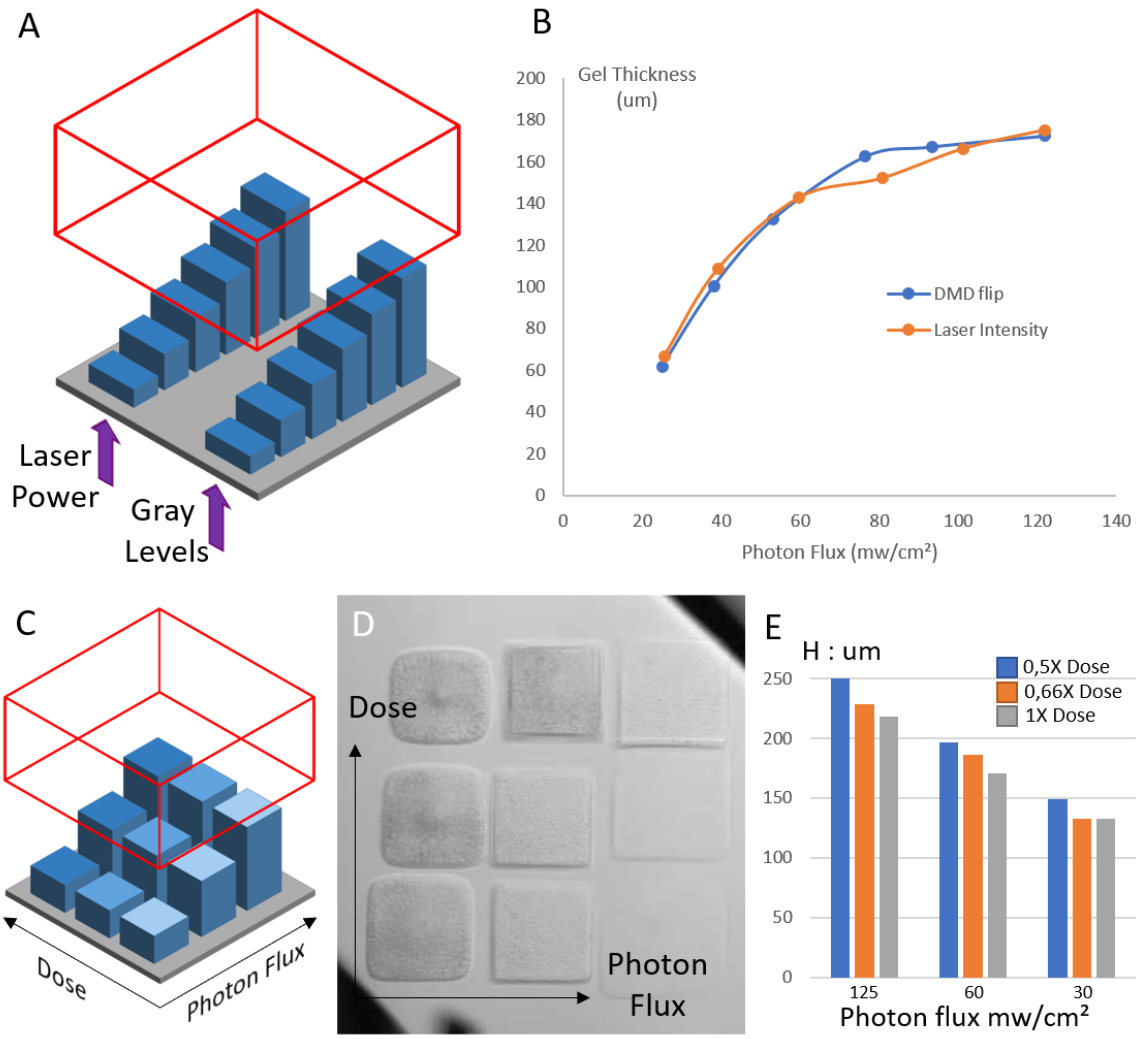

Figure 35 **| *Characterization of flux and dose dependence in flux-controlled polymerization***

A, Schematics of hydrogel 6-stage structures obtained via flux-controlled polymerization either using laser-tuning or projecting gray levels. **B,** Histogram displaying the resulting hydrogel thicknesses for each condition. **C,** Schematics of an array of nine pillars each resulting from the unique combination between three ultra-violet-doses and three photon fluxes. **D,** Brightfield microscopy image of the aforementioned structure. **E,** Histogram displaying the resulting hydrogel thicknesses for each condition.

Analysis:

Flux controlled polymerization allows much more thickness granularity at the expense of the capacity to reach the ceiling. Projected gray levels and laser tuning have roughly the same capacities in terms of thickness modulation **(Figure 35 B)** but the former can generate slopes in a single insolation step. Additionally, we confirm that the gel thickness mostly depends on the photon flux allowing orthogonal control over thickness and stiffness **(Figure 35 C-E)**. We observe a small effect of the ultra-violet-dose nonetheless: it can be attributed to shrinking and swelling of the hydrogel that are a consequence of the reticulation **(Figure 35 E)**. Another limitation arises: thinner structures appear trimmed **(Figure 35**

D) on the borders. This effect is due to sideways diffusion of oxygen which becomes prevalent when the photon flux lessens. We studied this phenomenon **(Figure 36)** and implemented a methodology to circumvent it **(Figure 37)**.

Methods:

Study of the trimming effect: A solution consisting of 5% 4-Arm-poly(ethylene-glycol)-Acrylate diluted in PLPP 0,5X was injected inside each well of a 9 wells microreactor. The same pattern was insolated thrice using the following parameters: 60 sec, 780, 390, 195 mw/cm² respectively. The ultra-violet signal was recorded during insolation and the resulting gels were imaged and compared to the former to extract the untrimmed area.

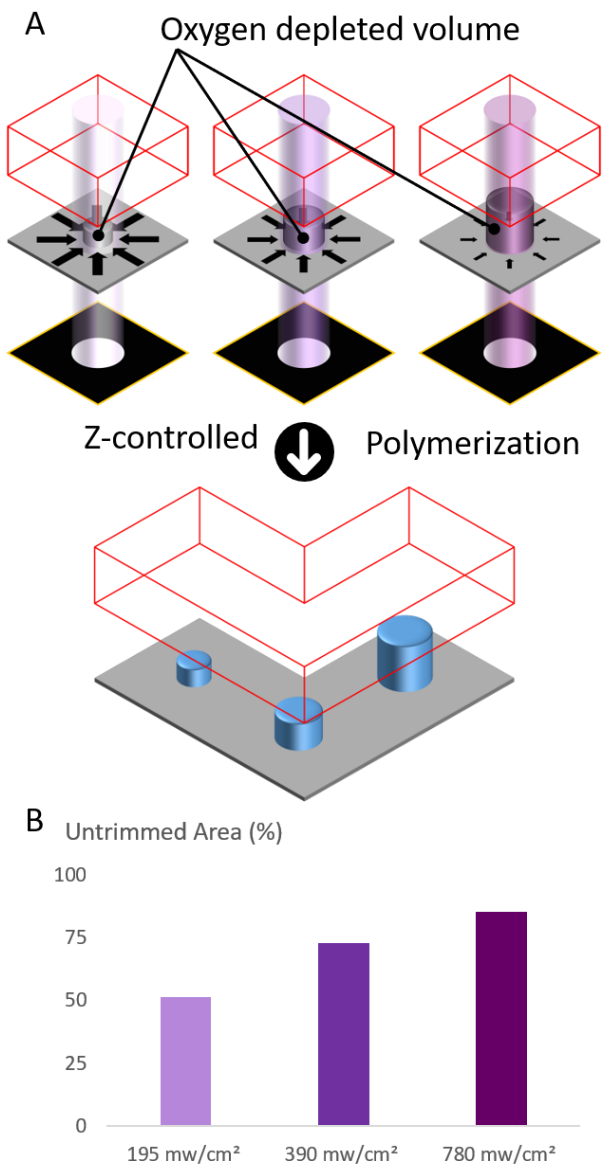

A, Schematics of hydrogel resulting from the same pattern with different laser power the weaker photon-flux induces a stronger lateral oxygen inhibition ultimately trimming the hydrogel. **B,** Histogram displaying the resulting hydrogel (untrimmed area) for each condition.

Figure 36 **|** ***Principle and characterization of the trimming effect***

Using oxygen consumption to counter the trimming effect: A solution consisting of 5% 4-Arm-poly(ethylene-glycol)-Acrylate diluted in PLPP 0,5X was injected inside each well of a 9 wells microreactor. A pattern consisting of a grayscale portrait was projected followed by a second pattern consisting of the same portrait with the null values replaced by a low grayscale value (18). In each case the insolation parameters were as follow: 10 x magnification, 60 sec, 780 mw/cm² (max power). The gel was then rinsed prior to imaging.

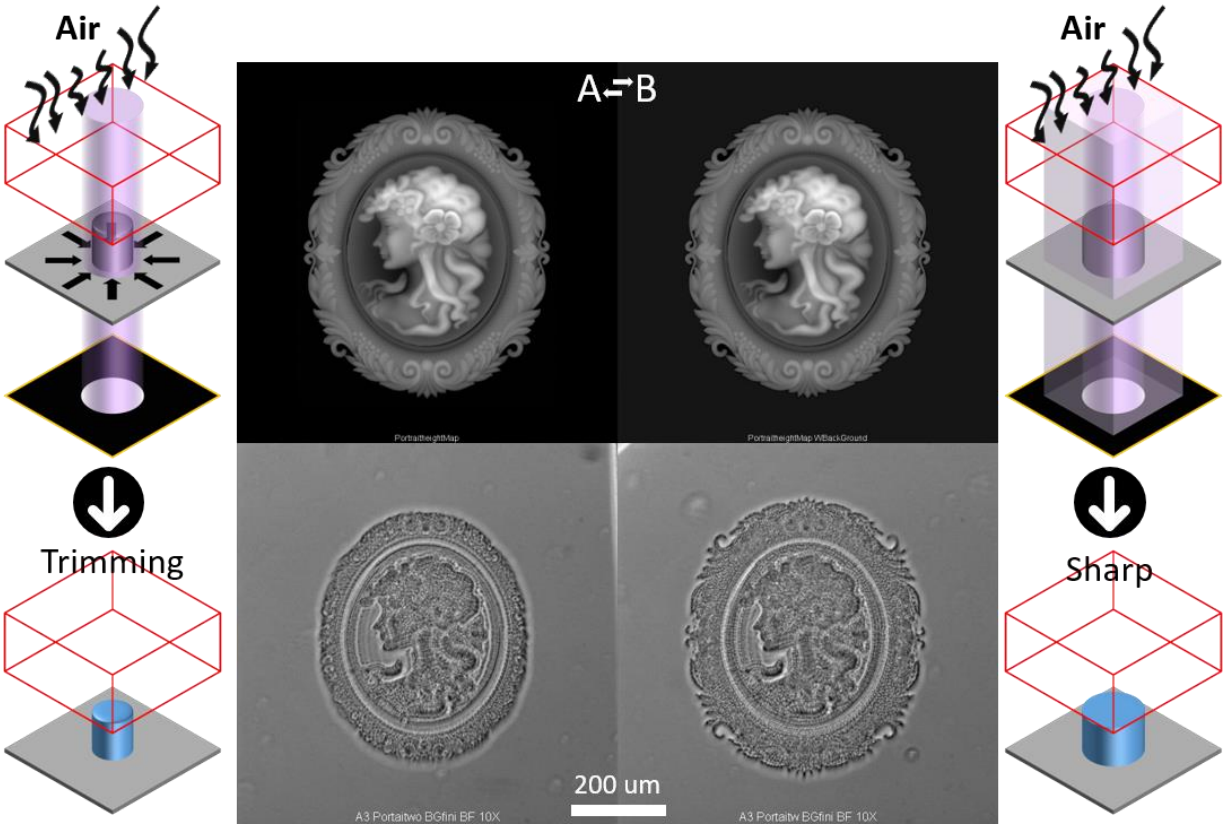

***Figure 37* | Grayscale background to reduce of the trimming effect**

A Left panel, Schematics, projected pattern and brightfield microscopy image illustrating hydrogel trimming resulting from the projection of pattern with fine lateral features. **B Right panel,** Schematics, projected pattern and brightfield microscopy image illustrating reduced hydrogel trimming resulting from the projection of pattern with fine lateral features complemented with a grayscale background.

Analysis:

Oxygen trimming becomes more prevalent when the photon flux grows dim **(Figure 36)** or when the pattern features are too thin **(Figure 37 A)**. In such cases, a simple optimization step consists in projecting a pattern with no “zero” value **(Figure 37 B)**. Replacing each black pixel with a low value ensure that oxygen is also consumed outside of the polymerized areas thus limits trimming. The exact value must be adjusted depending on the pattern and material to avoid unwanted polymerization.

Conclusions on flux-controlled polymerization

In this section we traded flexibility for more simplicity. We succeeded in controlling the gel's polymerization thickness by only using the platform's illumination capacities. It is important to note that due to the kinetic nature of our structuration method, the parameters presented above are likely to change depending on: the precursor's nature, the liquid's thickness (the reactor's height) and the photo-initiator's concentration.

Both gas and flux-controlled polymerization are nonetheless simple enough to support the fabrication of cell culture templates from photocurable precursors. In the next section we will thus illustrate how we can use pure precursors and blends to control the cell adhesion and favor the emergence of diverse cellularized structures.

Cell culture: Revert the antifouling or make use of it

Adhesion is a key factor in self organization and the material's properties directly influence it. Poly(ethylene-glycol) is notoriously bionert : since biomolecules cannot adsorb on its surface, cell adhesion is thus impaired[27]. As an hydrogel, it is commonly used as a blank-state : a meshwork devoid of biological activity that can be complemented with the required adhesion and differentiation factors[17,19]. In other words, poly(ethylene-glycol) helps the scientist design minimal matrixes where each cell culture factor can be tuned separately. This is a significant advantage over animal-extracted matrixes such as Matrigel which are as much biocompatible as they are poorly characterized in terms of biomolecule content.

Alternatively, there are 3D-cell culture configurations where adhesion must be prevented. Other bio-inert gels like agar-agar can be shaped into cups to standardize the aggregation of cells into spheroids[55–57]. In this situation, cell-cell contacts are favored over cell-substrate interactions leading to the formation of a cohesive sphere of cells that synthesize endogenous extracellular matrix[55–57].

In the following pages, we apply our poly (ethylene-glycol)-structuration capacities to each 3D cell culture strategy **(Figure 38)**. We first complement our hydrogels with adhesive biomolecules and poly-electrolytes to cultivate COS-7 cells within channels or on top of topographies **(Figure 38 A, B)**. We also use raw poly(ethylene-glycol) to create anti-adhesive templates that support and standardize the culture of HEK 293-T spheroids **(Figure 38 C)**.

Methods:

Cellularized Hydrogel Channels: the cell-coated hexagonal pillars come from a solution consisting of 2.5% 4-Arm-poly(ethylene-glycol)-Acrylate and 500ug/mL FITC labelled PLL diluted in 0.5X PLPP which was injected inside the channels of a 6 entry silicone reactor. All the ultra-violet illumination steps were performed using a 4X objective. During argon perfusion, an array of hexagons is insolated during 20 sec at max power: 128 mW/cm². The resulting gels were rinsed with PBS and incubated with 100ug/mL of fibronectin for 1 hour. Subsequently COS-7 cells were seeded in complete cell culture medium (DMEM, FBS). The cell culture was then carried for three days to allow cells to spread before fixing and imaging.

Cellularized Bumps: The cell coated waves were obtained with a solution consisting of 0.5% Matrigel with 1,25% 4-Arm-poly(ethylene-glycol)-Acrylate diluted in 0.75X PLPP injected inside the 9 microreactors of silicone device. All the ultra-violet illumination steps were performed using a 4X objective. Under air atmosphere, a first grayscale wave pattern was insolated is insolated during 3

minutes at max power: 128 mW/cm². A second pattern consisting of the lower grayscales was insolated for 3 additional minutes on top of the other. The resulting gels were rinsed with PBS. Subsequently COS-7 cells were seeded in complete cell culture medium (DMEM, FBS). The cell culture was then carried for three days to allow cells to spread before fixing and imaging.

Spheroïd MultiWells: the spheroids were obtained with a solution consisting of 5% 4-Arm-poly(ethylene-glycol)-Acrylate diluted in 1X PLPP injected inside the 9 microreactors of silicone device. For the purpose of this experiment the glass slide of the microreactor was pre-coated with and anti-adhesive layer (Schott HCoated, Schott Jena, Germany). All the ultra-violet illumination steps were performed using a 4X objective. Under air atmosphere, an array of wells with variable features is insolated during 1min 30 sec at max power: 128 mW/cm². The resulting gels were rinsed with PBS. Subsequently HEK 293T cells were seeded in complete cell culture medium (DMEM, FBS). The cell culture was then carried overnight to allows cells to aggregate then form spheroïds.

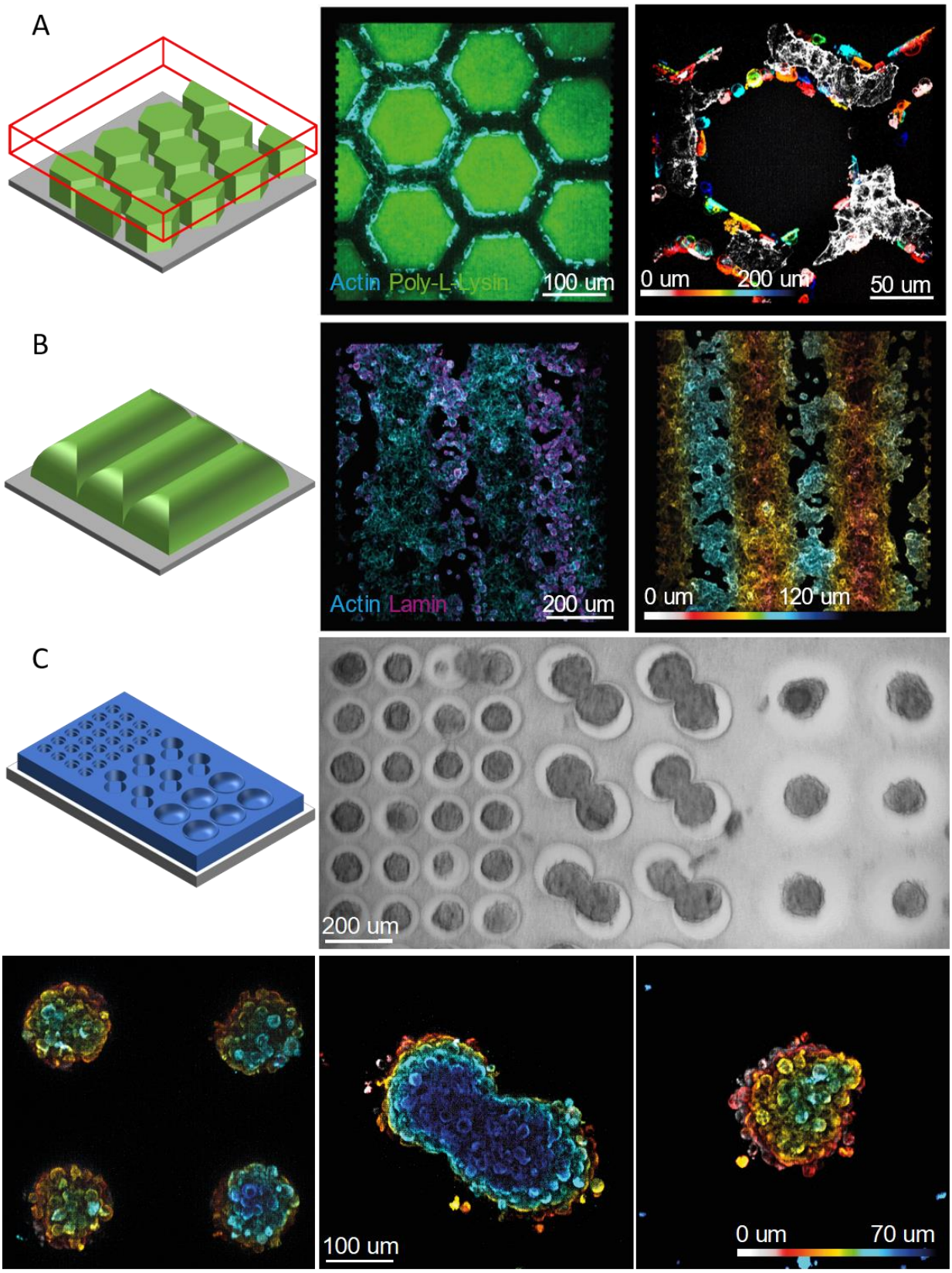

***Figure 38* | Gel structuration applied to cell-culture.**

A, right: schematics of hydrogel hexagonal pillars complemented with poly-l-lysin and fibronectin (green) inside the microreactor (gray and red). Left: multicolor and z-color coded confocal microscopy images of the resulting cellularized hydrogels. **B,** right: schematics of Matrigel-complemented hydrogel bumps (green) Left: multicolor and z-color coded confocal microscopy images of the resulting cellularized hydrogels. **C,** schematics of poly(ethylene-glycol) microwells with brightfield and z-color coded confocal images of the standardized spheroids growing within.

Analysis:

By complementing poly(ethylene-glycol) with adhesion factors such as poly-L-lysin, fibronectin or Matrigel we reverted the anti-adhesive properties of the structure **(Figure 38 A-B)**. This allowed cells to colonize the substrates after seeding often forming monolayers at the interface of the hydrogel. On the other hand, native poly(ethylene-glycol) promoted the formation of spheroids in the same way as agar microwells made by Rivron's and Kauer's respective teams[56,57] **(Figure 38 C)**. One advantage over this prior development however, is the smaller scale and greater flexibility in the shapes we can obtain. Interestingly, while the size of the pit had a direct and obvious effect on spheroid size, the many shapes we tested almost all led to the formation of spheres. Only the height-shaped wells had a strong effect on spheroid organization forcing the sphere to center and "divide" between the two wells. For later experiments would could take inspiration from the works of Rivron's laboratory were they demonstrated how increasing the edge's sharpness in the well could influence the spheroid's final shape[55].

Chapter's conclusion: kinetics to control Z

Here, we tested two strategies to tune the gel thickness: one based upon polymerization propagation (frontal) and the other taking advantage of oxygen inhibition (gas-controlled and flux-controlled). Front polymerization intended to control the gel thickness by initiating a spreading reaction from a photo-initiator-coated glass slide. Ultimately this reaction proved unpractical: The kinetic was too sensitive to environmental conditions and the reaction was limited to short di-acrylate monomers which were closer to resins than actual hydrogels.

Oxygen-controlled polymerization intended to control the gel thickness by exploiting the well documented dead-zone dependence on oxygen content and photon flux. This methodology was much more flexible and successful: It worked with many photopolymerizable hydrogels including the most relevant (long) ones. The transition from gas controlled to flux controlled further enhanced the simplicity and allowed the printing of topographical structures in a single insolation step. Gas-controlled polymerization is still relevant though, to date argon perfusion is the sole way to remove all oxygen and thus obtain hydrogel barriers and flow systems.

When applied to poly (ethylene-glycol), a bioinert material that can be complemented with adhesive factors, we could manufacture a range of cell culture substrates that promote or prevent cell adhesion. As such, cellularized vasculatures and standardized spheroids represent relevant application at the two ends of this spectrum.

In between these two extremes, lies an area where materials display adhesive and antiadhesive areas arranged in specific patterns. This requires to locally and hierarchically alter the bio-chemical properties of hydrogels and represent a different challenge from structuration. The next chapter of this manuscript will discuss the decoration (patterned functionalization) of hydrogels using light.

Introduction

During development, patterns of biomolecules guide the cells to specific architectures[78].

To experiment on that, scientists started engineering hard surfaces so they harbored functional motifs able to polarize and/or confine cells in a standardized manner[79]. This led to the emergence of the micropatterning techniques: the methods by which decorated surfaces are generated. As for structuration techniques, the need for more physiological materials as led in a transition from glass/plastic to hydrogels.

Confusingly, hydrogel micropatterning can both describe the controlled positioning of molecules[25] onto the gel or the structuration of the mesh[42]. **I chose the word decoration to describe the methods that graft or deposit molecules onto the mesh as opposed to structuration that is the art of modifying the shape.**

In hydrogel decoration, contact-based, light-based and flow-based methodologies are common solutions. Once again, scientists developed smart solutions to achieve hydrogel decoration with only limited amount of advanced technology. The goal of this introductory section is to study these works while also highlighting the critical features that define a successful hydrogel decoration protocol.

Microcontact Printing

In this first strategy, proteins are transferred from a microfabricated stamp down to the surface[79]. The surface does not require chemical modification and must be flat and stiff enough to withstand the stamping. Although, the fabrication of said stamp by soft lithography techniques can prove labor intensive, this workflow is being increasingly employed by researchers even on hydrogels[80–82]. Oftentimes, the hydrogel of choice is poly-acryl-amide[80,81] as it is sufficiently resilient but recently researchers used even softer materials[82]. In 2014, Castano and colleagues smartly froze the hydrogels to stamp fibronectin patterns despite using a notoriously frail gel such as Matrigel[82] **(Figure 39 A)**. The hydrogels were decorated with lines to promote cell alignment which proved instrumental in the differentiation of human embryonic stem cells into functional, beating cardiac cells **(Figure 39 B)**. Compared to randomly organized control populations the micropatterned populations showed an increasing number beating foci earlier in their development **(Figure 39 C)**.

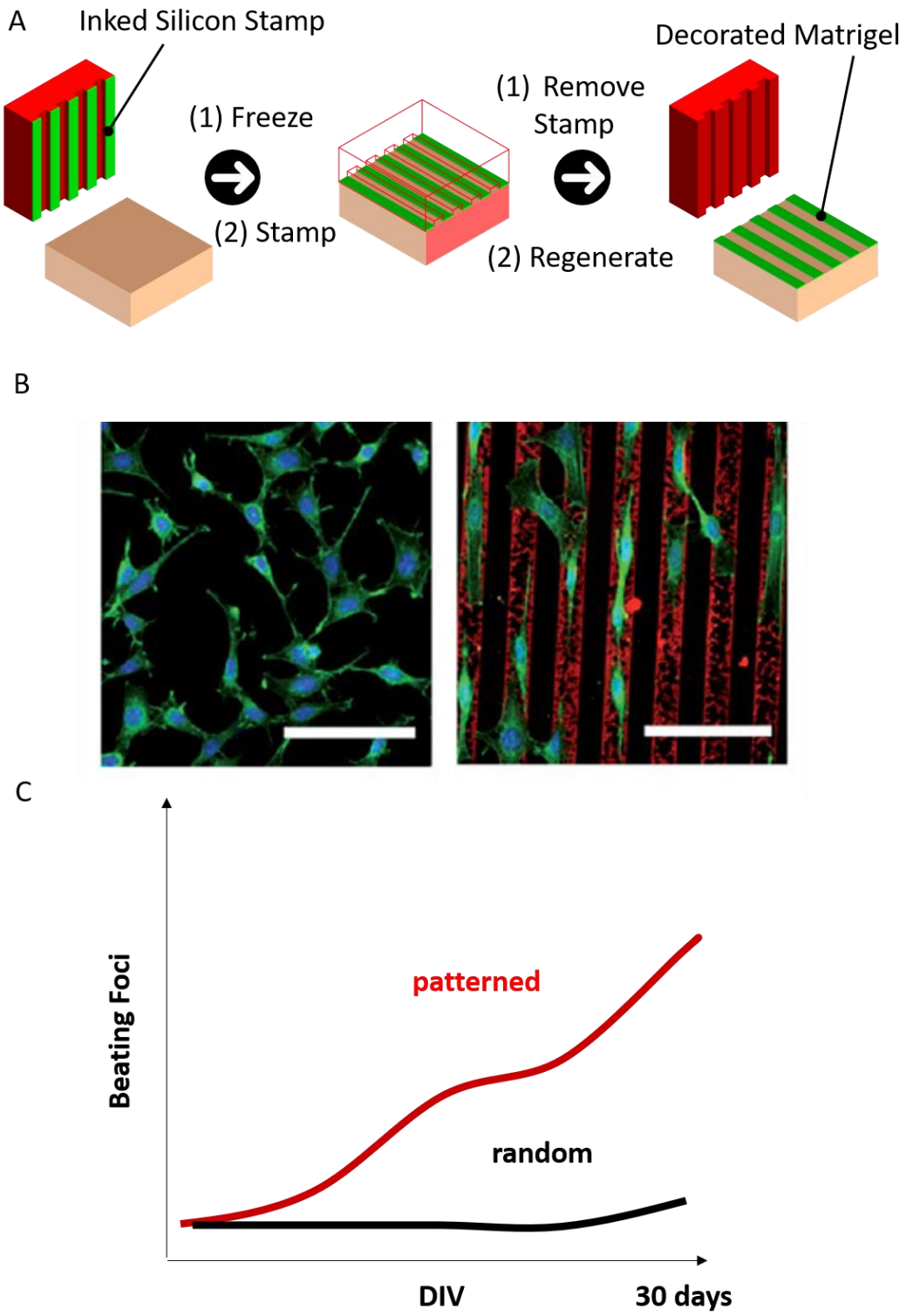

Figure 39 **| *Freeze drying to stamp Matrigel.***

Adapted from: Protein patterning on hydrogels by direct microcontact printing: application to cardiac differentiation. Elena Martinez Fraiz and colleagues RSC advances 2014[93] **Upper Panel,** Hydrogel decoration workflow consisting of Matrigel (orange) deposition on a glass slide (blue), freeze drying (orange to pink), stamping of proteins (red) with a silicone mold (gray), reconstitution and cell (green and blue) culture **Lower Panel,** Cell culture results from left to right epifluorescence microscopy images of cells cultivated in classic (top) and decorated (bottom) hydrogels with nuclei (DAPI blue) actin (Green) and decorated molecule (red). Alignment diagrams of the two populations. Evolution of beating foci over time.

Light-based micropatterning

In light based patterning, ultra-violet light is projected through a photomask to degrade repulsive layers (mostly poly(ethylene)glycol) or activate sensitive materials all in order to promote the local adsorption of proteins[79]. Soft and topographical substrates are compatible with this technique as long as they allow for the coating of an antifouling layer. There are early examples of this protocol applied to commonplace hydrogels such as poly-acryl-amide[83]. In 2011 Tseng et al. studied the combinatorial effects of cell shape and substrates stiffness during tumoral transformation using micropatterned poly-acrylamide gels **(Figure 40)**. The methodology implied ultra-violet activation of the poly-acrylamide surface using commercially available photomasks. The irradiated areas could subsequently react with commercially available crosslinkers to promote protein binding **(Figure 40 A)**. Cells thus only adhered in the activated areas leading to a highly standardized actin cytoskeleton's organization **(Figure 40 B)**. Traction force microscopy experiments could be prosecuted by following the micropattern's deformation upon cell contraction. The results demonstrated tumor transition was not always synonymous with increased contractility, in fact not all tumorigenic factors had an effect on cell contractility as was previously thought.

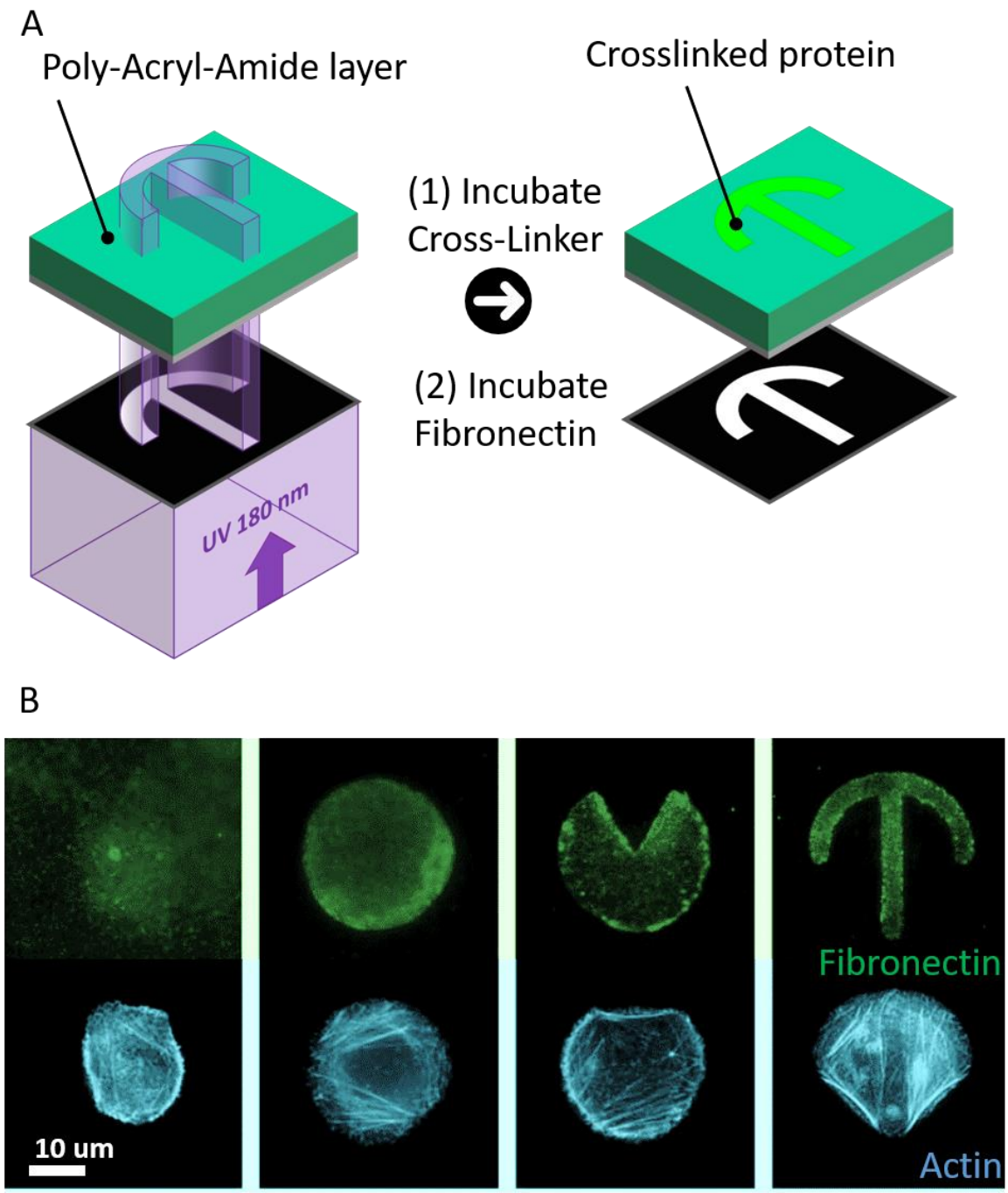

Figure 40 **| Decoration of polyacrylamide hydrogels to study cell contractility in the presence of tumorigenic factors.**

Extracted from: A new micropatterning method of soft substrates reveals that different tumorigenic signals can promote or reduce cell contraction levels. QingZong Tseng and Colleagues Lab On A Chip 2011[83] **A,** Decoration workflow where a chromo photomask (black with silvertrim) is used to shape short ultraviolet light in order to shine specific areas of a poly-acryl amide hydrogel (Turquoise). The gel is subsequently bathed with a solution of fibronectin (Green) which will adsorb on the insolated areas. **B,** Cell culture results: epifluorescence microscopy images of the fibronectin decoration motif in green and the actin cytoskeleton organization in light blue.

Flow-generated chemical gradients

Biomolecules gradients on hydrogels are as valuable as they are challenging to obtain. Flow chambers have been extensively used in this regard[84,85] **(Figure 41)**. Here, instead of physically trapping the biomolecules, the researchers seek to control their diffusion within the hydrogel templates and thus tune their local chemical composition.

In 2014, Cosson and colleagues built a hydrogel-based device comprising a microwell array to support the aggregation of stem-cells. Channels were built underneath the array to perfuse solutions containing retinoic acid. They could thus induce and study the stem cell's differentiation into neurons **(Figure 41 left)**.

More recently, Xu et al used silicone stencils as a way to suspend Matrigel spots. The resulting film could be topped over a flow chamber that would support the generation of gradients. The biomolecules would then diffuse upwards in the gel spots forming gradients of variable steepness in the vertical axis **(Figure 41 right)**. The researchers studied the response of neurons to various guidance cues such as netrin, nerve growth factor and semaphoring. They observed drastic effects of the gradient steepness in the neurite's responses.

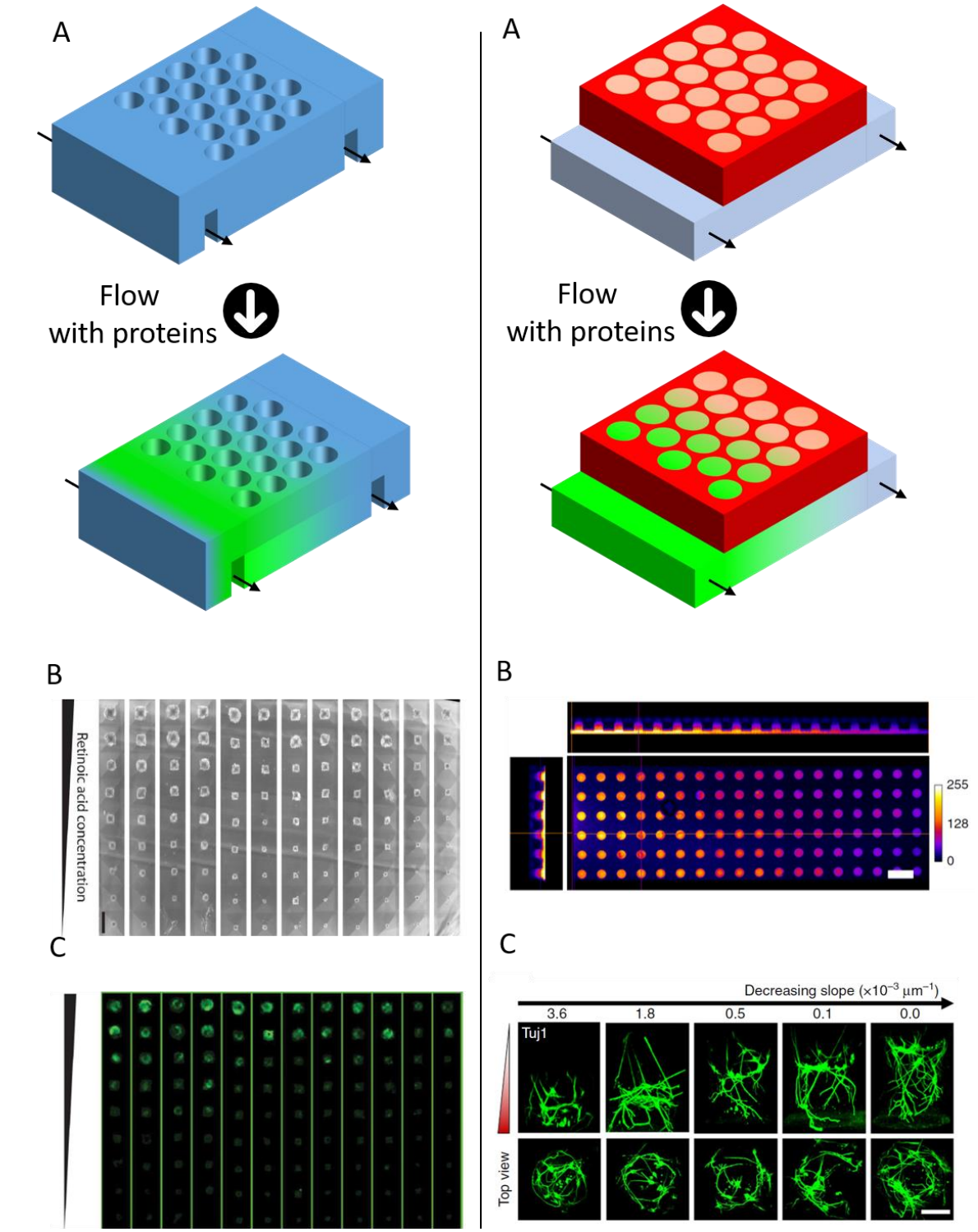

Figure 41 **| *Chemical gradients through flow chambers.***

Left Panel, stem cell differentiation in hydrogels. Extracted from: Hydrogel microfluidics for the patterning of pluripotent stem cells. Steffen Cosson and Colleagues Nature Scientifc reports 2014[84]. **A,** Decoration workflow where a diffusion gradient (green) is generated by perfusing channels (black arrows) incorporated within a poly(ethylene-glycol) microwell array (blue). **B,** Brightfield microscopy images of the resulting stem cell aggregates in the presence of retinoic acid gradient. **C,** epifluorescence microscopy images showing GFP expression along the axis of the gradient attesting for neurite differentiation. **Right Panel, axonal guidance in hydrogels.** Extracted from: High-throughput three-dimensional chemotactic assays reveal steepness-dependent complexity in neuronal sensation to molecular gradients. Zhen Xu and Colleagues Nature communications 2018[85] **A,** Decoration workflow where Matrigel spots (pink) are suspended on a silicone stencil (red) under which a flow gradient (black arrows) is established. **B,** Confocal microscope orthogonal slices showing the resulting gradient in the spots. **C,** Confocal microscopy images of neurites outgrowth within the spots in the presence of a Sema3 gradient.

Discussion

Ideally, decoration should be multiplexable and reversible to enable coculture and emulate the diverse dynamic protein environment that the cell encounter[10,11] **(Table 3 Column 3)**. To our knowledge, there is only a handful of scientific teams that have achieved this level of freedom on hydrogels. These scientists had to develop a complete chemical toolset to do so[16,44,45] which hints us that this is a very daunting task.

In the works above, the most basic decoration that is one single protein **(Table 3 Column 1)** was enough to serve two fundamental purposes: Positioning and Tutoring.

> Positioning seeks to confine cells or cell populations to specific configurations relative to each-other or pre-existing structures. Once organized, cells can be imaged and analyzed more easily and can be set in hierarchical cocultures. To be successful, this workflow requires precise control over the material's inertness to prevent cells from over-spreading. This is usually achieved through coating the gel's surface with cell repellant molecules.
>
> Tutoring refers to triggering differentiation, alignment or other signaling pathways in a way that is controlled by the experimenter. Being able to tutor the cells is especially valuable in stem cell research and disease modeling for example. As opposed to positioning, controlling the gel's adhesive properties is less important or can be even detrimental to cell transduction. Protein gradients are especially valuable for tutoring, much less so for positioning.

With the help of digital light processing, we sought to improve upon the existing methods by taking advantage of our grayscale projection and alignment capacities **(Table 3 Column 2)**. In the coming experimental section, we thus test two different protocols (indirect and direct):

In the indirect protocol we first decorate a sacrificial substrate that will transfer its protein content to the gel. Having the advantage of preserving the gel's properties, this protocol will unfortunately fail in inducing any cell response despite promising initial results.

Subsequently a direct protocol is tested. Here, a polymerized gel is functionalized through the use of photosensitive linkers. This latter protocol will prove easier to push towards cell culture applications.

	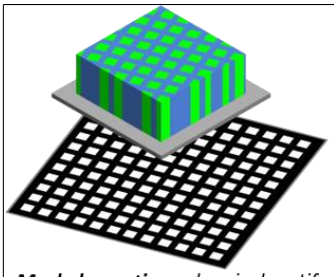 ***Mask decoration :*** *chemical motifs can be repeated over a flat gel or structure with no alignement.*	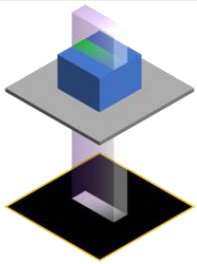 ***Digital decoration:*** *motifs and gradients can be aligned onto existing structures.*	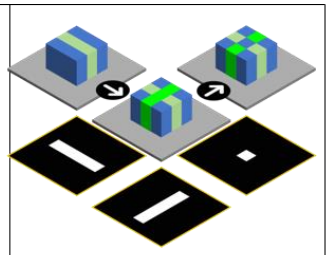 ***Dynamic Decoration:*** *motifs and gradients can be repeated and/or erased*
Cell Positionning 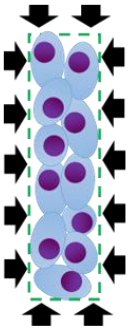	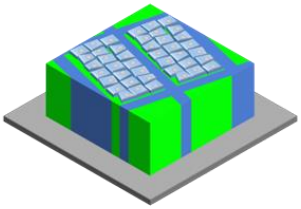 *Cells can be positionned on flat gels.*	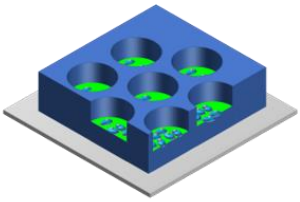 *Cells can be positionned on pre-existing objects.*	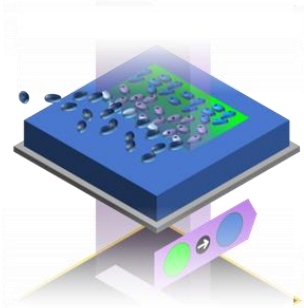 *Cocultures become possible, cells can be removed or added at will*
Cell Tutoring 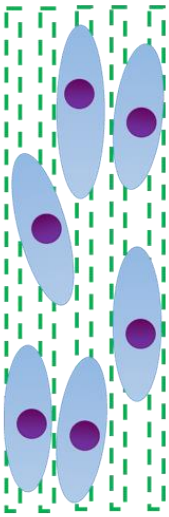	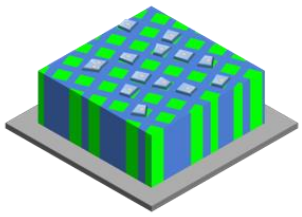 *Shapes induce differention* 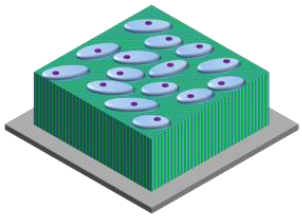 *Lines can induce cell alignement*	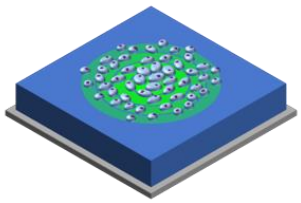 *Immobilized gradients can tune the cells response.* 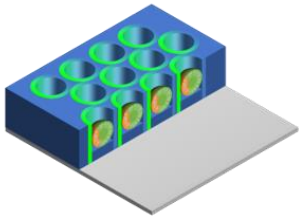 *Topographical and chemical cues can be combined*	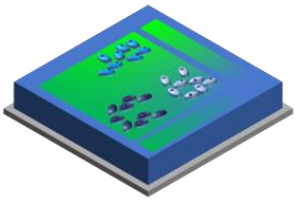 *Competitive chemical cues can be compared ...* 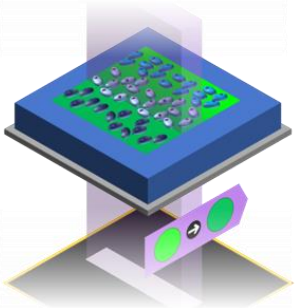 *... or switched*

Table 3 **| Hydrogel decoration from a practical and technical standpoint.**

Three levels of hydrogel decoration are presented in columns with their respective advantages when it comes to positioning or tutoring cells.

Experiments

Gel transfer: lift off patterning.

In gel transfer, micropatterns are first printed on a stiff substrate that serves as an intermediate. A hydrogel is then polymerized onto the micropatterns inducing the transfer of proteins into the mesh[86–88]. Although less straightforward than the modalities presented in the introduction, this technique is popular as it does not involve insolating or stamping the gel.

An application of the protocol can be found in the works of Seddiki, Narayana et al done in 2017[88] **(Figure 42)**. Here, they use a glass slide as the sacrificial substrate to transfer the proteins onto a poly(acryl-amide) gel. Poly-acryl amide has a tunable elasticity that depends on the precursor concentration. They were thus able to quantify protein expression as a function of gel stiffness. In this article, the protein micropatterns were obtained through stamping however light based methodologies can also replace the stamps as it was also demonstrated later in the works of Moeller Denisin and colleagues[86].

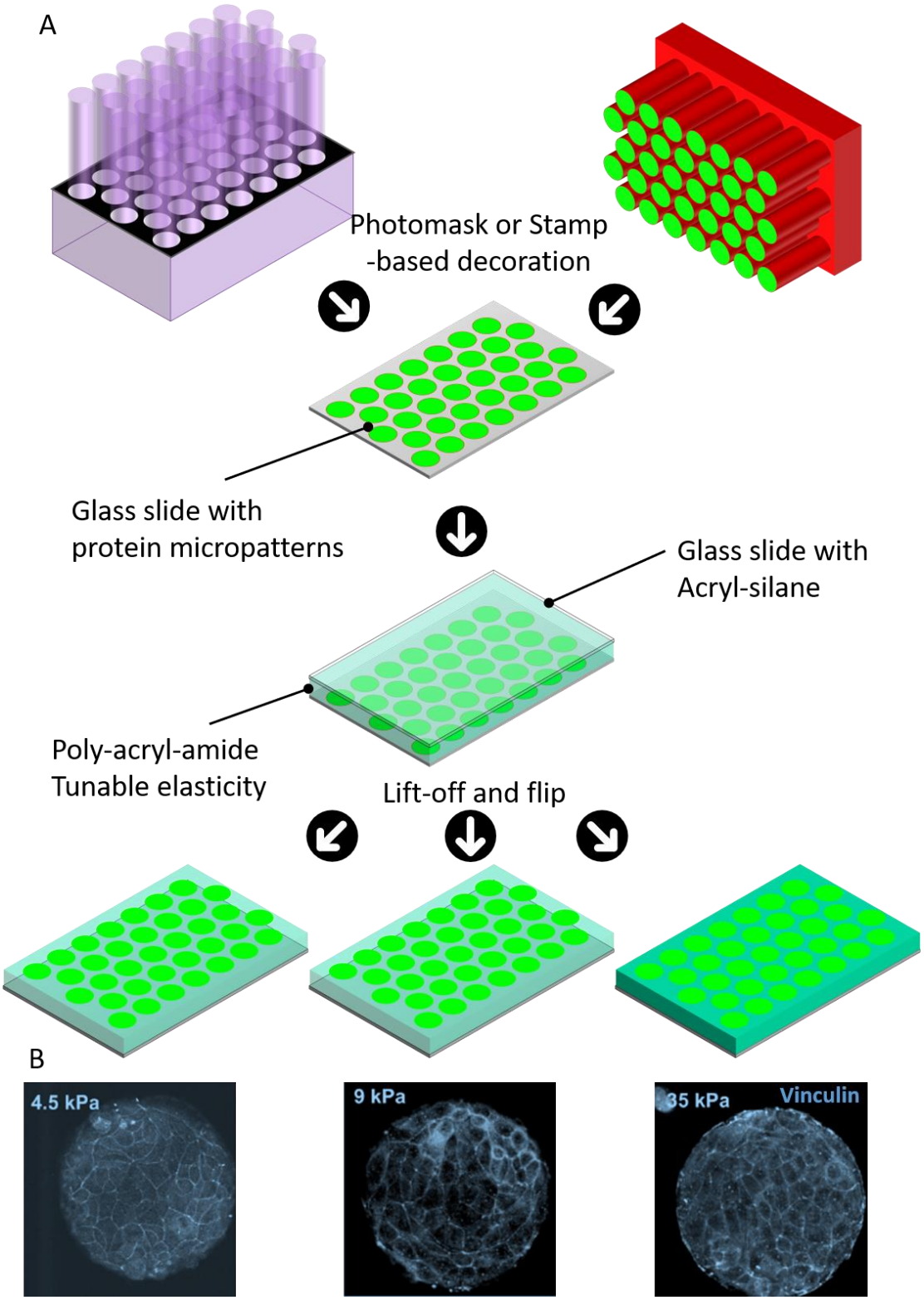

Figure 42 **| *Lift-off decoration workflow.***

Extracted from Force-dependent binding of vinculin to α-catenin regulates cell-cell contact stability and collective cell behavior B. Ladoux Molecular Biology of the Cell 2017[88].**A,** lift off workflow were a glass slide (gray) with protein micropatterns (green) is first realized following stamping (red). A poly-acryl amide (light blue) hydrogel is then let to reticulate onto the protein decorations. The proteins are tethered to the poly-acrylamide and removal of the glass slide exposes the decorated areas. Adequate adhesion of the hydrogel is ensured by silanization of the cell culture substrate. Alternatively, the protein micropatterns can be prepared through light-based decoration with a photomask (black with gray trim) and UV (violet) irradiation as was done in the works of Beth Pruitt's group[86]. **A,** epifluorescence microscopy images of the cell's vinculin signal when spread on the gels with varying stiffnesses.

Transferring proteins micropatterns onto an hydrogel was very attractive for us as we had previously developed a quantitative and multiprotein decoration method for glass substrates[22] **(Figure 43)**. We hypothesized that we could use our powerful glass slide decoration and subsequently polymerize hydrogels on top of the protein motif **(Figure 43)**. This would, in theory, allow us to locally tune the rheology via the insolation time which was equally promising. We thus made preliminary experiments **(Figure 44)**.

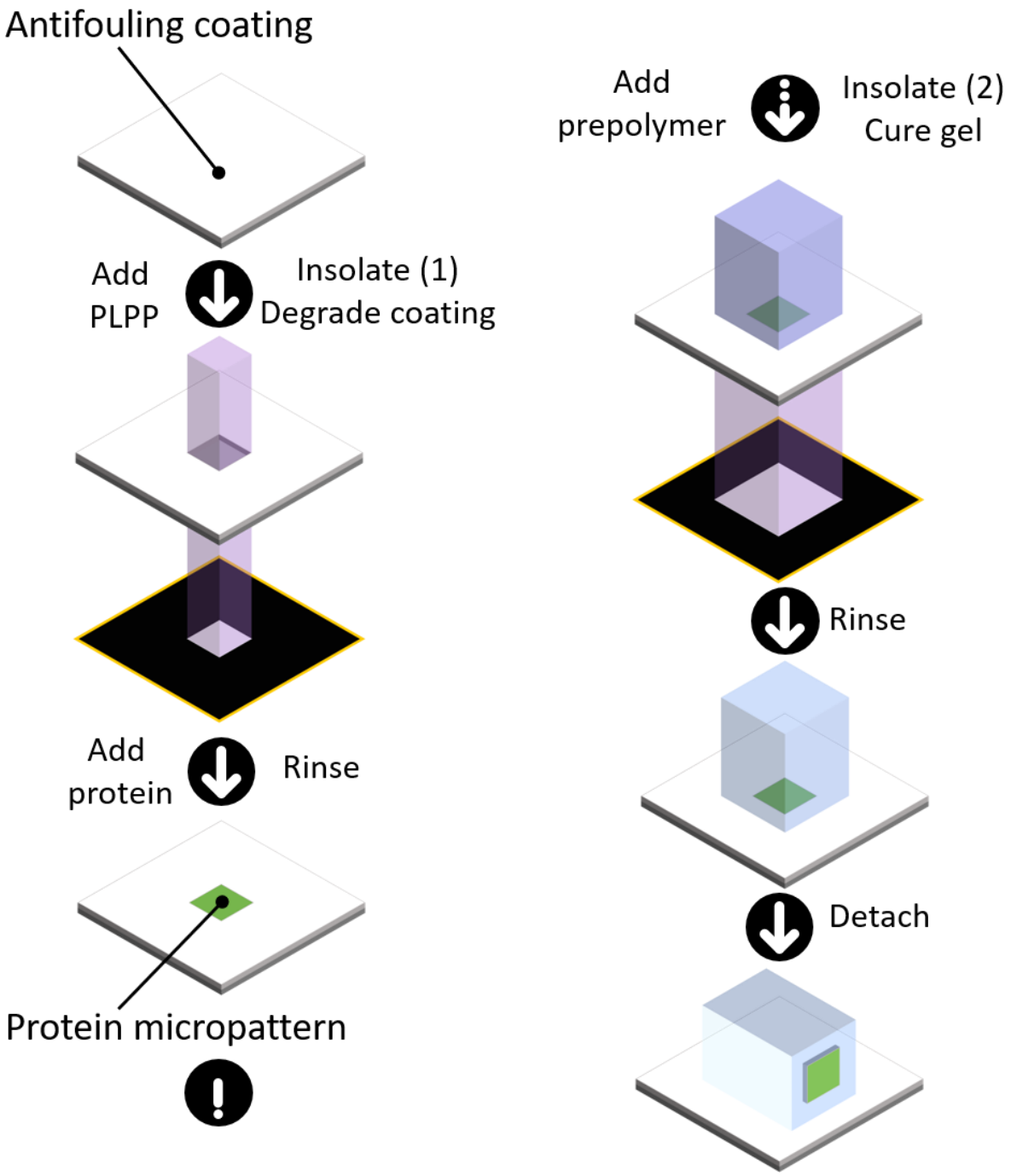

Figure 43 **| *Adapted lift-off decoration workflow.***

First a protein micropattern (green) on a glass slide (gray) with an antifouling coating (white) is generated via photo-induced (violet) degradation. A hydrogel (blue) is subsequently photopolymerized on top of the pattern, carrying the proteins upon detachment.

Methods:

Protein to gel transfer using poly(ethylene-glycol) di-acrylate hydrogels: A glass slide coated with an antifouling layer (Schott-H Coated, Schott Jena , Germany) was first micropatterned using a previously described protocol[22]. Briefly: a solution containing 1X PLPP was incubated and cross patterns were projected for 100 sec using maximum power (3120 mw/cm²) at 20X magnification. The glass slide was rinsed and incubated with 100 ug/mL of Cyanine-5 labelled protein A for 5 minutes before rinsing again. Subsequently a solution consisting of 5% poly(ethylene-glycol) di-acrylate (MW 700, Sigma Aldrich) diluted at 10% in 0.5X PLPP was polymerized on top of the patterns using two successive patterns. A circle and a surrounding square were projected for 15sec using maximal power at 10X magnification (128 mw/cm²).

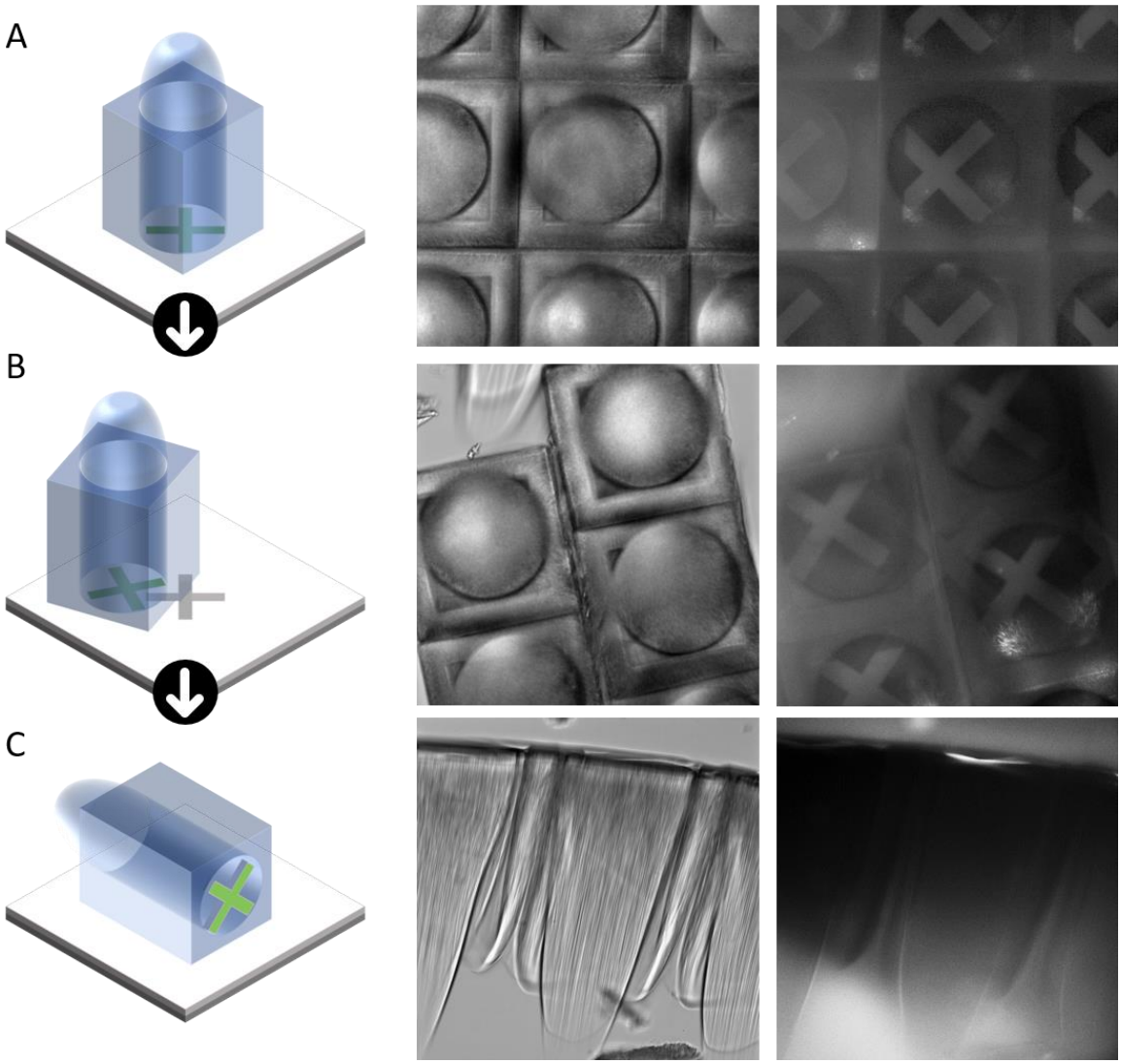

Figure 44 **| *Liftoff patterning using photopolymerized poly(ethylene-glycol) hydrogels.***

A, Schematics, brightfield and epifluorescence images of hydrogel photopolymerized on top of protein micropatterns. **B,** Schematics, brightfield and epifluorescence images of the same hydrogel detached from the glass slide displaying damage and transferred proteins. **C,** Schematics, brightfield and epifluorescence images of the same hydrogel lying from the side.

Analysis:

While the transfer principle works well, the cell culture is unpractical.

The small photopolymerized structures are especially sensitive to physical detachment as the damage in brightfield demonstrate **(Figure 44 B)**. Due to this, flipping the hydrogel blocs upside down once detached is almost impossible and in turn cells do not go in contact with the decoration **(Figure 44 C)**.

It is worth noting that we did not use a silanized substrate to lift the gels from their polymerization glass slide. We planned to implement that step if we were to demonstrate cell adhesion on the patterns. This was unfortunately never the case. A latter experiment shed light on the possible reasons : proteins transferred to the gel were not tagged using antibodies which hints that either the protein were not functional or not accessible anymore.

Conclusions on gel transfer

With sufficient efforts with respect to experimental set-up and choice of materials I am convinced that gel-transfer could work.

Nevertheless, this process showed three fatal flaws for our specific applications:

First and foremost, the decorated sacrificial layer is preferentially a flat glass slide meaning that this technology is not compatible with structured hydrogels which were our main interest.

Secondly, this process induces irradiation and radical reactions over proteins which may deteriorate their function and explain why cells could not attach on the decorated hydrogels. We could follow this effect through the photobleaching of our decorated proteins during the insolation.

Last but not least the protocol's results were highly dependent on the prepolymer's length:

> The transfer was efficient with short poly(ethylene-glycol) precursors (MW 700) yet it proved much more difficult to execute with longer prepolymers. This may explain why gel transfer is traditionally performed and successful with poly(acryl-amide), a very short-strand hydrogel precursor. Further confirming this fact, the works of Moeller and Denisin stated that when the acryl-amide concentration fell below a threshold, the transfer efficiency decreased likely due to changes in the gel's mesh size[86].
>
> The photobleaching effect was also more pronounced when using longer prepolymer strands such as 4-arm-poly(ethylene-glycol)-acrylate (MW > 10K) instead of short precursors. As for the results with frontal polymerization **(See <u>Conclusions on "NOA-Slides"</u>)** we think that the vinyl moieties' density is a critical factor.

These finding motivated our work on the second decoration strategy which was based on photo-linkers. With these molecules, we devised a protocol that would be compatible with structured gels while also preventing proteins from receiving irradiation.

Photo-linkers: bridging poly(ethylene-glycol) and biomolecules

Photo-linkers are hetero-bifunctional ligands made to close the gap between the gel and the biomolecules chemistries[25,46,47]. Each extremity of a photo-linker serves a different purpose: one is a photo-reactive moiety that binds to a vinyl functionalized surfaces under ultra-violet irradiation while the other is an activated-ester which reacts with the amino-groups found in the biomolecule's lysine's and N-terminus. **(Figure 45).**

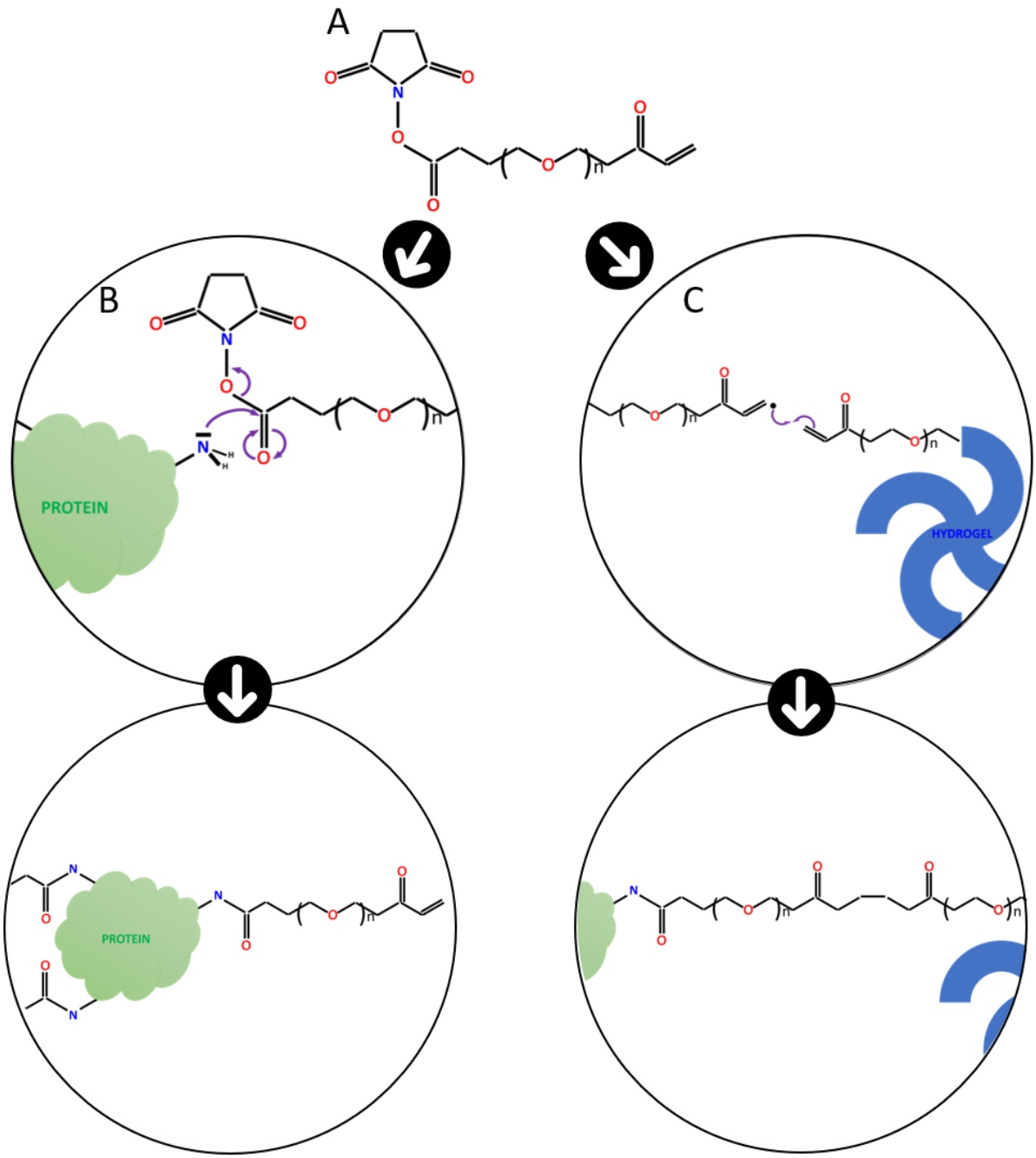

Figure 45 **| *Amide crosslinking and acryl crosslinking.***

A, Chemical structure of the acryl-poly (ethylene glycol)-succinimidyl-valerate photolinker **B,** Formation of an amide bond through nucleophilic substitution. **C,** Formation of a carbon-carbon bond under radical activation (reaction voluntarily simplified for clarity)

It is possible to graft the linker to the biomolecules prior to grafting the couple into the hydrogel via photo-crosslinking as was shown by Ali and colleagues [25] **(Figure 46)**.

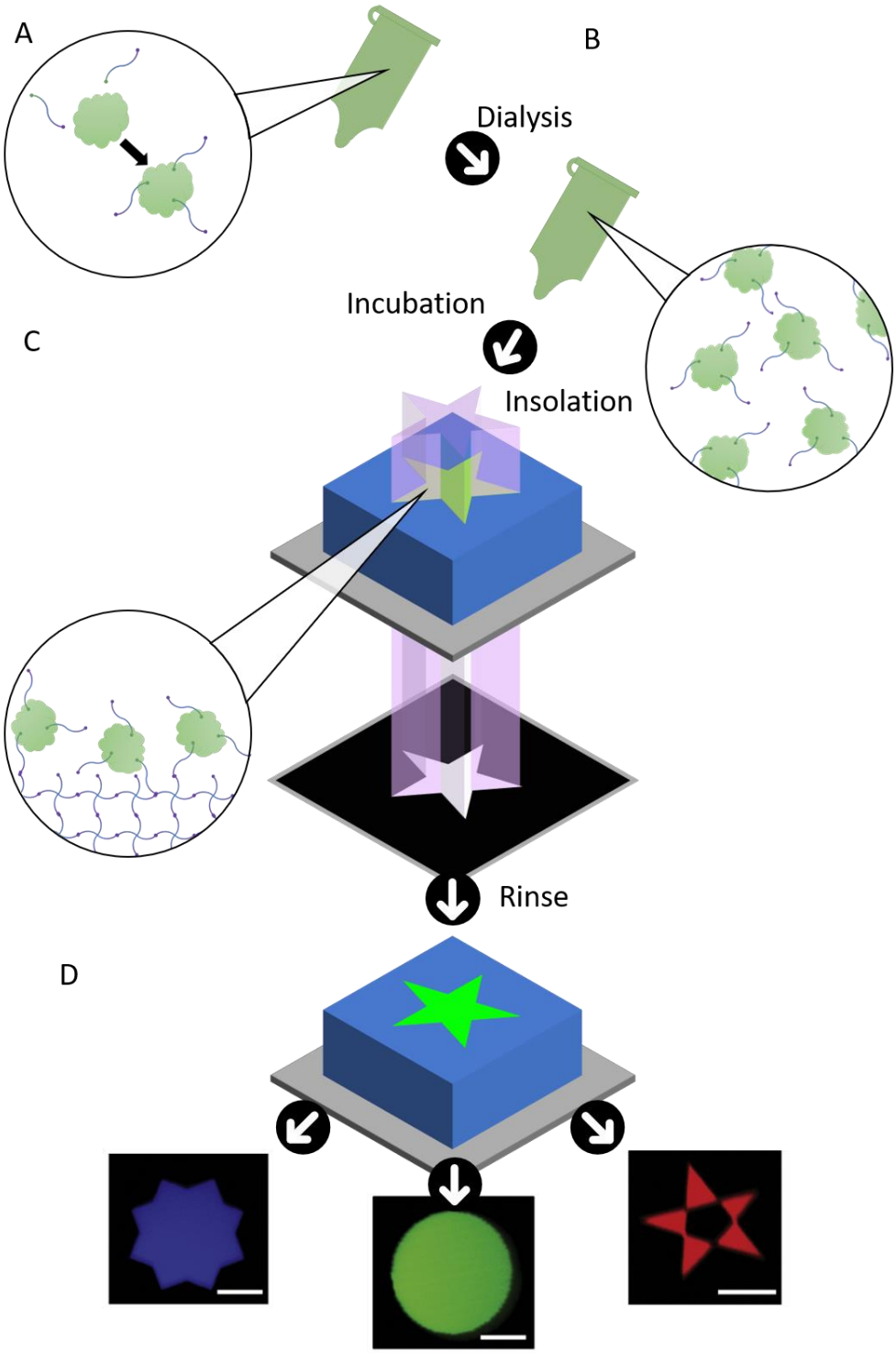

Figure 46* | *A bifunctional ligand to decorate hydrogels.

Adapted and adapted from: Micropatterning of poly(ethylene glycol) diacrylate hydrogels J.L. West Methods in Cell Biology 2014[25] A schematic of the protocol is presented with **A,** Synthesis of photo-graftable biomolecules (green) when mixed with the photo-linker (blue lines with green and purple dots). **B,** Dialysis and purification of the photo-graftable biomolecules **C,** photo-grafting of the biomolecules (green) onto of poly(ethylene-glycol) hydrogel (blue) using photomasks (black with gray trim). **D,** the resulting decorated hydrogel with epifluorescence microscopy images exemplifying the process and its flexibility.

On the upside, activated esters can graft most biomolecules available in a laboratory without any further modification. Additionally, numerous photo-linkers are commercially available making them a good entry-level decoration solution.

On the downside, the linkers must first be grafted to the protein to circumvent the rapid hydrolysis of activated esters in water. This implies a long subsequent dialysis to filter out the linkers that did not react. To make matters worse, the linkers will bind at random onto the protein, often multiple times, and may hinder the biomolecule's functionality. On this topic, the previously described work of Shadish and colleagues[44] **(see Figure 12)** made an extensive series of tests to illustrate the loss of function that random photo-linker binding can induce.

Comparatively, we knew our platform could send photon fluxes orders of magnitude stronger than the photomasks system used in this article. We thus suspected that the grafting time could be lowered down to a minute or two.

Knowing these factors, we twisted the protocol by grafting the linker to the hydrogel first then immediately rinsing and adding poly-L-lysin. Poly-L-lysin provides a cheap, highly-reactive biomolecule that can be concentrated to quickly saturate the grafted photo-linkers before they hydrolyze **(Figure 47)**. The resulting layer is stable, can sustain ethanol sterilization, and promotes proteins adsorption and cell adhesion. We subsequently tested whether this added poly-L-lysin step was hindering or improving cell adhesion **(Figure 48)**.

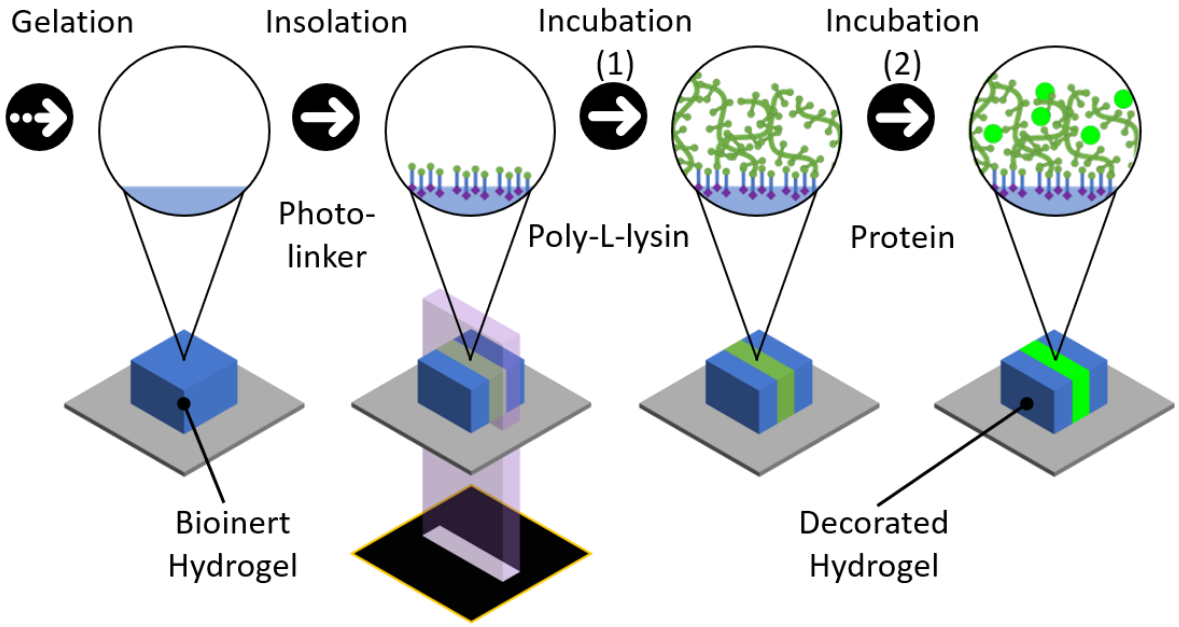

Figure 47 **| *Hydrogel decoration workflow with photo-linkers.***

A bioinert hydrogel (blue) is photopolymerized on a glass slide (gray). Photo-linkers (violet-blue-green sticks) are attached onto the gel surface using patterned illumination in order to subsequently graft poly-L-lysin (green). This creates an adhesive layer onto the hydrogel where proteins (fluo-green) can later adsorb in large quantities.

Methods:

Effect of the poly-L-lysin on cell adhesion: all decoration steps were performed with a 4X magnification objective. A prepolymer solution of 5% 4-Arm-poly(ethylene-glycol)-Acrylate diluted in PLPP 1X was injected inside two wells of a 9 wells microreactors. The gels were crosslinked following 2 minutes exposure inside a ultra-violet oven (UV-KUB). The gels were rinsed with PBS then incubated with PLPP 1X. A solution of 500 mg/mL Acryl-poly(ethylene-glycol)-succinimidyl-valerate (MW 2K) in dimethyl formamide was added to reach a 10% vol/vol final concentration and a square pattern was insolated for 40 sec at 128 mw/cm². Immediately after, one of the gels was rinsed and incubated with 100ug/mL Fibronectin for two hours. The other gel was rinsed with PBS and a 1 mg/mL solution of PolyLysine FITC conjugate was incubated for 1 hour followed by 100 ug/mL of fibronectin for 10 minutes. The two gels were incubated in cell culture medium at 37C° prior to cells seeding. Cells were allowed to sediment and adhere for 30 minutes. The non-adherent cells were washed away by pipetting up and down over the hydrogel. Brightfield images were taken before and after the washing procedure.

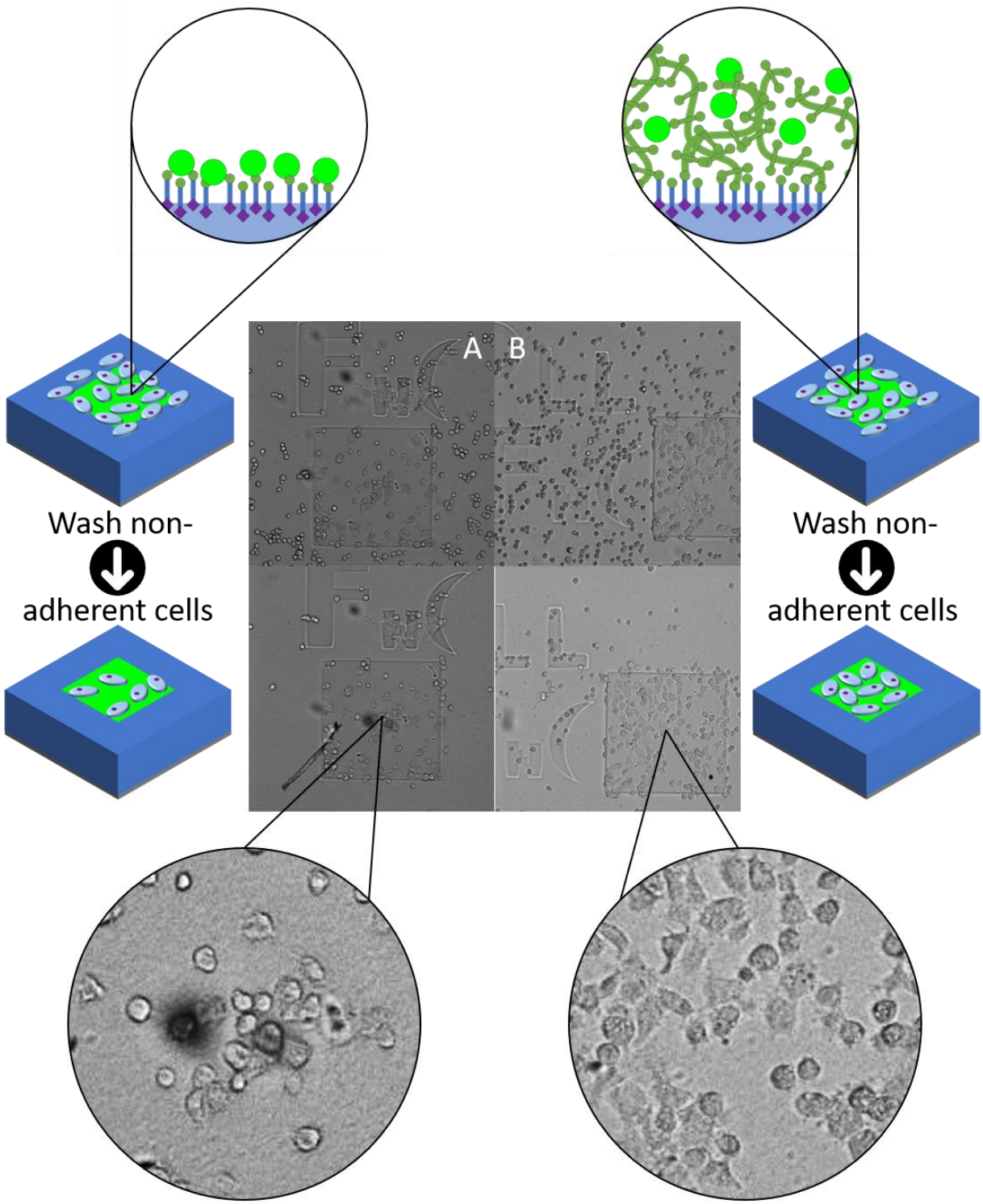

Figure 48 **| *Poly-L-lysin improves cell adhesion on poly(ethylene-glycol) hydrogels.***

A Left panel, Schematics and brightfield microscopy with close up image illustrating cell adhesion on hydrogels where proteins are directly attached to the photo-linker. **B Right panel,** Schematics and brightfield microscopy with close up image illustrating cell adhesion on hydrogels where proteins are adsorbed onto a poly-L-lysin layer.

Analysis:

As the result show, the intermediate step of poly-L-lysin incubation improves cell adhesion on hydrogels. The number of cells is not only higher in the right panel but they are also more spread **(Figure 48 B)**. This could be explained in two ways: i) There are more proteins adsorbed to the poly-L-lysin than grafted on the hydrogel. ii) The negatively-charged cell membrane physically adsorbs to the poly-cationic poly-L-lysin layer accelerating the cell adhesion.

The success of this methodology led us to expand to protocol on various applications such as the generation of immobilized gradients and the culture of neurons **(Figure 49)**. Both were highly important as neurons are sensitive cells that are better cultivated on soft substrates while gradients are key tools for the tutoring of cells.

Methods:

Controlling neural growth on hydrogels: All decoration steps were performed with a 4X magnification objective. A prepolymer solution of 5% 4-Arm-poly(ethylene-glycol)-Acrylate diluted in PLPP 1X was injected inside two wells of a 9 wells microreactors. The gels were crosslinked following 2 minutes exposure inside a ultra-violet oven (ultra-violetKUB). The gels were rinsed with PBS then incubated with PLPP 1X. A solution of 500 mg/mL Acryl-poly(ethylene-glycol)-succinimidyl-valerate (MW 2K) in dimethyl formamide was added to reach a 10% vol/vol final concentration and a grid of 6-pointed stars was projected for 40 sec at 128 mw/cm².Immediately after, the gels were rinsed with PBS and a 1 mg/mL solution of PolyLysine FITC conjugate was incubated for 1 hour. The gels were rinsed again with PBS and incubated with a 100 ug/mL solution of laminin for 10 minutes at 37C°. At last, E18 rat primary cortical neurons were seeded in complemented neurobasal. The cell culture was then carried for one day to allow cells to spread before fixing and imaging.

Gray scale decoration: All decoration steps were performed with a 4X magnification objective. A prepolymer solution of 5% 4-Arm-poly(ethylene-glycol)-Acrylate diluted in PLPP 1X was injected inside two wells of a 9 wells microreactors. The gels were crosslinked following 2 minutes exposure inside a ultra-violet oven (ultra-violetKUB). The gels were rinsed with PBS then incubated with PLPP 1X. A solution of 500 mg/mL Acryl-poly(ethylene-glycol)-succinimidyl-valerate (MW 2K) in dimethyl formamide was added to reach a 10% vol/vol final concentration and concentric circles with different gray values were projected for 40 sec at 128 mw/cm². Immediately after, the gel was rinsed with PBS and a 1 mg/mL solution of PolyLysine FITC conjugate was incubated for 1 hour. The gel was then rinsed with PBS and incubated with a 100 ug/mL solution of fibronectin for 10 minutes at 37C° prior cells seeding. The cell culture was then carried over for two weeks.

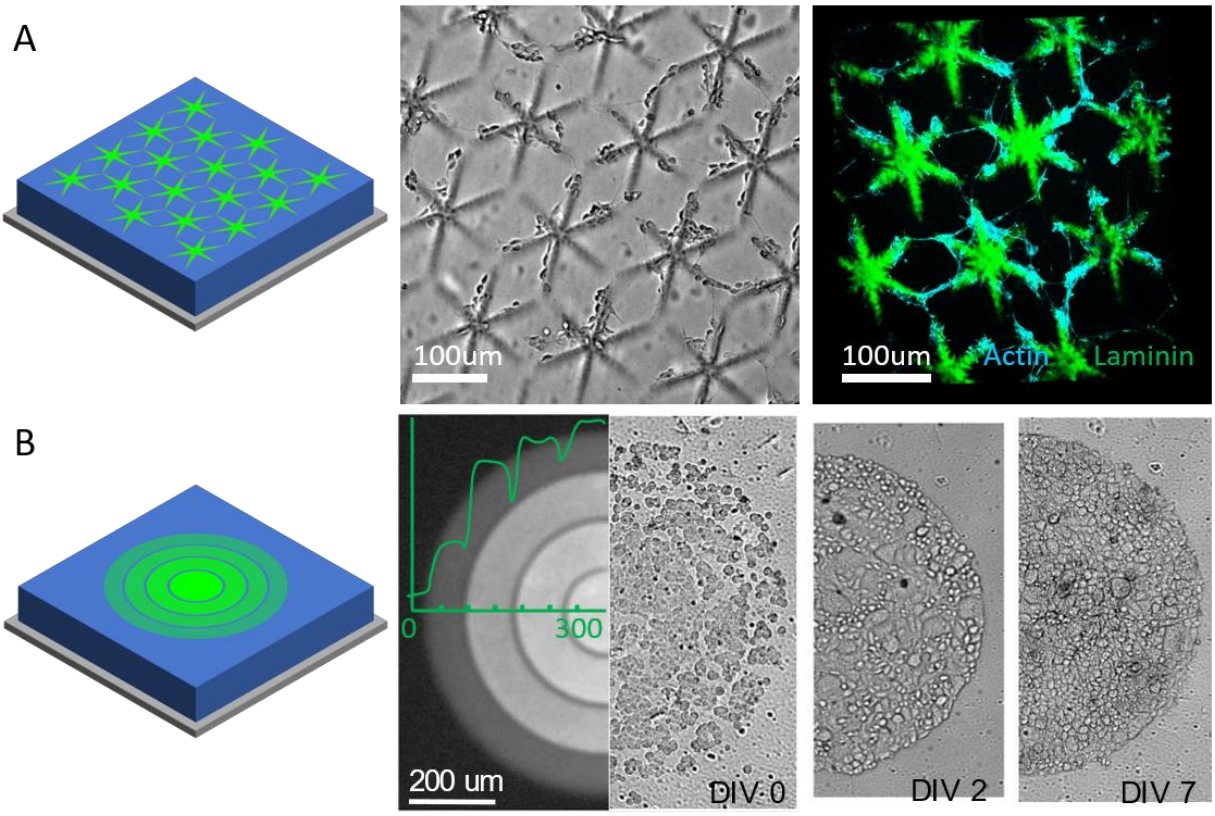

Figure 49 **| *Neuron and Cell culture on flat poly(ethylene-glycol) hydrogels.***

A, Schematics of a hydrogel (blue) decorated with an array of 6-pointed stars (green). Brightfield and epifluorescence microscopy image showing neurons growing on said hydrogel. **B,** Schematics of a hydrogel (blue) decorated with concentric circles of decreasing intensity (green). Brightfield and epifluorescence microscopy image showing cos-7 cells growing on said hydrogel.

Analysis:

The culture of neurons on standardized hydrogels represents an important validation step **(Figure 49 A)**. Neurons are sensitive to toxic compounds and their successful growth and polarization on the photopolymerized hydrogels confirms the latter's biocompatibility. We observed that the neuron's somas gather on the decorated areas however neurites seem to maintain a high degree of freedom despite the anti-adhesive properties of poly(ethylene-glycol).

We also demonstrate that the grayscale projection capabilities of the digital micromirror device allow for quantitative decoration **(Figure 49 B)**. In the experiment above, cell lines initially spread according to the decorated biomolecule's density. After seven days in culture, the cells populated the whole decorated area but didn't spread outside of it.

We pursued the application of the photo-linkers by combining decoration and structuration.

Synergy: queuing structure with decoration

Biochemical function and structure must work in concert to guide the cell behavior. The first part of this manuscript highlighted the structuration capacities of our platform **(See Chapter's conclusion: kinetics to control Z)** while the second presented photo-linkers as powerful chemicals able to decorate hydrogels. These molecules bypass the need for physical contact as in gel transfer and as such they are perfect to decorate topographies **(Figure 50)**. In this last part on hydrogel decoration, we design cell culture templates that combine topographical and biochemical features to highlight the synergy of structuration and decoration **(Figure 51)**.

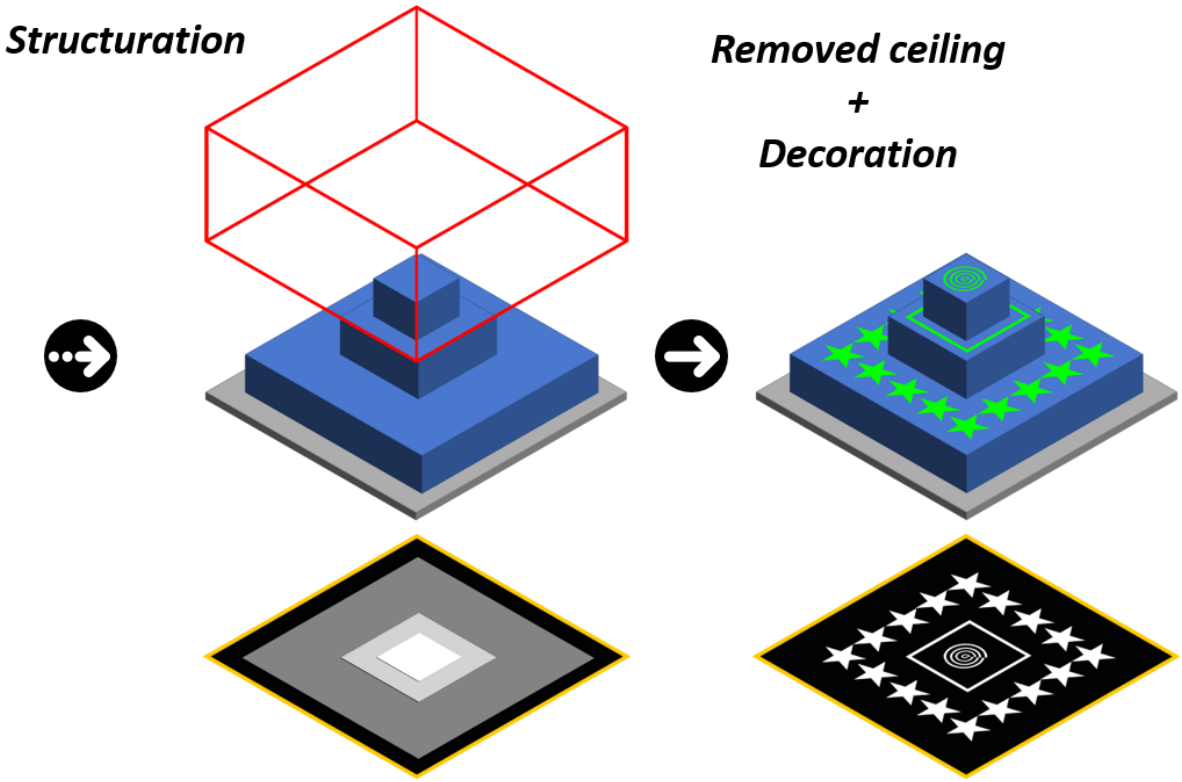

Figure 50 **| *The synergy between structuration and photo-linker decoration***

Schematics illustrating the capacity to create an hydrogel shape (blue) and subsequently decorate I (green) using the platform.

Methods:

Decoration of shaped hydrogels: The decorated "Aztec temple" hydrogel results from the gelation of a prepolymer solution of 5% 4-Arm-poly(ethylene-glycol)-Acrylate diluted in PLPP 1X. To create the pillar, a square pattern was insolated during 36 sec at max power: 128 mw/cm² with argon perfusion. A second and third stage were added when two peripheral square are successively projected at 128 mw/cm² during 36 sec and during 70 sec at 26,5 mw/cm² under air atmosphere respectively. The gels

were rinsed and PLPP 1X was then incubated inside the wells followed by a solution of 500 mg/mL Acryl-poly(ethylene-glycol)-succinimidyl-valerate (MW 2K) in dimethyl formamide to reach a 10% vol/vol final concentration. Immediately after, a pattern consisting of stars, square and spirals was aligned and insolated onto the preexisting structure for 120 sec at 128 mw/cm² using the registration features of the Leonardo software. Immediately after, the gel was rinsed with PBS and a 1 mg/mL solution of PolyLysine FITC conjugate (MW 15K-30K) was incubated for 1 hour. The gels were rinsed with PBS and imaged using a homemade confocal microscope.

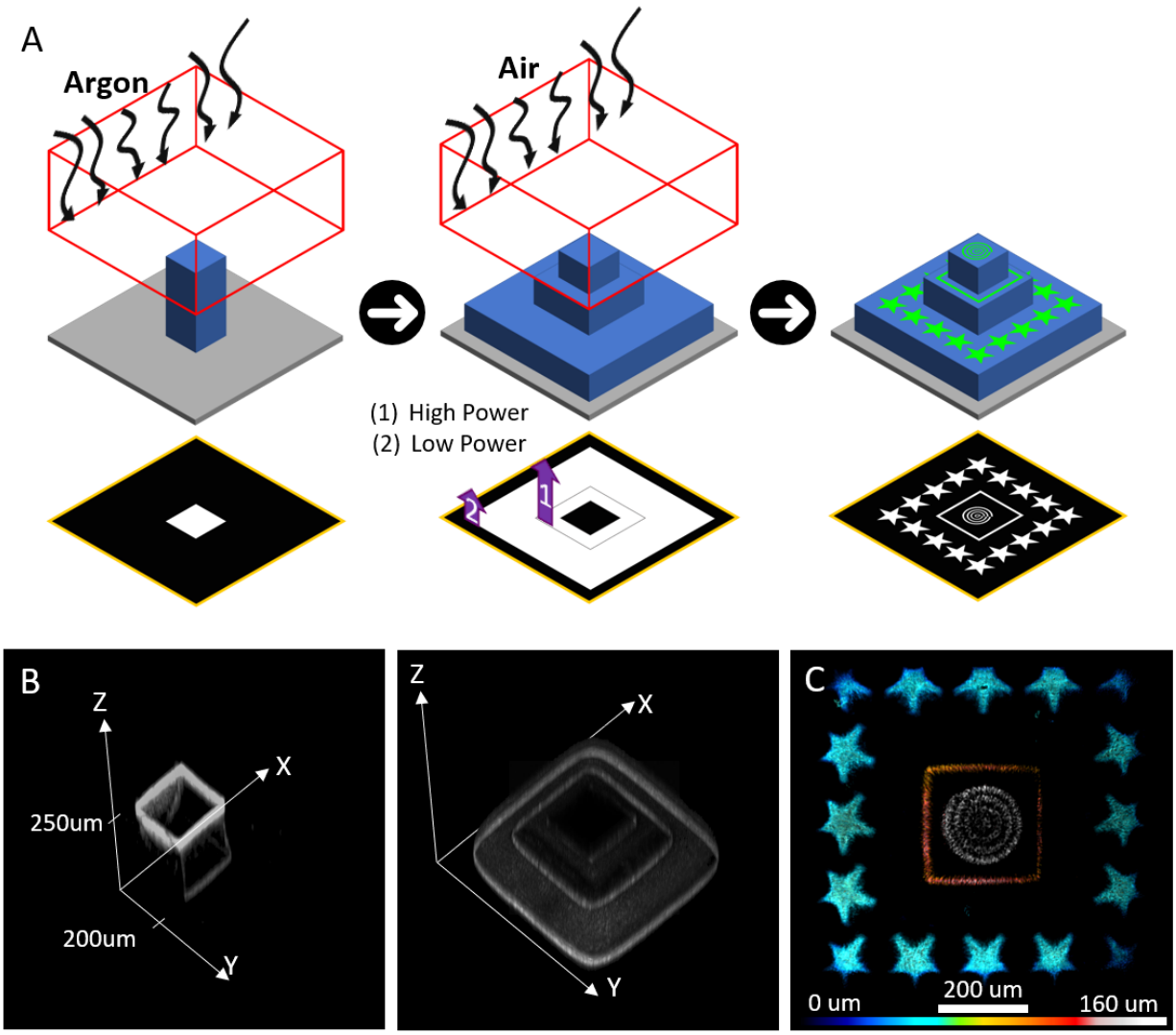

Figure 51 **| *Realization of a decorated hydrogel pyramid.***

A, Schematics of the process: a hydrogel pyramid (blue) is cured via gas-controlled and flux-controlled polymerization under a silicone ceiling (red). The ceiling is removed to ease the decoration (green) step that will add a spiral a cadre and 5-pointed stars on each stage respectively. **B,** 3D reconstruction of the hydrogels during the structuration steps. **C,** Z-color coded confocal microscopy image of the decorated hydrogel pyramid.

Analysis:

This experiment serves as a proof of concept highlighting that we can easily create hydrogels that have shape and biochemical patterns. We drew each pattern to align with each other and used the microscope's camera and software to align the decoration onto the structure. On the confocal imagery **(Figure 51 C)**, one can observe that the decoration is mostly located on the gel's surface: each decorated stage presents a single tone from the color code instead of a blend. This likely comes from two factors: First, our insolation time is kept low preventing the photo-initiator and photo-linker from diffusing deep in the gel. Second, the high molecular weight poly-L-lysin we used could not easily diffuse through the short mesh in the subsequent incubation.

This workflow served as the starting point for the fabrication of standardized cell-culture templates both for cell lines and neurons **(Figure 52)**.

Cell culture: topographical and chemical cues combined

With this synergistic structuration and decoration package we tested the possibility to precisely position cells on topographies. We were particularly interested in studying neuron's behavior on such templates as neurons are known to be sensitive to both chemical[89] and structural[90] patterns. We thus generated simple shape such as domes , waves, and wells and sought to decorate these shapes with aligned motifs of adhesion.

Methods:

Shaping and decoration of hydrogels for cell culture:

All structuration and decoration steps were performed with a 4X magnification objective. The polymerization steps were done as follow for each specific structure:

To generate the microwells and domes for cell lines, a prepolymer solution of 5% 4-Arm-poly(ethylene-glycol)-Acrylate diluted in PLPP 1X was injected inside one well of a 9 wells microreactors. An all-white pattern was insolated at 26.5 mw/cm² during 90 seconds. Then a second pattern consisting of wells was projected at 128 mW/cm² during 30 sec. Alternatively, a second grayscale pattern consisting of big domes (pattern 10 Supp.3) was projected at 128 mw/cm² for 3 minutes.

To generate Big domes and Waves for neurons, grayscale of the corresponding structures were insolated at 128 mW/cm² during 3 minutes. Afterwards a support pattern was added at 128 mW/cm² during 40 sec. in order to facilitate further neurons seeding. The gel were rinsed with PBS and incubated with PLPP 1X prior to decoration. A solution of 500 mg/mL Acryl-poly(ethylene-glycol)-SVA MW 2K in DMF was added to reach a 10% vol/vol final concentration and a doughnut pattern for the wells and small domes an array of 6-pointed stars for the big domes and waves, was insolated for 120 sec at 128 mW/cm².

Immediately after the gel were rinsed with PBS and a 1 mg/mL solution of PolyLysine FITC conjugate was incubated for 1 hour. The gels were rinsed again with PBS and incubated with a 100 ug/mL solution of fibronectin (Wells, small domes) or laminin (Big domes, waves) for 10 minutes at 37C° prior cells seeding. In wells and on small domes COS-7 cells were seeded in complete cell culture medium (DMEM, FBS). On big domes and waves E18 rat primary cortical neurons were seeded in complemented neurobasal. The cell culture was then carried for one day to allow cells to spread before fixing and imaging.

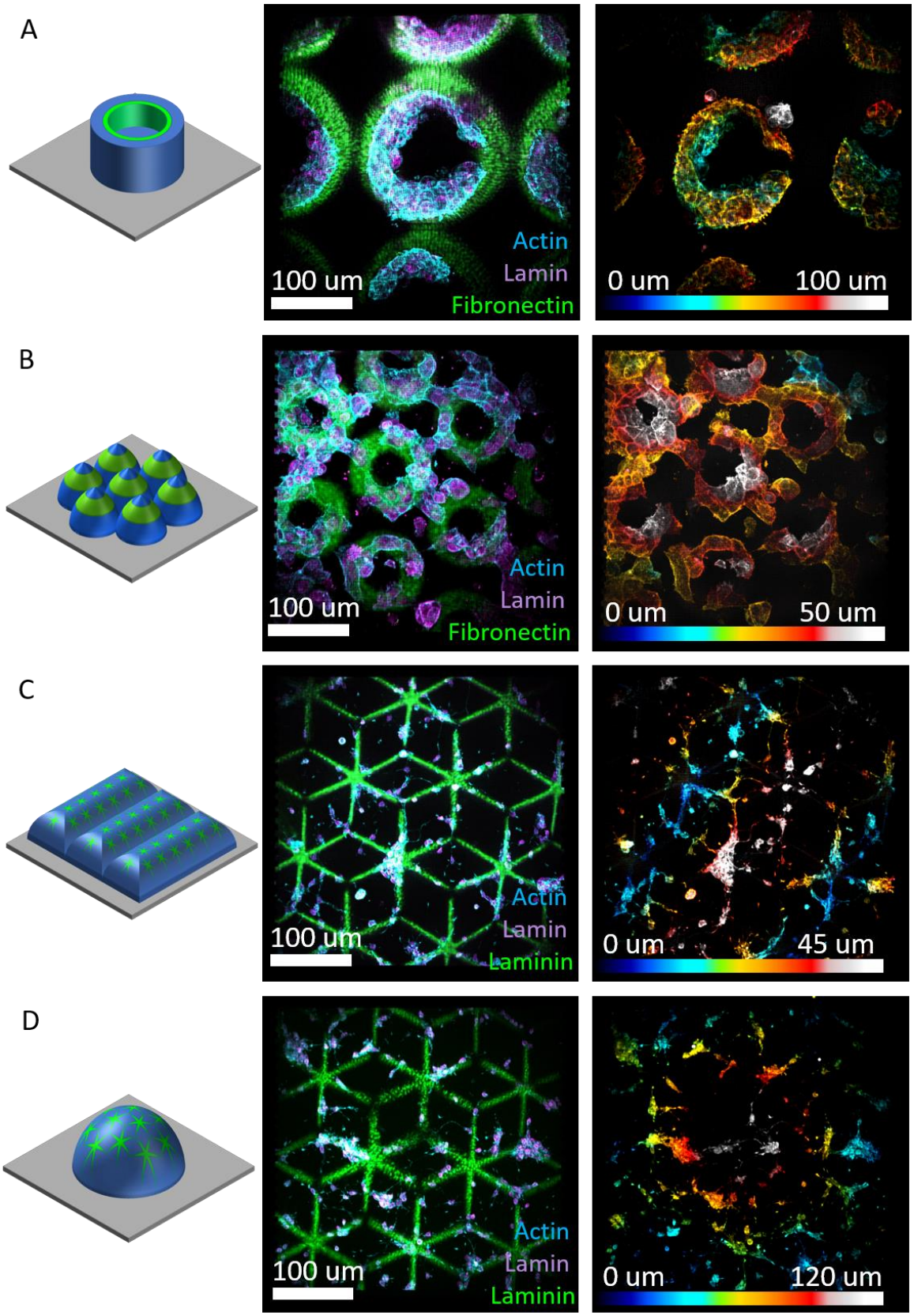

Figure 52 **| *Queuing structuration and decoration for cell culture.***

Left Panels, Schematics of the hydrogel structure (blue) and decoration (green). **Middle panels,** Multicolor confocal microscopy images of the respective hydrogels populated with cells (A,B) and neurons (C,D) **Right panels,** Z-color coded confocal microscopy image of the cellularized templates showing the actin signal each time.

Analysis:

The results show the same previously observed tendency: cell lines grew with respect to both the topographies and the chemical cues **(Figure 52 A B)**. The neuron's soma did the same however the neurites spread almost at random **(Figure 52 C D)**.

This can be explained in two ways. First, there is a tendency for neurites to stretch once they come in contact often bridging across non adhesive area. Second, poly(ethylene-glycol) may not be antiadhesive enough so that the neurites can grow regardless. Numerous efforts have been made to create materials that are more cell repellant than poly-ethylene glycol such as poly-2-methyl-oxazoline[89] however, to date, these material do not exist as hydrogel precursors.

Here we only promoted adhesion on specific places of the structures. With neurons we are especially interested in finding configurations where the decoration and structure actually compete for the neurite's guidance. On this prospect, the work from Virlogeux et Al in 2018[91] should provide a starting point for axonal guidance through structural cues.

It would also be interesting for later experiment to decorate non-adhesive molecules such as guidance and polarization cues on cups that promote spheroid formation. In such case the poly-L-lysin may be detrimental however as it would promote nonspecific adherence.

Chapter's conclusion: Are linkers superior?

In this chapter, we first tried to transfer proteins from micropatterns to photopolymerized hydrogels. Despite numerous attempts we couldn't observe cellular adhesion on the patterns transferred onto hydrogels. Stiff gels (molecular weight < 700) had a good transfer yield which did not translate in cellular adhesion likely because the proteins were not accessible/functional anymore. Additionally, detaching the hydrogel from the glass slide in a gentle manner became increasingly difficult as softer (and longer) gels were implemented.

Photo-linkers were then tested. Used in conjunction with poly-L-lysine, they proved to be an effective solution. The poly-L-lysine acted like an intermediate, ensuring fast reaction time at critical step while subsequently allowing protein adsorption and cell adhesion. We demonstrated that this workflow could be adapted to multiple cell types. We also applied it to quantitatively graft biomolecules and thus generate adhesion gradients. Photo-linker decoration was successfully queued with hydrogel structuration to tailor hydrogel micro-niches that supported the culture of cell lines and neurons.

From this perspective photo-linkers may appear strictly superior but as the next paragraph will demonstrate, each technology has to face a tradeoff:

Gel transfer was not suitable for tridimensional structures but it was perfect at preserving the gel's rheology which is not the case for our photo-linker protocol. Our photo-linker works in conjunction with a photo-initiator and the latter is likely to induce further crosslinking within the mesh while we decorate. We tested initiator-free alternatives to this linker yet they were less stable because of a different activated ester (N-hydroxy-succinimide).

Gel transfer could also theoretically decorate hydrogels that weren't light sensitive such as agar-agar while this vinyl-terminated photo-linker would only work on gels that display the same vinyl moieties … or so it seemed.

In fact, we successfully performed the decoration protocol on amide linked-poly (ethylene glycol) and agar-agar demonstrating that acryl-displaying gels were not a necessity. We were puzzled as to why this process was possible and it became clearer when we looked at our photo-initiator properties.

As it shows, we had greatly underestimated the implications and applications of our photo-initiator. The next chapter will thus cover the unique properties of our photo-initiator such as native crosslinking and photo-scission.

Chapter 3
Going Wide

Introduction

In the coming years, photo-engineering commonplace-hydrogels may become a serious concern.

Photo-chemistry on hydrogels is traditionally supported by two mandatory components: photo-initiators as a source of radicals and precursors with adequate chemical modifications. Native hydrogels with no chemical modifications are considered insensitive towards photo-initiators.

Hydrogel-centric laboratories invested in chemistry to photo- gelify[31–34], degrade[9,16,41,42] or decorate[16,44,45] their favorite matrix but for the same to happen in a biological context is very unlikely. Biologists mostly stick to commonplace (and native) materials namely : Matrigel[20,30,53,59,82], Agar[56,57] and poly-(acryl-amide)[80,83,87].

When it comes to engineering Matrigel or Agar, benzophenone-based photo-initiators have unique properties which may prove instrumental. Often shunned because other photo-initiators display better cytocompatibility and/or yield, this chapter aims at shedding new light on these molecules.

As an introduction, we will take a closer look at the topic of photo-initiators to better highlight the unique properties of the benzophenone photophore and its potential applications.

Benzophenones: a deeper dive in the world of photo-initiators.

Photo-initiators are classified in two categories **(Table 4)**: Type I photo-initiators which break upon irradiation forming two radicals and type II which abstract hydrogen from molecules (co-initiators) to form the radicals **(Table 4 column 1)**. The generated radicals then start reactions (gelation, grafting or scission) granted that the gels are properly functionalized.

For gelation and grafting, free radicals react preferentially with electron rich sites such as double-bonds and atoms with many free electron pairs such as Sulphur. For photo-release and photo-degradation, ortho-nitrophenyl moieties are embedded within the gel's backbone and will degrade upon insolation with ultraviolet light.

Three photo-initiators are commonly used in hydrogel engineering each with distinct yield or cytocompatibility advantages **(Table 4 column 2, column 3)**.

Our photo-initiator (PLPP), and benzophenones in general, are type II initiators with the capacity to abstract hydrogens from C-H bonds upon 365 nm irradiation[23]. Said otherwise, benzophenone can effectively generate radicals from essentially anything that has C-H bonds and all hydrogels register in this category. This is what makes benzophenone equally liked and despised: the chemistry is generic and thus difficult to canalize into a specific reaction.

In the experimental section below, the combination of gas permeable microreactors and digital light processing set-up great conditions to precisely monitor and study these reactions.

In a first part, we'll pick up where we left in the second chapter with the decoration of native hydrogels. We will subsequently demonstrate the gelation of native hydrogels under the same conditions. Together these results will devise a generic crosslinking mechanism tying decoration and gelation.

Doing so will also unravel another, long-suspected, oxygen-driven mechanism that we describe in the second section. Here, the combination of oxygen inhibition and hydrogen abstraction yields to photo-scission: the photo-induced liquefaction of hydrogels. Oxygen will thus expand the mechanism described above by linking thickness control and subtractive manufacturing.

Type	Chemical	Main Advantages
Type I 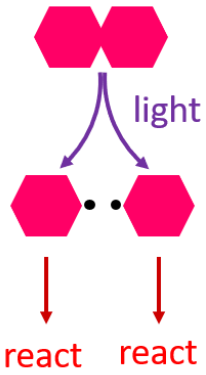	Irgacure 2959 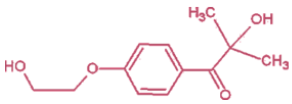	Well documented Optimized for photopolymerization
	Lithium phenyltrimethyl benzoylphosphinate 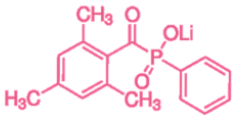	Well documented Optimized for cytocompatibility Degradation products are non-toxic
Type II 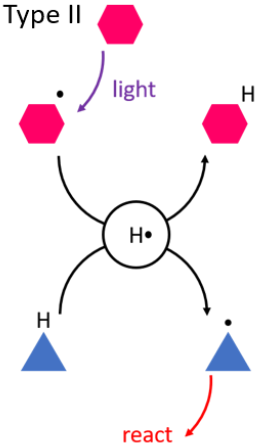	Eosin Y 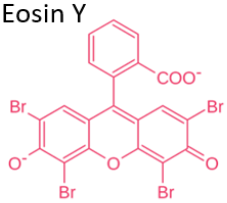	Optimized for cytocompatibility Uses low energy (green) light
	PLPP's benzophenone core 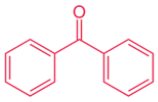	Hydrogen abstraction of carbon Sensitivity towards oxygen Initiates a wide array of reactions

Table 4 **| *Common photo-initiators in hydrogel engineering.***

The type, chemical formula, and properties of each photo-initiator are display in the left, idle and right columns respectively.

Experiments

Decoration of native gels

Benzophenone can graft the photo-linker at the surface of native gels despite the absence of vinyl functionalities **(Figure 53)**. The proposed mechanism is the following:

In the insolated bulk, benzophenone is activated by ultraviolet light **(Figure 53 B)** and in turn abstracts a hydrogel from the vinyl moiety of the linker **(Figure 53 C)**. At the surface benzophenone, abstracts a hydrogen from the hydrogel's back bone **(Figure 53 D)**. This creates a carbo-radical which will subsequently crosslink with the activated photo-linker **(Figure 53 E)**.

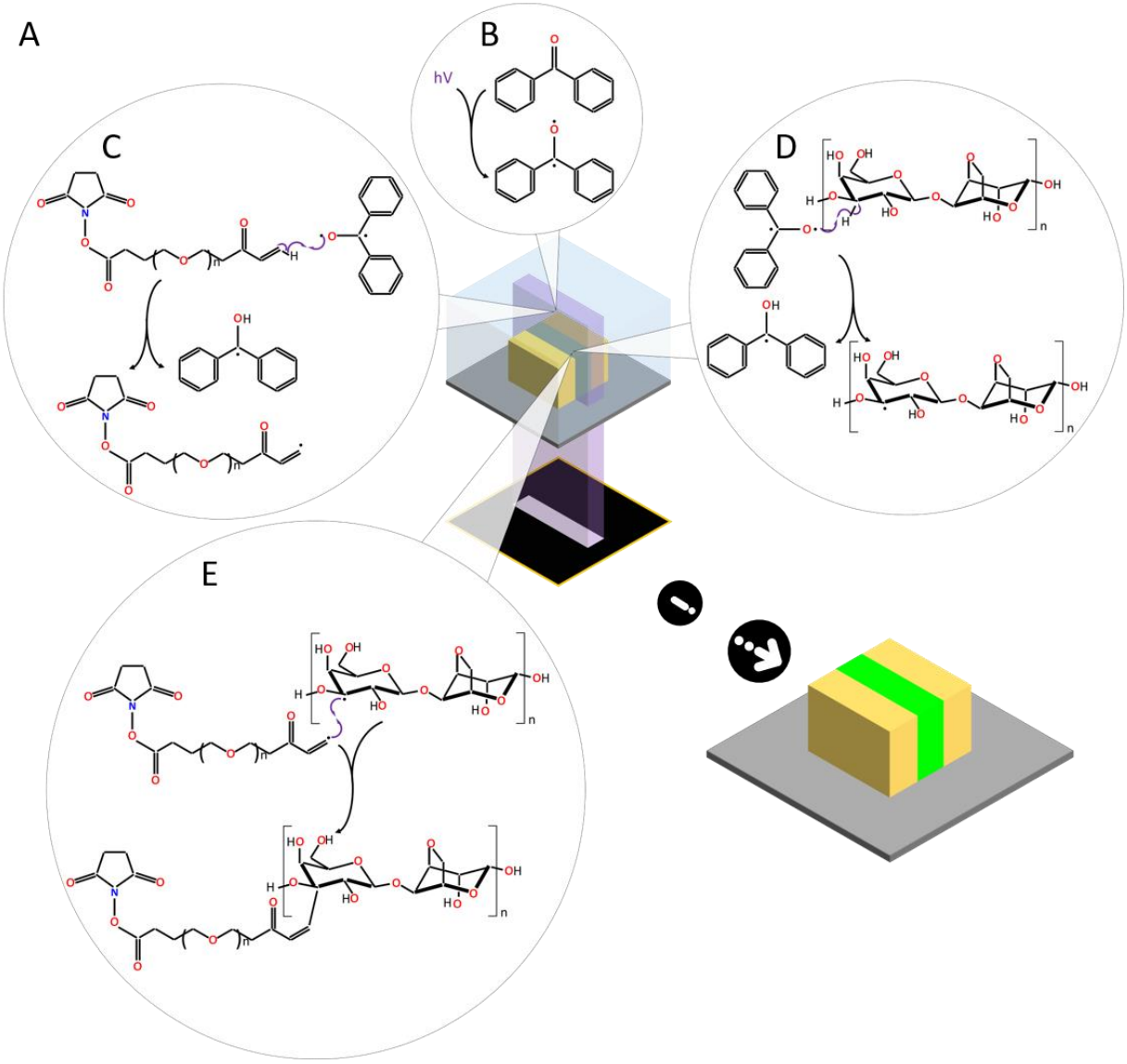

Figure 53 **| PLPP can decorate native materials.**

A, Schematics illustrating the different reactions happening during the insolation (violet) of agar (yellow) in the presence of a photolinker leading to it's subsequent decoration with biomolecules (green). **B,** benzophenone activation under ultra-violet light **C,** hydrogen abstraction of the photolinker **D,** hydrogen abstraction on agar. **E,** crosslinking of the photolinker and agar.

We thus applicated this reaction in the decoration on two relevant hydrogels **(Figure 54)**:

An amide crosslinking poly(ethylene-glycol) hydrogel which, here, serves as an ersatz to other chemically crosslinked hydrogels commonly found in other papers.

And agar, which is the commonplace alternative to poly(ethylene-glycol) as it is also a bio-inert material.

Methods:

Gelation of amide crosslinked poly(ethylene-glycol) : two solutions respectively containing 200mg/mL 4-arm- poly(ethylene-glycol)-succinimidyl-amido-succinate in dimethyl formamide and 200 mg/mL 4-arm- poly(ethylene-glycol)-amine in PBS were diluted and mixed together at a 50/50 ratio to reach 12 mg/ml for each solution. After thoroughly vortexing , the solution was cast into the chambers of silicone microreactors and let to cure for 15 minutes at 70 C° before removing the silicone ceilings.

Gelation of agar: 20mg/mL of agar was diluted in PBS by boiling using a micro-wave oven. the solution was cast into the chambers of silicone microreactors and let to cure for 30 minutes at ambient temperature before removing the silicone ceilings.

Decoration of amide crosslinked poly(ethylene-glycol) and agar-agar:

Amide-linked gels were rinsed with PBS then incubated with PLPP 0,5X mixed with 100 mg/mL of Acryl-poly(ethylene-glycol)-succinimidyl-valerate (MW 2K). The gels were then immediately insolated for 30seconds using maximal power (128mw/cm²) using a 10X magnification. Agar gels were rinsed with PBS and incubated with PLPP 1X prior to decoration. A solution of 500 mg/mL Acryl-poly(ethylene-glycol)-SVA MW 2K in DMF was added to reach a 10% vol/vol final concentration and were then immediately insolated for 100seconds using maximal power (128mw/cm²) using a 10X magnification. Once insolated the gel were promptly rinsed with PBS and a 1 mg/mL solution of PolyLysine FITC conjugate was incubated for 1 hour. The gels were rinsed again with PBS and imaged using brightfield fluorescence microscopy.

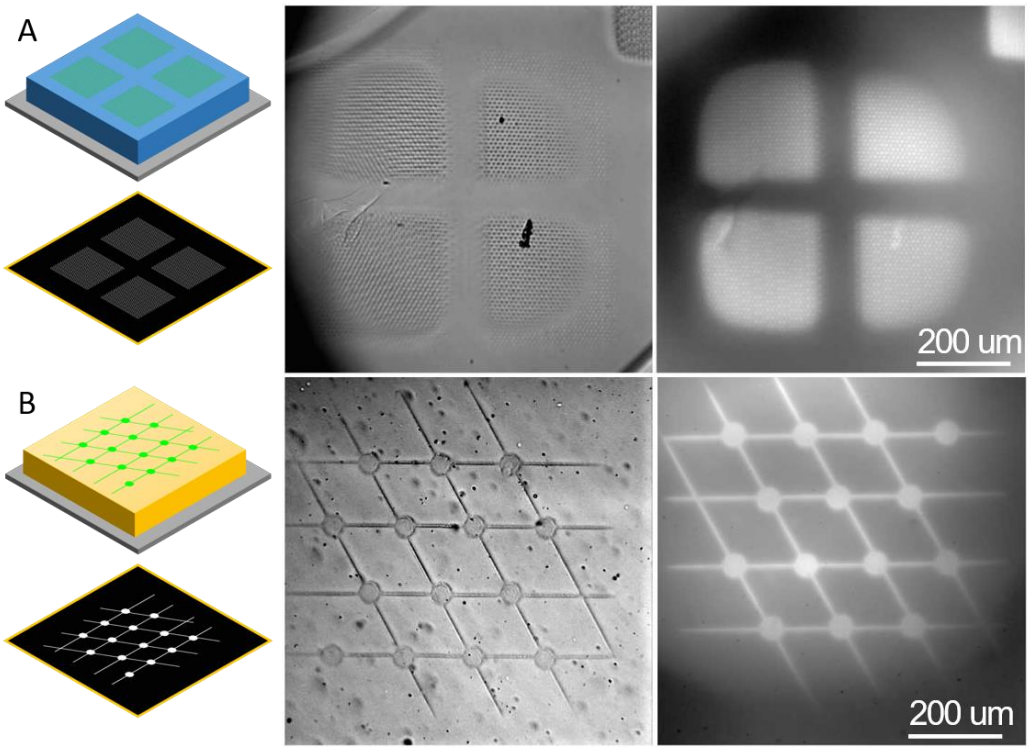

Figure 54 **| *Decoration of native materials: demonstration with amide-poly(ethylene-glycol) and agar.***

A, Schematics brightfield and epifluorescence images showing the decoration of amide linked poly(ethylene-glycol). **B,** Schematics brightfield and epifluorescence images showing the decoration of agar.

Analysis:

In these experiments we used 10X magnification (increasing the power) in order keep the insolation step within reasonable time frames with respect to photo-linker moisture sensitivity. The results show the successful decoration of hydrogels albeit with a lesser yield than vinyl-functionalized hydrogels **(Figure 54)**. This is not surprising: we didn't expect a generic reaction to be as fast and efficient as the dedicated chemistries. On this topic, agar is especially resilient to decoration; this could be explained by the high steric hindrance that comes with hydrogen abstraction in the case of this prepolymer **(Figure 53 E)**. Also, tri substituted carbo-radicals formed upon the abstraction of agar chains are more stable and thus less reactive than bi-substituted (formed upon poly(ethylene-glycol) abstraction).

In the brightfield image for poly(ethylene-glycol) **(Figure 54 A)** one can clearly see an oxygen trimming effect reminiscent to what we previously described during oxygen-controlled polymerization **(see Figure 37)**. From similar and repeated observations, we deduced that "gelation" and "decoration" were in fact the respective bulk and surface facets of "crosslinking" a more generic mechanism which obeys to the rules of oxygen inhibition and depletion. We logically hypothesized that benzophenone would also be able to generate hydrogels out of native precursors.

Gelation of native precursors.

The mechanism we propose for native gelation looks similar to decoration albeit in this case only benzophenone and the precursor are implied and the reaction must happen in bulk **(Figure 55)**. After hydrogen abstraction **(Figure 55 C)**, the carbo-radicals formed on the precursors must reach with each other to form crosslinks **(Figure 55 D)**. Above a material-specific threshold, the number of crosslinks lead to the formation of a mesh: gelation occurs.

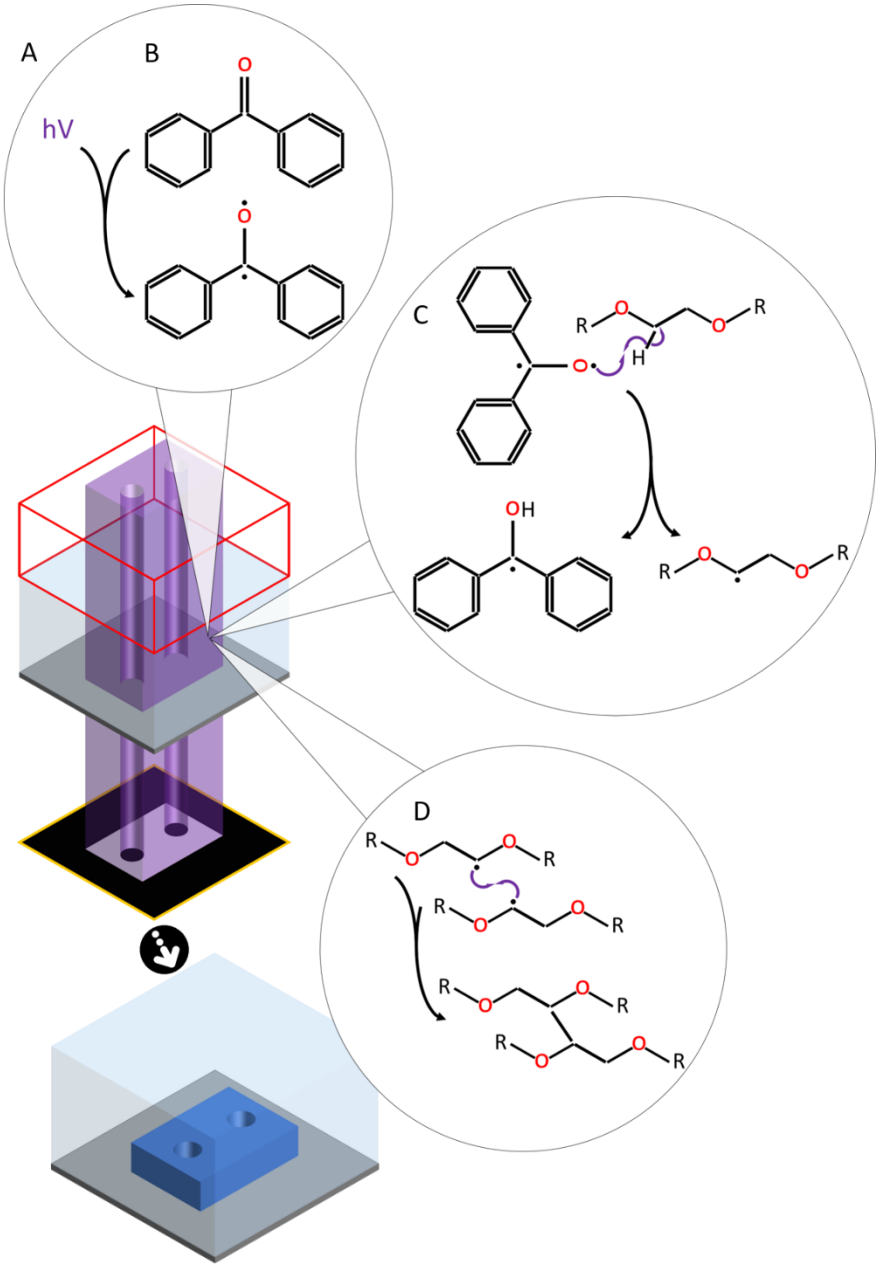

Figure 55 **| PLPP can cure native precursors.**

A, Schematics illustrating the different reactions happening during the insolation (violet) of poly(ethylene-glycol) in the presence of benzophenone leading to the formation of a gel (blue). **B,** benzophenone activation under ultra-violet light **C,** hydrogen abstraction of the precursor **D,** crosslinking of precursors.

As we show in the following experiments, benzophenone are the only photo-initiators capable of such a feat **(Figure 56)**. However, the precursor's chain length and ramification also play a crucial role: the probability to form a stable tridimensional network within the insolated boundaries depends on these two parameters **(Figure 57)**.

Methods:

Comparing photo-initiators in the crosslinking of native molecules: Three solutions containing 10% poly(ethyleneglycol) (Molecular Weight = 20 KDa) were supplemented with 7mg/mL of Irgacure 2959 , Lithium phenyltrimethyl benzoyl phosphinate and PLPP. Each solution was incubated in a separate microreactor and insolated with ultra-violet at maximum power (128 mw/cm^2) and 20X magnification for 120, 80 and 40 sec respectively. The reactors were then rinsed with PBS. Bright field pictures were taken before and after the rinsing.

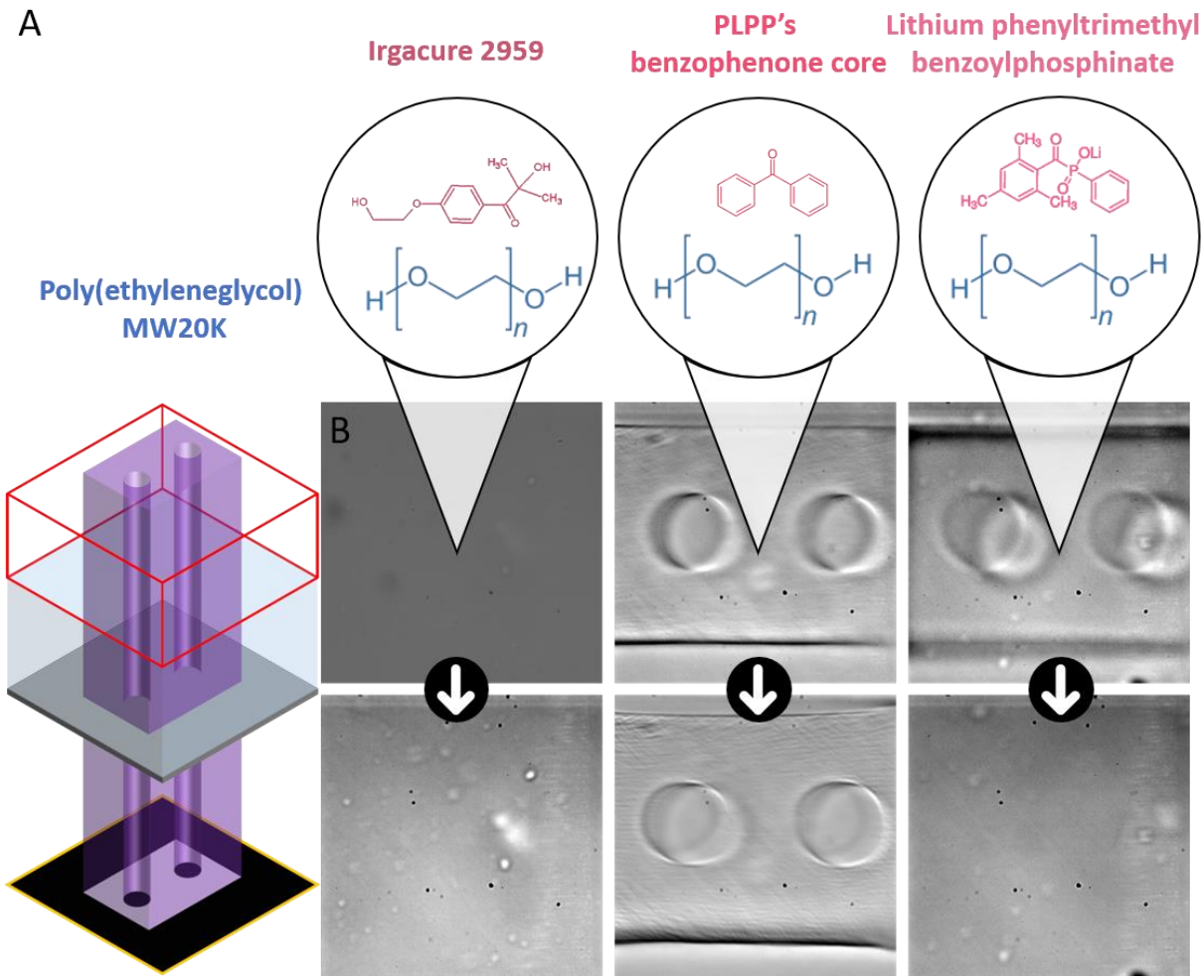

Figure 56 **| *PLPP is critical for native gelation.***

A, Schematics of the experimental conditions displaying the experimental set-up (left panel) and the monomer (blue) and photo-intiators (pink) chemical structures. **B,** Brightfield microscopy images taken during the insolation (above) and after rinsing the unreacted monomer (below).

Effect of chain length on native crosslinking: Three solutions respectively containing 50mg/mL of poly(ethylene-glycol) molecular weight 8000, poly(ethylene-glycol) molecular weight 20000 and 4-arm-poly(ethylene-glycol)-acrylate molecular weight 10000 were mixed with 0.75X PLPP . Each solution was separately insolated at maximal power (128 mw/cm²) with 10X magnification until a gel was observed.

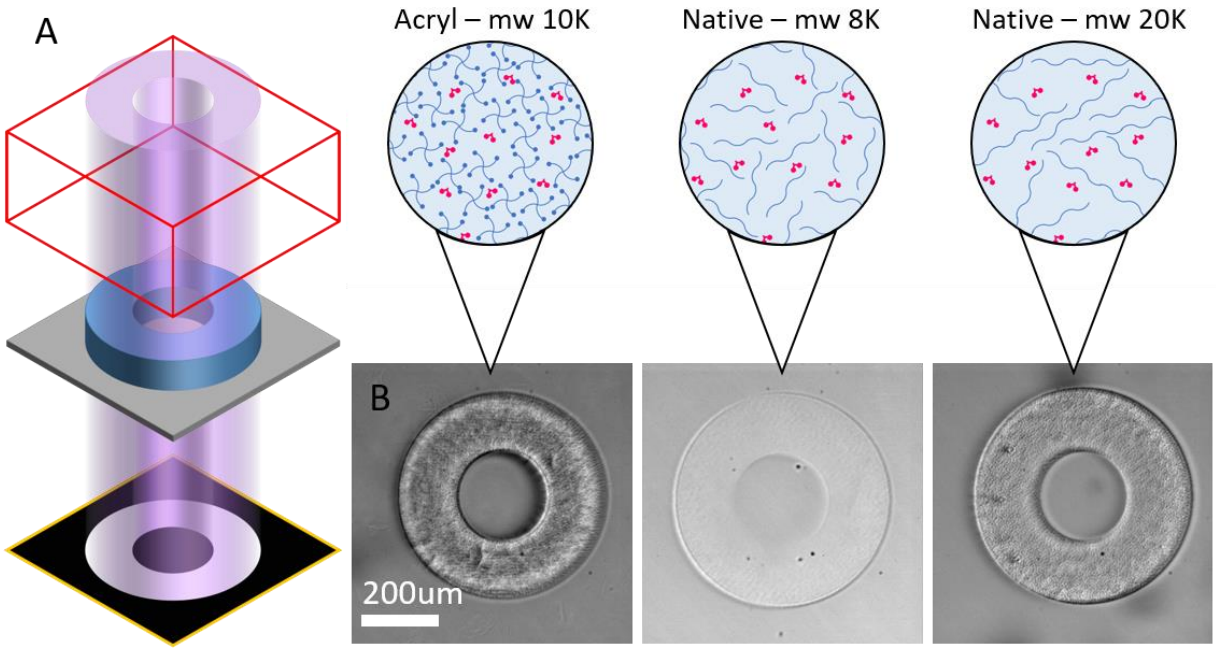

Figure 57 **| *Monomer chain length impacts the crosslinking yield.***

A, Schematics of the experimental conditions displaying the experimental set-up (left panel) and the monomer (blue) and photo-intiators (pink) schematic representation. **B,** Brightfield microscopy images taken after rinsing the unreacted monomer (below).

Analysis:

In the first experiment, PLPP emerges as the only photo-initiator able to cure hydrogels from prepolymers lacking photopolymerizable groups **(Figure 56)**. We insolated with Irgacure for a long period of time without noticing any effect **(Figure 56 B left)**. When using Lithium phenyltrimethyl benzoyl phosphinate, a distinct insolation motif appears then progressively fades to completely disappear upon rinsing **(Figure 56 B right)**. With the benzophenone photo-initiator, a gel forms and stays after rinsing, one can also observe that the gel starts to swell **(Figure 56 B middle)**. This may be the consequence of a few numbers of crosslinks within the mesh as a same tendency was observed with acrylate-terminated precursors when insolated for short periods (**see Figure 35**).

Chain's length is also a decisive factor to reach the crosslinking threshold (upon which the gel becomes stable) **(Figure 57)**. We observed that shorter strands led to unstable hydrogels that would collapse and eventually dissolve upon rinsing **(Figure 57 middle)**. Longer chains formed swelling but stable gels **(Figure 57 left)**.

Conclusions on native-crosslinking

Through hydrogen-abstraction, PLPP is able to decorate and crosslink hydrogels that lack vinyl moieties. Both reactions display a sensitivity towards oxygen hinting that they are in fact two facets of the same crosslinking mechanism. Even though the native precursors take longer to react, this offers new decoration and structuration routes for commonplace materials.

Regarding oxygen, the decoration of poly(ethylene-glycol) brought evidence of a second mechanism occurring beyond the depletion volume **(Figure 58)**. The study of this phenomenon unveiled the photo-scission, an equally generic reaction that leads to hydrogel liquefaction under irradiation. The next section will provide an extensive study of this mechanism as well as providing preliminary cell culture applications.

Photo-scission: Debuts

Decoration and gelation are both crosslinking reactions and are thus both subject to oxygen trimming **(gelation : Figure 37, decoration : Figure 53)**. During decoration however, a gel is already present when oxygen inhibits crosslinking and, together with benzophenone, it can act on the gel's structure **(Figure 58)**. Under the right conditions, one can observe alteration of the gel inside the once-called deadzone **(Figure 58 A D)**.

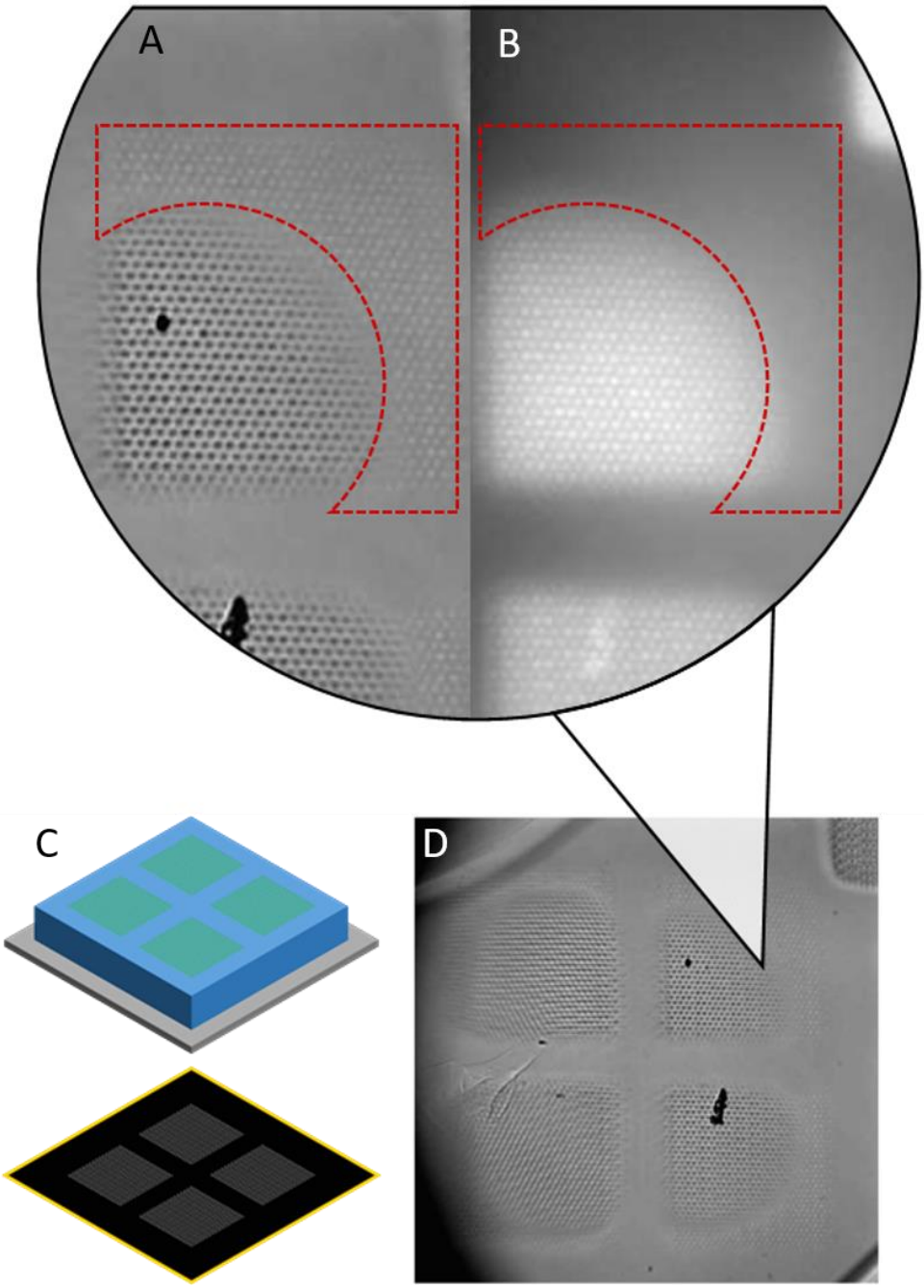

***Figure 58* | Evidence of an oxygen driven reaction observed during native decoration.**

A, Close up of the brightfield microscopy image showing hydrogel alteration (red dotted line) beyond the oxygen depleted volume. **B,** Epifluorescence microscopy image showing the decorated motif with respect to the altered area (red dotted line). **C,** Schematics of the experimental conditions. **D,** Brightfield microscopy image showing the complete decorated motif.

Analysis:

On the gel, one can see the insolated motif split in two zones: core-located "dark" areas and boundary-located "white" areas **(Figure 58 A D)**. The dark area corresponds logically to the crosslinking volume as only these areas were successfully decorated **(Figure 58 B)**. By extension, the white areas are the ones where oxygen inhibited crosslinking just like it does for gelation **(See Figure 37)**. Additionally, the white areas likely correspond to a looser gel because the more a material resembles water is and the whiter it appears in brightfield microscopy. From these observations we deduced that i) a second, oxygen-driven, reaction was at play and ii) this reaction was locally liquefying the gel.

Of note, we highly suspected that this reaction could be photoscission. Indeed we had previously demonstrated the oxygen-driven degradation of brushes made of poly(ethylene-glycol) [22] and reports of polystyrene degradation with oxygen and benzophenone existed in the litterature[51] **(see Figure 14 and Figure 15)**. At the early stages of the project I looked after this reaction without finding any evidence until I started juggling with oxygen inhibition and photon flux. Since tuning the photon flux allowed to monitor oxygen depletion, I wondered what could happen when the flux was low enough to nullify oxygen depletion **(Figure 59)**.

We pursued our experimentations by simplifying the experimental set-up: square patterns where repeatedly projected onto a gel bathed in PLPP. The photon flux was tuned while the overall ultra-violet-dose remained constant.

Methods:

Linking photo-scission with oxygen trimming and crosslinking with oxygen-depletion: to study the relationship between oxygen consumption and scission yield a thin layer of 4-arm-poly(ethylene-glycol)-acrylate was cured inside a 1well microreactor using a ultra-violet-oven for 2 minutes. After incubating 1X of PLPP, photo-scission was carried out at 128 mw/cm² using 1sec laser pulses with 40, 10 and 1% duty cycles. The photo-scissionned gels were subsequently imaged.

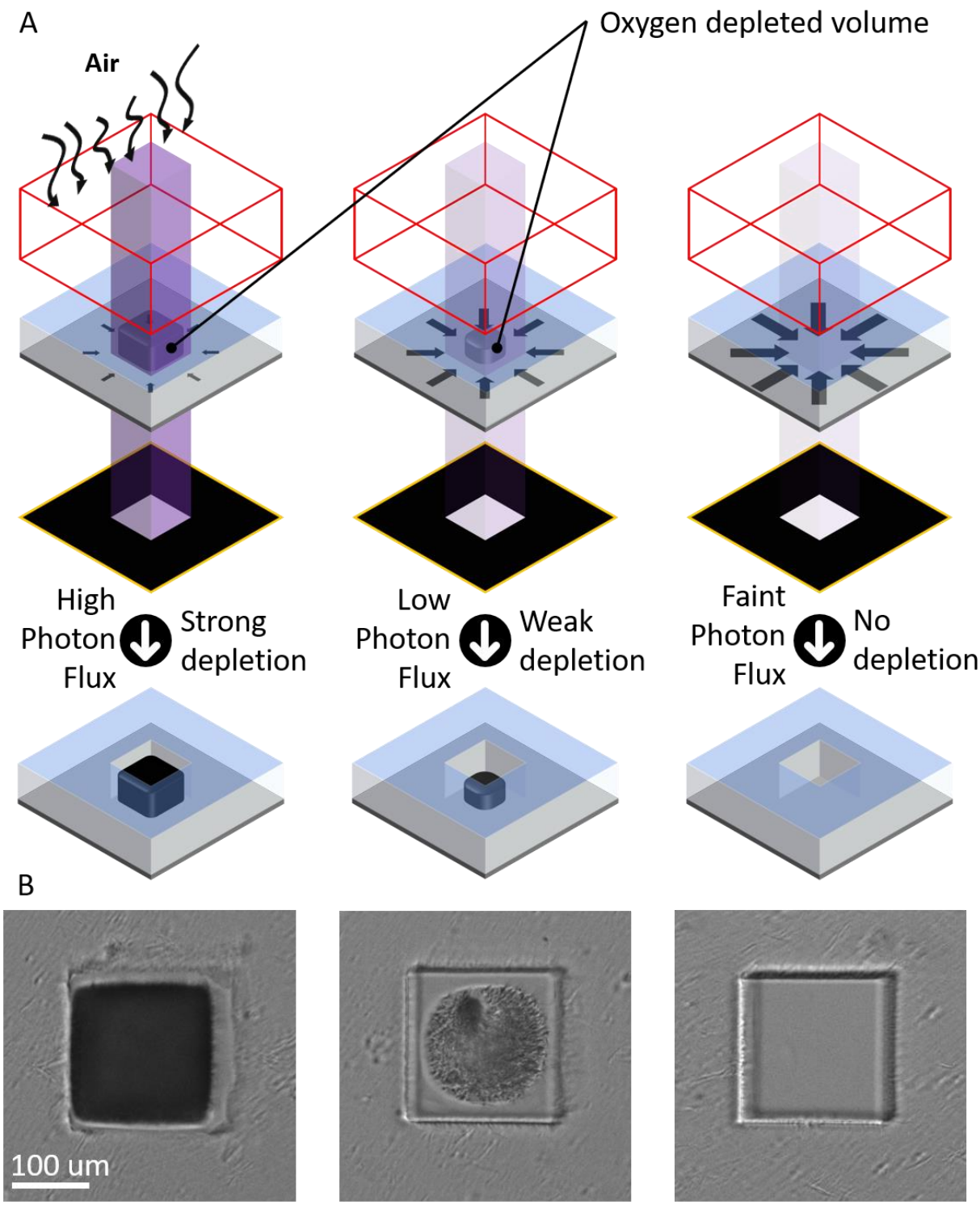

***Figure 59* | Photo-scission depends on oxygen consumption and diffusion.**

A, Schematics of three experimental conditions: in each case a layer of poly(ethylene-glycol) hydrogel (blue) is first cured and rinsed within a micro-reactor (glass in gray and silicone ceiling in red) with air (black arrow) as a source of oxygen. In the first two cases the photon flux (violet) leads to oxygen depletion (black) that induces crosslinking in the core hydrogel while the borders are photo-scissionned. The latter case presents how a faint photon flux prevents depletion and ensures photo-scission. **B,** Brightfield microscopy images of the hydrogels resulting from each experimental condition.

Analysis:

Insolating a cured hydrogel with PLPP will induce its crosslinking: the core of the insolated volume is depleted in oxygen until it reaches a crosslinking threshold **(Figure 59 left and middle panel)**. The insolated area will become darker and may shrink as water exits the mesh **(Figure 59 left and middle panel)**. Core-crosslinking can be reduced by lowering the photon flux or the photo-initiator concentration and in doing so another chemical reaction will take place. In the "oxygen-dominated" boundaries around the crosslinking core, the gel will progressively loosen until it completely fades into small debris in a process, we call photo-scission **(Figure 59 right panel)**.

In this study we used short (centiseconds: cs) laser pulses with a 1Hz frequency to modulate the photon flux and follow its effect on photo-scission. While crosslinking is the dominant reaction above 40 cs, one can still observe photo-scission at the borders of the insolated area **(Figure 59 B left)**. These boundary areas are those most replenished in oxygen due to diffusion clearly indicating that photo-scission depends on oxygen. Photo-scission becomes dominant as the photon flux lowers (10 cs) eventually eclipsing photo-crosslinking completely (1cs) **(Figure 59 B middle and right)**.

In short, photo-scission is characterized by oxygen dependence and is a boundary starting reaction as opposed to core-crosslinking. Like crosslinking, photoscission is generic and can be applied to many hydrogels including the most common. The above-mentioned characteristics made a basis to first optimize the photo-scission of poly(ethylene-glycol) and later extend the reaction to other materials.

Photo-scission: improvements

Taking inspiration from the work of pinto et al[51] on poly-styrene we devised a similar mechanism that explains the photo-scission of poly(ethylene-glycol) **(Figure 60)**.

Upon light activation the PLPP's photophore will abstract a hydrogen from the hydrogel's backbone thus forming a carbo-radical on the mesh **(Figure 60 B C)**.. Alternatively, Di-Oxygen can add onto the carbo-radical forming an hydroperoxyl group which initiates a chain reaction **(Figure 60 D)**. Indeed, the hydroperoxyl will also abstract hydrogens from other meshes leading to the further generation of carbo-radicals **(Figure 60 D)**. From this point on, the mechanism is highly hypothetical: two scission pathways are possible. The hydroperoxyl group may either break upon irradiation forming an oxy-radical and a hydroxyl-radical **(Figure 60 E)**. This oxyradical will then further break leading to chain scission **(Figure 60 E)**. Alternatively, the hydroperoxyl can decompose, breaking the chain while releasing water **(Figure 60 F)**.

There are also parasitic reactions during the photo-scission: two carbo-radicals can bind leading to unwanted crosslinking in the absence of oxygen **(Figure 60 D')**

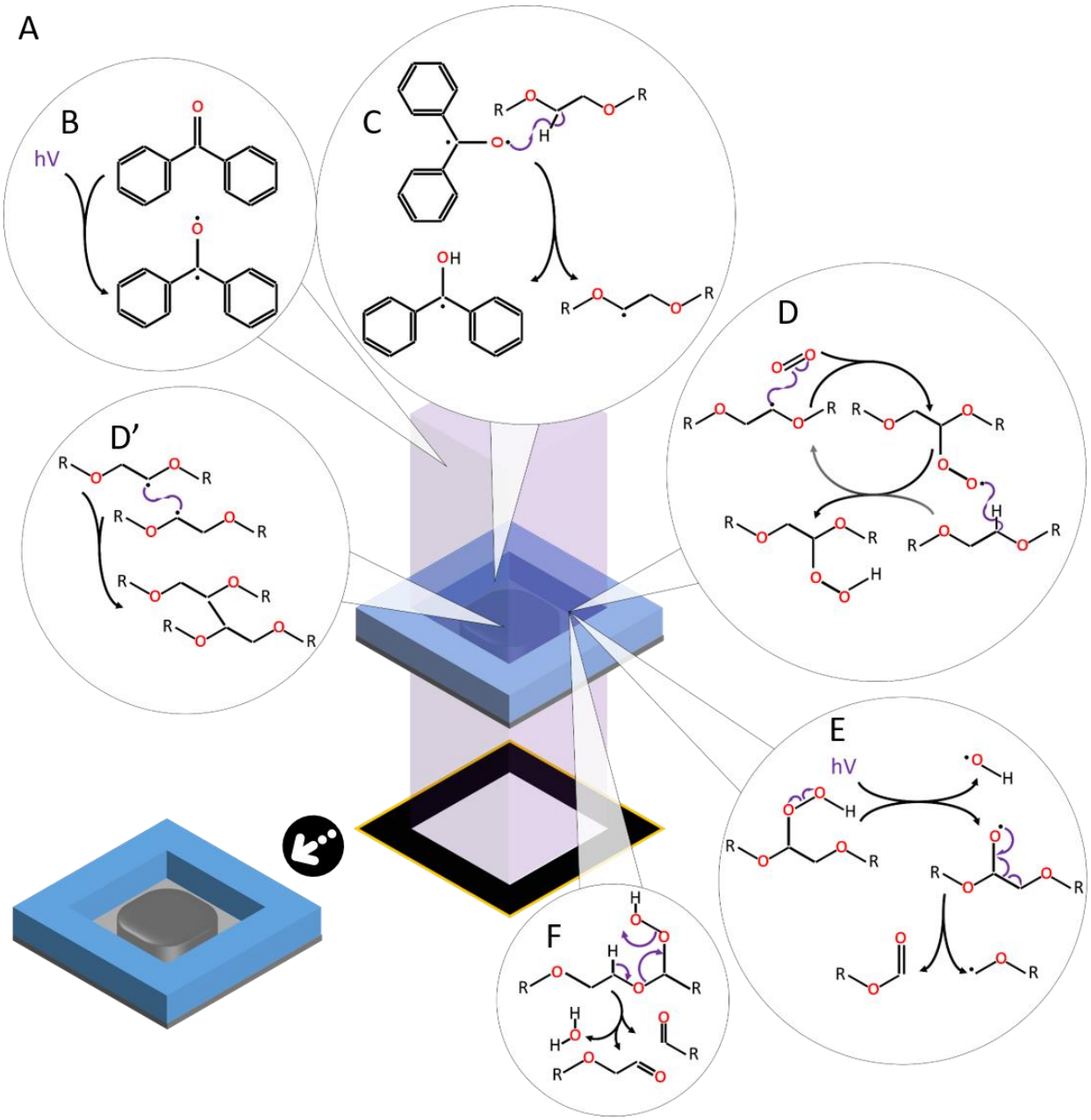

Figure 60 **| *Putative Photo-scission mechanism including parasitic reactions.***

A, here we illustrate the different reactions happening during the insolation (violet) of poly(ethylene-glycol) (blue) in the presence of a photo-linker leading to the co-existence of photo-scission and crosslinking. **B,** benzophenone activation under ultra-violet light **C,** hydrogen abstraction of the gel's mesh forming a carbo-radical **D,** addition of oxygen on the carbo-radical forming a hydro-peroxyl group. Of note, this reaction can loop and further generate other carbo-radicals. **D',** "Parasitic" crosslinking of the mesh. **E,** light induced scission pathway. **E,** Recombination induced scission pathway

The photon flux and the PLPP's concentration are two key parameters in this reaction. They both favor hydrogen abstraction **(Figure 60 B C)**. Additionally, while ultra-violet light also induces hydroperoxyl breaking **(Figure 60 E)**, the photo-initiator may participate in other radical side-reactions that are not displayed for visibility purposes. Ideally one wants to maximize both parameters but in practice this is

not possible due to crosslinking. The appearance of crosslinked areas during photo-scission is tantamount to failure as these areas become increasingly difficult to liquefy the further they reticulate. To ensure successful scission, one must avoid oxygen depletion and thus either decrease the photon flux or photo-initiator concentration. We sought to better understand the contribution of each of these two parameters by testing two extreme cases: low photon flux with concentrated initiator and vice versa **(Figure 61)**.

Methods:

Two modes of photo-scission: a precursor solution of 4-arm-poly(ethylene-glycol)-acrylate at 50mg/mL in PLPP was incubated inside a microreactor. A cube was cured using a short (17sec) illumination at maximum power (128mw/cm²) using 10X magnification. In the first case, after incubating 1X of PLPP, photo-scission was carried out at 1,6 mw/cm² during 3500 seconds. In the second case, after thoroughly rinsing with deionized water and ethanol 0,0125 X of PLPP was incubated. Photo-scission was carried out at 128 mw/cm² during 1200 seconds. In each case a time-lapse of the photo-scission was taken during the reaction.

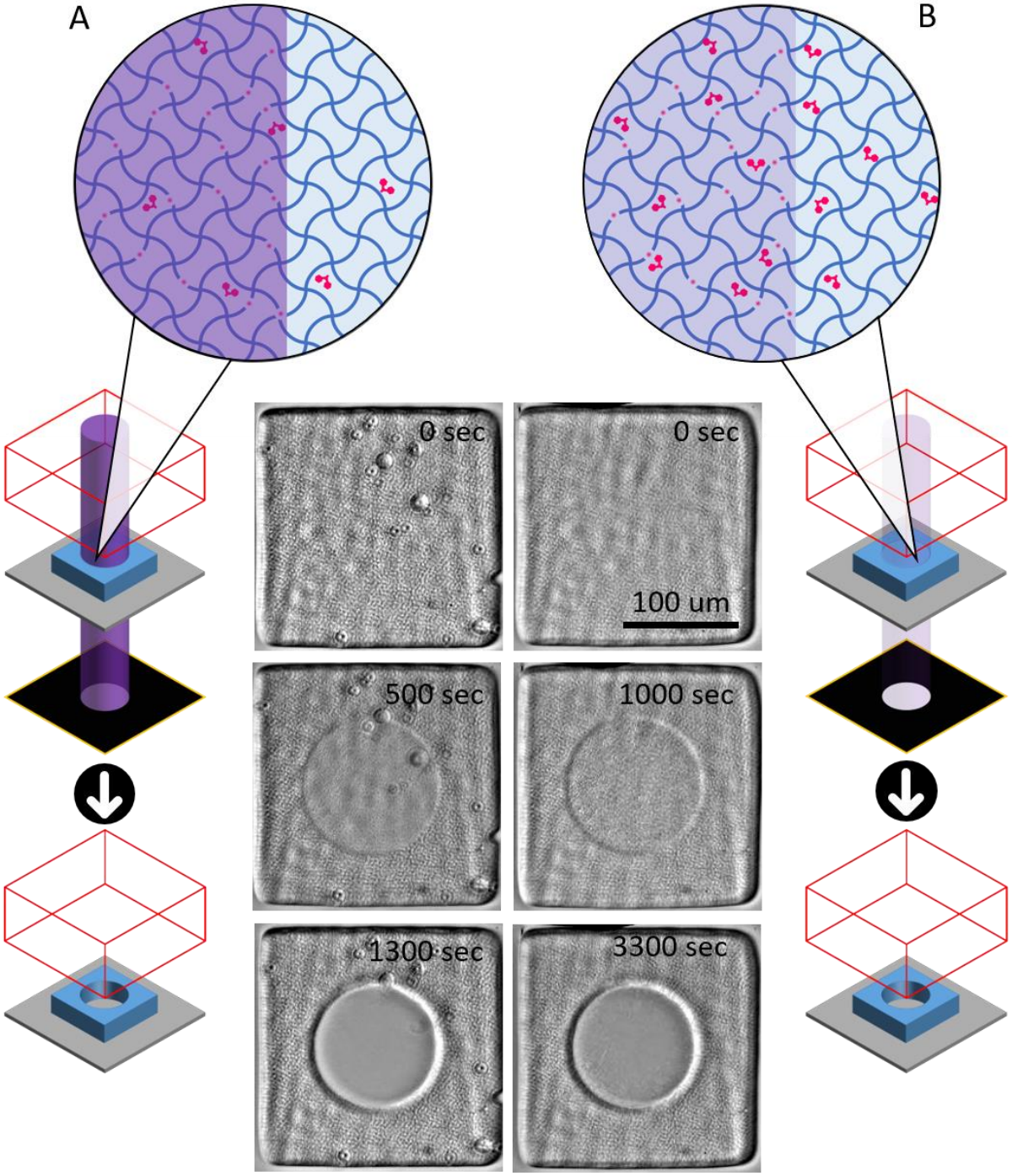

Figure 61 **| *Two photo-scission modes exist.***

Schematics of the protocol: In each case a cube of poly(ethylene-glycol) hydrogel (blue) is first cured and rinsed within a micro-reactor (glass in gray and silicone ceiling in red). PLPP photo-initiator (pink) is let to diffuse inside the mesh. The cylinder shaped ultra violet beam (violet) is shone through the hydrogel inducing photo-scission. In the center panel: Brightfield microscopy images of the hydrogel during the photo-scission reaction when testing two extreme conditions: **A,** Here the photo-initiator is scarce while the photon flux is strong **B,** There, the photo-initiator is concentrated and the photon flux is faint.

Analysis:

Each condition leads to photo-scission but with differing results **(Figure 61)**. The reaction appears to be faster when the photo-initiator is highly diluted. This may be explained due to the more important role that ultraviolet light plays during scission while an increasing amount of initiator may prove detrimental as it may react with itself and other radicals stopping the chain-breaking. One can also observe that the gel swells during the early steps of photo-scission. A possible explication is a rise in osmotic forces as fragments of the gel get trapped inside the liquefying mesh causing water to flow inwards.

Once optimized for poly(ethylene-glycol) we subsequently tested photo-scission for other hydrogels precursors such as poly-acryl-amide, agar-agar and Matrigel **(Figure 62)**. This highlighted that the reaction was generic and that each photo-scission mode was useful. Indeed, each material displayed a specific kinetic requiring varying amount of photo-initiator. **(Figure 63)**.

Methods:

Photo-scission of native hydrogels: all insolations steps were performed under a microreactor using 10X magnification. A 50/50 mix of 4-arm-poly(ethylene-glycol)-amine and 4-arm-poly(ethylene-glycol)-succinimide-amino-succinate at 1,2% in PBS, were cured by mixing and waiting for 30 minutes. They were scissionned in 150 seconds with 1X PLPP at 3,6 mw/cm². 1% Agar-Agar in PBS were boiled then cured at room temperature for 10 minutes. They were scissionned in 120 minutes at 45 mw/cm² after adding 1X PLPP. A precast Poly(acrylamide) layer at 7,5% was incubated in PLPP 1X and scissionned in 180 minutes at 7,4 mw/cm². 2% Matrigel was thawed and a thin layer was let to cure at 37C° for 10 minutes. Photoscission was achieved in 120 minutes using 0.0125X of PLPP and maximum laser power (128mw/cm²).

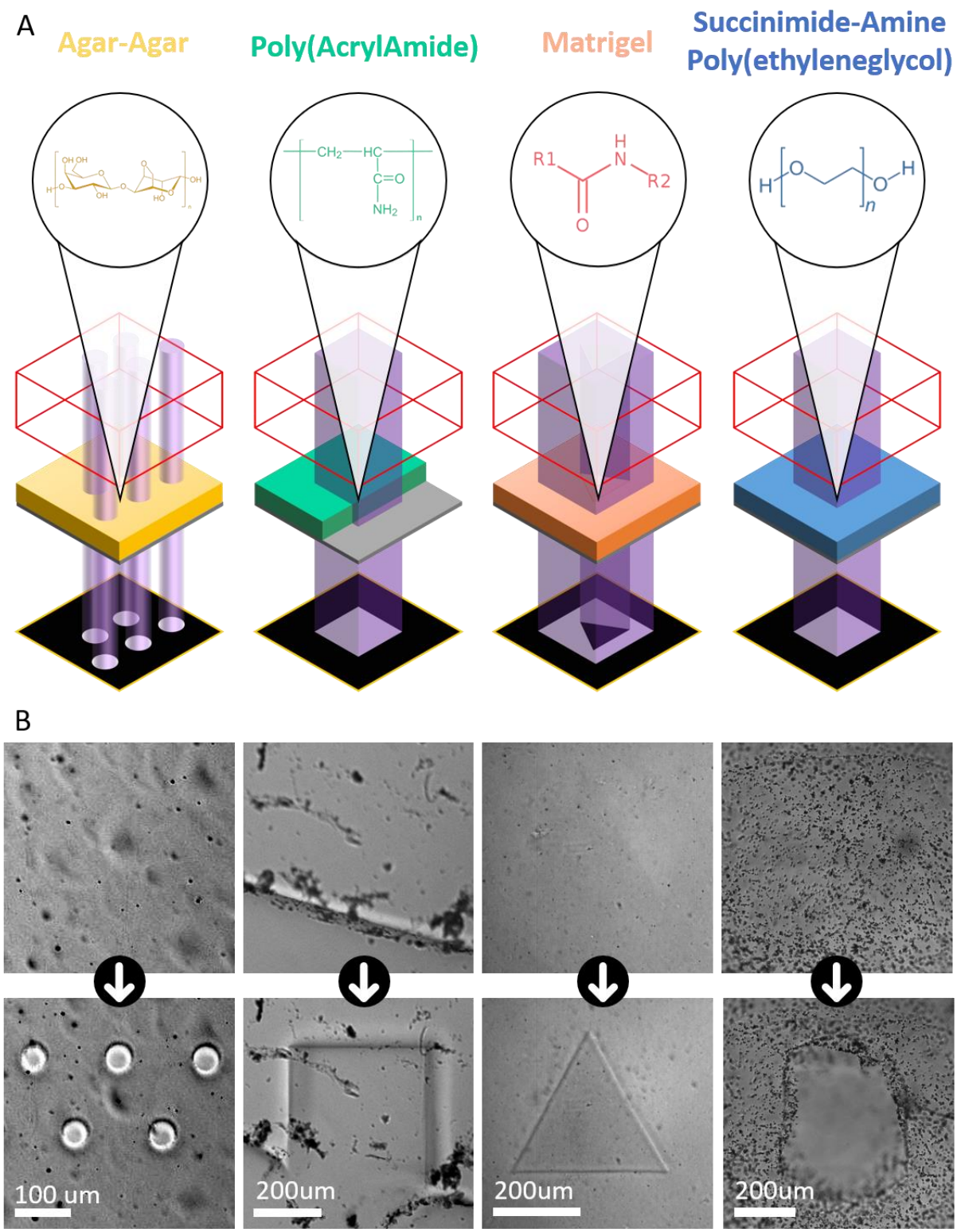

Figure 62 **| *Photo-scission works on many hydrogels.***

A, Schematics of four experimental conditions: photo-scission is performed on a layer of several hydrogels including: Agar-Agar (yellow), Poly-Acryl-Amide (Turquoise), Matrigel (Pink), Ester poly(ethylene-glycol) (blue). Above each schematic lies the chemical structure of each material (albeit oversimplified for Matrigel). **B,** Brightfield microscopy images of the hydrogels before and after the photo-scission process.

Scission time histogram: to measure the scission time of different materials four different hydrogels were each let to cured inside the wells of an inverted silicone microreactor. The gels were as follow: 4-Arm-poly(ethylene-glycol)-amine at 50/50 with 4-Arm- poly(ethylene-glycol)-succinimidyl-amino-succinate, 4-Arm-poly(ethylene-glycol)-acrylate, Agar-Agar, and Matrigel. All gels were at 2% in PBS. Photo-scission was achieved by incubating PLPP and insolating a single round with 10X magnification at max power 128 mw/cm²during. In the case of Matrigel in 4-arm-poly(ethylene-glycol)-acrylate the photo-initiator concentration had to be diluted (0.0125X) to prevent oxygen depletion.

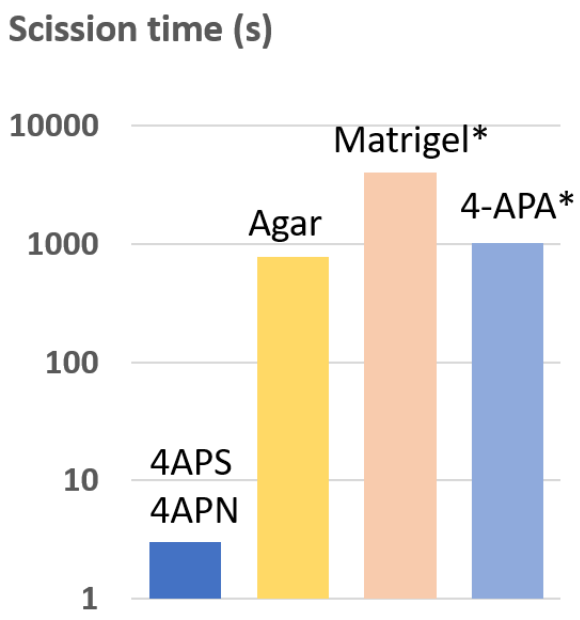

A histogram representing the photo-scission time in logarithmic scale for four different hydrogels at the same mass to volume concentration. The asterisk represents cases where the photo-initiator concentration had to be lowered.

Figure 63 | ***Scission time and conditions are material dependent.***

Analysis:

Photo-scission performs on many hydrogels despite their chemical differences however, each material requires optimization to successfully liquefy **(Figure 62)**. Previous undisclosed experiments showed that agar could not undergo photo-scission with a low photo-initiator concentration while Matrigel would entirely liquefy with high concentrations of photo-initiator. After optimization steps, we found parameters allowing us to liquefy our most-used hydrogels **(Figure 62)**.

In a second experiment we tried to compare the scission time of different materials while using the exact same initial conditions: gel concentration, photo-initiator concentration, and photon flux **(Figure 63)**. To keep the photon flux as high as possible, a small (10 um diameter) pattern size was chosen ensuring optimal oxygen replenishment in the insolated volume. Unfortunately, acryl-functionalized poly(ethylene-glycol) and Matrigel still displayed crosslinking so we had to decrease the photo-initiator

concentration in both cases. It may be because the molecules composing these gels have a higher propensity to induce crosslinking. This is further suggested when comparing amide-linked poly(ethylene-glycol) with the acryl-counterpart. The former did not require diluted PLPP and was very fast to undergo photo-scission.

Among the materials we tested, agar is unique in that it displays a slow scission time even when both the photon flux and the photo-initiator concentration are high. This scission resilience is reminiscent to the challenging decoration of the same material **(see Figure 53)** and may very well have the same origins: the mesh's steric hindrance with added carbo-radical stability protects it from photo-scission.

Being a subtractive structuration method has the advantage of preserving the gel properties outside of the photo-scissionned areas. We thus tested the possibility to create structures out of fragile materials such Matrigel and highly diluted Agar.

Cell culture : controlling cell growth on visco-elastic gels

Soft, viscoelastic matrixes such as Matrigel and Agar are highly valuable because they let cells expand and invade their mesh. They are notoriously difficult to shape with conventional stamps due those properties. With photo-scission we have access to a contactless structuration method that can maintain the material properties. We thus applied this process to the generation of agar cups and Matrigel pillars and subsequently cultivated cells in those templates **(Figure 64)**.

Methods:

Photo-scission of agar-agar wells: to photocleave agar-agar a thin layer of 0.5% agar-agar was deposited unto the wells of an inverted silicone microreactor. Photo-scission is achieved by incubating 0.05X of PLPP and insolating rounds with 10X magnification at max power 128 mw/cm² during 6 hours. The resulting micro-structured gel is rinsed with PBS. HEK 293T cells were seeded in complete cell culture medium (DMEM, FBS).

Matrigel Pillars with neurons: to generate the pillars shown in a thin layer of 2.1% Matrigel was deposited unto the wells of an inverted silicone microreactor. Photo-scission is achieved by incubating 0.0125X of PLPP and insolating a frame containing black hexagons with 10X magnification at max power 128 mw/cm² during 1 hour and 40 minutes. The scission is stopped a few minutes before total liquefaction of the gel. The resulting micro-structured gel is rinsed with PBS, then E18 rat primary cortical neurons were seeded in complemented neurobasal. After a few hours the temperature and osmotic pressures achieve the photoscission while cells stay mostly on top. The cell culture was then carried for a week to allow cells to spread. Pictures were taken at day 4 in brightfield and at day 7 using a fluorescent actin probe (Sir-Actin, Molecular devices,).

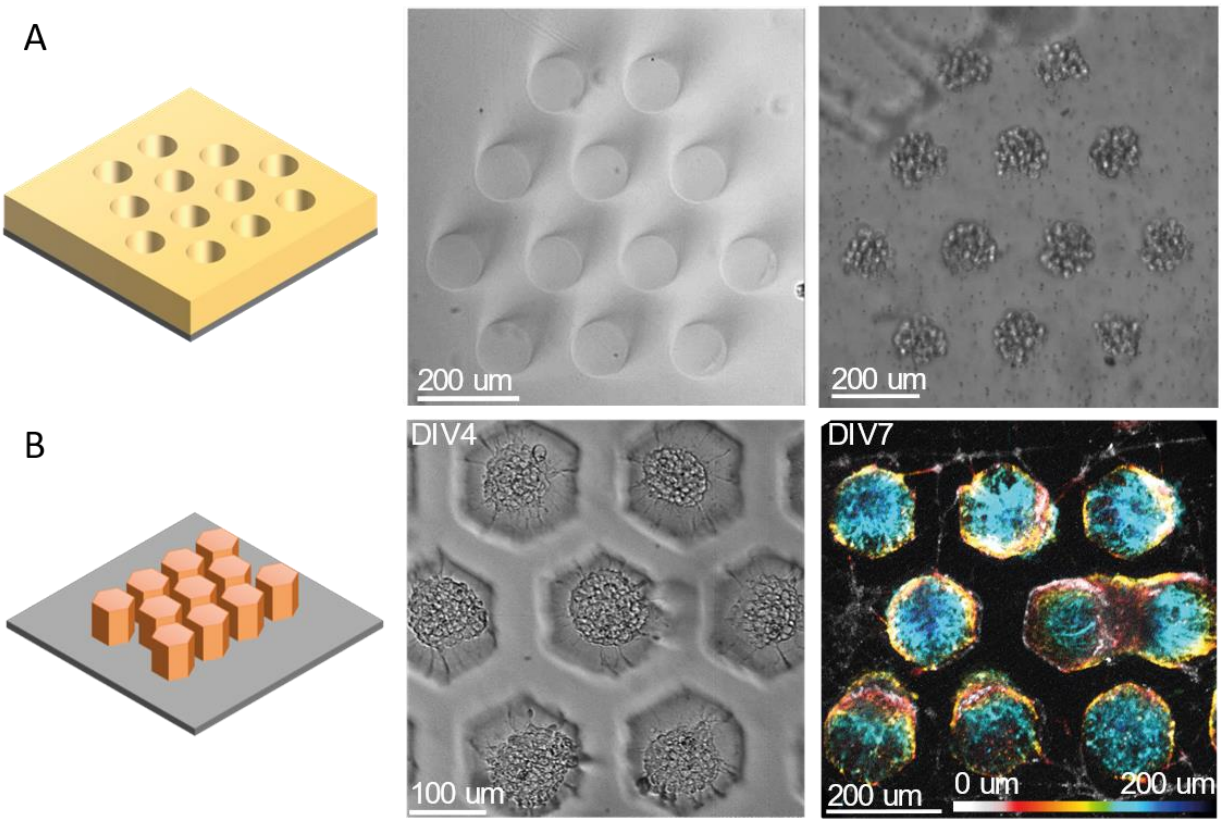

Figure 64 **| *Scission of soft hydrogels for cell culture.***

A, Fabrication of microwells made in agar-agar with from left to right : schematics of said structure showing agar in yellow. Brightfield images of the microwells before and after cells seeding. **B,** Fabrication of Matrigel micropillars with from left to right : schematics showing Matrigel in pink. Brightfield microscopy images of neurons seeded on said pillars after four days in culture. Z-color coded confocal fluorescence microscopy image showing the neurites spreading after a week in culture.

Analysis:

In the experiments above, we applied photo-scission on very soft materials: 0.5% agar is around 1 Kpa and Matrigel at 21mg/mL is around 400 Pa. Which such frail materials molding is close to impossible (and really not scalable). With photo-scission, we succeeded in creating agar microwells to aggregate HEK cells **(Figure 64 A)** as well as cultivating neurons on Matrigel pillars **(Figure 64 B)**. In this last example, some of the pillars were bent by the neurons during the culture demonstrating that the Matrigel retains its visco-elastic properties. Fluorescence calcium imaging demonstrated that the networks were spontaneously firing.

These preliminary results show promising avenues for photo-scission; despite being a slow reaction, it is appealing when working with the most fragile materials and as yet to show the extent of its possibilities.

Chapter's conclusion: uncharted territories

In this last chapter we looked more closely at the chemical reactions that are supporting our engineering processes. We shed light on three reactions: native decoration, native gelation and photo-scission each time highlighting the central role of oxygen and benzophenone chemistries.

We demonstrated that each reaction was generic and could thus be applied to a wide variety of hydrogels and precursor molecule. PLPP was crucial to successfully abstract hydrogens from the hydrogel's backbone creating carbo-radicals that would subsequently induce these reactions.

Oxygen had a distinct effect on each reaction. Decoration and gelation were both subject to oxygen inhibition suggesting they are facets of the same general crosslinking mechanism. Conversely, photo-scission only occurred within oxygen replenished areas. From these results, we deduced that crosslinking and scission were opposite reactions originating from hydrogen abstraction in the absence or presence of oxygen respectively.

In short, native gelation and decoration were an extension of the structuration and decoration protocols devised in the first and second chapter. With photo-scission however, we went in uncharted territories.

Literature on the subject of benzophenone / oxygen interactions is very scarce and, to our knowledge, this is the first time such a reaction is demonstrated on hydrogels. We took advantage of our platform's capacity to precisely control oxygen consumption and photon flux to study the interplay between crosslinking and photo-scission. Thanks to this we optimized the photo-scission to adapt to each hydrogel sensitivity.

As of now we are still struggling with the slow and sometimes puzzling nature of the three reactions. The relatively low amount of cell culture applications in this last chapter attests for that. Nevertheless, we successfully made pioneering experiments showing that organized cell culture was possible on some of the most fragile matrixes thanks to these engineering operations.

The realization that PLPP can crosslink or scission many materials led us to the pending question: How far are we from using these reactions to their full potential?

We could envision using crosslinking to locally change the rheology of hydrogels.

We could potentially graft any precursor onto any preexisting gel.

And likely many others …

On that specific subject, the following pages will conclude this manuscript with a specific focus towards new applications and current limits. We will notably discuss each technology's stage of advancement and the necessary steps to improve upon them.

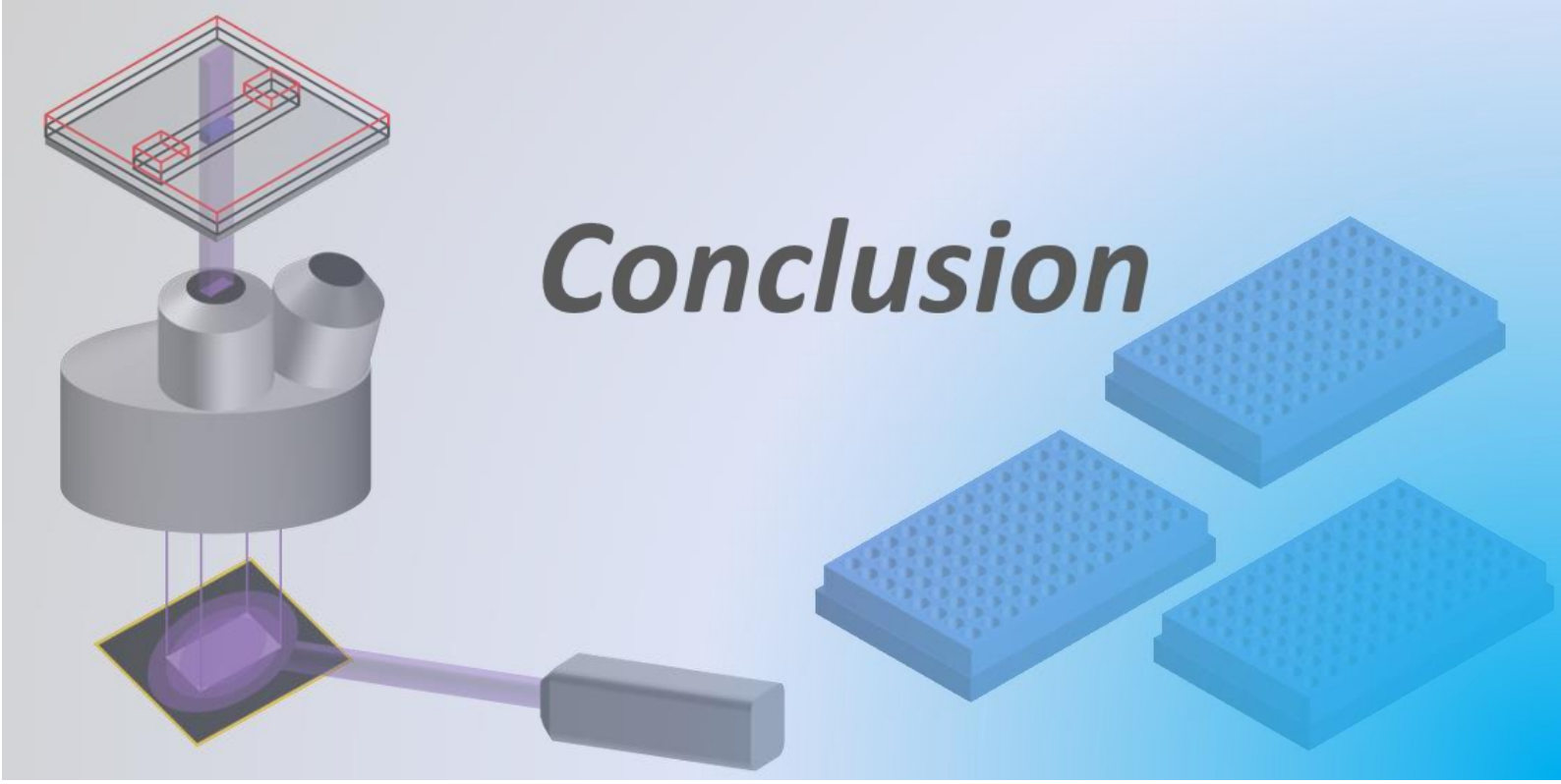

Preamble:

Tailoring hydrogels into tridimensional cell culture templates is as promising as it is challenging.

There is a high demand for hydrogel structuration and decoration solutions in an effort to standardize organoid culture and thus improve in-vitro models. However, this represents a frontier of micro-fabrication: engineering a frail material while preserving its delicate properties.

The contact-based and chemically supported methodologies, once developed for hard (silicium, glass) and later elastic (silicones, thermoplastics) substrates, quickly become obsolete and a lot of innovation is still ongoing in order to improve hydrogel engineering.

In this manuscript, I tried to offer a broad view of the many hydrogel tailoring strategies that were implemented with or without the help of structured light. Inspired by these methodologies and taking advantage of our unique capabilities, I meant to implement an original method for hydrogel structuration. I ended up with a platform and a set of chemical reactions that assemble into an effective toolbox to tailor 3D cell culture templates.

This solution is a balance between complexity, performance and flexibility favoring generic (albeit crude) chemistry over dedicated chemicals and parallel over raster-scanned illumination.

In the following paragraphs I'd like to argue on this deliberate choice, with a specific focus on technical limitations, orthogonality and scalability.

Impossible structures:

Here, we discuss the technical limitations of our platform and terms of structuration and decoration. Despite its flexibility there are tasks which our process cannot handle well:

We monitor reactions in the Z-axis through oxygen gradients instead of mechanical moving parts or voxel illumination. Thus, our control in this dimension is very dependent on each reaction we use **(Table 5)**:

> Gelation is only controlled in thickness: our method essentially creates landscapes that start form a base which is the glass slide. Bridges and complete tunnels (with all four walls being made of gel) are not feasible. This control z control is also relative rather than absolute: the resulting thickness depends on each material's kinetic parameters and must be calibrated.
>
> Decoration is surface-controlled: usually a few microns at the surface of the irradiated gel are functionalized. Controlling penetration depth in the gel has yet to be studied. Thus, z-control of decoration is mostly tied to our control with gelation. Oxygen could be exploited to control the reaction in the Z axis although as long as structuration creates landscapes this won't be necessary.
>
> Photo-scission is not controlled in the Z axis at all. The mechanism relies on the (omni)presence of oxygen to perform and any starvation invariably switches the photo-initiator towards crosslinking reactions. As such any attempt at inhibiting scission through oxygen depletion would be counter-productive. A potential solution would to be generate photo-initiator gradients instead.

Overall: the silicone microreactors create oxygen gradients that are fit to control the gelation thickness but ill-suited for the other reactions especially photo-scission. In the future, new kinds of microreactors could be fashioned to make use of more/ different chemical gradients helping us in better controlling each reaction in the Z-axis.

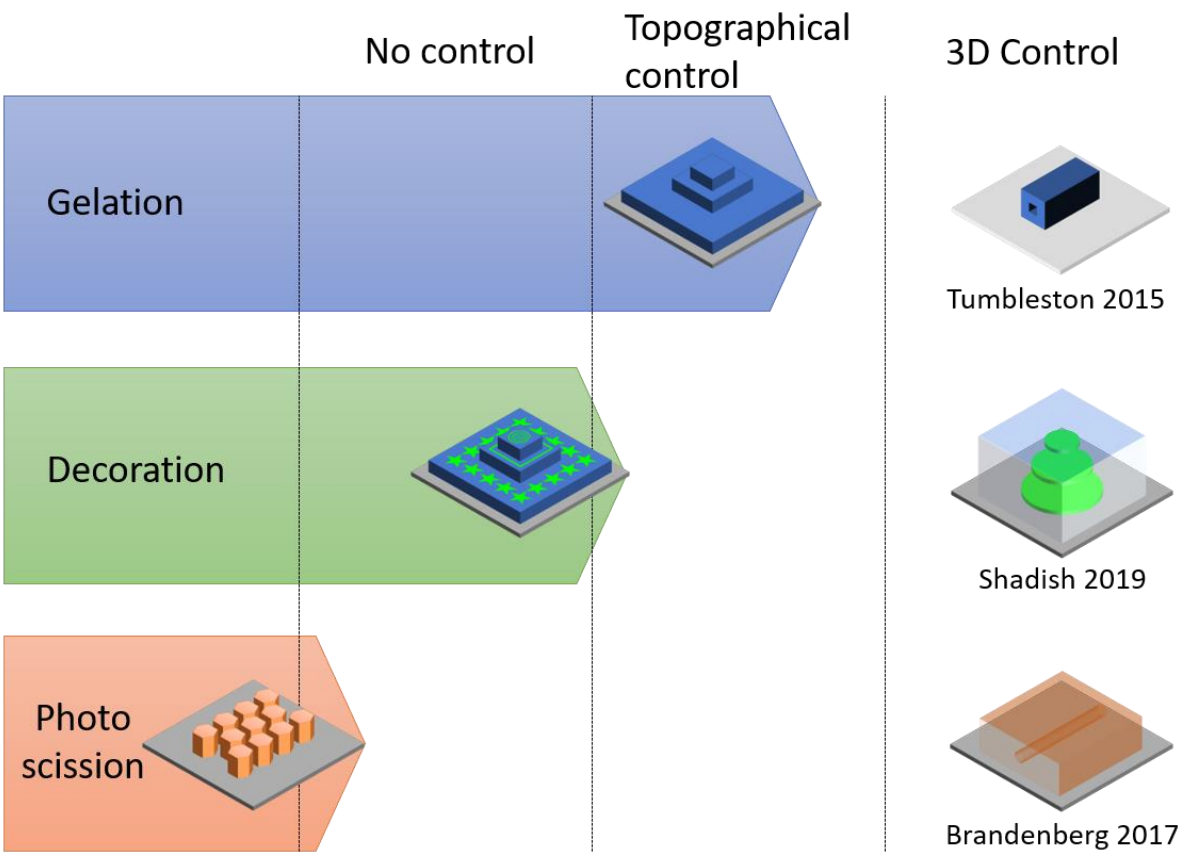

Table 5 **| *Advancing towards tridimensional control.***

Schematic of our most telling examples for each hydrogel engineering operation when compared to the most advanced platform presented during this manuscript.

It is also worth noting that some of those limitation can be by-passed by combining the three engineering operations and taking full advantage of their capacities **(Figure 65)** for example: Using the materials varying sensitivity towards photo-scission, one could use a photopolymerizable gel as a sacrificial ink and thus create channels inside a resilient gel. One could also sandwich a decoration step between successive layers of gelation to virtually localize the decoration in Z.

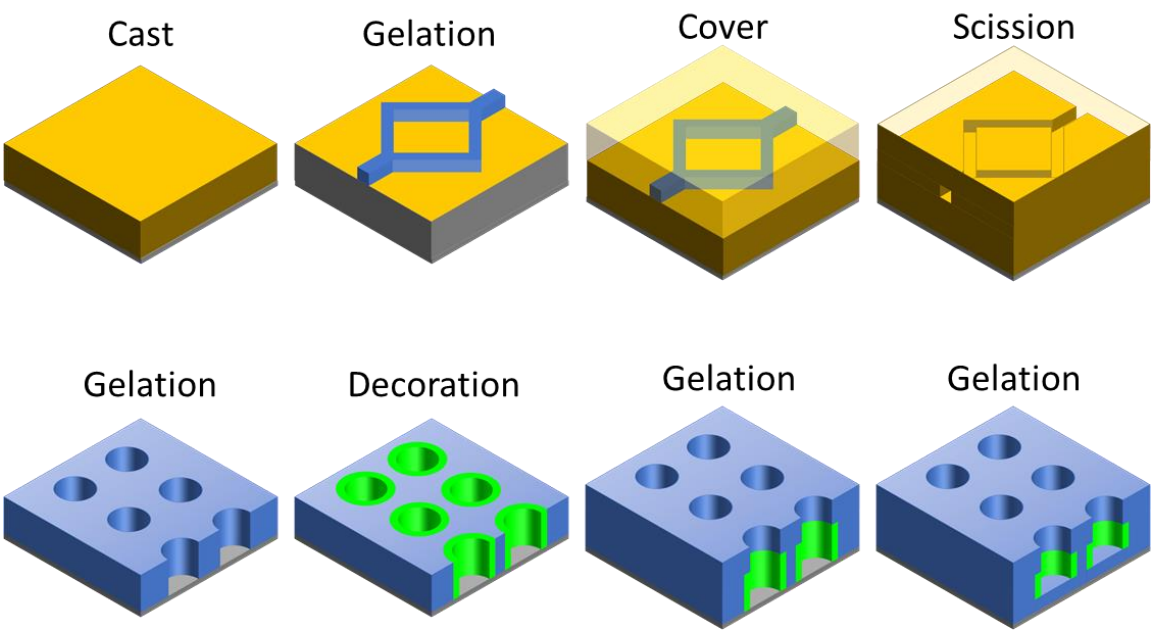

Figure 65 **| *Queuing and combining engineering steps.***

Schematic illustrating how the combination of successive engineering steps can produce structures with **A,** complete channels or **B,** decorations localized in Z.

As this last paragraph has highlighted, there is a lot of unhinged potential with this platform. As we discuss the orthogonality in the next section, we will also disclose potential directions this platform could go to overcome existing hurdles.

Preserving the gel and the cells: The orthogonality conundrum

It is hard to alter a single property of a given material while also preserving the others. It is especially hard when the material is as frail as the photo-initiator is powerful. The most valuable properties of hydrogels are: rheology, transparence and cells that may be already present **(Figure 66)**. When trying to preserve those properties, a clear line can be drawn between the crosslinking reactions (gelation, decoration) and photo-scission.

First and foremost, the three engineering operations are not equally respectful of the gel mechanical properties. When it comes to shaping hydrogels while preserving the rheology photo-scission is best suited. Photo-gelation induces crosslinking and thus drastically alters the gel elasticity and viscosity. Photopolymerization of Matrigel, while it can be done, is a good example as it completely nullifies the gel's softness. Our decoration protocol suffers from the same issues as the photo-initiator crosslinks the gel likely causing alteration of the stiffness.

Decoration and polymerization also raise the issue of opacity: crosslinking alters the material refractive index up to a point where the mesh is no longer translucent. When it comes to imaging the sample through the hydrogels this becomes an issue. In contrast, photo-scission is unique in that it alters areas of the gel that are supposed to be removed, on top of that it positively affects the gel refractive index.

At last, comes the daunting challenge of cytocompatibility. As K.S. Anseth, T.E. Brown and later M.P. Lutolf suggest in their review[4,10], hydrogel modification should be feasible during the cell culture. In essence, the reaction's portfolio that we developed is better suited to tailor the initial seeding conditions instead of changing the substrates properties during the cell culture. Radical reactions are notoriously cytotoxic especially when paired with oxygen, the only possible exception being photo scission. To date this reaction has been successfully performed in the presence of cells with minimal cell death by lowering the photo-initiator concentration to its minimum. Nonetheless, we suspect that no matter the cytocompatibility, the most sensitive cells like neurons and stem cells are unlikely to emerge unscathed from any engineering operation involving radicals.

In summary, this illustrates the expected difficulty of achieving orthogonal and gentle reactions when using crude chemistry.

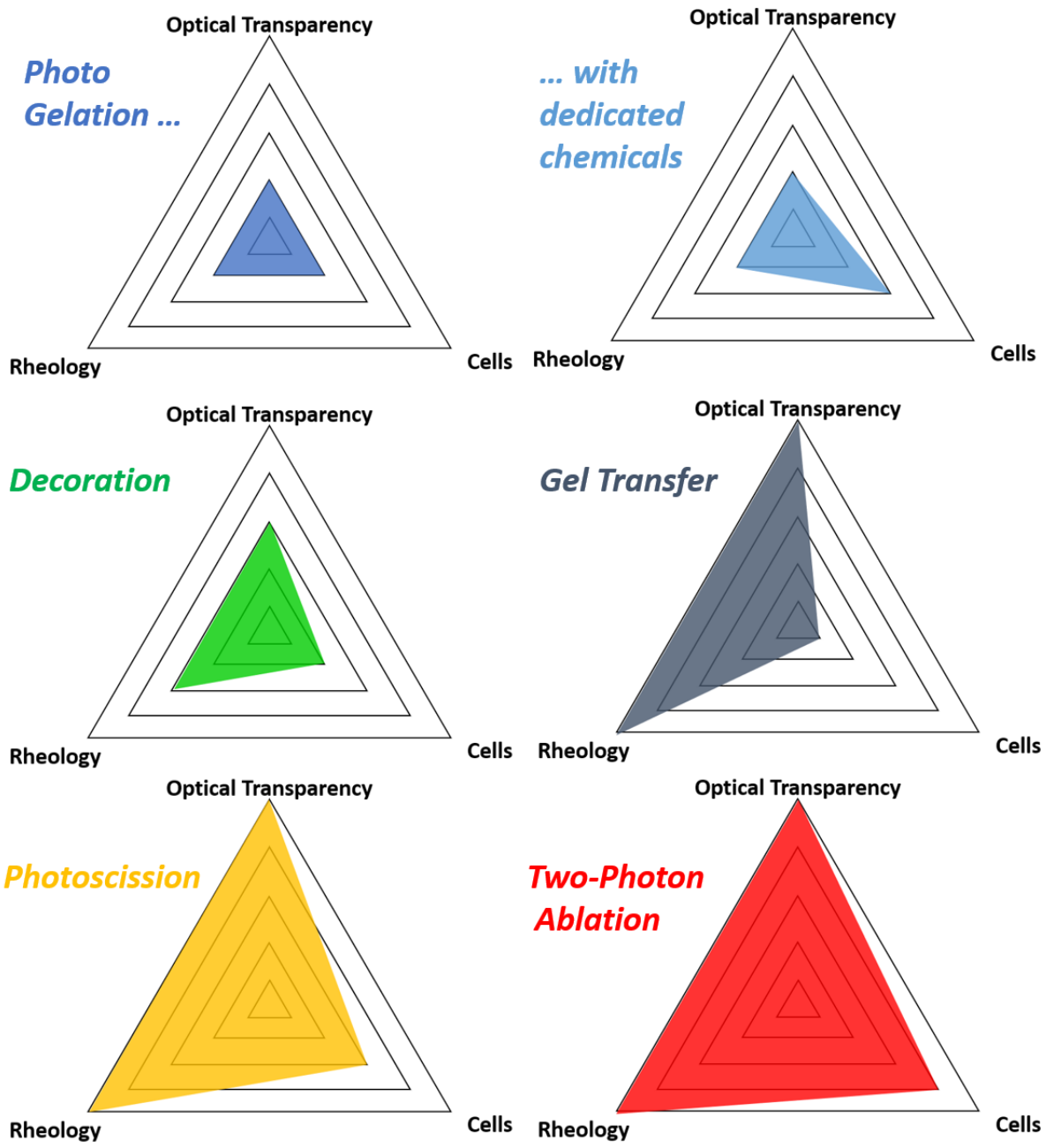

Figure 66 **| *Orthogonality conundrum from the prism of each engineering operation.***

For each process, the difficulty of preserving the material's rheology, transparency and embedded cells is given: the deeper the edge goes the more the property is preserved.

Nonetheless, some solutions can be devised to tackle the conundrum especially with regards to cytocompatibility and/or dynamic environments. The general strategy would be to use gentle, enzymatic reactions as a follow up to the radical engineering. For example, one could use biotinylated linkers and proteins to create dynamic decoration motifs. In another example, we could structure degradable and non-degradable gels to promote cell growth or migration in specific areas **(Figure 67)**.

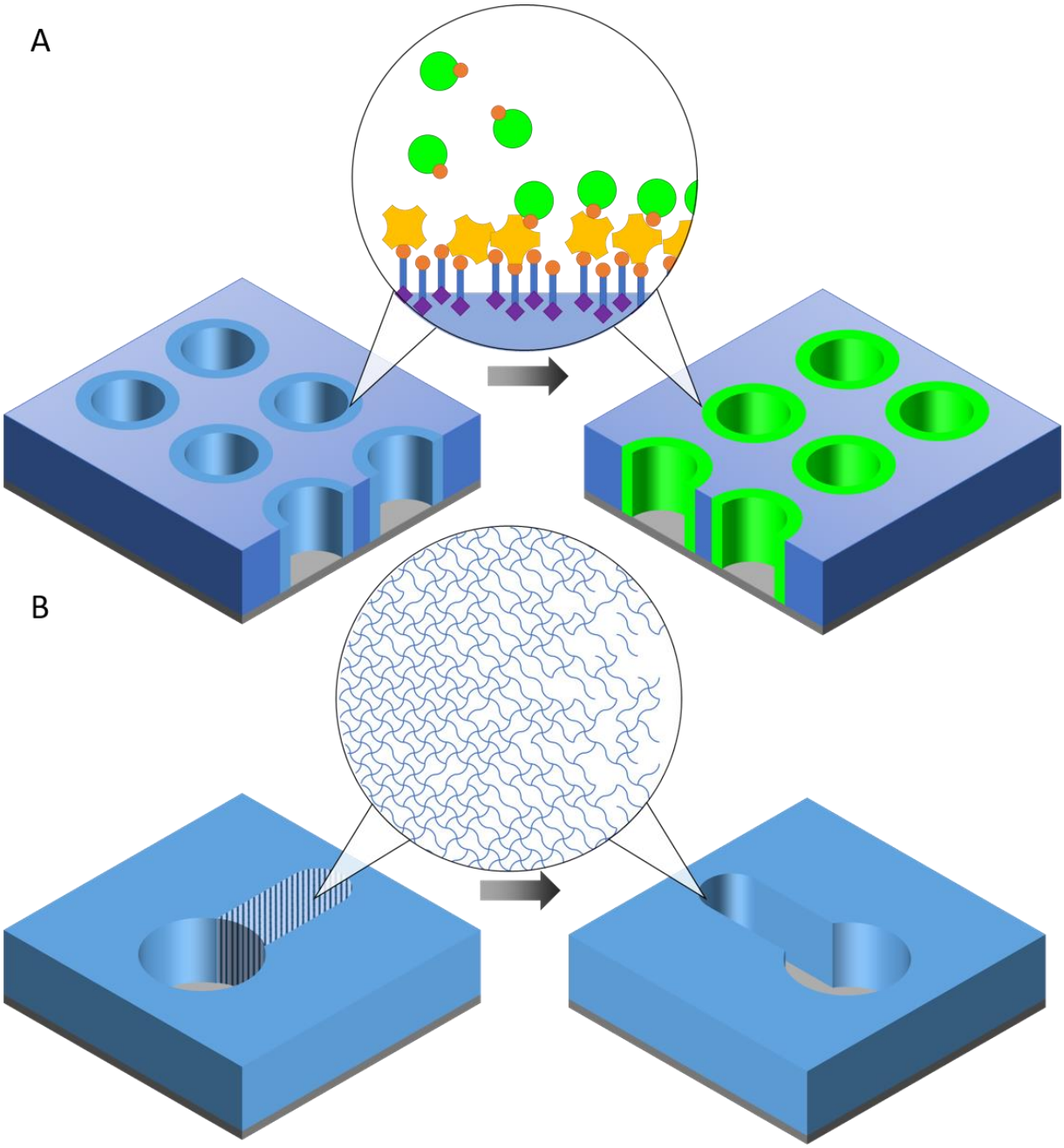

Figure 67 **| *Integrating a gentler chemistry to create dynamic environments.***

Example schematics of gentle solutions to promote **A,** dynamic decoration or **B,** dynamic structures within the template.

Setting the "stage" in advance would also minimize the amount of light-based operations that one as to perform during the cell culture. This is especially relevant since the time these engineering operations take is actually significant. The next part of this conclusion will go on this topic in further details as we discuss the challenge of scale-up.

Square meters of micron sized niches? The question of scale

Most reviews point towards the necessity of large-scale manufacturing of advanced (3D) in vitro models. No matter the degree of physiological relevance, biology requires a lot of statistics and thus organoids will soon have to be mass-produced.

In the event that we would need to fill a 96-well plate using our method we would need at least one of the following modifications **(Figure 68)**.

Either the reaction kinetics should be sped up by an order of magnitude in order to keep the same set-up while being time-efficient **(Figure 68 left)**. This development would keep the flexibility of the set-up but the reagents would probably become more expensive.

Otherwise, the structured illumination field should be increased to cover the whole plate. In the present day, digital micromirror devices could not fulfill this task and grayscale photomasks will be necessary **(Figure 68 right)**. This represent the least flexible yet most scalable option.

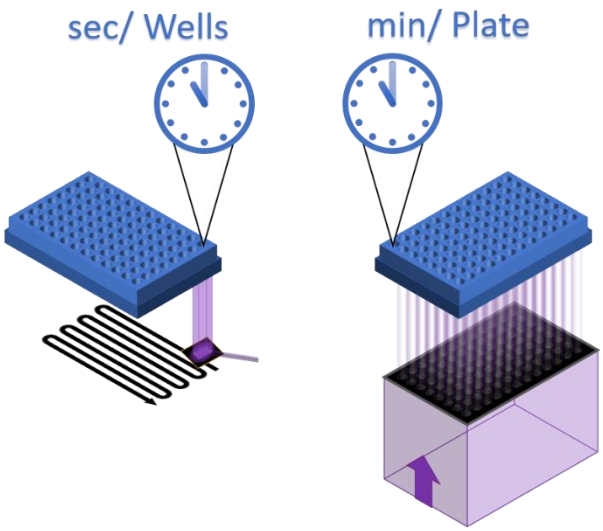

Schematics illustrating the two possibilities. In the left case, a light-motif is raster scanned across the 96-well plate. The operation is performed with the actual set-up however the chemistry allows a single well to be treated in seconds. In the right case, all wells are treated at once using a photomask. This operation does not require a faster chemistry but loses the initial platform's flexibility.

Figure 68 **| Two path towards large scale exist.**

Photo-crosslinking reactions are amenable to the first path: these are fast reactions that rely on oxygen depletion which can always be made quicker. This could be perfect for decoration however thickness control will likely become more difficult. Additionally, a stable and planar air liquid interface will be required in each well which present an engineering challenge.

Photo-scission is likely to benefit the most from a large field of projection: the fact that it's a slow reaction makes it more appealing when applied on massively parallelized workflow. On top of that many of the existing gel-coated

substrates are made of materials which we readily photo-scissionned in this document. Last but not least, if oxygen depletion is avoided, photo-scission can perform without the need for a gas permeable window.

These two pathways are not antagonists and will likely benefit from one another. Overall, a right balance between tailoring time and reagent cost will have to be found.

Closing words:

Looking back at my work, I can now envision important standards for successful hydrogel tailoring:

- genericity: be able to use the hydrogels you want or the one you developed
- rheology: preserve / generate visco-elasticity as it is key for cell culture
- opacity: make sure that the template does not interfere with imaging
- cytocompatibility: make sure that the engineering does not interfere with the cells
- scalability: be able to mass produce and achieve statistical relevance
- straightforwardness: ensure the shortest possible gap between idea and result

In the closing section of this manuscript, I'd like to discuss about what may be the coming tendencies in hydrogel engineering for cell culture and the interest of photo-scission in such a context.

As more scientists will adopt tridimensional cell culture, hydrogel diversity is likely going to explode even more while the staples (Matrigel, agar, acryl-amide) will be even more popular. Most of the hydrogels being developed won't be light sensitive and will likely emulate some properties of Matrigel such as visco-elasticity. In other words, I expect photo-crosslinking to be more and more lackluster as new hydrogels will be designed because it cannot efficiently structure all materials and cannot prevent them from stiffening during the shaping (or decoration) process. Photo-crosslinking of gels is in use since more than a decade and many pioneering laboratories already move away from it.

Despite being the slowest, least straightforward reaction, photo-scission is a unique parallel and subtractive engineering process. It has much more appeal to me. Over the course of this conclusion I highlighted the benefits of this reaction with regards to most of the points cited above **(See Figure 65, Figure 66)**. It is also worth noting scission likely turns elastic hydrogels into visco-elastic hydrogels the further they degrade. On top of structuration, photo-scission could thus be a generic tool used to locally print rheological patterns onto hydrogels. To me, photo-scission truly is the reaction adapted to the softest materials.

My bet is that with sufficient developments, photo-scission will become a staple in hydrogel engineering by overcoming its current shortcomings: becoming faster, controlled in the Z axis and gentler to the cells.

Appendix I : Common methods

Experimental Setup: For all the experiments, we used a Nikon TI-E inverted microscope (Nikon Instruments) equipped with a digital micromirror device-based ultra-violet patterned illumination device (PRIMO, Alveole, France) together with its dedicated software (LEONARDO V3.3, Alveole). The wavelength of the illumination laser is 375 nm. 4X S-Fluor and 10X Plan Fluor (Nikon) were used to ensure efficient ultra-violet transmission. A homemade version of this illumination device was previously described in 22.

Modular Microreactors: We used custom silicone chips made of two superposed silicone thin films with holes fabricated by xurography (silicone Stencils, Alveole, France, previously described in 22). These stencils were stacked onto a 22x22 mm 170 um thick glass coverslip (Schott Nexterion, Schott Jena, Germany) forming silicone microchambers of various geometries (Fig 1). Depending on the application, the upper silicone film was removed after the building steps to ease the seeding of cells or beads. In gas-controlled structuration experiments, the device is placed in a custom enclosure allowing argon or oxygen perfusion during the insolation steps.

Reagents were purchased as follow: 4-Arm-poly(ethylene-glycol)-Acrylate MW 10K, Acryl-poly(ethylene-glycol)-SVA MW 2K, 4-Arm-poly(ethylene-glycol)-Amine MW 10K, 4-Arm-poly(ethylene-glycol)-SAS MW 10K. Laysan Bio (Arab, USA). Matrigel Corning (USA). PLPP 1X (14.6 mg/mL) (Alvéole, France). Human Fibronectin (Roche).Agar low melting point, poly(ethylene-glycol) 8K, poly(ethylene-glycol) 20K , poly(ethylene-glycol)DA MW700, Laminin from mouse EHS, PolyLysine, PolyLysine FITC conjugate (P3543), NH4Cl, Triton X100, Paraformaldehyde, Bovine Serum Albumin (BSA), Phosphate Buffered Saline (PBS), N,N-DimethylFormamide (DMF), Dulbecco Modified Eagle Medium, NeuroBasal (Sigma Aldrich). Phalloidin-Alexa647 conjugate (Invitrogen), anti-Lamin (Abcam, ab16048) and Goat Anti-rabbit antibody Alexa 568 conjugate (Abcam, ab175471). 0.3 um diameter carboxy-fluorescent latex beads (Invitrogen).

Cell Culture: COS-7 and HEK 293T cells were seeded and cultivated in complete cell culture media (DMEM, FBS). E18 rat primary cortical neurons were seeded and cultivated in complemented neurobasal.

Staining and imaging: Fixation and staining of cells was conducted using standard procedures. Staining of gels structures was performed by coating with 0.3 um carboxy-fluorescent beads. Neurons on Matrigel (Fig4E) were imaged using Sir-Actin and Fluo5F live markers. Spheroids (Fig3C) were stained using membright™ live marker. 3D imaging was achieved using a homemade digital micromirror device based confocal microscope.

Appendix II : BioRxiv Preprint

Tailoring 3D cell culture templates with common hydrogels.

Aurélien Pasturel[1,2,3], Pierre-Olivier Strale[3], Vincent Studer[1,2,*]

[1] University of Bordeaux, Interdisciplinary Institute for Neuroscience, Bordeaux, France.

[2] CNRS UMR 5297, F-33000 Bordeaux, France.

[3] ALVEOLE, Paris, France.

*vincent.studer@u-bordeaux.fr

Hydrogels are the simplest and most widespread 3D cell culture materials, but turning these homogeneous substrates into biomimetic templates proves difficult. To this end, we introduce a generic solution compatible with the most biologically relevant and often frail materials. Here we take control of the chemical environment driving radical reactions to craft common gels with patterned light. In a simple microreactor, we harness the well-known inhibition of radicals by oxygen to enable topographical photopolymerization. Strikingly, by sustaining an oxygen rich environment, we can also induce hydrogel photo-scission, which turns out to be a powerful and generic subtractive manufacturing method. We finally introduce a flexible patterned functionalization protocol based on available photo-linkers. Using these tools on the most popular hydrogels, we tailored soft templates where cells grow or self-organize into standardized structures. The platform we describe has the potential to set a standard in future 3D cell culture experiments.

Hydrogel | 3D Cell Culture | Photo-chemistry | Micro-fabrication

Hydrogels are commonplace in 3D cell culture i.e. the art of organ-izing cells by cultivating them in configurations that more closely mimic the in-vivo environment(1). Whether to fill scaffolds with cells(2), exploit cell self-organization(3–5), or both(6), their high hydric content, modulable mechanical properties(3) and access to chemical functionalization(7–9) make hydrogels a staple for most applications.

With the help of light, the ability to shape(10), cleave(11, 12) or functionalize(8, 9) these materials has improved in tandem with the idea that standardized organoid models will emerge from spatially defined micro-niches(6, 13). To this end, an array of light-based devices and photo-controllable hydrogels have been designed with the intent of turning these homogeneous matrixes into heterogeneous micro-environments(8, 11). Alternatively, laser-scanning photoablation has been used to degrade natural matrixes(12) like Matrigel or agar-agar which are commonplace(5, 14) but lack photo-responsive moieties.

Unfortunately, despite their respective successes, these technologies cannot favor widespread adoption as they either lack the required flexibility, accessibility or speed. To keep biology at the center of focus, an ideal toolbox should alleviate labor-intensive developments in chemistry, hardware and 3D modelling thus simplifying the conception of microniches out of common place materials.

In this report, we introduce a setup consisting of a commercially available widefield patterned light illuminator and oxygen permeable PDMS micro-reactors. This platform can spatially control the kinetics of light-based reactions by locally tuning the photon flux over the entire insolated field.

This flexible solution performs: (i) additive manufacturing of photopolymerizable hydrogels with control over thickness (ii) subtractive manufacturing of many gels such as PEG, Agar, Matrigel or poly-acrylamide (iii) decoration (patterned functionalization) of hydrogels.

Queuing and combining the above capabilities, we turned common hydrogels into topographically and chemically heterogeneous micro-environments. Cells were then seeded onto those templates, growing or self-organizing into various designs: standardized spheroids, patterned cells on hydrogels and colonized perfusable channels.

In short, a flexible platform, common materials and a simple workflow open an avenue of hydrogel engineering for 3D cell culture.

Results

A set-up to control the photo-initiator's chemical context. To engineer hydrogels with light, our platform makes extensive use of a benzophenone-based photo-initiator. Upon irradiation, benzophenone forms highly reactive radicals that can induce polymer crosslinking, degradation and functionalization depending on its immediate chemical environment (gas, pre-polymers, photo-linker)(15). To harness this sensitivity towards the environment, we developed modular microreactors into which reagents are injected and gas-gradients can be generated, while photochemical reactions occur (Fig.1A).

These microreactors are made of two gas-permeable PDMS stencils(16) stacked onto a glass microscopy slide enabling oxygen gradients as well as changes in atmospheric content. These foils of calibrated thickness are perforated by xurography(17) and constrain the liquid height. Their assembly is simple and their geometry modular, thus allowing to create channels or wells that can fit the end-user application. (Fig.1B).

The micro-reactors are mounted onto the motorized stage of a microscope coupled with a DMD-based widefield illuminator that shines spatially modulated UV light. The DMD (digital micro-mirror device) allows arbitrary forms and gray levels (via pulse

Significance

Light based, engineering of hydrogel should not be solely restricted to chemically modified materials. Indeed, many researchers rely on common hydrogels to organ-ize cells but lack the structuration and functionalization methods to develop standardized in vitro models with human-like properties. We unlock this limitation by providing a scalable toolbox that operates on widespread generic hydrogels or hydrogel blends such as PEG, Agar, or Matrigel. We crafted tailored 3D cell culture templates with these materials, growing and self-organizing cell lines and primary neurons in a controlled manner. More largely, we encourage all engineers with a knack for hydrogels but who are not experts in organic chemistry, to adopt our toolbox.

width modulation) to be projected. The radical generation rate is thus controlled in space and time (Fig.1C).

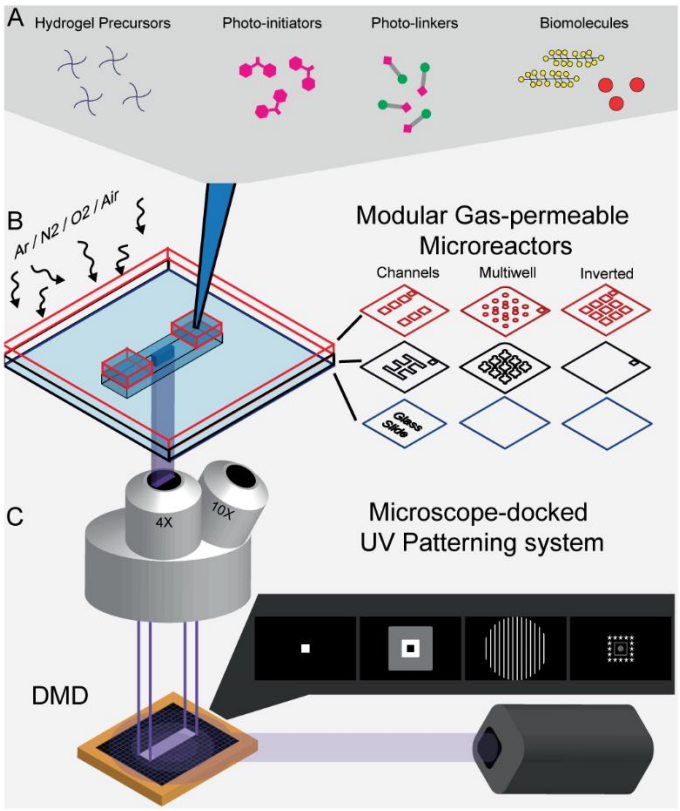

Fig. 1. A flexible set-up to control reagents, gas and photon distribution. (A) Schematics of the potential reagents used in the platform with hydrogel precursors (blue 4-branched stars), photo-initiator (pink), photo-linkers (pink and green), biomolecules (yellow, red). (B) Schematics of the gas permeable PDMS microreactors used in this paper showing the upper (red) and lower (black) PDMS stencil designs stacked onto a glass slide (blue). (C) Schematics of the DMD-based (gold) UV projection set-up with microscope objectives (gray), projected patterns and 375nm expanded and collimated laser beam (purple).

Overall the complete platform locally tunes the reagent concentration, the gas content and the UV-power. This control over the chemical context enables four hydrogel engineering operations with immediate applications in cell culture. We now describe these operations starting with total polymerization of hydrogel channels under inert atmosphere.

Total polymerization. Perfusion channels and chemical gradients are critical to provide cells with essential nutrients and differentiation factors during growth. To this end we aimed at building walls and permeable barriers of arbitrary shape (movieS1) in our micro-reactors.

Yet, photopolymerization of hydrogels is impaired at the vicinity of PDMS as the perfusing oxygen forms an inhibition layer (deadzone)(18, 19). By generating an inert gas atmosphere over our microreactors, we deplete oxygen from the PDMS roof.

In such anoxic condition, the deadzone disappears and the cured structure reaches the ceiling forming a wall in the chamber (Fig.2A). Successive illumination patterns can be aligned in order to generate hydrogel-based millimeter-sized circuits (movieS2). Capillary driven flow is achieved by deposition of liquid drops at the micro-reactor's entries. The perfusion of a solution of 1um fluorescent beads inside a hydrogel spiral showed no leakage demonstrating the total polymerization (Fig.2C, movieS2).

Secondly, hydrogel-channels can be tailored into semi-permeable membranes, letting small molecules pass through (Fig.2D). As an example, solution of purified GFP was let to perfuse through a photo-polymerized barrier, showing the establishment of a diffusing gradient over time (Fig.2D).

To turn these microfluidic channels into cellularized vasculatures, we complemented bioinert PEG hydrogels with cell adhesion molecules (Poly-L-Lysine, fibronectin). Hexagonal networks of such materials were entirely polymerized and used as cell culture templates. COS-7 cells colonized the hydrogel walls as revealed by 3D fluorescence imaging of the labelled cells after 3 days in culture (Fig.2E).

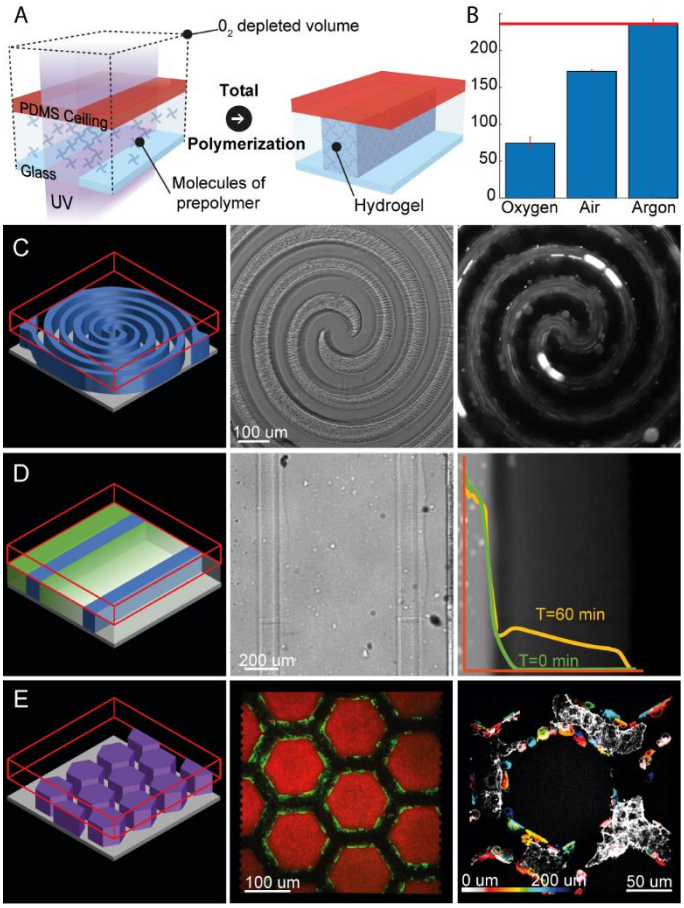

Fig. 2. Building perfusable hydrogel channels with total-polymerization. (A). Schematics of the total polymerization procedure: hydrogel precursors (blue 4-branched stars) and photo-initiators are incubated. Argon perfusion generates an oxygen depleted volume (black dotted lines). After UV illumination (purple, purple arrows) the gel is polymerized(blue) in the whole insolated volume. Polymerized gel height (µm) is inversely correlated with the oxygen content, reaching the PDMS ceiling in its absence (B). Total polymerized hydrogels create leak tight barriers that support flow (C) and the generation of diffusive gradients (D). Biocompatible hydrogels can allow for the growth of cells in arbitrary vascular structures (E).

Additionally, we observed that the height of the hydrogel depends on the oxygen content of the atmosphere (Fig.2B). This can be used to globally control the thickness. However, the much-needed topographical structures, favoring spheroid organization or mimicking the complexity of organs, require local thickness control. Hereafter, we introduce a second engineering operation suited for the above purpose.

Z-Controlled Polymerization. At a given oxygen content, the deadzone thickness is inversely correlated with the photon-flux(18). In our set-up, under air atmosphere, the PDMS ceiling simply imposes a constant oxygen boundary condition.

In turn, varying the laser power or the gray level intensity from 20 to 140 mW/cm^2 dictates the resulting gel thickness from 65 to 175 µm respectively (Fig.3B).

Taking advantage of this structuration mode we created cup-shaped PEG templates ideal for spheroid culture (Fig.3C). Spheroïds are cell aggregates which can be readily used as physiological models or serve as a starting point for complex organoïds. Yet the lack of adequate culture substrates induces a high variability in shape and cell count leading to unreliable results.

Here, HEK cells seeded on topographically structured PEGs aggregated into standardized spheroids the size and shape of which coincided with the features of the micro-wells (Fig.3C).

The inertness, transparency, permeability and simple structuration of this hydrogel make it the go-to material to dictate spheroid growth.

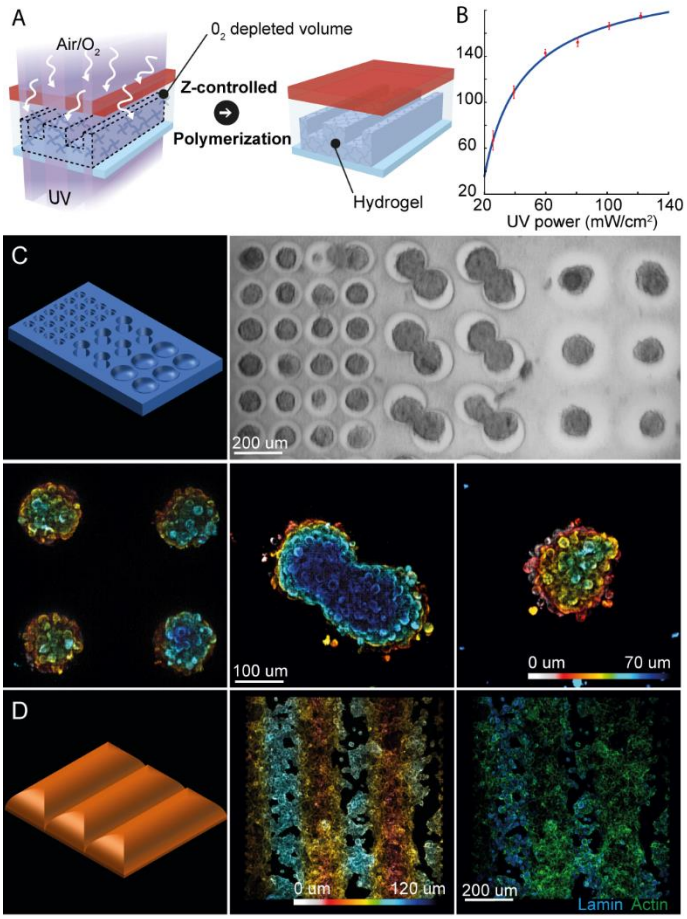

Fig. 3. Controlling the gel topography with z-controlled polymerization. (A) Schematics of the z-controlled polymerization procedure: hydrogel precursors (blue 4-branched stars) and photo-initiators are incubated, air serves as an oxygen source. UV illumination (purple, purple arrows) generates an oxygen depleted volume (black dotted lines) with features corresponding to the photon flux distribution (darker and lighter purples). The polymerized gel (blue) will correspond to the oxygen depleted volume during the insolation. The gel thickness(µm) correlates with the local photon flux (mW/cm²) (B). Using this principle, grayscale pattern can generate topographical structures out of bioinert hydrogels to grow standardized spheroids (C). Alternatively the surface of biocompatible hydrogels can be colonized with cells (D).

When needed, the inertness of the PEG can be reverted to allow for cells to colonize the topographies. Here, cell-adherent waves were created by mixing Matrigel with a photopolymerizable PEG precursor. Matrigel is a temperature-curing hydrogel enriched in laminin, collagen and other adhesion factors ensuring high cellular compatibility. On these hybrid hydrogels, seeded cells quickly spread homogeneously, forming a confluent layer on top of the structure (Fig.3D).

Even in the absence of photopolymerizable precursors, some prepolymers can undergo total and z-controlled polymerization, as shown for Matrigel (MovieS3). However, UV-induced crosslinking drastically alters the gel rheological properties which are critical for cell behavior(20). To overcome this limitation, we introduce a third engineering operation where most hydrogels can be structured without significantly altering their final mechanical properties.

Photo-scission. Photo-scission removes areas of hydrogels while the remaining mesh is left unscathed. While oxygen is known to inhibit radical photo-polymerization and induce the photo-scission of PEG chains, the latter reaction has found only few applications in material science(21). In this report, we show how photo-scission unlocks the structuration of bulk, native hydrogel such as PEG, Poly-acrylamide, Agar-agar and Matrigel. (MovieS4).

This reaction occurs when a cured gel, perfused with photo-initiators, is exposed to UV light in the presence of a sustained supply of oxygen. Indeed, anoxic conditions inside the insolated volume would favor crosslinking instead of chain scission. Here again, a permeable PDMS ceiling or floor (Fig.4A) is in contact with the air atmosphere thus providing a continuous oxygen supply during the reaction. The gel will then progressively liquefy in material-specific kinetics (Fig.4B).

Soft, visco-elastic hydrogels such has Matrigel are widespread but lack simple structuration means. Indeed, the replica molding of such frail material is notoriously difficult. Here, we exemplify our contactless photo-scission on very soft materials (Matrigel, Agar 0,5%), to engineer high aspect ratio (>2) structures.

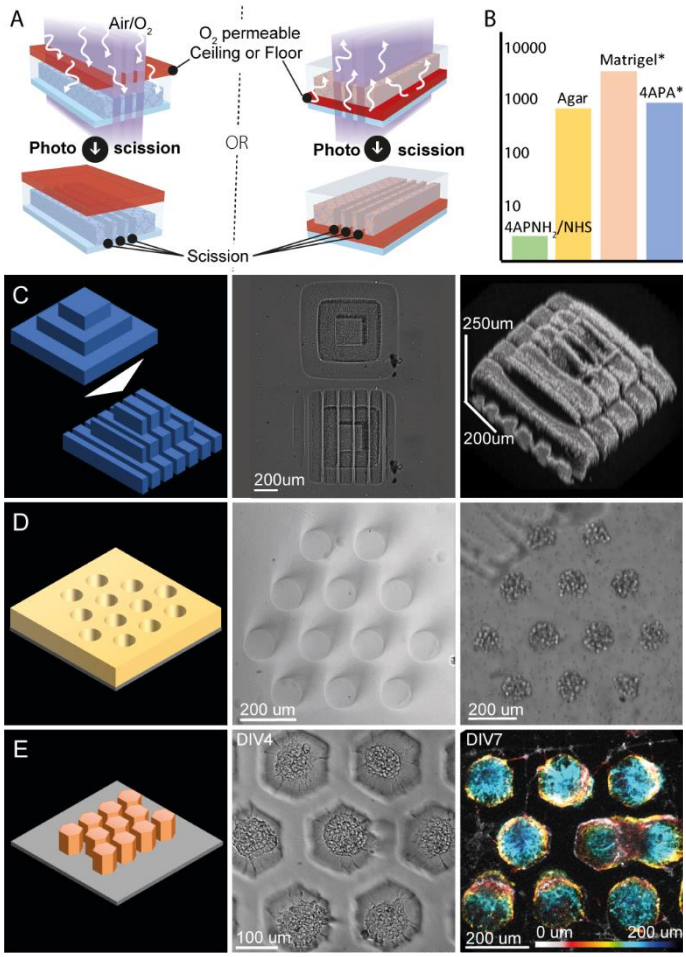

Fig. 4. Subtractive manufacturing of common hydrogels with photo-scission. (A) Schematics of the photo-scission procedure: cured hydrogels (blue, and pink) are exposed to patterned UV irradiation (purple, purple arrows) in the presence of photo-initiators. The PDMS ceiling or floor (red) ensures that oxygen is renewed in the insolated areas. This ultimately leads to the local liquefaction of the hydrogel. For the same pattern, scission time (s) is material dependent and may require dilution of the photo-initiator (*) (B, logarithmic scale). Photopolymerized hydrogels can also undergo photo scission (C). Soft bio-inert agar can be photo-scissionned to form spheroid assembly templates (D). Biocompatible pillars of Matrigel can be created to grow neurons (E).

An agar-agar template consisting of an array of 100um diameter microwells served as a spheroid culture substrate. (Fig.4D)

With the same method, hexagonal pillars were carved out of a Matrigel layer. These structures were among the softest we created (400 Pa) and were especially suited for neurons cell culture. As the pictures demonstrates, the neurons soma aggregated on top of the pillars while the axons spread out

(Fig.4E) forming interconnected spontaneously firing networks after a week (MovieS5). Of note photo-polymerized hydrogels can be subsequently photo-scissioned. In this example, a photo-polymerized "Aztec temple" was generated using the two previously described engineering operations: a square pillar was total-polymerized while two stages were added by z-controlled polymerization. The structure was then sliced demonstrating that cross-linked objects can be photo-scissionned (Fig.4C, MovieS6)

So far, the structures we've described were either cell repellant or fully adhesive. In the latter part we'll show how to decorate (locally functionalize) inert hydrogels with adhesive biomolecules.

Hydrogel Decoration. PEG or agarose hydrogels are bio-inert: they prevent biomolecules from adsorbing and thus cells from adhering(22). Previously , they have been either homogeneously(3) or locally(9) complemented with biomolecules to promote cell adhesion and differentiation. Photo-linkers like Sulfo-Sanpah or Acryl-PEG-Sva (APSv) are a family of commercially-available molecules capable of hydrogel decoration. One extremity of these hetero-bifunctional molecules can photo-graft to a hydrogel while the other moiety can bind amine-rich adhesion molecules like poly-L-lysin via esterification.

Here, we attach an acryl-PEG-Sva linker onto a PEG hydrogel in a spatially controlled manner by the conjugated action of the acryl moiety, the photo-initiator, and the patterned UV illumination (Fig.5A).

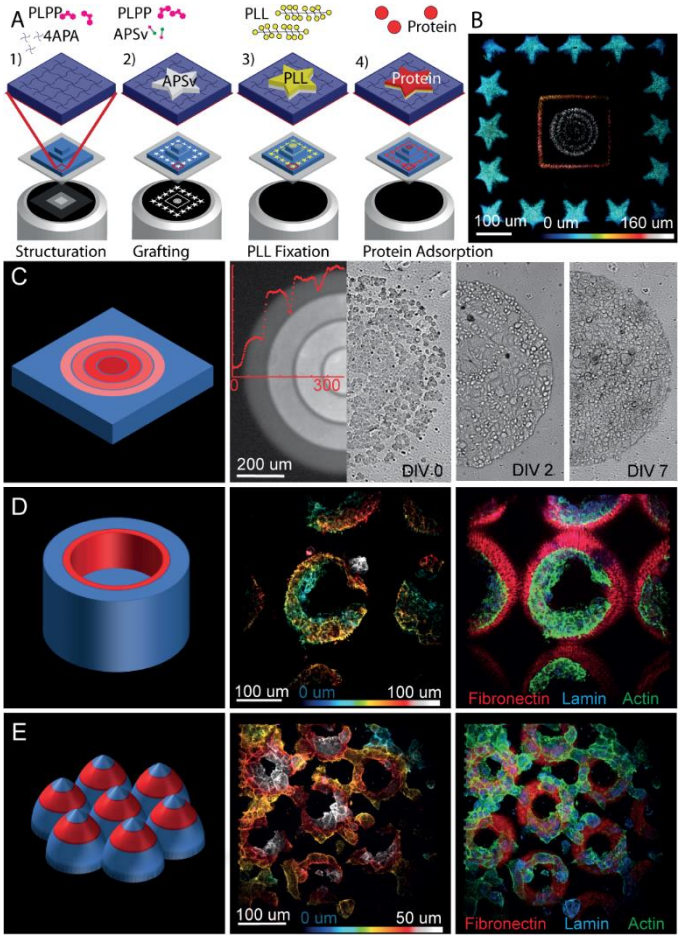

Fig. 5 | Decoration: quantitative and patterned functionalization of hydrogels. (A) Schematics of the micro-structuration and decoration of an "Aztec temple" hydrogel. First a gel is formed (dark blue) via height-controlled polymerization of 4-arm-PEG-acrylate (blue) with PLPP (pink). Then acryl-peg-sva (pink and green, white layer) is photo-grafted in the presence of PLPP according to the projected UV pattern. This allows covalent ester-binding of poly-L-lysin (yellow) and the subsequent adsorption of biomolecules (red). Complex decoration patterns can be easily aligned on previously generated topographies (B). Additionally, the process is dose dependent and can create adhesive gradients (C). It is thus possible to cultivate cells in microwells (D) or topographies (E) that combine adhesive and structural cues.

The photo-grafted succinimide-ester will subsequently react with the many amino-groups of the poly-L-lysin. This locally reverses the gel antifouling properties and permits subsequent adsorption of a wide range of proteins (23).

The photo-addition of acryl-PEG-Sva is UV dose-dependent and as such the density of grafted poly-L-lysin can be modulated. In Fig.5C, 4 concentric levels of photo-linkers were grafted on a flat PEG hydrogel leading to differential covalent binding of poly-L-lysin-FITC. We were able to induce differential cell adhesion by adsorbing fibronectin on this pattern. Using the same approach, laminin, a neuron specific adhesion molecule, was successfully grafted to orient neuron growth (S1).

With this maskless decoration method we can easily align biomolecule motifs onto previously built topographies. As a proof of concept, a 3-stage Aztec temple was polymerized as described in Fig.4 and each stage was decorated with a distinct motif (Fig.5B).

We now demonstrate that our platform precisely controls cell positioning on tridimensional objects. First, PEG Hydrogels were polymerized with power and grayscale modulation to obtain topographies. They were subsequently decorated with the aforementioned method allowing COS-7 cells to colonize these structures reminiscent of capillaries (Fig.5D) and intestinal villi (Fig.5E).

In summary, we combined UV-patterned illumination with gas permeable reactors to obtain 4 hydrogel engineering operations: total polymerization, z-controlled polymerization, photo-scission and decoration. We highlighted that they can readily address hydrogel engineering challenges alone or in combination.

Discussion

As any fast-growing field, 3D cell culture has known a burst in material and application diversity. Our platforms aim at embracing many materials (generic) and protocols (flexible) while being user-friendly (accessible). We'll now discuss these three aspects with emphasis on structuration, decoration and the role of the DMD.

Together, our results suggest that the chemical reactions leading to hydrogel structuration are driven by oxygen, light and benzophenone regardless of the material. This is the root of our multi-material capability.

As a result, total and z-controlled polymerization do not require prepolymers with photo-polymerizable moieties (movieS3). Even though, acrylated polymers display a faster crosslinking rate, our benzophenone-based initiator is able to induce polymer photo-crosslinking by itself. We also observed that chain length is critical to achieve sharp structures with good shape replication fidelity (S2C).

Indeed, polymerization of short prepolymer is impossible for native molecules and uncontrollable with acryl-moieties probably due to their high diffusivity. In our hands, long branched acrylated prepolymers are ideal to quickly form sharp structures (S2C).

In contrast, photo-scission liquefies all the hydrogels we have encountered so far regardless of their chain length. Nevertheless, this oxygen-consuming process is slower than photo-polymerization. Oxygen starvation prevents photo-scission and leads to crosslinking at depleted points in the insolated volume. Higher laser power and photo-initiator concentration increase the scission rate. Nevertheless, for a given geometry they must be low enough to prevent oxygen depletion. Finally, the above parameters together with material specific kinetics lead to highly variable scission times. For instance, the scission of dense agar structures can take hours while it only takes seconds to obtain sparse PEG gel geometries.

In line with the multi-material capabilities of our structuration method, a decoration operation supporting a wide range of hydrogels and biomolecules was needed.

Fortunately, there are plenty of available linkers which can be chosen depending on the material. Photo-linkers such as Sulfo-SANPAH can be grafted onto most substrates while avoiding further gel crosslinking(24). However, they are moisture and light sensitive making them very unstable and thus dispendious. To cope with those limitations, we combine our light stable photo-initiator with accessible Acryl-PEG-Sva linkers. This provides a user-friendly alternative at the expense of unwanted crosslinking inside the insolated area.

The poly-L-lysin incubation step was implemented to increase to robustness and flexibility of the decoration. Indeed, the photo-linker's succinimide ester hydrolyze in water limiting incubation time. Thus, optimal grafting would require highly concentrated biomolecules with many available amino groups but protein solutions are often highly diluted and can lack free amines. In contrast, poly-L-lysin quickly grafts onto the succinimide due to its high number of free amines. This now-stable grafting intermediate allows for the enrichment of most biomolecules even when highly diluted or poorly reactive.

We previously emphasized that our platform was suitable for structuring and decorating many hydrogels each having its own reaction rate. Here we introduce patterned light as a straightforward method to locally control the kinetics of the photoreactions that occur in the micro-reactor.

The DMD is the only hardware capable of locally tuning the UV photon flux within an entire illumination field. In essence, a DMD is a binary light modulator, the mirrors can only flip between ON and OFF state. It interprets grayscales by quickly switching between those two states in a process called pulse width modulation (PWM). The flipping rate of the mirrors is fortunately faster than the reaction kinetics so that PWM can control the thickness as efficiently as the laser intensity (S2A). This gives us local control over the photon flux. We also implemented an alternative insolation mode which interprets gray levels as UV doses. In this scenario, each pixel has a continuous insolation time proportional to the gray level. Together with the tunable laser power, this gives us enough flexibility to quickly optimize the illumination settings leading to the desired template.

We previously demonstrated that UV dose was instrumental in quantitative decoration and the photon flux was key to the generation of topographical structures. To give an insight into the possibilities offered by these illumination modes, one can fix the overall thickness with the laser power and locally tune the crosslink density with the UV dose(10). Hydrogel structures with orthogonal structural and rheological features are then feasible (S2D).

Lateral diffusion of oxygen during polymerization makes patterns with fine features especially difficult to print. The resulting structures appear as trimmed on the sides. To overcome this limitation, we optimized patterns design by offsetting the "zero" to a low value (S1B). This generates a photon flux sufficient to induce oxygen consumption without initiating polymerization ultimately reducing the trimming effect.

To summarize, the illumination set-up turned multiple 4-dimensional reaction kinetics into a playground where simple grayscale images sets the rules of the desired hydrogel micro-niches.

Outlook

Engineering soft gels for 3D cell culture is usually a difficult task. Here, by combining gas-permeable reactors together with patterned UV illumination, we ended up with a flexible yet simple hydrogel design solution:

When applied to its fullest, this principle can make perfused systems in short time scales. It can also generate topographically complex structures in one step. It gives new structuration means for photo-inert hydrogels. It can decorate gels to promote cell adhesion. Each of the engineering operations above can be queued since alignment steps are easy.

As biologists are striving to create standardized and physiologically relevant in vitro models using many materials, cells and protocols, our set-up can address many of their challenges. Overall, this platform has the potential to offer a common frame work for the scientists to share and expand their 3D cell culture discoveries.

Acknowledgments

The authors thank Nikon Instruments France for loaning some of their equipment. We thank our readers on bioRxiv for their comments and ideas in order to improve the impact of our work. We thank Corey Butler for careful reading of the manuscript.

Author Contributions

AP conducted the experiments. All authors designed the experiments and wrote the manuscript.

Additional information

Correspondence and requests for materials should be addressed to V.S.

Competing financial interests

A.P. and P-O.S. are employed by and V.S. is co-founder and shareholder of Alvéole (France).

References:

1. Caliari SR, Burdick JA (2016) A practical guide to hydrogels for cell culture. Nat Methods 13(5):405.
2. Shin Y, et al. (2012) Microfluidic assay for simultaneous culture of multiple cell types on surfaces or within hydrogels. Nat Protoc 7:1247.
3. Gjorevski N, et al. (2016) Designer matrices for intestinal stem cell and organoid culture. Nature 539(7630):560–564.
4. Dolega ME, Abeille F, Picollet-D'hahan N, Gidrol X (2015) Controlled 3D culture in Matrigel microbeads to analyze clonal acinar development. Biomaterials 52(1):347–357.
5. Kauer JA, et al. (2015) Three-Dimensional Neural Spheroid Culture: An In Vitro Model for Cortical Studies. Tissue Eng Part C Methods 21(12):1274–1283.
6. Laurent J, et al. (2017) Convergence of microengineering and cellular self-organization towards functional tissue manufacturing. Nat Biomed Eng 1(12):939–956.
7. Brown TE, Anseth KS (2017) Spatiotemporal hydrogel biomaterials for regenerative medicine. Chem Soc Rev 46(21):6532–6552.
8. DeForest CA, Anseth KS (2011) Cytocompatible click-based hydrogels with dynamically tunable properties through orthogonal photoconjugation and photocleavage reactions. Nat Chem 3(12):925–931.
9. Ali S, Cuchiara ML, West JL (2014) Micropatterning of poly(ethylene glycol) diacrylate hydrogels (Elsevier Inc.). 1st Ed. doi:10.1016/B978-0-12-800281-0.00008-7.
10. Yin H, Ding Y, Zhai Y, Tan W, Yin X (2018) Orthogonal programming of heterogeneous micro-mechano-environments and geometries in three-dimensional bio-stereolithography. Nat Commun 9(1):4096.
11. Tsang KMC, et al. (2015) Facile one-step micropatterning using photodegradable gelatin hydrogels for improved cardiomyocyte organization and alignment. Adv Funct Mater 25(6):977–986.
12. Pradhan, S., Keller, K. A., Sperduto, J. L. & Slater, J. H. (2017) Fundamentals of Laser-Based Hydrogel Degradation and Applications in Cell and Tissue Engineering. Adv Health Mat 1700681, 1–28.
13. Marina S, Bissell MJ (2017) Organoids: a historical perspective of thinkin in three dimensions. J Cell Biol 216:1–10.
14. Benton G, George J, Kleinman HK, Arnaoutova IP (2009) Advancing science and technology via 3D culture on basement membrane matrix. J Cell Physiol 221(1):18–25.
15. Dormán G, Nakamura H, Pulsipher A, Prestwich GD (2016) The Life of Pi Star: Exploring the Exciting and Forbidden Worlds of the Benzophenone Photophore. Chem Rev 116(24):15284–15398.
16. Folch A, Jo B, Hurtado O, Beebe DJ, Toner M (2000) Microfabricated elastomeric stencils for micropatterning cell cultures. J Biomed Mater 52(2):1–8.
17. Bartholomeusz DA, et al. (2012) Rapid prototyping of micro-structures using a cutting plotter. 14(6):1364–1374.
18. Tumbleston JR, et al. (2015) Continuous liquid interface production of 3D objects. Science (80-) 347(6228):1349–1351.
19. Dendukuri D, Pregibon DC, Collins J, Hatton TA, Doyle PS (2006) Continuous-flow lithography for high-throughput microparticle synthesis. Nat Mater 5(5):365–369.
20. Chaudhuri O, et al. (2016) Hydrogels with tunable stress relaxation regulate stem cell fate and activity. Nat Mater 15(3):326–334.

21. Strale PO, et al. (2016) Multiprotein Printing by Light-Induced Molecular Adsorption. Adv Mater 28(10):2024–2029.
22. Falconnet D, Csucs G, Michelle Grandin H, Textor M (2006) Surface engineering approaches to micropattern surfaces for cell-based assays. Biomaterials 27(16):3044–3063.
23. Mazia D, Schatten G, Sale W (1975) Adhesion of cells to surfaces coated with polylysine: Applications to electron microscopy. J Cell Biol 66(1):198–200.
24. Kumari A, et al. (2018) Actomyosin-driven force patterning controls endocytosis at the immune synapse. bioRxiv:452896.
25. York AG, et al. (2012) Resolution doubling in live, multicellular organisms via multifocal structured illumination microscopy. Nat Methods 9(7):749–754.

Methods:

Experimental Setup: For all the experiments, we used a Nikon TI-E inverted microscope (Nikon Instruments) equipped with a DMD-based UV patterned illumination device (PRIMO, Alveole, France) together with its dedicated software (LEONARDO V3.3, Alveole). The wavelength of the illumination laser is 375 nm. 4X S-Fluor and 10X Plan Fluor (Nikon) were used to ensure efficient UV transmission. A homemade version of this illumination device was previously described in 21. The patterns projected with PRIMO for all the experiments can be found in S4.

Modular Microreactors: We used custom PDMS chips made of two superposed PDMS thin films with holes fabricated by xurography (PDMS Stencils, Alveole, France, previously described in 21). These stencils were stacked onto a 22x22 mm 170 um thick glass coverslip (Schott Nexterion, Schott Jena, Germany) forming PDMS microchambers of various geometries (Fig.1). Depending on the application, the upper PDMS film was removed after the building steps to ease the seeding of cells or beads. In gas-controlled structuration experiments, the device is placed in a custom enclosure allowing argon or oxygen perfusion during the insolation steps.

Reagents were purchased as follows: 4-Arm-PEG-Acrylate MW 10K, Acryl-PEG-SVA MW 2K, 4-Arm-PEG-Amine MW 10K, 4-Arm-PEG-SAS MW 10K. Laysan Bio (Arab, USA). Matrigel Corning (USA). PLPP 1X (14.6 mg/mL) (Alvéole, France). Human Fibronectin (Roche). Agar low melting point, PEG 8K, PEG 20K, PEGDA MW700, Laminin from mouse EHS, PolyLysine, PolyLysine FITC conjugate (P3543), NH4Cl, Triton X100, Paraformaldehyde, Bovine Serum Albumin (BSA), Phosphate Buffered Saline (PBS), N,N-DimethylFormamide (DMF), Dulbecco Modified Eagle Medium, NeuroBasal (Sigma Aldrich). 0.3 um diameter carboxy-fluorescent latex beads, Phalloidin-Alexa647 conjugate (Invitrogen), anti-Lamin (Abcam, ab16048) and Goat Anti-rabbit antibody Alexa 568 conjugate (Abcam, ab175471). Sir-Actin (Spirochrome), Fluo4AM (Thermo Fisher), Membrite (Biotium).

Total Polymerization: precursor gel solutions containing monomer and PLPP as photo-initiator were incubated inside the PDMS microreactors. Under inert atmosphere (argon, N2), gels were polymerized using maximal laser intensity. The insolation times varied from 20sec to 5 minutes depending on the monomer polymerization yield. Precursor gel solutions used in the article were as follow: 50 mg/mL 4-arm-PEG-Acrylate diluted in 1X PLPP (Fig.2B, C, D, MovieS2, MovieS6), 25 mg/mL 4-Arm-PEG-acrylate with 0.5 mg/mL of Poly-L-Lysine in 0.5X PLPP (Fig.2E, MovieS1). To functionalize the hydrogels in Fig 2E, 100 ug/mL of Fibronectin were incubated for 15 minutes prior to cell seeding.

Z-controlled / Topographical Polymerization: Precursor gel solutions containing monomer and PLPP as photo-initiator were incubated inside the PDMS microreactors. Gels were polymerized in the presence of air using a combination of grayscale projection and/or variable light intensity. In one mode a gray scale pattern is insolated with gray levels interpreted as photon fluxes leading to a topographical structure. In another mode the gray levels are interpreted as UV dose and the laser intensity is set to obtain the desired thickness. In this second mode multiple projections must be done to obtain topographies. The insolation times varies from 20sec for 4 arm-PEG-acrylate to 5 minutes for Matrigel alone depending on the monomer polymerization yield and photon flux. Precursor gel solutions used in the article were as follow: 50 mg/mL 4-arm-PEG-Acrylate diluted in 1X PLPP (Fig.3B, C, S2A, B, D, E, MovieS6), Matrigel 5mg/mL in 0.5X PLPP (MovieS5),1.250 mg/mL 4-Arm-PEG-Acrylate with 5mg/mL Matrigel in 0.75X PLPP (Fig.3D). 100 mg/mL PEG 8K, 100 mg/mL PEG 20K, 100 mg/mL 4-arm-PEG-Acrylate and 100 mg/mL PEGDA 700 all in 0.5X PLPP (S2C).

Photo-scission: Hydrogel precursor solutions were allowed to cure inside the PDMS microreactors. PLPP was left to perfuse in the hydrogels for 10 minutes prior to UV projection. The PLPP concentration was also adjusted depending on the material: 0.0125X for Matrigel or 4-arm-PEG-acryl and 1X for agar-agar or 4-arm-PEG-amine / 4-arm-PEG-SAS. Photo-scissionned hydrogels in the article were the following: 50 mg/mL 4-Arm-PEG-Acrylate (Fig.4C, MovieS3, MovieS6), 20 mg/mL 4-Arm-PEG-Acrylate(Fig.4B), 20 mg/mL Agar (Fig.4B),0.50 mg/mL Agar (Fig.4D, MovieS3) 20 mg/mL Poly-Acryl-Amide (MovieS3) , 20 mg/mL 4-Arm-PEG-Amine /4-Arm-Peg SAS (Fig.4B , MovieS3) , 21mg/mL Matrigel (Fig.4B,E, MovieS3)

Decoration: Solutions consisting of 50 mg/mL 4-arm-PEG-acrylate in 1X PLPP were photopolymerized with z-control inside the PDMS microreactors. For agar and 4-arm-PEG-amine/4-arm-PEG-SAS (S3) solutions of 20mg/mL of precursor were let to cure in the microreactors. After rinsing with PBS, a solution of 100mg/mL of APSV in 1X PLPP was incubated. These solutions were prepared immediately before use. 1g/mL aliquots of APSV in DMF can alternatively be used, they are stable for 2 months at -20C°. The photo-linkers were grafted onto the surface of the gel by the subsequent insolation which last for 30 sec to 2 minutes depending on photon flux and substrate. The gels were rinsed and incubated with 1mg/mL PLL immediately after the insolation step to prevent the activated esters to hydrolyze. After one hour of PLL incubation the gels were rinsed. To promote cell adhesion, 100 ug/mL of Fibronectin (Fig.4) or 25ug/mL laminin (S1) were incubated for 15 minutes prior to cell seeding.

Cell Culture: COS-7 and HEK 293T cells were seeded and cultivated in complete cell culture media (DMEM, FBS). E18 rat primary cortical neurons were seeded and cultivated in complemented neurobasal.

Staining and imaging: Fixation and staining of cells was conducted using standard procedures. Staining of gels structures was performed by coating with 0.3 um carboxy-fluorescent beads. Neurons on Matrigel (Fig.4E MovieS5) were imaged using Sir-Actin and Fluo4AM live markers. Spheroids (Fig.3C) were stained using membrite live marker. 3D imaging was achieved using a homemade DMD based confocal microscope(25).

SI APPENDIX

Supplementary Figures

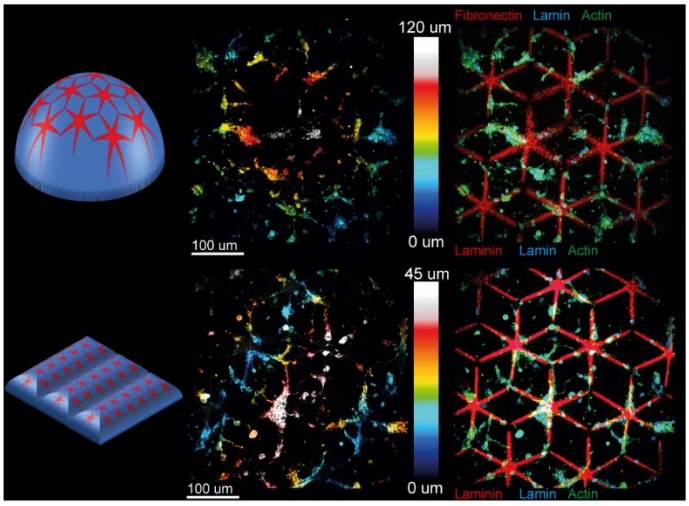

S1 Decoration of hydrogels for neurons. left panels: schematic representation of 4-arm-PEG-hydrogels (blue) decorated with Poly-L-lysin(red) and laminin. Middle panels: Z-color-coded confocal fluorescence microscopy images of neurons seeded on the gels and stained for actin. Right panels: 3-color max-projection of confocal microscopy z-stack showing the patterned molecules (red), the actin cytoskeleton (green) and the nuclear envelope (blue).

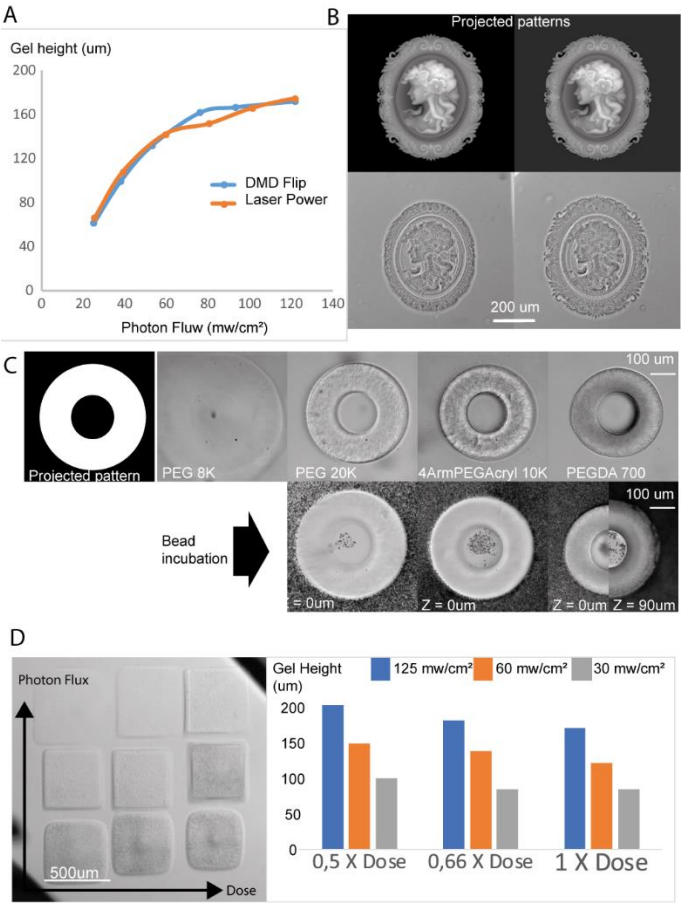

S2 Optimization of photo-polymerization. The gel height is equally modulated by the laser power or the projected gray levels (A). A gray background can nullify oxygen trimming (B). Polymerization fidelity depends on precursor length (C). Gel thickness and reticulation are decorrelated (D).

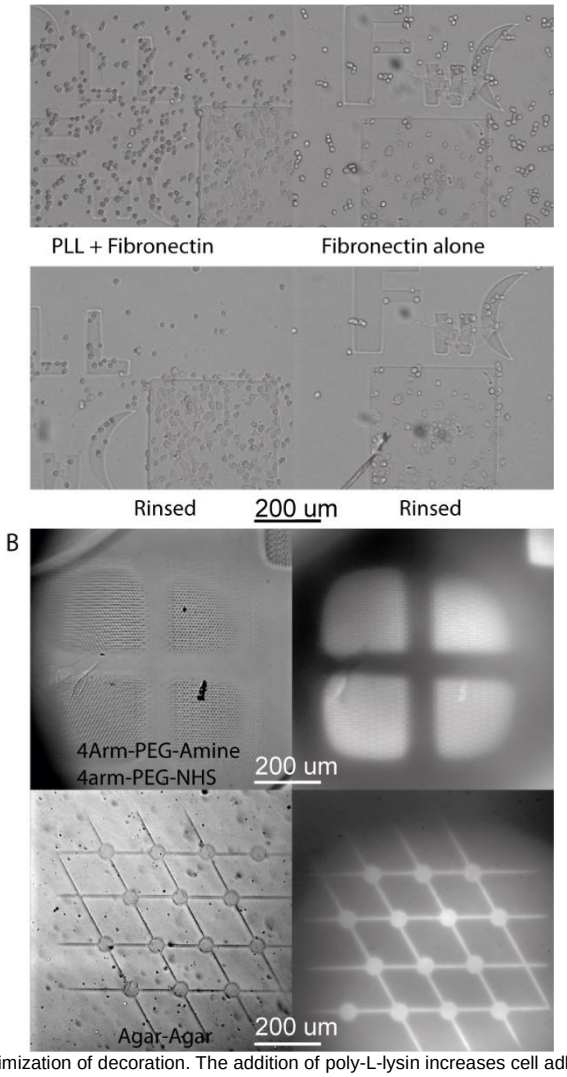

S3 Optimization of decoration. The addition of poly-L-lysin increases cell adhesion (A). Non acryls hydrogels can be decorated (B).

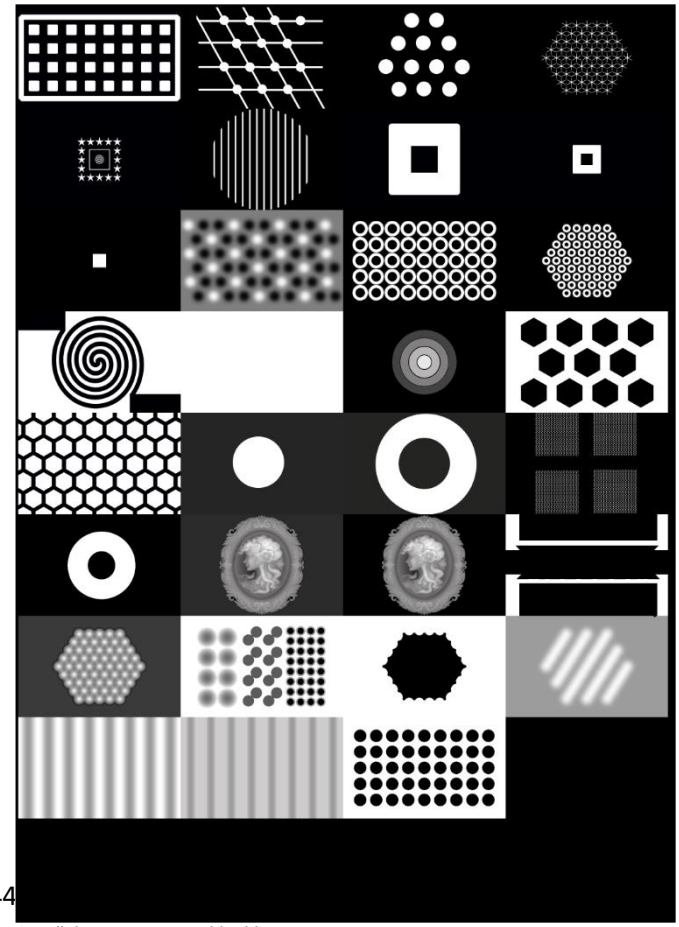

S4 All the patterns used in this report

Bibliography

1. Marina, S. & Bissell, M. J. Organoids: a historical perspective of thinkin in three dimensions. *J. Cell Biol* **216**, 1–10 (2017).

2. Kelava, I. & Lancaster, M. A. Stem Cell Models of Human Brain Development. *Cell Stem Cell* **18**, 736–748 (2016).

3. Laurent, J. *et al.* Convergence of microengineering and cellular self-organization towards functional tissue manufacturing. *Nat. Biomed. Eng.* **1**, 939–956 (2017).

4. Brassard, J. A. & Lutolf, M. P. Engineering Stem Cell Self-organization to Build Better Organoids. *Stem Cell* **24**, 860–876 (2019).

5. Li, X., Sun, Q., Li, Q., Kawazoe, N. & Chen, G. Functional Hydrogels With Tunable Structures and Properties for Tissue Engineering Applications . *Frontiers in Chemistry* **6**, 499 (2018).

6. Pradhan, S., Keller, K. A., Sperduto, J. L. & Slater, J. H. Fundamentals of Laser-Based Hydrogel Degradation and Applications in Cell and Tissue Engineering. *Adv. Healthc. Mater.* **6**, 1700681 (2017).

7. Murphy, S. V, Skardal, A. & Atala, A. Evaluation of hydrogels for bio-printing applications. *J. Biomed. Mater. Res. Part A* **101A**, 272–284 (2013).

8. Choi, J. R., Yong, K. W., Choi, J. Y. & Cowie, A. C. Recent advances in photo-crosslinkable hydrogels for biomedical applications. *Biotechniques* **66**, 40–53 (2019).

9. Kloxin, A. M., Kasko, A. M., Salinas, C. N. & Anseth, K. S. Photodegradable hydrogels for dynamic tuning of physical and chemical properties. *Science* **324**, 59–63 (2009).

10. Brown, T. E. & Anseth, K. S. Spatiotemporal hydrogel biomaterials for regenerative medicine. *Chem. Soc. Rev.* **46**, 6532–6552 (2017).

11. Burdick, J. A. & Murphy, W. L. Moving from static to dynamic complexity in hydrogel design. *Nat. Commun.* **3**, (2012).

12. Yao, H., Wang, J. & Mi, S. Photo Processing for Biomedical Hydrogels Design and Functionality: A Review. *Polymers (Basel).* **10**, 11 (2017).

13. Nerger, B. A., Siedlik, M. J. & Nelson, C. M. Microfabricated tissues for investigating traction forces involved in cell migration and tissue morphogenesis. *Cell. Mol. Life Sci.* **74**, 1819–1834 (2017).

14. Warner, J. J., Soman, P., Zhu, W., Tom, M. & Chen, S. Design and 3D Printing of Hydrogel Scaffolds with Fractal Geometries Department of NanoEngineering , University of California , San Diego. (2016). doi:10.1021/acsbiomaterials.6b00140

15. Miri, A. K. *et al.* Microfluidics-Enabled Multimaterial Maskless Stereolithographic Bioprinting. *Adv. Mater.* **30**, 1800242 (2018).

16. DeForest, C. A. & Anseth, K. S. Cytocompatible click-based hydrogels with dynamically tunable properties through orthogonal photoconjugation and photocleavage reactions. *Nat. Chem.* **3**, 925–931 (2011).

17. Gjorevski, N. *et al.* Designer matrices for intestinal stem cell and organoid culture. *Nature* **539**, 560–564 (2016).

18. Chaudhuri, O. *et al.* Hydrogels with tunable stress relaxation regulate stem cell fate and activity. *Nat. Mater.* **15**, 326–334 (2016).

19. dos Santos, B. P. *et al.* Development of a cell-free and growth factor-free hydrogel capable of inducing angiogenesis and innervation after subcutaneous implantation. *Acta Biomater.* (2019). doi:10.1016/j.actbio.2019.08.028

20. Benton, G., George, J., Kleinman, H. K. & Arnaoutova, I. P. Advancing science and technology via 3D culture on basement membrane matrix. *J. Cell. Physiol.* **221**, 18–25 (2009).

21. Lancaster, M. A. *et al.* Cerebral organoids model human brain development and microcephaly. *Nature* **501**, 373 (2013).

22. Strale, P. O. *et al.* Multiprotein Printing by Light-Induced Molecular Adsorption. *Adv. Mater.* **28**, 2024–2029 (2016).

23. Dormán, G., Nakamura, H., Pulsipher, A. & Prestwich, G. D. The Life of Pi Star: Exploring the Exciting and Forbidden Worlds of the Benzophenone Photophore. *Chemical Reviews* **116**, 15284–15398 (2016).

24. Tumbleston, J. R. *et al.* Continuous liquid interface production of 3D objects. *Science (80-.).* **347**, 1349–1351 (2015).

25. Ali, S., Cuchiara, M. L. & West, J. L. *Micropatterning of poly(ethylene glycol) diacrylate hydrogels*. *Methods in Cell Biology* **121**, (Elsevier Inc., 2014).

26. Mazia, D., Schatten, G. & Sale, W. Adhesion of cells to surfaces coated with polylysine: Applications to electron microscopy. *J. Cell Biol.* **66**, 198–200 (1975).

27. Caliari, S. R. & Burdick, J. A. A practical guide to hydrogels for cell culture. *Nat. Methods* **13**, 405 (2016).

28. Horvath, P. *et al.* Screening out irrelevant cell-based models of disease. *Nat. Rev. Drug Discov.* **15**, 751–769 (2016).

29. Fang, Y. & Eglen, R. M. Three-Dimensional Cell Cultures in Drug Discovery and Development. *SLAS Discov.* **22**, 456–472 (2017).

30. Barcellos-Hoff, M. H., Aggeler, J., Ram, T. G. & Bissell, M. J. Functional differentiation and alveolar morphogenesis of primary mammary cultures on reconstituted basement membrane. *Development* **105**, 223–235 (1989).

31. Zhao, X. *et al.* Photocrosslinkable Gelatin Hydrogel for Epidermal Tissue Engineering. *Adv. Healthc. Mater.* **5**, 108–118 (2016).

32. Yue, K. *et al.* Visible light crosslinkable human hair keratin hydrogels. *Bioeng. Transl. Med.* **3**, 37–48 (2018).

33. Valmikinathan, C. M. *et al.* Photocrosslinkable chitosan based hydrogels for neural tissue engineering. *Soft Matter* **8**, 1964–1976 (2012).

34. Qi, A. *et al.* Hydroxypropyl Cellulose Methacrylate as a Photo-Patternable and Biodegradable Hybrid Paper Substrate for Cell Culture and Other Bioapplications. *Adv. Healthc. Mater.* **3**, 543–554 (2014).

35. Yin, H., Ding, Y., Zhai, Y., Tan, W. & Yin, X. Orthogonal programming of heterogeneous micro-mechano-environments and geometries in three-dimensional bio-stereolithography. *Nat. Commun.* **9**, 1–7 (2018).

36. Sunyer, R., Jin, A. J., Nossal, R. & Sackett, D. L. Fabrication of Hydrogels with Steep Stiffness Gradients for Studying Cell Mechanical Response. *PLoS One* **7**, e46107 (2012).

37. Sheth, S. *et al.* UV Dose Governs UV-Polymerized Polyacrylamide Hydrogel Modulus. *Int. J. Polym. Sci.* **2017**, (2017).

38. Lee, S.-H., Moon, J. J. & West, J. L. Three-dimensional micropatterning of bioactive hydrogels via two-photon laser scanning photolithography for guided 3D cell migration. *Biomaterials* **29**, 2962–2968 (2008).

39. Lunzer, M. *et al.* A Modular Approach to Sensitized Two-Photon Patterning of Photodegradable Hydrogels. *Angew. Chemie - Int. Ed.* **57**, 15122–15127 (2018).

40. Sarig-Nadir, O., Livnat, N., Zajdman, R., Shoham, S. & Seliktar, D. Laser photoablation of guidance microchannels into hydrogels directs cell growth in three dimensions. *Biophys. J.* **96**, 4743–4752 (2009).

41. Kharkar, P. M., Kiick, K. L. & Kloxin, A. M. Designing degradable hydrogels for orthogonal control of cell

microenvironments. *Chem. Soc. Rev.* **42**, 7335–7372 (2013).

42. Tsang, K. M. C. *et al.* Facile one-step micropatterning using photodegradable gelatin hydrogels for improved cardiomyocyte organization and alignment. *Adv. Funct. Mater.* **25**, 977–986 (2015).

43. You, S. *et al.* Nanoscale 3D printing of hydrogels for cellular tissue engineering. *J. Mater. Chem. B* **6**, 2187–2197 (2018).

44. Shadish, J. A., Benuska, G. M. & DeForest, C. A. Bioactive site-specifically modified proteins for 4D patterning of gel biomaterials. *Nat. Mater.* (2019). doi:10.1038/s41563-019-0367-7

45. DeForest, C. A. & Anseth, K. S. Photoreversible patterning of biomolecules within click-based hydrogels. *Angew. Chemie - Int. Ed.* **51**, 1816–1819 (2012).

46. Chaudhuri, T., Rehfeldt, F., Sweeney, H. L. & Discher, D. E. Preparation of collagen-coated gels that maximize in vitro myogenesis of stem cells by matching the lateral elasticity of in vivo muscle. *Methods Mol. Biol.* **621**, 185–202 (2010).

47. Sunyer, R., Jin, A. J., Nossal, R. & Sackett, D. L. Fabrication of Hydrogels with Steep Stiffness Gradients for Studying Cell Mechanical Response. *PLoS One* **7**, 1–9 (2012).

48. Shim, T. S., Yang, S. M. & Kim, S. H. Dynamic designing of microstructures by chemical gradient-mediated growth. *Nat. Commun.* **6**, 6584 (2015).

49. Yin, H., Ding, Y., Zhai, Y., Tan, W. & Yin, X. Orthogonal programming of heterogeneous micro-mechano-environments and geometries in three-dimensional bio-stereolithography. *Nat. Commun.* **9**, 4096 (2018).

50. Dendukuri, D., Pregibon, D. C., Collins, J., Hatton, T. A. & Doyle, P. S. Continuous-flow lithography for high-throughput microparticle synthesis. *Nat. Mater.* **5**, 365–369 (2006).

51. Pinto, L. F. A., Goi, B. E., Schmitt, C. C. & Neumann, M. G. Photodegradation of Polystyrene Films Containing UV-Visible Sensitizers. *J. Res. Updat. Polym. Sci.* **2**, 39–47 (2013).

52. Alimperti, S. *et al.* Three-dimensional biomimetic vascular model reveals a RhoA, Rac1, and N-cadherin balance in mural cell–endothelial cell-regulated barrier function. *Proc. Natl. Acad. Sci.* 201618333 (2017). doi:10.1073/pnas.1618333114

53. Nelson, C. M., VanDuijn, M. M., Inman, J. L., Fletcher, D. A. & Bissell, M. J. Tissue geometry determines sites of mammary branching morphogenesis in organotypic cultures. *Science (80-.).* **314**, 298–300 (2006).

54. Pavlovich, A. L., Manivannan, S. & Nelson, C. M. Adipose stroma induces branching morphogenesis of engineered epithelial tubules. *Tissue Eng. - Part A* **16**, 3719–3726 (2010).

55. Vrij, E. *et al.* Directed Assembly and Development of Material-Free Tissues with Complex Architectures. *Adv. Mater.* **28**, 4032–4039 (2016).

56. Rivron, N. C. *et al.* Blastocyst-like structures generated solely from stem cells. *Nature* **557**, (2018).

57. Dingle, Y. L. *et al.* Three-Dimensional Neural Spheroid Culture: An In Vitro Model for Cortical Studies. *Tissue Eng. Part C Methods* **21**, 1274–1283 (2015).

58. Yu, L. *et al.* Core-shell hydrogel beads with extracellular matrix for tumor spheroid formation. *Biomicrofluidics* **9**, 24118 (2015).

59. Laperrousaz, B. *et al.* Direct transfection of clonal organoids in Matrigel microbeads: A promising approach toward organoid-based genetic screens. *Nucleic Acids Res.* **46**, (2018).

60. Alessandri, K. *et al.* Cellular capsules as a tool for multicellular spheroid production and for investigating the mechanics of tumor progression in vitro. *Proc. Natl. Acad. Sci. U. S. A.* **110**, 14843–14848 (2013).

61. Sugiura, S. *et al.* Size control of calcium alginate beads containing living cells using micro-nozzle array. *Biomaterials* **26**, 3327–3331 (2005).

62. Dolega, M. E., Abeille, F., Picollet-D'hahan, N. & Gidrol, X. Controlled 3D culture in Matrigel microbeads to analyze clonal acinar development. *Biomaterials* **52**, 347–357 (2015).

63. Onoe, H. *et al.* Metre-long cell-laden microfibres exhibit tissue morphologies and functions. *Nat. Mater.* **12**, 584–590 (2013).

64. Andrique, L. *et al.* A model of guided cell self-organization for rapid and spontaneous formation of functional vessels. *Sci. Adv.* **5**, 1–13 (2019).

65. Gilardi, M. *et al.* Human 3D vascularized organotypic microfluidic assays to study breast cancer cell extravasation. *Proc. Natl. Acad. Sci.* **112**, 214–219 (2014).

66. Xiao, Y. *et al.* Senescent Cells with Augmented Cytokine Production for Microvascular Bioengineering and Tissue Repairs. *Adv. Biosyst.* **3**, 1900089 (2019).

67. Jang, M., Kleber, A., Ruckelshausen, T., Betzholz, R. & Manz, A. Differentiation of the human liver progenitor cell line (HepaRG) on a microfluidic-based biochip. *J. Tissue Eng. Regen. Med.* **13**, 482–494 (2019).

68. Xiao, Y. *et al.* Ex vivo Dynamics of Human Glioblastoma Cells in a Microvasculature-on-a-Chip System Correlates with Tumor Heterogeneity and Subtypes. *Adv. Sci.* **6**, 1801531 (2019).

69. Moreno, E. L. *et al.* Differentiation of neuroepithelial stem cells into functional dopaminergic neurons in 3D microfluidic cell culture. *Lab Chip* **15**, 2419–2428 (2015).

70. Pojman, J. A. *Frontal Polymerization*. *Polymer Science: A Comprehensive Reference, 10 Volume Set* **4**, (Elsevier B.V., 2012).

71. Cabral, J. T., Hudson, S. D., Harrison, C. & Douglas, J. F. Frontal photopolymerization for microfluidic applications. *Langmuir* **20**, 10020–10029 (2004).

72. Vitale, A., Hennessy, M. G., Matar, O. K. & Cabral, J. T. A Unified Approach for Patterning via Frontal Photopolymerization. *Adv. Mater.* **27**, 6118–6124 (2015).

73. Zhao, Z. *et al.* Origami by frontal photopolymerization. *Sci. Adv.* **3**, e1602326 (2017).

74. Stoecklin, C. *et al.* A New Approach to Design Artificial 3D Microniches with Combined Chemical, Topographical, and Rheological Cues. *Adv. Biosyst.* **2**, 1700237 (2018).

75. Zhao, W., Li, X., Liu, X., Zhang, N. & Wen, X. Effects of substrate stiffness on adipogenic and osteogenic differentiation of human mesenchymal stem cells. *Mater. Sci. Eng. C* **40**, 316–323 (2014).

76. Bartholomeusz, D. A. *et al.* Rapid prototyping of micro-structures using a cutting plotter. **14**, 1364–1374 (2012).

77. Decock, J., Schlenk, M. & Salmon, J.-B. In situ photo-patterning of pressure-resistant hydrogel membranes with controlled permeabilities in PEGDA microfluidic channels. *Lab Chip* **18**, 1075–1083 (2018).

78. Blin, G., Picart, C., Théry, M. & Puceat, M. Geometrical confinement guides Brachyury self-patterning in embryonic stem cells. *bioRxiv* 1–46 (2017).

79. Thery, M. Micropatterning as a tool to decipher cell morphogenesis and functions. *J. Cell Sci.* **123**, 4201–4213 (2010).

80. Grevesse, T., Versaevel, M., Circelli, G., Desprez, S. & Gabriele, S. A simple route to functionalize polyacrylamide hydrogels for the independent tuning of mechanotransduction cues. *Lab Chip* **13**, 777–780 (2013).

81. Hynd, M. R., Frampton, J. P., Dowell-Mesfin, N., Turner, J. N. & Shain, W. Directed cell growth on protein-functionalized hydrogel surfaces. *J. Neurosci. Methods* **162**, 255–263 (2007).

82. Castaño, A. G. *et al.* Protein patterning on hydrogels by direct microcontact printing: application to cardiac differentiation. *RSC Adv.* **4**, 29120–29123 (2014).

83. Tseng, Q. *et al.* A new micropatterning method of soft substrates reveals that different tumorigenic signals can promote or reduce cell contraction levels. *Lab Chip* **11**, 2231–2240 (2011).

84. Cosson, S. & Lutolf, M. P. Hydrogel microfluidics for the patterning of pluripotent stem cells. *Sci. Rep.* **4**, 4462 (2014).

85. Xu, Z. *et al.* High-throughput three-dimensional chemotactic assays reveal steepness-dependent complexity in neuronal sensation to molecular gradients. *Nat. Commun.* **9**, 4745 (2018).

86. Sim, J. Y. *et al.* Controlling cell shape on hydrogels using lift-off protein patterning. *PLoS One* **13**, e0189901 (2018).

87. Vignaud, T., Ennomani, H. & Théry, M. Polyacrylamide Hydrogel Micropatterning. *Methods Cell Biol.* **120**, 93–116 (2014).

88. Seddiki, R. *et al.* Force-dependent binding of vinculin to α-catenin regulates cell-cell contact stability and collective cell behavior. *Mol. Biol. Cell* **29**, 380–388 (2018).

89. Weydert, S. *et al.* Easy to Apply Polyoxazoline-Based Coating for Precise and Long-Term Control of Neural Patterns. *Langmuir* **33**, 8594–8605 (2017).

90. Renault, R., Durand, J.-B., Viovy, J.-L. & Villard, C. Asymmetric axonal edge guidance: a new paradigm for building oriented neuronal networks. *Lab Chip* **16**, 2188–2191 (2016).

91. Virlogeux, A. *et al.* Reconstituting Corticostriatal Network on-a-Chip Reveals the Contribution of the Presynaptic Compartment to Huntington's Disease. *Cell Rep.* **22**, 110–122 (2018).

Index of Figures

Figure 1 | Introducing the platform and the chapters. 4
Figure 2 | Naturally derived matrixes have paved the history of three-dimensional cell culture. 8
Figure 3 | Engineered matrixes can improve organoid generation. 9
Figure 4 | Engineered matrixes allow better control of mechanical parameters. 10
Figure 5 | Engineered matrixes allow better control of biological factors. 11
Figure 6 | When hydrogel and micro-engineering meet: rationalizing organoid generation. 13
Figure 7 | Principles of light-matter interaction with the oversimplified example of benzophenone. 15
Figure 8 | The three major light structuration methodologies. 16
Figure 9 | Using light structuration to photo-cure hydrogel precursors. 18
Figure 10 | Using light structuration to photo-degrade hydrogels. 19
Figure 11 | Chemically engineered hydrogels for photodegradation. 20
Figure 12 | Chemically engineered hydrogels for dynamic and spatial presentation of biomolecules. 21
Figure 13 | Oxygen inhibited stereolithography. 23
Figure 14 | Oxygen induced photo-scission. 24
Figure 15 | Using photo-scission to tutor cell adhesion. 25
Figure 16 | Molding Agar to produce cortical neurospheres. 29
Figure 17 | Molding Agar to produce blastoïds. 30
Figure 18 | Molding Collagen into tubules. 31
Figure 19 | Flow focusing to create clonal organoid capsules 33
Figure 20 | Flow focusing to create tubules and vessels 34
Figure 21 | Meniscus pinning as a tool to create hydrogel barriers and vasculatures. 36
Figure 22 | Frontal photopolymerization. 40
Figure 23 | Fabrication of NOA-slides for photopolymerization and use thereof. 41
Figure 24 | Frontal polymerization is unreliable 42
Figure 25 | Oxygen inhibition is easily observed near silicone. 44
Figure 26 | Inhibition depends on oxygen concentration and photon flux. 45
Figure 27 | From wells to microreactors. 46
Figure 28 | The xurography process 47
Figure 29 | Assembly of gas permeable microreactors and use thereof. 48
Figure 30 | Gas-controlled photopolymerization and use thereof. 50
Figure 31 | Characterization of hydrogel thickness in gas-controlled polymerization 51
Figure 32 | In-situ polymerization of chambers and channels. 52
Figure 33 | Fabrication of fluidic devices using gas-controlled polymerization 54
Figure 34 | Flux-controlled polymerization, principle and uses. 56
Figure 35 | Characterization of flux and dose dependence in flux-controlled polymerization 58
Figure 36 | Principle and characterization of the trimming effect 59
Figure 37 | Grayscale background to reduce of the trimming effect 60
Figure 38 | Gel structuration applied to cell-culture. 64
Figure 39 | Freeze drying to stamp Matrigel. 69
Figure 40 | Decoration of polyacrylamide hydrogels to study cell contractility in the presence of tumorigenic factors. 71
Figure 41 | Chemical gradients through flow chambers. 73
Figure 42 | Lift-off decoration workflow. 77
Figure 43 | Adapted lift-off decoration workflow. 78
Figure 44 | Liftoff patterning using photopolymerized poly(ethylene-glycol) hydrogels. 79
Figure 45 | Amide crosslinking and acryl crosslinking. 82
Figure 46 | A bifunctional ligand to decorate hydrogels. 83
Figure 47 | Hydrogel decoration workflow with photo-linkers. 84
Figure 48 | Poly-L-lysin improves cell adhesion on poly(ethylene-glycol) hydrogels. 86
Figure 49 | Neuron and Cell culture on flat poly(ethylene-glycol) hydrogels. 88
Figure 50 | The synergy between structuration and photo-linker decoration 89
Figure 51 | Realization of a decorated hydrogel pyramid. 90
Figure 52 | Queuing structuration and decoration for cell culture. 93
Figure 53 | PLPP can decorate native materials. 101
Figure 54 | Decoration of native materials: demonstration with amide-poly(ethylene-glycol) and agar. 103
Figure 55 | PLPP can cure native precursors. 104
Figure 56 | PLPP is critical for native gelation. 106
Figure 57 | Monomer chain length impacts the crosslinking yield. 107
Figure 58 | Evidence of an oxygen driven reaction observed during native decoration. 109
Figure 59 | Photo-scission depends on oxygen consumption and diffusion. 111
Figure 60 | Putative Photo-scission mechanism including parasitic reactions. 114
Figure 61 | Two photo-scission modes exist. 116
Figure 62 | Photo-scission works on many hydrogels. 118
Figure 63 | Scission time and conditions are material dependent. 119
Figure 64 | Scission of soft hydrogels for cell culture. 122
Figure 65 | Queuing and combining engineering steps. 128
Figure 66 | Orthogonality conundrum from the prism of each engineering operation. 130
Figure 67 | Integrating a gentler chemistry to create dynamic environments. 131
Figure 68 | Two path towards large scale exist. 132

Index Of tables

Table 1 | A wide array of hydrogels support different types of cell culture studies. 6
Table 2 | Three functional bricks support hydrogels templates, Z structuration is crucial in their production by light. 38
Table 3 | Hydrogel decoration from a practical and technical standpoint. 75
Table 4 | Common photo-initiators in hydrogel engineering. 99
Table 5 | Advancing towards tridimensional control. 127

Contexte : Culture Cellulaire, Hydrogels et Micro-fabrication

Depuis près d'un demi-siècle, la culture cellulaire évolue vers des modèles qui se veulent de plus en plus représentatifs des conditions physiologiques. De façon traditionnelle les cellules sont cultivées sur des lames en verre ou des boîtes de Petri, des substrats très éloignés des conditions naturelles de par leur extrême rigidité et leur absence totale d'eau. Les scientifiques ont donc cherché à développer des matériaux plus fidèles aux conditions *in-vivo* en essayant notamment de mimer la matrice extracellulaire : l'ensemble des molécules qui entourent les cellules dans les organes et qui soutiennent et influencent leur comportement.

Les hydrogels, des réseaux de fibres polymères enchevêtrées et gorgées d'eau sont progressivement devenus le substrat de choix pour la culture cellulaire physiologique. Ils sont obtenus par extractions des composants de la matrice extracellulaire ou par synthèse chimique de molécules mimétiques. Au sein de ces matériaux les cellules sont susceptibles de pousser en trois dimensions et de s'auto-organiser en structures complexes telle que les sphéroïdes ou les organoïdes. Ces dix dernières années, l'utilisation de cellules souches (induites ou embryonnaires) combinée à l'usage d'hydrogels comme substrat a permis l'élaboration de modèles *in-vitro* de différents organes comme l'intestin, la glande mammaire ou plus récemment le cerveau. Ces modèles sont d'ores et déjà promis à des applications à visée pharmacologique néanmoins leur fabrication hasardeuse et leur structure assez anarchique reste un frein à leur adoption.

Afin de standardiser la production de modèles in-vitro sur hydrogels, il est désormais nécessaire de pouvoir structurer ces matériaux ainsi que de contrôler leurs propriétés physicochimiques à l'échelle des cellules (quelques dizaines de micromètres). Malheureusement, les méthodes de micro-fabrication traditionnelles basées sur l'usage de moules ou tampons en silicone sont peu adaptées à la grande fragilité des hydrogels : ces derniers supportent très mal le contact physique. Ainsi, des méthodes basées sur la structuration de la lumière et l'emploi de la photochimie ont vu le jour pour permettre l'ingénierie d'hydrogels sans contact.

Cette thèse industrielle s'inscrit dans cette démarche, elle est le fruit d'une collaboration entre le CNRS, ici représenté par l'institut interdisciplinaire de neurosciences (IINS) et Alvéole : entreprise française qui commercialise une plateforme de photo-impression de protéines. L'enjeu global était de permettre la structuration et la décoration d'hydrogels par le biais de la plateforme susmentionnée sans la modifier afin de permettre l'adoption des procédés par les utilisateurs.

Développements : Structuration, décoration et généricité

Le travail s'est décomposé en trois jalons complémentaires d'égale importance :

Le premier jalon a consisté à débloquer la photo-gelation d'hydrogel en trois dimensions. De nombreux précurseurs d'hydrogels ont été modifiés chimiquement pour leur permettre de former un gel en présence de lumière ultraviolette. Cependant en l'absence de contrôle sur les zones illuminées l'ensemble du volume éclairé serait polymérisé. Notre outil de photo-imprimerie étant d'ores et déjà capable de structurer la lumière de façon bidimensionnelle, nous avons donc concentré nos efforts pour parvenir à contrôler l'épaisseur de gélation. Pour ce faire, nous avons tiré profit de l'effet d'inhibition de la gélation provoqué par l'oxygène. Cet effet appelé zone morte a pour propriétés d'être moins prononcé si on diminue la teneur en oxygène dans le réacteur ou qu'on illumine avec des intensités plus fortes. Pour pouvoir appliquer ce processus au contrôle de l'épaisseur de gels nous avons conçu des micro-réacteurs avec une toiture en silicone : un matériau très perméable à l'oxygène. Les effet de zones mortes ont étés ainsi concentrés à proximité de cette toiture perméable nous permettant ensuite de jouer sur la concentration en oxygène ou l'intensité lumineuse pour contrôler l'épaisseur du gel.

Le second jalon concernait la décoration des gels c'est à dire le contrôle local des molécules présentées par le gel. Pour y parvenir nous avons employé des photo-ligands, des réactifs développées pour pouvoir s'accrocher au gel sous l'effet de la lumière ultraviolette et permettre ensuite l'accrochage l'accrochage de biomolécules comme par exemple protéines d'adhésion. Notre principal objectif était justement de parvenir à créer des zones adhésives pour les cellules à la surface de matériaux bio-inertes (non-adhésifs). Les photo-ligands sont des molécules très réactives ce qui les rend assez instables, elles sont notamment connues pour s'hydrolyser rapidement dans l'eau. Pour rendre le protocole plus simple nous avons employé une bio-molécule de synthèse, la poly-L-lysine, qui a le triple avantage d'être peu onéreuse, très réactive vis-à-vis des photo-ligands et de promouvoir l'adhésion des cellules. Cette molécule a servi d'intermédiaire entre le photo-ligand est des protéines d'adhésion naturelles telle que la fibronectine et la laminine.

Le troisième jalon a cherché à étendre les méthodes précédemment développées au plus grand nombre possible d'hydrogels. En effet les hydrogels sont très répandus mais aussi très variés en terme de composition chimique, il est donc difficile de trouver des réactions génériques susceptibles de fonctionner pour beaucoup d'hydrogels. Ici c'est l'usage d'un photoinitiateur basé sur la benzophénone qui nous aura permis de progresser. Nous avons mis en évidence que ce photoinitiateur est capable de déclencher des réaction de gélation et de greffage même à partir de gels dépourvus de fonctions chimiques adéquates. Plus intéressant encore, nous avons fait la découverte de la réaction de photo-scission. Cette méthode de photo-liquéfaction d'hydrogels est basée sur l'interaction entre l'oxygène et la benzophénone. Ce procédé liquéfie la partie de gel insolée tout en préservant les propriétés mécanique du gel alentour , il est très adaptée aux matériaux les plus fragiles.

Résultats : culture cellulaire en micro-niches standardisées

Par le biais des développements, nous avons créé une boîte à outils photochimique à même de créer des environnements en hydrogels structurés et décorés à l'échelle des cellules : des micro-niches. Nous avons en parallèle mené des expériences de culture cellulaire au sein des ces structures pour valider leur fonctionnement.

La structuration nous a permis de créer des topographies ou des microcanaux adhésifs rappelant les replis de l'intestin ou encore des vaisseaux dans lesquelles les cellules peuvent s'étaler et former des épithéliums rudimentaires. Nous avons aussi exploité les propriétés bio-inertes de matériaux comme le poly-éthylène glycol pour réaliser des puits ou les cellules s'agrègent en sphéroïdes de taille et de forme contrôlée.

Nos premières expériences sur la décoration ont démontré le rôle bénéfique de la poly-lysine dans l'adhésion des cellules au gels. Nous avons ensuite validé qu'il était possible de créer des gradients d'adhésion cellulaire en modulant par la lumière la cinétique de greffage du photo-ligand à la surface du gel. Enfin, nous avons combiné la structuration et la décoration pour créer des environnements encore plus complexes. Nous avons démontré que les cellules au sein de ces micro-niches réagissent et s'organisent en respectant la structure et les facteurs d'adhésion.

Par l'emploi de la benzophénone pour la photo-scission, nous avons créé des piliers en matrigel et des puits en Agar : deux matériaux très répandus et particulièrement fragiles.Les cellules cultivés dans les puits en agar ont formé des sphères. Des neurones ont été cultivés sur les piliers en matrigel, ils se sont polarisés formant des neurites et se connectant au bout de quelques jours.

Perspectives : cytocompatibilité et grande échelle

L'ensemble de ces expériences a montré l'utilité de cette boite à outil pour la culture cellulaire en micro-niches. Un brevet sur la photo-scission a été déposé, une publication est en cours et Alvéole peut dès à présent communiquer sur ces travaux car ils ne nécessitent pas de changements sur la plateforme.

Les futurs développement vont concerner la cytocompatibilité et l'application à grande échelle :

Le contrecoup d'une photochimie puissante c'est qu'elle peut s'avérer toxique pour les cellules. En l'état, notre plateforme est utile pour créer des niches en gel et y ensemancer des cellules mais elle ne permet pas d'effectuer des modifications durant la culture. Pour y parvenir il sera nécessaire d'améliorer la chimie ou d'opter pour des solutions plus douces. Grâce à ces développements nous espérons pouvoir encapsuler des cellules ou encore modifier la décoration au gré des besoins durant la pousse des cellules.

Le deuxième défi à relever sera d'augmenter le débit de production de ces structures pour atteindre des échelles satisfaisantes pour les tests *in-vitro*. Notre plateforme a été optimisée pour façonner des millimètres carrés dans des temps de l'ordre de la dizaine de minutes. Afin de pouvoir façonner des hydrogels dans des substrats standards que sont la plaque 96 puits et la boîte de pétri nous allons devoir mettre nos procédés à l'échelle. Cela sous entend d'accélérer nos réactions par un facteur dix ou cent et/ou augmenter notre champ d'illumination pour couvrir des aires plus grandes.